Études des interactions hôte-microbiote chez l'algue brune Saccharina latissima

Bertille Burgunter-Delamare

▶ **To cite this version:**

Bertille Burgunter-Delamare. Études des interactions hôte-microbiote chez l'algue brune Saccharina latissima. Botanique. Sorbonne Université, 2022. Français. ⟨NNT : 2022SORUS212⟩. ⟨tel-03813790v2⟩

HAL Id: tel-03813790

https://theses.hal.science/tel-03813790v2

Submitted on 13 Oct 2022

HAL is a multi-disciplinary open access archive for the deposit and dissemination of scientific research documents, whether they are published or not. The documents may come from teaching and research institutions in France or abroad, or from public or private research centers.

L'archive ouverte pluridisciplinaire **HAL**, est destinée au dépôt et à la diffusion de documents scientifiques de niveau recherche, publiés ou non, émanant des établissements d'enseignement et de recherche français ou étrangers, des laboratoires publics ou privés.

HAL Authorization

Sorbonne Université

Ecole Doctorale 227 Sciences de la Nature et de l'Homme, Ecologie et Evolution

Laboratoire de Biologie Intégrative des Modèles Marins UMR 8227

Equipe Biologie des algues et interactions avec l'environnement

Etudes des interactions hôte-microbiote chez l'algue brune *Saccharina latissima*

Par Bertille BURGUNTER-DELAMARE

Thèse de doctorat de Biologie Marine

Dirigée par Catherine BOYEN et Simon DITTAMI

Présentée et soutenue publiquement le 28 janvier 2022

Devant un jury composé de :

Dr. Claire PRIGENT-COMBARET	CNRS, LEM, Lyon	Rapportrice
Dr. Sophie ARNAUD-HAOND	IFREMER, Sète	Rapportrice
Pr. Christophe DESTOMBE	Sorbonne Université - CNRS	Examinateur
Dr. Alexis DUFRESNE	CNRS, ECOBIO, Rennes	Examinateur
Dr. Catherine BOYEN	Sorbonne Université - CNRS	Directrice de thèse
Dr. Simon DITTAMI	Sorbonne Université - CNRS	Directeur de thèse

Except where otherwise noted, this work is licensed under
http://creativecommons.org/licenses/by-nc-nd/3.0/

« Ensemble, on n'est pas tout seul »

- Piotr

Tous à l'Ouest,

- Olivier Jean-Marie, 2007

« Le tout c'est pas d'y faire, c'est d'y penser ;

mais le difficile c'est pas d'y penser, c'est d'y faire »

La Plaisante Sagesse Lyonnaise

- Catherin Bugnard, 1920

Remerciements

« Il y a plus d'idées dans deux têtes que dans une »

Je tiens à remercier chaleureusement, Claire Prigent-Combaret et Sophie Arnaud-Haond, rapportrices, Alexis Dufresne et Christophe Destombe, examinateurs, d'avoir accepté de faire partie de mon jury de soutenance et d'évaluer mes travaux de thèse.

Je remercie également les membres de mon comité de suivi de thèse : Angélique Gobet, Marc-André Selosse, Frédérique Viard et Frédéric Partensky, pour leurs précieux conseils.

« Faire du vélo sans les petites roues »

Un énorme merci à mes encadrants, Catherine B. et Simon. Vos conseils, votre engagement et votre soutien m'ont énormément apporté, autant sur le plan humain que scientifique. Catherine, merci d'avoir été là quand il le fallait. Simon, merci d'avoir cru en moi dès le début de mon stage de M2 puis au long de ces années de thèse ; merci pour ton calme efficace et ta bienveillance, oh combien précieux pendant cette dernière ligne droite.

« Holobionte »

Je remercie toute l'équipe *ABIE*, pour m'avoir accueillie en ce début de janvier 2018 (avec la grippe en plus) et avec qui je viens de passer 4 années enrichissantes : Catherine L., Sylvie, Philippe, Elham, Ludo, et les autres. Merci à tous pour vos précieux conseils ; Sylvie, merci de m'avoir aidé avec toutes ces cultures et ces plantules, sans toi je n'y serais jamais arrivée !

Merci aussi à nos collaborateurs en Allemagne et en Norvège, grâce à qui j'ai pu avoir accès à de superbes échantillons de *Saccharina latissima*. Stein, Kai and Nora, thank you so much, tusen takk, Vielen Dank !

Merci à Emilie Adouane et Soizic Prado du MNHN pour leur aide précieuse avec les biosenseurs, les protocoles et tout le reste …

Merci à Gwenn et Erwan de la plateforme Genomer, pour leur soutien technique lors des nombreuses sessions de métabarcoding 16S.

« BONJOUR ! »

Un énorme merci aux « adultes » de cette histoire : Lionel et Laurence, Sabine, Stéphane E., Sandrine, Fred L., Nathalie, François, Maryvonne, Alexandra, Tristan et les autres. Merci à tous pour vos conseils, les discussions sur l'Avenir dans la recherche, les ateliers Microbio / Fêtes de la Science / Nuit des Chercheurs. Merci pour le café 60X, les cuberdons et les chocolats (ceux qui comprennent comprendrons…)

Enormes pensées pour Gaëlle ; on sera toujours des super-scientifiques !

« Chien-assis, piles du pont et dos collé-carré »

Mathilde, Ulysse G, Kévin, Léna, Martin, Jade, Damien, Camille P., Erwan, Lisa, Louison, Yasmine, Aurélien, Dan, Marie-Morgane, Yacine, Mathurin, Ulysse F. (= Meilleur Stagiaire), Samuel… et j'en oublie.

Merci pour les verres partagés au Typ (et merci aussi à l'équipe du Typ), à l'Albat ou ailleurs (oui, même le Vasco), les blablas, les bleubleus, les pas bobets, les raclettes, les tartiflettes, et les pâtes en rentrant. Merci d'avoir été là (de A à Z !) dans les moments moins drôles, parce que mêmes si « c'est évident », ça fait toujours chaud au cœur de savoir que vous êtes là :)

Merci aussi pour les sessions de jardinage nocturne (oh ! camaïeu de rose !), les hurlements de certains et les danses endiablées des autres, les histoires à dormir debout et les « tu sais pas la dernière !? »

Prochaines étapes, VOS gâteaux de thèse ;)

« Bureau 353, en face des stagiaires »

Maéva, super collègue de thèse, avec qui nous avons partagé l'espace vital du bureau. Tu as supporté mes moments de craquage, mes ronchonnements et le bruit de la cafetière pendant ces 3 années… et aussi le meilleur : les pains au chocolat, les chouquettes et quelques fous rires somptueux.

Vielen Dank, Marie-Katherine ! Post-doc de choc, tu as sur-vécu nos 3 derniers mois avec Maéva. Merci pour le chocolat et pour ton oreille attentive à nos déboires.

« Tout le monde peuvent pas être de Lyon »

Mathieu, Louis et Axel : merci d'être encore là après tout ce temps.

Les anciens du master BV, 3 ans plus tard, on a bien grandi …

« Les chiens ne font pas des chats »

Papa & Maman, Quentin & Aymeric, Grand-Père & Paulette, merci à vous d'avoir été là depuis le début, et de m'avoir supportée ces dernières années, merci de m'avoir transmis ce caractère particulier et l'envie d'apprendre.

Parce que finalement,

« A taaaableeeee ! »

Merci à vous de lire ce manuscrit (ou du moins les remerciements…)

Bonne lecture !

Table des matières

Table des matières 9

Liste des figures 13

Liste des tables 15

INTRODUCTION 21

I. L'holobionte 21

1. Le concept d'holobionte 21

2. Holobionte marin 27

3. Holobionte macroalgue 30

II. De l'importance des macroalgues et des kelps en particulier 36

1. Importance écologique et économique des macroalgues brunes, populations naturelles .. 36

2. Systèmes holobionte algue brune : *Ectocarpus* sp. et *Saccharina latissima* 38

III. Le projet de thèse : problématique et objectifs 42

CHAPITRE I - Effects of sampling and storage procedures on 16S amplicon sequencing results of kelp microbiomes 47

Abstract 49

I. Introduction 50

II. Material & Methods 51

1. Biological material 51

2. Sample preparation technics 51

3. DNA extraction 52

4. 16S metabarcoding 52

5. Analyses 53

III. Results 53

1. Comparison of apex and meristem samples with the three storage methods 54

2. Direct comparison of storage methods 55

IV. Discussion & Conclusion 57

Declarations 59

Acknowledgements 59

Supplementary Data 59

CHAPITRE II - The *Saccharina latissima* microbiome: algal tissue matters more than region, season, and physiology 63

Abstract 65

I. Introduction 67

II. Material & Methods 68

1. Biological material & Environmental Variables 68

2. DNA extraction 69

3. 16S Metabarcoding 70

4. Analyses 71

III. Results 71

1. General taxonomy 71

2. Comparison of apex and meristem samples 72

3. Comparison of regions 72

4. Seasonality 74

5. Comparison Healthy / Symptoms 76

IV. Discussion 77

1. The blade part is the primary driver of samples separation 78

2. Regional specificities: tides, seawater, and genetics 79

3. Shifts in bacterial communities depending on the season 80

4. Is microbiota a characteristic signature for algae in poor health? 81

V. Conclusion 82

VI. Tables 84

VII. Declarations 88

VIII. Acknowledgements 88

IX. Supplementary data 88

CHAPITRE III - Etude des interactions algues-bactéries : Croissance & Quorum-Sensing 93

I. Contexte 94

1. *Ectocarpus,* microbiote et transcriptome 94

2. *Ectocarpus et l'impact de son microbiote* 94
3. Cocultures croisées *S. latissima* et bactéries d'*Ectocarpus* 95
4. Le phénomène de Quorum-Sensing 96
5. Hypothèses de travail 100
II. Sélection de souches bactériennes d'intérêt 101
1. Partie cultivable du microbiote de *S. latissima* 101
2. Sélection des souches 104
III. Cocultures 104
1. Préparation des solutions bactériennes 104
2. Préparation des plantules 106
3. Composition des cocultures 106
4. Incubation 107
IV. Étude de l'impact sur la croissance de l'algue 109
1. Méthodes 109
2. Résultats & Discussion 110
V. Corrélation QS & Croissance 116
1. Méthodes 116
2. Le QS dans les cocultures 118
3. Corrélation Croissance des algues et QS 125
VI. Etude de l'impact de l'inoculation sur la composition de la communauté bactérienne 127
1. Matériel & Méthodes 127
2. Résultats 128
VII. Discussion 130
VIII. Données Supplémentaires 133
CONCLUSION & PERSPECTIVES 139
REFERENCES BIBLIOGRAPHIQUES 147
ANNEXES 177
Annexe I - Présentations orales 178
Annexe II - Poster 179

Annexe III - Article M2 N°1 180

Annexe IV - Article M2 N°2 191

Annexe V - Article *Ectocarpus* Australie 203

ABSTRACT 215

RESUME DE THESE 216

Liste des figures

Figure 1 – Définition de l'holobionte selon Adolf Meyer-Abich et Lynn Margulis 21

Figure 2 – Définition de l'holobionte d'après Theis et al. (2016) 22

Figure 3 – Le microbiote de la plante d'après Gopal and Gupta (2016). La rhizosphère, l'endosphère et la phyllosphère sont les compartiments principaux du microbiote de la plante (Dicotylédones à gauche et Monocotylédone à droite). 25

Figure 4 – L'holobionte et les facteurs influençant la colonisation bactérienne sur l'hôte algue (Egan et al., 2013). 30

Figure 5 – Répartition mondiale des forêts de laminaires, d'après Steneck et al. (2002) et Bolton (2010) 36

Figure 6 – Position phylogénétique des *Phaeophyceae*, *Ectocarpales* et *Laminariales*. (A) Position des algues brunes au sein de l'arbre des eucaryotes d'après Burki et al. (2020). Les algues brunes (*Phaeophyceae*) appartiennent au clade SAR, à la division des Straménopiles (Hétérocontes), et sont phylogénétiquement distantes des plantes terrestres et des algues vertes et rouges. (B) Position des *Ectocarpales* et des *Laminariales* au sein des algues brunes d'après Bringloe et al. (2020). 39

Figure 7 – Morphologie et croissance de *Saccharina latissima* 40

Figure 8 – Cycle de vie de *Saccharina latissima*, adapté de Visch et al., (2019) et Theodorou and Charrier (2021) 41

Figure 9 – Sampled parts of the thallus. Two discs (Ø2cm) were punched out in immediate proximity for each part of the blade, and an area of 2cm² was swabbed 51

Figure 10 – Distribution of 16S rRNA gene metabarcoding sequences per phylum 54

Figure 11 – Box plot of alpha-diversity (Shannon H index) across sample types. P-values correspond to the results of a two-sided t-test; n.s. = not significant ($p > 0.05$). 55

Figure 12 – NMDS analysis of the microbiome composition. Results show a clear separation of the apex and meristem samples for the (A) liquid nitrogen, (B) silica gel, and (C) swab method, as well as (D) all methods combined. The points of the same colours and connected by lines correspond to the same "parent" sample. . 55

Figure 13 – Venn diagram illustrating shared genera between the liquid nitrogen (pink), silica gel (blue), and swab (green) datasets. Numbers in parentheses indicate the percentage of total reads represented by the genera in each section. 56

Figure 14 – Correlation of log10-transformed mean sequence abundance across the sampling protocols. Only genera shared by at least two of the protocols were considered. R=Pearson correlation coefficient, red line = linear regression, $p < 0.0001$ 57

Figure 15 – Samples part of *Saccharina latissima*'s thallus. Two discs (Ø2cm) were punched out in immediate proximity for each part of the blade. 69

Figure 16 – Algal blade part analysis A) NMDS analysis of the microbiome composition. Results show a clear separation of the apex and meristem samples for all the samples. B) Box plot of alpha-diversity (Shannon H index) across different sample types. *p-value <0.0001*. C) Comparison of microbiome composition between apex and meristem samples. Distribution of 16S rRNA gene metabarcoding sequences per phylum. *Proteobacteria_NA*: not classified as *Alpha-* or *Gammaproteobacteria*. D) Venn diagram illustrating shared core genera between the apex (blue) and the meristem (yellow) part. Those are classified genera present in 90% of replicate for each group. The percentage of total reads of each subset are shown in parentheses. 73

Figure 17 – Regions analysis. A) NMDS analysis of the microbiome composition. Results show a clear separation of the samples according to their origin. B) Box plot of alpha-diversity (Shannon H index) across different sample types. p-value>0.005. C) Microbiome composition of samples from Roscoff, Helgoland and Norway. Distribution of 16S rRNA gene metabarcoding sequences per phylum. *Proteobacteria_NA*: not classified as *Alpha-* or *Gammaproteobacteria*..... 74

Figure 18 – Season analyses. A) NMDS analysis of the microbiome composition. Results show a separation of the samples depending on the sampling's season. B) Box plot of alpha-diversity (Shannon H index) across different sample types. P-value>0.005. C) Seasonal microbiome composition tracking in Roscoff. Distribution of 16S rRNA gene metabarcoding sequences per phylum. *Proteobacteria_NA*: not classified as *Alpha-* or *Gammaproteobacteria*..... 75

Figure 19 – Examples of symptoms observed on "diseased" *S. latissima* individuals. A) twisted blade, B) hole and C) bubbling in blade 76

Figure 20 – Symptoms analyses. A) NMDS analysis of the microbiome composition. Results do not show a separation of the healthy and symptoms samples. B) Box plot of alpha-diversity (Shannon H index) across different sample types. *p-value=0.046*. C) Microbiome composition of healthy and symptoms samples. Distribution of 16S rRNA gene metabarcoding sequences per phylum. *Proteobacteria_NA*: not classified as Alpha- or Gammaproteobacteria. D) NMDS analysis of the microbiome composition depending on the symptoms. ... 77

Figure 21 – Croissance en mm des algues (*Ectocarpus*) après 4 semaines de coculture, adapté de Burgunter-Delamare et al. (2020) ..... **Erreur ! Signet non défini.**

Figure 22 – Taux de croissance relatif (mm) des plantules de *S. latissima* T0-T5 95

Figure 23 – Voie de biosynthèse des AHL par LuxI, d'après Dickschat (2010) 98

Figure 24 – Voie de biosynthèse des AI-2, d'après Zhu et al. (2004) 99

Figure 25 – Photos d'une « boite mère » et stries d'étalement pour purification 102

Figure 26 – Part cultivable du microbiote de *S. latissima* 103

Figure 27 – Photo d'une plantule de *S. latissima* sur lame millimétré (à gauche) et sa conversion pour l'analyse de la surface (à droite) 110

Figure 28 – Croissance relative journalière des plantules de *S. latissima* entre T0-T5 (T5) et T5-T1week (T1week). Les lettres du test post hoc sont distinctes entre les deux séries. Zb : Zobell. Tutti : mélange des souches du groupe de coculture. Slat CTRL : plantules non inoculées. Cf Table 8. 115

Figure 29 – Taux de croissance et concentration en Zobell. On considère le taux de croissance par rapport au contrôle comme très faible : -0.3-0.2, faible : 0.2-0.5, moyen :0.5-1 et élevé >1. On considère la concentration en Zobell comme très faible : <1 µl/ml, faible : 1-1.75 µl/ml, moyenne : 1.75-3.5 µl/ml, élevée : 3.5-5 µl/ml et très élevée : >5 µl/ml. 116

Figure 30 – Induction des biosenseurs par les différents surnageants de cocultures. 120

Figure 31 – Induction des biosenseurs par les différentes souches bactériennes..... 121

Figure 32 – Induction de MM32 par les surnageants de cocultures bactéries et algues + bactéries 123

Figure 33 – Induction de MM32 dans CC algues-bactéries..... 124

Figure 34 – Induction de MM32 en fonction de la concentration en Zobell 125

Figure 35 – Taux de croissance en fonction de l'induction de MM32 126

Figure 36 – Induction des biosenseurs AHL par les cocultures 126

Figure 37 – NMDS générale sur les données d'abondance pour tous les groupes de cocultures 129

Figure 38 – NMDS pour chaque groupe de cocultures. Croissance relative forte : >1, moyenne : entre 0.5 et 1, mi-faible : entre 0.02 et 0.5, et faible : <0.02. n.t. : non testée = plantules prélevées avant l'inoculation. CTRL : le taux de croissance relatif est calculé à partir de la croissance du contrôle. 130

Figure 39 – Schéma récapitulatif des principaux résultats de thèse. L'épaisseur des flèches caractérisent l'importance des facteurs d'influence. 142

Liste des tables

Table 1 – Sampling dates and sites 69

Table 2 – Taxonomic affiliations of the ASVs specific to the apex and meristem samples, compared with their occurrence in the entire dataset. 84

Table 3 – Taxonomic affiliations of the ASVs specific to Roscoff, Helgoland, or Norway samples compared with their occurrence in the entire dataset. 84

Table 4 – Taxonomic affiliations of the ASVs specific to each season from Roscoff samples, compared with their occurrence in the entire dataset..... 85

Table 5 – Taxonomic affiliations of the ASVs specific to the healthy and symptoms samples compared with their occurrence in the entire dataset..... 86

Table 6 – Les molécules du QS 97

Table 7 – Souches bactériennes sélectionnées pour les cocultures 105

Table 8 – Composition bactérienne des cocultures et concentration finale après inoculation..... 108

Table 9 – Cocultures algues-bactéries & induction du QS. Les taux de croissance sont ceux de la section IV.2 Figure 8 de ce chapitre. Pour la concentration en Zobell, très faible : <1 µl/ml, faible : 1-1.75 µl/ml, moyenne : 1.75-3.5 µl/ml, élevée : 3.5-5 µl/ml et très élevée : >5 µl/ml. 122

Liste des abréviations

ADN / DNA	Acide désoxyribonucléique / Deoxyribonucleic acid
AHL	Acyl Homoserine Lactone
AI-1	Autoinducteur de type 1
AI-2	Autoinducteur de type 2
ANOVA	Analysis of variance
ARN / RNA	Acide ribonucléique / Ribonucleic acid
ASV	Amplicon Sequence Variant
ASW	Artificial SeaWater
ATB	Antibiotiques
CC	Cocultures
CTRL	Contrôle
DAPG	2,4-Diacetylphloroglucinol
DGTA	diacylglyceryl hydroxymethyltrimethyl-β-alanine
DMSP	Dimethylsulfoniopropionate
Eau milliQ	Eau ultra pure
EDTA	Ethylenediaminetetraacetic acid
HSL	Homo Serine Lactone
LB	Luria-Bertani (milieu)
MB	Marine Broth
NA	Non Assigné
NMDS	Non-Metric Multidimensional Scaling
NSW	Natural SeaWater
PAM	Pulse amplitude modulation
PCR	Polymerase chain reaction - Réaction en chaîne par polymérase
PES	Provasoli Enrichissement SeaWater
PGPR	Plant Growth Promoting Rhizobacteria
QS	Quorum Sensing
R2A	Reasoner's 2A Agar
UV	Ultra-Violet

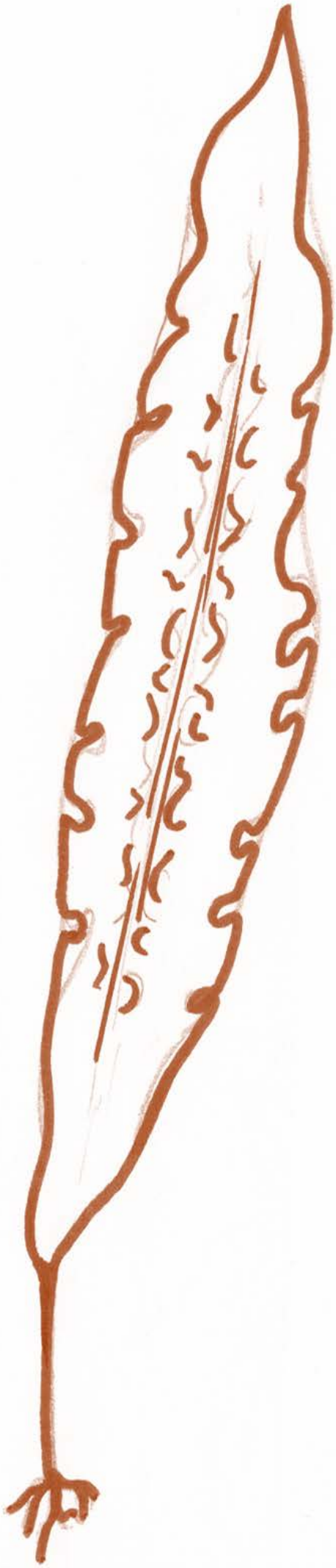

- INTRODUCTION -

INTRODUCTION

I. L'holobionte

1. Le concept d'holobionte

a. Définitions de l'holobionte

Le terme de symbiose dans un contexte biologique fut introduit par Heinrich Anton de Bary en 1879, alors professeur de botanique à l'Université de Strasbourg. Lors d'une conférence donnée à *l'Association of German Naturalists and Physicians* (De Bary, 1879), il caractérise de symbiose une « interaction à long terme entre des organismes de différentes espèces ».

Dans les années 40, le biologiste Allemand Adolf Meyer-Abich a développé une théorie de l'évolution par l'holobiose (Meyer-Abich, 1943), qui explique que les organismes complexes se sont développés au travers de phénomènes d'association (parasitisme → sym-biose → holo-biose), et que les ensembles d'organes résultent d'organismes indépendants à la base. Il explique également que pour comprendre un changement évolutif, il faut se concentrer sur les organismes d'abord en tant que tels, puis en tant que partenaires symbiotiques, en tant qu'« holobionte » ensuite, et enfin en système entier. Il décrit l'holobionte comme l'assemblage de biotes spécifiques, dû à un phénomène d'holobiose, plutôt que comme un ensemble complet (**Figure 1**), ce qui est légèrement différent du concept indépendamment développé par Lynn Margulis (1991). Elle définit l'holobionte comme un complexe symbiotique, formé de plusieurs biotes (organismes individuels), et qui résulte d'une association entre ces biotes (**Figure 1**).

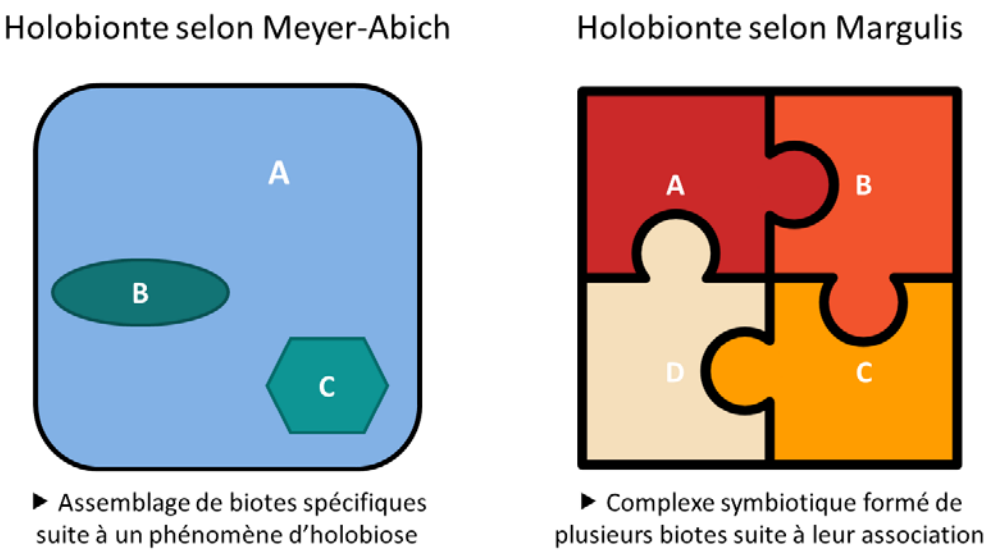

Figure 1 – Définition de l'holobionte selon Adolf Meyer-Abich et Lynn Margulis

Dans cette thèse, la définition de Theis et al. (2016) sera retenue, définissant un holobionte comme une entité formée de l'hôte et de tous les microbes associés, y compris ceux qui affectent le phénotype de l'holobionte et qui ont co-évolué avec l'hôte, ceux qui affectent le phénotype de l'holobionte mais n'ont pas co-évolué avec l'hôte, et ceux qui n'affectent pas du tout le phénotype de l'holobionte. Les microbes peuvent être transmis verticalement ou horizontalement, peuvent être acquis à partir de l'environnement et peuvent être présents de manière constante ou non. Ainsi, l'holobionte est capable d'évoluer dans le temps et l'espace à mesure que les microbes l'intègrent. Les microbes présents dans l'environnement ne font pas partie de l'holobionte (**Figure 2**).

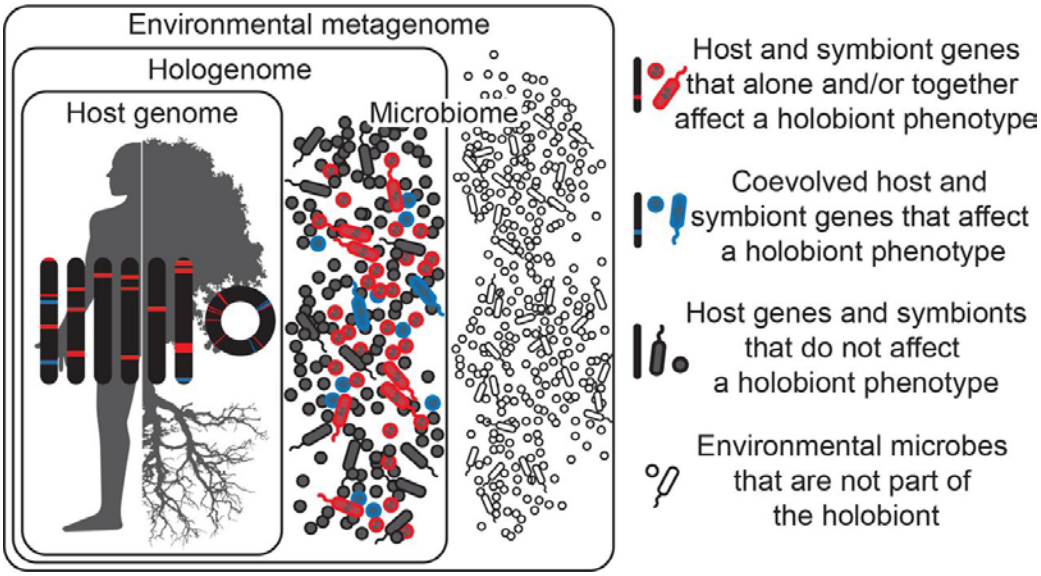

Figure 2 – Définition de l'holobionte d'après Theis et al. (2016)

Suite au développement des études sur l'holobionte, le concept d'hologénome s'est également développé (Rosenberg and Zilber-Rosenberg, 2012, 2018; Bordenstein and Theis, 2015). Ce concept d'évolution postule que l'holobionte (=hôte + symbiotes) et son hologénome (=génome hôte + génome symbiotes) sont des « blocs » de sélections dans l'évolution.

Un holobionte est donc un assemblage de plusieurs partenaires, avec un hôte et ses microbes associés. Au sein de cet assemblage, les partenaires microbiens sont nombreux et diversifiés comme nous le verrons par la suite.

b. Holobionte & Microbiote

Les partenaires microbiens peuvent être procaryotes comme les virus, les *Archaea* et les bactéries, mais aussi eucaryotes comme les champignons.

Dans le monde marin, les virus sont les organismes les plus abondants, dépassant fortement en nombre les bactéries (Suttle, 2005, 2007) et peuvent infecter des formes de vie extrêmement variées (Rohwer et al., 2009), dont les macroalgues comme *Chondrus crispus*, colonisées par des totivirus (Rousvoal et al., 2016). Chez *Delisea pulchra* (Lachnit et al., 2016), l'étude de son virome a montré la présence de plusieurs types de virus (Virus à ARN simple et double brin), certains qualifiés de pathogènes potentiels pour cette algue connue pour être infectée aussi par des bactéries. Cette corrélation entre la présence de virus particuliers (simple brin) et des symptômes de blanchiment a aussi été trouvée chez l'algue *Ecklonia radiata* (Beattie et al., 2018). D'autres macroalgues brunes, comme *Ectocarpus* (Müller et al., 1990; Müller, 1996) ou *Saccharina* (McKeown et al., 2017; Schroeder and Mckeown, 2021) sont aussi infectées. Chez l'hydre, *Hydra* sp. (Grasis et al., 2014) la plupart des virus associés sont des bactériophages, ce qui implique leur rôle de régulation du microbiote au sein de l'holobionte, et met également en lumière le fait que les virus ne sont pas tous pathogènes. De la même manière pour le monde terrestre, les plantes sont infectées par des virus dits cryptiques, ne déclenchant pas de symptômes chez leur hôte (Boccardo et al., 1987). Il persistent au sein de la plante (Roossinck, 2010), et y restent associés de génération en génération par transmission verticale. L'abondance de ces virus persistants semble indiquer une participation au fonctionnement biologique de l'hôte (Roossinck, 2015).

Les plantes ne sont pas seulement colonisées par des virus, mais également par des champignons. Les associations mycorhiziennes sont formées lors de l'association d'un champignon mycélien avec le système racinaire de deux ou plusieurs plantes. Environ 90% des plantes terrestres participent à ces mycorhizes (Selosse et al., 2006), et les champignons associés sont d'une très grande diversité (Vandenkoornhuyse et al., 2002). Côté marin, des champignons pathogènes ou saprophytes (Kohlmeyer and Demoulin, 1981) infectent aussi les algues, de manière parasitique ou symbiotique (Potin et al., 2002; Jones, 2012). Ainsi, chez l'algue brune *Ascophyllum*, l'infection par le champignon endophyte *Mycophycias* protège l'algue de la dessiccation (Garbary and London, 1995; Garbary and Deckert, 2001). Par ailleurs, lors d'une interaction bénéfique, le champignon peut produire des composés bioactifs et ainsi protéger l'hôte contre des infections pathogènes (Vallet et al., 2018; Tourneroche et al., 2020).

Un des composants du microbiote les moins connus sont les *Archaea*, même s'il est évident qu'elles sont diverses et abondantes dans de nombreux microbiotes de plantes, animaux et humains (revue par Borrel et al., 2020) ou même dans le milieu marin (DeLong, 1992; Karner et al., 2001; DeLong and Karl, 2005). Pour le moment, leur impact sur l'hôte est inconnu (bénéfique, neutre ou délétère) aucune *Archaea* pathogène n'ayant été décrite (Borrel et al., 2020), même si Bang and Schmitz (2018) rapporte que les *Archaea* peuvent interagir et activer le système immunitaire humain. Chez les macroalgues, les *Archaea* pourraient participer à la fitness de l'algue en prenant part à la dégradation du DMSP (Taylor and Visscher, 1996), composé clivé chez les algues lors de mécanismes de défense (anti-brouteurs, cryoprotection, antioxydant ; Van Alstyne et al., 2001; Van Alstyne and Puglisi, 2007).

La composante bactérienne est la plus étudiée, aussi bien chez les humains (NIH Human Microbiome Portfolio Analysis Team, 2019), que chez les animaux (Ley et al., 2008), les plantes (Vandenkoornhuyse et al., 2015) et le milieu marin (Egan et al., 2013; Stal and Cretoiu, 2016; Dittami et al., 2021). Cet environnement fera l'objet d'une description plus détaillée dans la suite de cette introduction.

c. Les systèmes holobionte

De plus en plus de systèmes holobiontes font l'objet d'études, mais certains systèmes sont déjà bien connus, comme chez l'humain, les plantes ou les lichens.

De 2007 à 2016, l'*Human Microbiome Project* (HMP) a eu pour but de générer des données de séquençage pour caractériser le microbiote humain et essayer de comprendre comment il impacte la santé humaine. La première phase du projet (2007-2012) s'est concentrée sur les communautés microbiennes associées à 5 zones du corps humain (bouche, peau, narines, voies gastro-intestinales et urogénitales), pour évaluer si un microbiote caractéristique était associé à un état de santé particulier (The NIH HMP Working Group et al., 2009). Cette phase a aussi permis de créer une base de données de séquences des microbes détectés (bactéries, archées, bactériophages, virus et champignons). La deuxième phase (2013-2016), nommée iHMP (pour integrative HMP), s'est focalisée sur trois conditions cliniques pour étudier le microbiote associé à ces conditions, à partir des cohortes de la première phase. Elle porte sur la grossesse et les naissances prématurées (Stout et al., 2017; Fettweis et al., 2019), maladies inflammatoires chroniques de l'intestin (Morgan et al., 2012; Kostic et al., 2014; Walters et al., 2014; Lloyd-Price et al., 2019), et le diabète de type 2 (Hartstra et al., 2015; Zhou et al., 2019).

La production massive de données a mené à plus de 790 publications évaluées par les pairs depuis 2007.

Les plantes sont connues pour abriter un microbiote depuis longtemps, avec les travaux de Lorenz Hiltner sur la rhizosphère au début du 20ème siècle (Hiltner, 1904; Hartmann et al., 2008), expliquant que la nutrition de la plante est impactée de manière considérable par la composition bactérienne de la rhizosphère (Hartmann et al., 2008). Le système racinaire n'est pas le seul compartiment de la plante à posséder un microbiote. En effet, le microbiote de la plante se décompose en plusieurs parties (**Figure 3**) : la rhizosphère (racines), l'endosphère (tissus), et la phyllosphère (feuilles). Le sol est la principale source de diversité microbienne pour la plante (Bulgarelli et al., 2012; Gopal and Gupta, 2016). La sélection et le tri des microbes en vue de leur intégration au microbiote de la plante sont faits par l'hôte (Berg and Smalla, 2009; Hartmann et al., 2009; Hirsch and Mauchline, 2012), grâce à la production de composés (phénols, hormones, acides aminés, sucres, composés organiques) qui sont diffusés au niveau des racines (Badri et al., 2013; Lebeis et al., 2015).

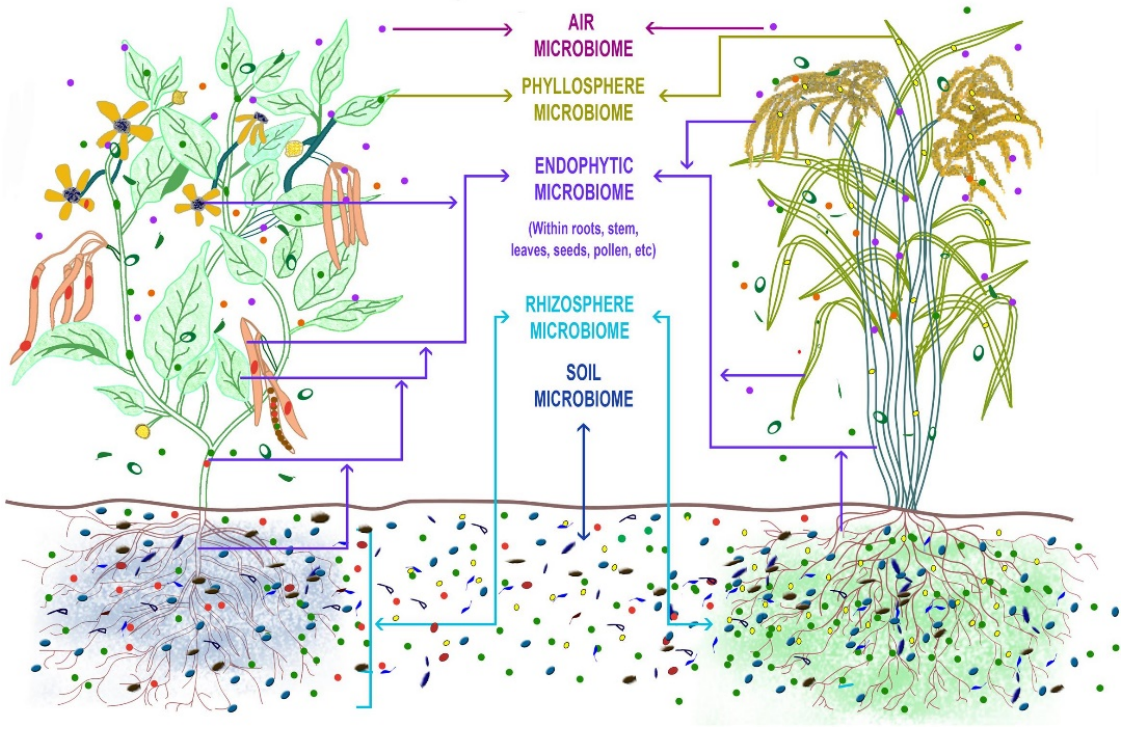

Figure 3 – Le microbiote de la plante d'après Gopal and Gupta (2016). La rhizosphère, l'endosphère et la phyllosphère sont les compartiments principaux du microbiote de la plante (Dicotylédones à gauche et Monocotylédone à droite).

Parmi ces taxa bactériens, sont retrouvées des bactéries phytobénéfiques associées aux racines des plantes, dites PGPR (*Plant Growth-Promoting Rhizobacteria*), qui favorisent la croissance et la santé du végétal par différents modes d'action (Richardson et al., 2009), tels que la fixation de l'azote atmosphérique, l'augmentation de la disponibilité des nutriments, la production d'hormones capables de favoriser la croissance de la plante (effet phytostimulateur) ou de métabolites antimicrobiens (effets phytoprotecteurs). Plusieurs études ont amené des connaissances sur la réponse des plantes hôtes à l'interaction avec les PGPR (Walker et al., 2011; Drogue et al., 2014). Il a été montré que les génotypes de plantes, à un niveau infraspécifique, diffèrent dans leur capacité à interagir avec une ou plusieurs PGPR inoculées et à bénéficier de leurs propriétés phytobénéfiques (Chamam et al., 2013, 2015; Vacheron et al., 2016). Les PGPR appartiennent à de nombreux genres bactériens (*Azospirillum*, *Achromobacter*, *Pseudomonas,* etc.) (Vacheron, 2015). Un genre d'importance majeure dans la rhizosphère est le genre *Pseudomonas* (*Gammaproteobacteria*), particulièrement le groupe des *Pseudomonas* fluorescents. Parmi le genre *Pseudomonas*, certains sont connus pour avoir un effet positif sur la croissance et la santé de nombreuses céréales (Couillerot et al., 2009). L'effet phytobénéfique des bactéries PGPR dépend de leur capacité à se développer dans la rhizosphère en utilisant des sources de carbone présentes dans le sol, afin de coloniser efficacement les racines de leur plante hôte, notamment en formant des biofilms (Couillerot et al., 2009). Le rôle phytoprotecteur des *Pseudomonas* fluorescents est médié par la production d'antimicrobiens tels que le DAPG (2,4-diacétylphloroglucinol), la phénazine, la pyrolnitrine, l'acide cyanhydrique ou des surfactants (Couillerot et al., 2009). Ils peuvent également avoir un rôle phytostimulateur en modulant les voies hormonales des plantes (Brazelton et al., 2008).

Dès 1867, Schwendener caractérise les lichens comme une association entre un champignon et une algue (Mitchell, 2007). Aujourd'hui, il est connu que les microorganismes qui lui sont associés sont diversifiés et que le lichen peut être caractérisé d'holobionte, avec un champignon dominant et son microbiote (Simon et al., 2019). Il a été montré que chez les lichens, le microbiote joue un rôle dans la nutrition et dans la résistance aux facteurs biotiques et abiotiques (Grimm et al., 2021). Par exemple, le lichen *Lobaria pulmonaria* est un holobionte à 5 composantes : un mycobionte (champignon *Ascomycete* hétérotrophe), un cyanobionte (cyanobactérie du groupe *Nostoc*), un photobionte (microalgue verte *Dictyochloropsis reticulata*), un microbiote et des champignons lichéniques. Le mycobionte est responsable de la morphologie, de la stabilité mécanique et de la reproduction, il protège

et supporte les photo- et cyanobiontes et gère la communauté microbienne. Le photobionte est en charge de la fixation du carbone photosynthétique. Le cyanobionte fixe le carbone et l'azote. Le rôle des champignons lichéniques est encore peu clair (Eymann et al., 2017).

Ainsi, les systèmes holobiontes sont abondants et quasiment omniprésents dans l'environnement, avec des composants microbiens pro- et eucaryotes, qui remplissent des rôles essentiels au bon fonctionnement de leurs hôtes. Pour le moment, les exemples présentés ici appartiennent au milieu terrestre, mais les milieux aquatiques ne sont pas dépourvus d'holobionte.

2. Holobionte marin

Les holobiontes présents dans les systèmes aquatiques diffèrent sur plusieurs points des systèmes terrestres. Tout d'abord, les propriétés physico-chimiques de l'eau permettent une connexion plus fine entre les organismes d'un point de vue chimique et fonctionnel (Mitra et al., 2014). Ensuite, les mécanismes de dispersion sont facilités par le continuum eau-surface favorisant les changements rapides au sein des communautés microbiennes (composition et/ou communication) des holobiontes (Kinlan and Gaines, 2003; Burgess et al., 2016). Enfin, la diversité phylogénétique à de grandes échelles taxonomiques est plus élevée dans les milieux aquatiques que dans les milieux terrestres, et une grande partie de la diversité aquatique reste à découvrir (Thompson et al., 2012; de Vargas et al., 2015; Middelboe and Brussaard, 2017; Gregory et al., 2019).

a. Rôle des biofilms marins

Le microbiote associé à la surface de l'hôte peut l'être sous forme d'un biofilm. Dans un environnement marin, dès qu'une surface entre en contact avec de l'eau de mer, de la matière organique dissoute adhère à cette surface sous la forme d'un film fin (<100nm), appelé fouling moléculaire (Little and Zsolnay, 1985). Cette surface reçoit alors de nouvelles propriétés physicochimiques qui attirent des colonisateurs primaires (Schneider and Marshall, 1994) dont de très nombreuses bactéries, puisqu'elles sont extrêmement abondantes dans l'eau de mer (entre 10^5 et10^6 cellules/ml ; Dang and Lovell, 2000). Ainsi, les biofilms, systèmes complexes et dynamiques, sont constitués d'organismes pro- et eucaryotes et colonisent toutes les surfaces immergées (Wahl et al., 2012).

La composition des biofilms marins diffère de celle des autres types de biofilms, et comprend plusieurs types bactériens, des *Archaea* et des organismes unicellulaires comme les

diatomées. La densité et la composition d'un biofilm peuvent varier à différentes échelles : inter- et intra-espèces, en fonction d'une partie de l'hôte, des habitats ou des saisons (Wahl et al., 2012)

Les biofilms sont impliqués dans divers processus, bénéfiques ou non pour l'hôte, en fonction des conditions environnementales et des espèces bactériennes présentes. Ils jouent un rôle dans l'attachement des larves (coraux et invertébrés) et des spores d'algues (Qian et al., 2007). Cet attachement est possible grâce à la chimie du biofilm, sa microtopographie et une grande quantité de métabolites et polymères microbiens. En retour, les organismes qui se sont attachés peuvent modifier la composition microbienne du biofilm et donc ses propriétés et sa dynamique. Ainsi, un biofilm mature n'est jamais figé car en étroite relation avec son hôte, ses composants et son habitat (Qian et al., 2007). Ce biofilm mature peut aussi affecter les flux d'informations, d'énergie et de matières à la surface de l'hôte, et ainsi moduler les interactions biotiques et abiotiques de l'hôte avec son environnement (Wahl et al., 2012). Il peut réduire l'accès à la lumière et aux nutriments, mais également limiter les interactions avec des prédateurs ou des pathogènes.

b. Métazoaires

Les coraux et éponges sont des organismes marins qui sont colonisés par de nombreux micro-organismes et dont ils dépendent pour de nombreuses fonctions. Grâce à leurs partenaires microbiens, les éponges et les coraux participent au bon fonctionnement des récifs, jouant un rôle dans les cycles de nutriments (Raina et al., 2009; Fiore et al., 2010; Cardini et al., 2015; Pita et al., 2018).

Chez les éponges, il a été montré que le microbiote aide aux échanges de nutriments, à la détoxification de l'hôte et à son homéostasie en général (Karimi et al., 2018). Par ailleurs, les éponges sont les hôtes d'une diversité microbienne exceptionnelle et ainsi, des contributeurs majeurs de la diversité microbienne des océans (Thomas et al., 2016).

Le microbiote peut également évoluer pour protéger son hôte contre des pathogènes. Chez le corail *Oculina patagonica,* une souche de *Vibrio* semble jouer un rôle de prévention de l'infection par *V. shiloi* (responsable de blanchiment), en produisant un composé inhibiteur de croissance (Mills et al., 2013). Les coraux sont également colonisés par des microalgues photosynthétiques de la famille des *Symbiodiniaceae*, dont les produits sont nécessaires à la survie sur le long terme de leur hôtes et à leur protection, en particulier contre le blanchiment (Berkelmans and van Oppen, 2006; Sampayo et al., 2008).

Un troisième exemple intéressant est les Octocorallia (Cnidaires), qui possèdent un microbiote très stable dans le temps et dans l'espace, ou en condition de stress. Cette stabilité est due à une régulation fine de leur microbiote par la production de molécules antimicrobiennes et de quorum sensing (van de Water et al., 2018).

c. Microalgues

La micro-algue *Emiliania huxleyi* (Haptophyta) est un modèle d'étude du phytoplancton, qui produit des intermédiaires clefs dans les cycles biogéochimiques du carbone et du soufre. Plusieurs des bactéries qui lui sont associées appartiennent aux *Roseobacter,* qui aident à la croissance algale en synthétisant et sécrétant des antibiotiques et des facteurs de croissance (auxines) (Seyedsayamdost et al., 2011). Parmi ces bactéries, *Phaeobacter gallaeciensis,* devient un pathogène opportuniste quand elle détecte que l'algue vieillit, en produisant des roseobacticides, algicides puissants et sélectifs (Seyedsayamdost et al., 2011). Une autre souche, *P. inhibens*, vit en étroite relation avec *E. huxleyi*, et favorise sa croissance par apport d'auxine, mais finit par tuer son hôte. La mort de l'algue est due à l'activation de voies de biosynthèse spécifiques à la réponse au stress oxydatif et à la mort cellulaire programmée. Ainsi, les bactéries peuvent influencer la physiologie et le métabolisme de l'hôte algal (Segev et al., 2016).

Les diatomées, par leur agrégation, participent à de nombreux processus importants dans les systèmes marins, en particulier le dépôt de particules de carbone organique sous forme de neige marine (Passow et al., 2001). Les produits d'exsudation du phytoplancton forment des particules d'exopolymères transparents (*transparent exopolymer particles* (TEP) en anglais), qui jouent le rôle de colle pour les particules de carbone. Les bactéries hétérotrophiques qui interagissent avec le phytoplancton influencent positivement la formation de ces TEP et le dépôt de la neige marine (Gärdes et al., 2011) améliorent ainsi la pompe biologique (cycle marin du carbone).

En étudiant le microbiote associé à deux microalgues marines, une diatomée *Phaeodactylum tricornutum* et un eustigmatophyte *Microchloropsis salina*, Kimbrel et al. (2019) ont également montré que l'hôte exerce une influence sur la composition de son microbiote associé lors d'expérimentations de mésocosme, et que les conditions de cultures et le microbiote initial jouent également un rôle dans la sélection des communautés associées.

Ainsi, dans le milieu marin, les biofilms et par extension les holobiontes auxquels ils appartiennent, participent à des processus importants de l'écosystème. Ils colonisent des

hôtes divers allant des coraux aux algues, en passant par les éponges et d'autres formes de vie. L'holobionte macroalgue étant un sujet à part entière, il sera développé dans la prochaine partie de cette introduction.

3. Holobionte macroalgue

a. Composition du microbiote chez les macroalgues

Les macroalgues sont caractérisées par une importante diversité de microorganismes à leur surface (Hollants et al., 2013) avec la présence de bactéries, protistes, champignons et microalgues (diatomées et des dinoflagellés benthiques). Parmi ces microorganismes, les bactéries constituent un des groupes les plus abondants (**Figure 4** ; Egan et al., 2013).

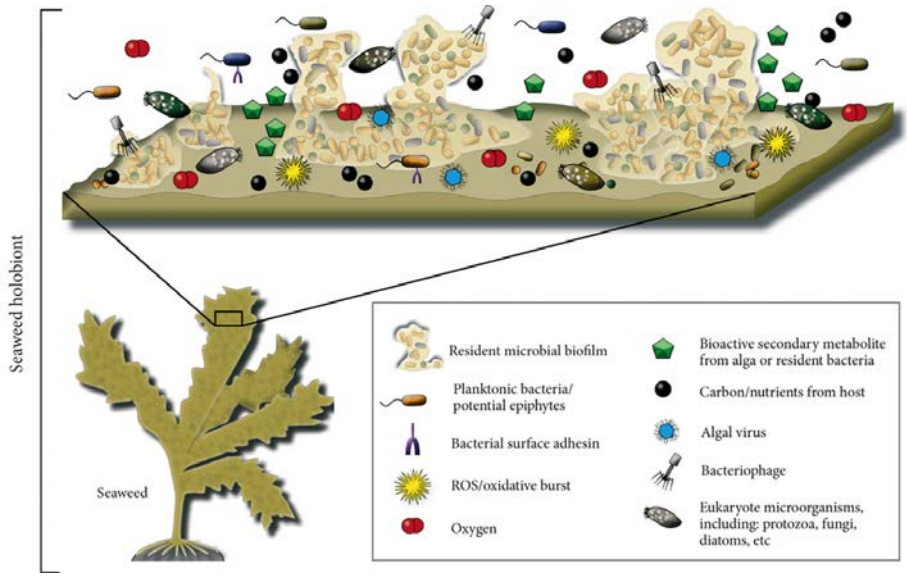

Figure 4 – L'holobionte et les facteurs influençant la colonisation bactérienne sur l'hôte algue (Egan et al., 2013).

La diversité bactérienne de l'eau de mer est grande et variée (Sunagawa et al., 2015; Overmann and Lepleux, 2016) et dominée par les *Alpha-*, *Gammaproteobacteria* et *Flavobacteria* (~40%, 25% et 15% respectivement ; Zinger et al., 2011). Les communautés bactériennes associées aux macroalgues sont différentes en composition et en proportions (Longford et al., 2007; Lachnit et al., 2009). De manière générale, ces bactéries appartiennent aux phylums *Proteobacteria, Actinobacteria, Bacteroidetes*, *Cyanobacteria, Firmicutes, Planctomycetes, Verrucomicrobia, Chloroflexi, Deinococcus-Thermus, Fusobacteria, Tenericutes*, et à la division OP11 (Hollants et al., 2013). Les *Gammaproteobacteria* sont les

bactéries le plus souvent associées aux macroalgues, tout comme les *Alphaproteobacteria* et les *Bacteroidetes*, ainsi que les *Firmicutes* et *Actinobacteria*. Les proportions d'*Alphaproteobacteria* et de *Bacteroidetes* sont plus importantes chez les algues vertes. Les algues rouges et brunes contiennent plus de *Firmicutes*, *Actinobacteria*, et de *Planctomycetes* (Hollants et al., 2013).

Nous allons voir par la suite que chez les macroalgues, le microbiote se distribue différemment en fonction de l'hôte, que celui-ci peut le modifier en fonction de ses besoins, et que la communauté bactérienne peut impacter le développement de l'hôte algal et son adaptation à un environnement.

b. Répartition et sélection du microbiote par l'hôte algal

Répartition en fonction de la zone de la lame et de la morphologie

La composition du microbiote algal peut varier en fonction de sa localisation sur l'algue. Chez l'algue rouge *Porphyra umbilicalis* par exemple, Quigley et al. (2018) ont mis en évidence une différence de composition du microbiote entre le crampon et la marge de la lame, avec une augmentation de l'abondance de *Planctomycetes* et d'*Alphaproteobacteria* au niveau du crampon.

Le même patron de répartition se retrouve chez les laminaires. Au début des années 90, une étude basée sur des isolements et portant sur la densité et la morphologie des bactéries épiphytes de *Laminaria digitata* rapporte un changement de la communauté bactérienne en fonction de l'âge des tissus (Corre and Prieur, 1990). Les tissus jeunes du méristème, en phase active de croissance, sont colonisés par des bactéries de type cocciforme, alors que les tissus plus anciens sont de plus en plus colonisés par des bactéries en forme de bacille. Plus récemment, Ihua et al. (2020) ont analysé la composition du microbiote de quatre parties de cette algue (crampon, stipe, méristème et lame) par métabarcoding 16S. Bien que le méristème et le stipe possèdent un microbiote très proche, le microbiote est spécifique à chaque zone de l'algue et les résultats supportent l'hypothèse que les communautés bactériennes sont spécifiques de niches morphologiques.

Chez *Laminaria setchellii,* l'étude du microbiote suivant un gradient d'âge des tissus a montré que le microbiote est différent en fonction de la zone de l'algue et que les surfaces avec des tissus plus âgés ont une plus grande diversité bactérienne que les tissus jeunes (Lemay et al., 2021) .

Sélection par composés chimiques

La sélection des communautés bactériennes au niveau des différents tissus peut se faire par l'hôte au moyen de composés chimiques.

Chez l'algue brune *Taonia atomaria*, l'étude du métabolome de surface et du microbiote montre que les communautés bactériennes des différents tissus ne sont pas les mêmes, que la diversité est plus grande chez les apex et que le métabolome de surface est aussi spécifique de la zone étudiée. En effet, des sesquiterpènes, des phosphatidylcholines et des lipides (DGTA) sont retrouvés en quantité importante au niveau des apex, alors que la zone méristématique est enrichie en caroténoïdes et en DMSP. Cette production de composés est probablement due au fonctionnement physiologique de l'algue, et pourrait expliquer la spécificité et les variations du microbiote de surface tout au long du thalle (Paix et al., 2020). Le même type d'analyse a été faite sur l'algue brune *Fucus vesiculosus* avec le même type de résultats (Parrot et al., 2019).

L'algue rouge *Delisea pulchra* interagit et contrôle son microbiote au moyen de composés de défenses, des furanones halogénées, qui ciblent les mêmes récepteurs que les acyl homoserine lactone (AHL), impliquées dans le quorum sensing. Ce mode de communication bactérien régule de nombreux processus, et son inhibition limite et module la composition du microbiote (Harder et al., 2012).

c. Impact sur la morphologie et la croissance

Le microbiote peut avoir un impact sur la croissance et la morphologie de son hôte. Depuis les années 60, plusieurs études ont montré que certaines bactéries favorisent la croissance des *Ulvales* tandis que d'autres induisent une morphogenèse (Wichard, 2015). Ces algues perdent leur morphologie typique quand elles sont cultivées en conditions axéniques ou sans le microbiote approprié, formant des morphotypes de types cals ou aberrants (Provasoli, 1958). La thallusin, molécule isolée d'une bactérie épiphyte de *Monostroma oxyspermum,* induit une croissance normale et restaure le morphotype foliacé de l'algue (Matsuo et al., 2005). De la même manière, il a été montré que la croissance et la morphogenèse en conditions axéniques d'*Ulva mutabilis* peuvent être sauvées par l'ajout de deux bactéries spécifiques appartenant aux *Rhodobacteraceae* et *Flavobacteriaceae,* formant ainsi une association tripartite au travers de communications chimiques (Spoerner et al., 2012), les bactéries apportant de la thallusin (Alsufyani et al., 2020) et des composés semblables aux phytohormones cytokinines.

Des effets similaires ont été observés chez l'algue brune *Ectocarpus,* où le microbiote est nécessaire au maintien de la morphologie filamenteuse de cette algue, morphologie perdue en condition asymbiotiques (Tapia et al., 2016; Burgunter-Delamare et al., 2020). Le microbiote apporte aussi des composés nécessaires à la bonne croissance de l'algue, comme de l'iode (Pedersén, 1969b), des cytokinines (Pedersén, 1968, 1973) ou la vitamine B12 (Pedersén, 1969a). L'apport de composés par les bactéries rentre aussi dans le cadre des interactions métaboliques bénéfiques. En effet, il a été montré qu'à la manière d'un puzzle, le partenaire bactérien va pouvoir compléter les fonctions métaboliques manquantes chez l'algue, favorisant ainsi la croissance de l'hôte algal grâce à la production de métabolites clefs chez *Ectocarpus* (Burgunter-Delamare et al., 2020; cf **Annexe IV**).

d. Dysbiose

Un phénomène de dysbiose peut se déclencher au sein de l'holobionte en cas de perturbation du microbiote et ainsi impacter négativement l'hôte au niveau de sa croissance ou de sa condition physiologique. Par exemple, une étude sur l'impact de l'urbanisation sur *Ecklonia*, une espèce qui participe à la formation des forêts de laminaires le long des côtes australiennes, a montré que le microbiote des algues des zones urbaines et celui des zones naturelles sont différents, parce que ces habitats n'ont pas les mêmes apports en lumière ou que la faune y est moins diversifiée (Marzinelli et al., 2018). Les bactéries isolées des algues de zones artificielles appartiennent à des taxas responsables de maladies chez les macroalgues (Vairappan et al., 2001; Marzinelli et al., 2015; Kumar et al., 2016), comme le blanchiment chez *Ecklonia*. Les zones de mariculture peuvent aussi être un lieu de diffusion de pathogènes. Dimitrieva et Dimitriev (1997) rapportent qu'en condition d'aquaculture, le rendement de l'algue *Saccharina japonica* diminue fortement à cause d'un fouling excessif et certains poissons ont disparu de cette zone. Le microbiote de ces algues malades est dominé par le genre *Alteromonas* et les *Actinomycetes* en sont absents. Les *Alteromonadales* sont connues pour produire des enzymes hydrolytiques qui suppriment le microbiote naturel de l'algue. Le genre *Alteromonas* est aussi responsable de symptômes chez l'algue rouge *Delisea* (Kumar et al., 2016), avec d'autres genres bactériens, pourtant retrouvés en faible abondance chez les algues saines. Les communautés bactériennes des algues infectées sont moins diversifiées que celles des algues saines. Cette étude a aussi montré que plusieurs pathogènes opportunistes peuvent déclencher les mêmes symptômes chez *D. pulcra*.

Le phénomène de dysbiose peut être compensé par d'autres souches bactériennes au sein du microbiote de l'algue. En effet, le groupe *Phaeobacter* contient des souches qui sont pathogènes pour les coraux mais certaines sont bénéfiques pour les algues. Ainsi, *Phaeobacter* sp. BS52, isolée de *D. pulchra* saines, a une action de prévention contre les pathogènes responsables du blanchiment (Li et al., 2021a), en limitant la dysbiose. Cet effet protecteur de certaines souches du microbiote est également présent chez *Agarophyton* (Saha and Weinberger, 2019) et une étude récente a montré qu'une souche probiotique peut avoir un effet positif chez son hôte habituel mais également chez une autre algue, comme *Phaeobacter* sp. BS52 sur *Agarophyton* (Li et al., 2021b).

En réponse à cette dysbiose, l'hôte peut aussi mettre en place des stratégies de défenses/restauration. Ainsi, lorsque le microbiote de surface de *D. pulcra* est perturbé, la communauté microbienne va évoluer de manière successive, jusqu'à ressembler à celle de départ, dans une sorte de restauration. Si la restauration est perturbée, un phénomène de blanchiment se développe (Longford et al., 2019). La colonisation primaire par certaines souches protège l'hôte d'une colonisation secondaire par des pathogènes. Les défenses chimiques de l'hôte le protègent également des maladies, de sorte que lorsqu'elles sont inhibées, le microbiote prend le relais et les communications en son sein sont plus importantes dans ces conditions. Ainsi, la capacité d'une algue à entretenir son microbiote protecteur de manière chimique a été démontrée pour la première fois chez *Agarophyton vermiculophyllum* (Saha and Weinberger, 2019). La production de métabolites de surface favorise le recrutement de bactéries bénéfiques et réduit celui de souches pathogènes. Ces métabolites de surfaces peuvent être de plusieurs sortes, comme les furanones halogénées de l'algue *Delisea*, impliquées dans le quorum sensing (Harder et al., 2012).

e. Adaptation à un environnement changeant

Le microbiote peut être une aide précieuse pour une adaptation de l'hôte à un environnement changeant, des exemples de cette adaptation sont retrouvés dans les trois grandes lignées de macroalgues.

Ulva rigida voit la composition de son microbiote et de l'eau environnante changer en fonction de son environnement de croissance (aquaculture ou milieu sauvage). Les systèmes d'aquaculture favorisent la présence de bactéries connues comme impactant de manière positive la morphologie d'*Ulva* (Califano et al., 2020).

Agarophyton vermiculophyllum est une algue rouge invasive et son microbiote semble être une des clefs de cette capacité d'acclimatation. En comparant le microbiote d'algues invasives ou non, des différences au niveau de la composition et des groupes fonctionnels apparaissent, suggérant un changement des bactéries de surface au cours du processus d'invasion (Bonthond et al., 2020). *A. vermiculophyllum* possède un microbiote qui varie fortement au niveau local mais possède un core bactérien stable à une plus grande échelle géographique, lui conférant le rôle d'hôte généraliste (Rodríguez-Echeverría, 2010), ce qui pourrait expliquer sa forte capacité invasive. En parallèle, il a été montré que les communautés microbiennes de ces *Agarophyton* invasives s'ajustent plus facilement à l'environnement qui les entoure par rapport aux *Agarophyton* endémiques (Bonthond et al., 2021).

Le microbiote peut également changer en fonction de la saison, comme chez *L. hyperborea* (Bengtsson et al., 2010) où les changements dans la composition de l'algue et de la température de l'eau entraînent un renouvellement au sein du biofilm. La salinité d'un milieu peut aussi influencer une acclimatation de l'hôte algal. Ainsi, chez *Ectocarpus* sp., l'adaptation à un changement de salinité passe par une modification de son microbiote (Dittami et al., 2016). Sans lui, l'algue ne peut pas survivre dans l'eau douce, mais l'ajout de sa microflore restaure sa capacité d'acclimatation. Le changement de milieu impacte également la communauté microbienne, qui subit des changements de composition. Ce changement peut entraîner une baisse de la diversité bactérienne, comme chez *F. vesiculosus* (Stratil et al., 2014).

Chez les macroalgues, la composition du microbiote varie en fonction de la lignée d'appartenance de l'hôte algal, avec une majorité de *Gamma-*, *Alphaproteobacteria* et *Bacteroidetes*. Ce microbiote va jouer un rôle dans la condition physiologique de l'algue, dans son adaptation à un environnement, ou dans sa morphologie et sa croissance. Un déséquilibre au sein de ce microbiote (dysbiose) peut entrainer des symptômes, parfois irréversibles, mais l'hôte et le microbiote peuvent mettre en place des stratégies de défense pour répondre à cette attaque. Il est fondamental de connaitre et de comprendre l'impact de ce microbiote sur son hôte. En effet, les macroalgues et en particulier les macroalgues brunes, sont des éléments essentiels des écosystèmes marins, avec des intérêts écologique et économique non négligeables.

II. De l'importance des macroalgues et des kelps en particulier

1. Importance écologique et économique des macroalgues brunes, populations naturelles

a. Importance écologique

Les laminaires, ou « kelps » en anglais, appartiennent à l'ordre des *Laminariales sensu stricto* (Bartsch et al., 2008; Bolton, 2010). Ces algues peuplent les substrats rocheux des régions côtières (Bold and Wynne, 1985), classiquement de la zone infralittorale jusqu'à une centaine de mètres, voire plus profondément (>200m), dans des zones de refuge et d'upwelling des régions tropicales (Graham et al., 2007).

La plupart des kelps appartiennent à des genres mono-espèces (*Nereocystis, Macrocystis*), en particulier ceux retrouvés dans le Pacifique Nord, tandis que l'Arctique et l'Atlantique Nord sont peuplés d'algues d'espèces variées (*Alaria*, *Laminaria*, *Saccharina*). Dans l'hémisphère sud, la famille *Lessoniaceae (Ecklonia, Lessonia, Eisenia)* est majoritairement présente, et contient les *Lessonia*, seul genre introuvable dans le Nord (**Figure 5** ; Bolton, 2010).

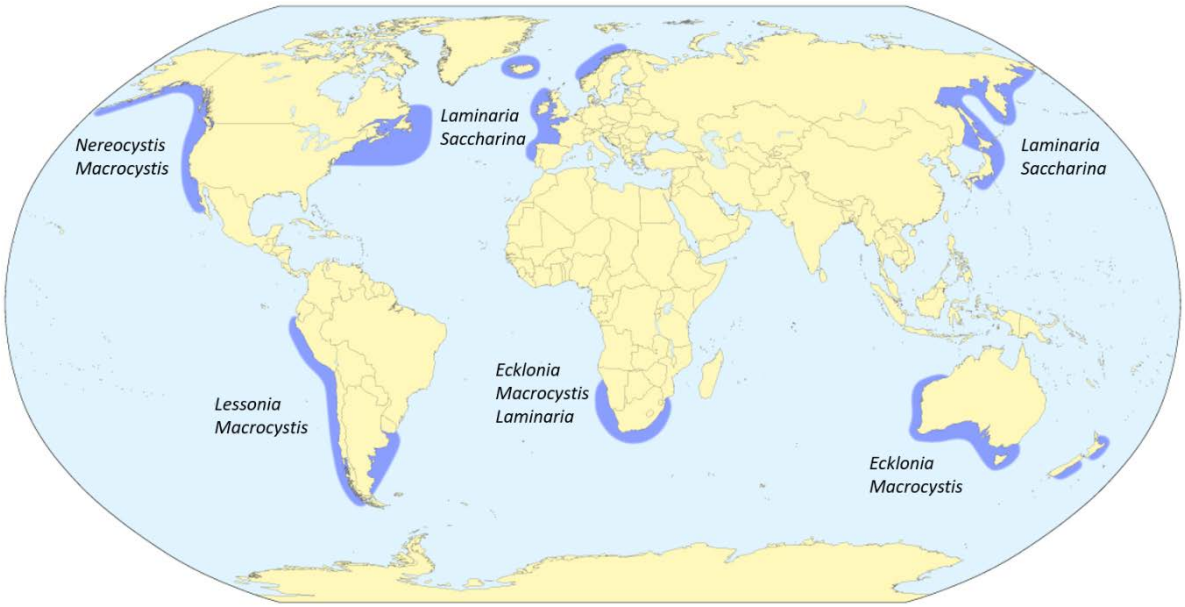

Figure 5 – Répartition mondiale des forêts de laminaires, d'après Steneck et al. (2002) et Bolton (2010)

Les kelps forment des systèmes complexes appelés forêts de laminaires, qui sont considérés comme les écosystèmes les plus divers et productifs au monde (Mann, 1973; Dayton, 1985). Ces algues dites ingénieures déterminent la structure physique de cet habitat (Schiel and Foster, 2006), et sont des producteurs primaires majeurs qui participent activement à la

séquestration du carbone (Chung et al., 2013). Comme les laminaires forment une canopée pérenne, elles peuvent influencer les conditions hydrodynamiques (Jackson, 1983) et lumineuses, ce qui permet de former un habitat stable (Schiel and Lilley, 2007), servant de refuge pour de nombreuses formes de vie macro- et microscopiques (Wilson et al., 1990; Bulleri et al., 2002; Steneck et al., 2002; Bartsch et al., 2008; Christie et al., 2009).

b. Importance économique

Les kelps sont utilisés dans de nombreux domaines allant de l'alimentation à l'agriculture, en passant par la cosmétique, la santé et des procédés industriels.

Les kelps sont couramment utilisés en alimentation humaine et animale. Les aliments à base d'algues font partie de la cuisine traditionnelle en Asie depuis plusieurs siècles (Tseng, 1987; McHugh, 2003) et certaines espèces de *Saccharina* ont été introduites dans certaines régions uniquement pour la consommation humaine (Suzuki et al., 2007; Li et al., 2008). Comme les kelps contiennent des quantités importantes d'iode (Hou et al., 1997), de minéraux et de vitamines (Fleurence, 1999; Ruperez, 2002; McHugh, 2003; Schmid et al., 2003), elles permettent d'améliorer les apports nutritionnels chez les mammifères, de manière directe (consommation d'algue) ou indirecte chez l'humain, via la consommation de poissons nourris avec des poudres d'algues (McHugh, 2003; Schmid et al., 2003). Ces poudres sont également utilisées dans les fourrages pour le bétail (McHugh, 2003). Les kelps frais sont utilisés en aquaculture pour nourrir les ormeaux (McHugh, 2003; Roussel et al., 2019).

Les polysaccharides issus des macroalgues (alginates, agars et carraghénanes) sont utilisés dans en industrie pour leur rôle de gélifiant, d'épaississant, d'émulsifiant et leur capacité de rétention des liquides (Indergaard and Ostgaard, 1991). Seuls les alginates sont présents chez les laminaires. Ils entrent dans la composition de nombreux desserts, sauces, crèmes de beauté, peintures (Peteiro, 2018) et même dans le brassage de certaines bières (Jackson et al., 1980), souvent sous l'appellation « E400 ».

En dehors de ces utilisations, les macroalgues sont aussi des sources potentielles de nouvelles molécules d'intérêt médical comme des antiviraux, des antibiotiques, des anti-inflammatoires ou des anti-tumoraux ou anti-cancers (revues par Mayer and Hamann, 2002, 2005; Smit, 2004; Stein and Borden, 1984).

L'utilisation des laminaires comme engrais en agriculture est une méthode traditionnelle utilisée en France et en Europe depuis très longtemps (Kain and Dawes, 1987; Blunden, 1991;

McHugh, 2003) et d'autres macroalgues brunes comme *Fucus* et *Ascophyllum* sont aussi utilisées en horticulture (McHugh, 2003). Les algues produisent également de nombreuses molécules qui peuvent avoir un intérêt en agrochimie (Smit, 2004), comme des pesticides naturels ou des composés antifoulings (Kjelleberg and Steinberg, 1999; Dworjanyn et al., 2006; Longford et al., 2019).

Les laminaires sont importantes d'un point de vue écologique, en fournissant un habitat adapté à de nombreuses formes de vie marines et en protégeant les côtes de l'érosion et des inondations lors des tempêtes (Duarte et al., 2013; Morris et al., 2019). Seulement, plusieurs populations naturelles de kelps sont en déclin (Bekkby and Moy, 2011; Araújo et al., 2016; Layton et al., 2019), et le changement climatique ou l'eutrophisation pourraient en être la cause. L'étude et la compréhension de la biologie et du fonctionnement de ces algues est donc un point clef pour la sauvegarde des populations naturelles. Ainsi, plusieurs algues brunes font l'objet d'études, deux en particulier seront étudiées dans cette thèse, *Ectocarpus* sp. et *Saccharina latissima*.

2. Systèmes holobionte algue brune : *Ectocarpus* sp. et *Saccharina latissima*

Au sein des algues brunes (*Phaeophyceae*, Stramenopila ; **Figure 6A**), *Ectocarpus* sp. est considéré comme modèle d'étude génétique et génomique (Peters et al., 2004; Coelho et al., 2012; Theodorou and Charrier, 2021). Sa petite taille, sa grande fertilité, la maitrise complète de son cycle de vie en laboratoire (en 3 mois ; Müller et al., 1998) et la facilité avec laquelle les croisements génétiques peuvent être effectués (Peters et al., 2004, 2008) ont été des arguments importants pour ce choix. Les nombreux outils qui ont été développés sont maintenant à l'étude pour une utilisation sur d'autres algues brunes, dont *Saccharina latissima*.

a. Ectocarpus sp.

Ectocarpus siliculosus est une algue brune issue de la famille des *Ectocarpales* (**Figure 6B**). Son génome a été entièrement séquencé (Cock et al., 2010), et son réseau métabolique reconstruit (Prigent et al., 2014). *Ectocarpus* n'est pas seulement un modèle d'étude génétique, mais aussi un modèle d'étude de l'impact du microbiote sur l'algue. Son adaptation à un changement de salinité (cf. section **I-3-c**), sa morphologie et son fonctionnement métabolique (cf. section **I-3-b**) sont possibles grâce à son microbiote. La composition en est

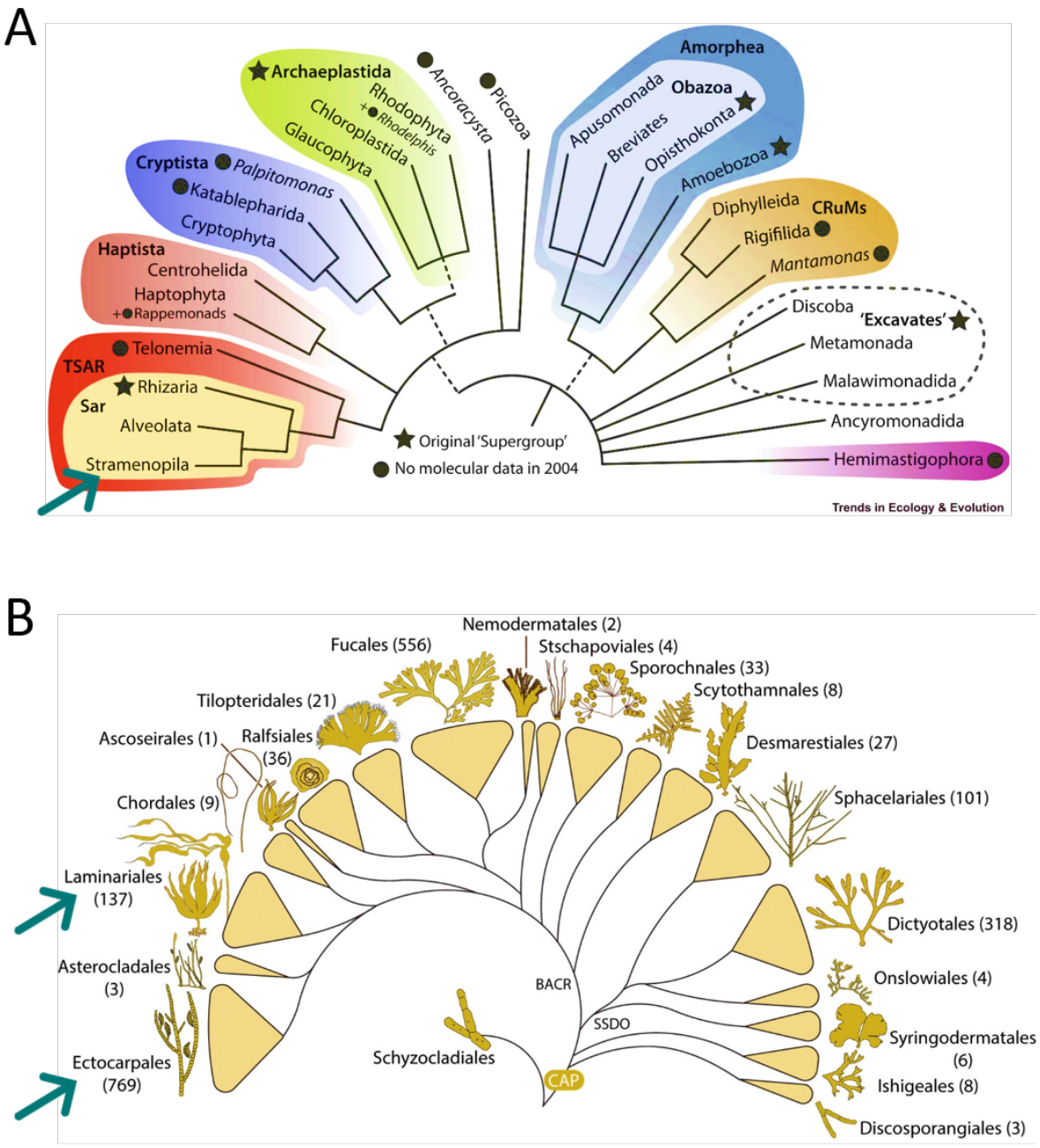

Figure 6 – Position phylogénétique des *Phaeophyceae*, *Ectocarpales* et *Laminariales*. (A) Position des algues brunes au sein de l'arbre des eucaryotes d'après Burki et al. (2020). Les algues brunes (*Phaeophyceae*) appartiennent au clade SAR, à la division des Straménopiles (Hétérocontes), et sont phylogénétiquement distantes des plantes terrestres et des algues vertes et rouges. (B) Position des *Ectocarpales* et des *Laminariales* au sein des algues brunes d'après Bringloe et al. (2020).

connue (KleinJan et al., 2017) et a permis, grâce à la réalisation de cocultures algues-bactéries, de valider *in vivo* des outils bioinformatiques de prédiction d'interactions métaboliques (Dittami et al., 2014; Prigent et al., 2017; Burgunter-Delamare et al., 2020).

b. Saccharina latissima

Saccharina latissima (L.) est une algue brune appartenant aux *Laminariales* (**Figure 6B**). Cette grande algue brune possède une lame entière, gaufrée en son centre et ondulée sur les bords, un stipe rond, lisse et fin, et est attachée au substrat à l'aide de crampons fins et peu nombreux (**Figure 7**). Les algues les plus âgées possèdent des lames pouvant mesurer jusqu'à 5 mètres de long. Cette algue est pérenne et a une durée de vie d'environ 2 à 4 ans (Handå et al., 2013). La croissance des nouveaux tissus se fait dans la zone méristématique de la lame, juste au-dessus du stipe, repoussant les tissus plus âgés vers l'apex où l'érosion et la sénescence se font plus fortes. En général, la croissance est amorcée en hiver, culmine au printemps et diminue pendant l'été et l'automne (Parke, 1948; Kain, 1979; Lüning, 1979; Sjøtun, 1993; Bartsch et al., 2008). A l'inverse, le phénomène saisonnier d'érosion est à son apogée entre juillet et décembre (Parke, 1948).

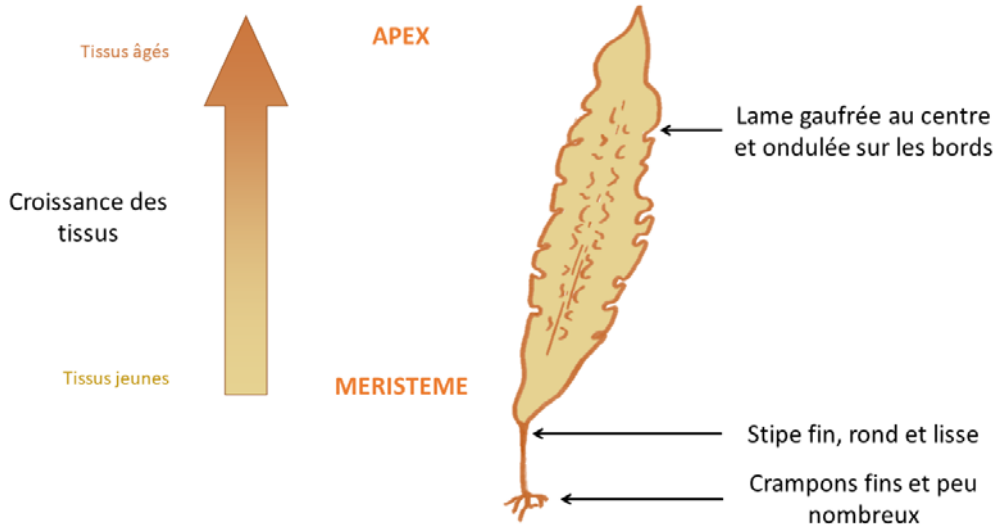

Figure 7 – Morphologie et croissance de *Saccharina latissima*

Les laminaires, dont *S. latissima*, sont caractérisés par un cycle de vie haplo-diplophasique hétéromorphe, avec des gamétophytes haploïdes microscopiques et des sporophytes diploïdes qui peuvent atteindre plusieurs mètres de long (**Figure 8**). Les sporanges se développent au niveau des sores sur le sporophyte adulte (Bold and Wynne, 1985). Au sein de ces sporanges, des zoospores haploïdes (4-8 µm) sont formées, ensuite libérées sous l'influence de l'environnement (Amsler and Neushul, 1989) et dispersées par les courants (Dayton, 1985). La germination des spores donne naissance à une génération gamétophytique

microscopique, les gamétophytes mâles donnant des anthérozoïdes mobiles à partir des anthéridies et les gamétophytes femelles des oosphères à partir des oogonies. Après fécondation, le zygote diploïde évolue en un sporophyte macroscopique, tandis que les oosphères non fertilisées peuvent évoluer en parthenosporophytes haploïdes (Dayton, 1985). Le cycle de vie n'est achevé que partiellement en laboratoire, à cause de la grande taille des sporophytes adultes. Des cultures peuvent être faites à partir de stocks de gamétophytes ou de spores fraîchement relargués qui grandiront en jeunes sporophytes, pour des expérimentations futures.

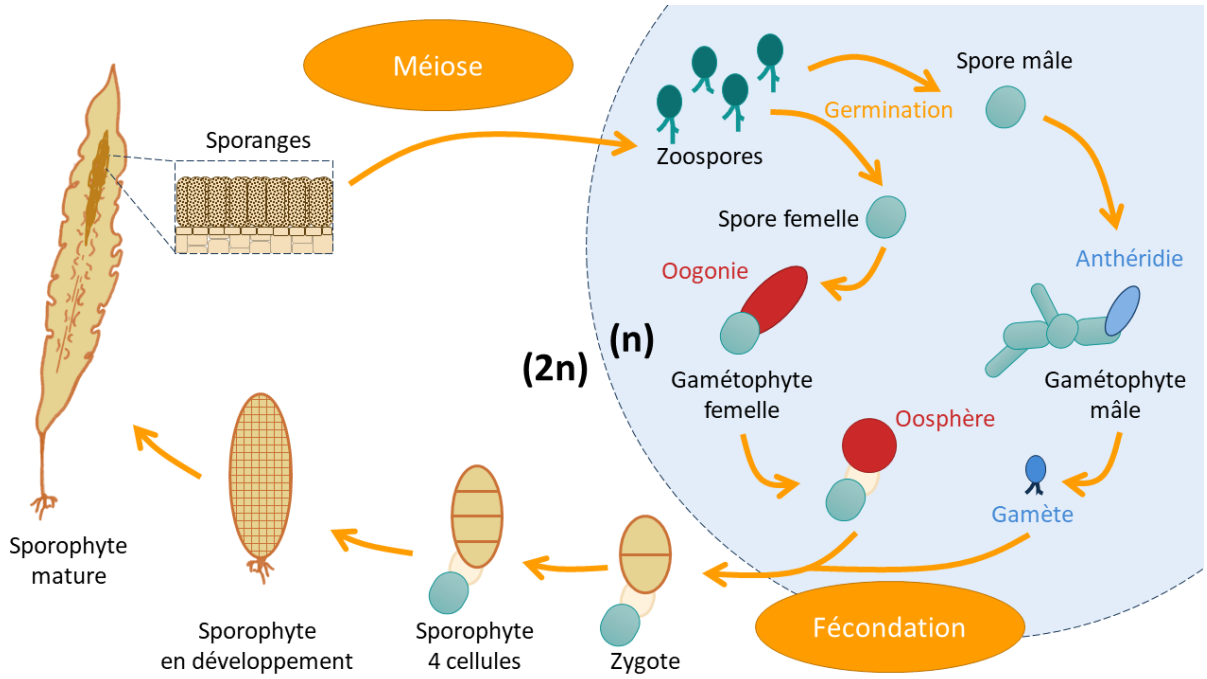

Figure 8 – Cycle de vie de *Saccharina latissima*, adapté de Visch et al., (2019) et Theodorou and Charrier (2021)

Les données sur le microbiote de *Saccharina latissima* sont peu nombreuses. L'étude de Staufenberger et al. (2008) analyse la composition bactérienne de *S. latissima* issues de deux sites distincts (Mer Baltique et Mer du Nord) à des périodes différentes (janvier et avril 2006), à l'aide de la technique d'électrophorèse sur gel en gradient dénaturant (DGGE en anglais), en se focalisant sur les crampons, le stipe et les zones méristématiques et apicales de l'algue. Les échantillons de la zone apicale ont aussi été utilisés pour les librairies de gènes 16S rRNA. Les résultats DGGE montrent que chaque zone de l'algue possède une communauté bactérienne spécifique, dont la spécificité diminue avec l'âge des tissus. Une différence de composition due à la saisonnalité et la géographie est aussi observée. L'affiliation taxonomique des

bactéries associées aux zones apicales donne les *Alphaproteobacteria* et les *Gammaproteobacteria* comme phylums majoritaires, suivi des *Bacteroidetes*.

L'étude plus récente de Tourneroche et al. (2020) utilise le métabarcoding 16S et ITS2 et de l'hybridation *in situ* en fluorescence (FISH) pour étudier le microbiote bactérien et fongique de jeunes tissus de *S. latissima*, échantillonnées en juillet 2017 sur la côte ouest de l'Ecosse. Les communautés bactériennes sont dominées par les *Proteobacteria*, *Actinobacteria*, et les *Bacteroidetes*, avec en particulier des *Hyphomonadaceae* et des *Cyclobacteriaceae*. Les communautés fongiques sont principalement composées d'*Ascomycota* et de *Basidiomycota*.

L'étude du microbiote d'*Ectocarpus* a mis au jour l'importance des partenaires bactériens pour cet hôte, et également permis la création de nombreux outils bio-informatiques. La transposition de ces outils sur l'hôte *Saccharina latissima* est à l'étude. A ce jour, les données disponibles sur son microbiote sont des données descriptives qui se basent sur des analyses différentes (DGGE vs Metabarcoding 16S), à partir d'échantillons plus ou moins différents de la lame mais il n'y a pas d'études (à notre connaissance) sur l'impact de ce microbiote sur l'hôte.

III. Le projet de thèse : problématique et objectifs

Saccharina latissima est une des espèces de macroalgues brunes dites ingénieures qui participent à la formation des forêts de laminaires. Plusieurs populations naturelles sont exploitées autour du monde et *S. latissima* fait également l'objet de développements croissants en aquaculture. Malgré l'importance économique et écologique de *S. latissima*, il existe actuellement peu de données sur la composition de son microbiote associé, sur le rôle de celui-ci dans la physiologie de l'algue et sur l'holobionte *Saccharina latissima* dans son ensemble.

Le but de ma thèse est de caractériser le microbiote bactérien et d'étudier les interactions hôte-microbiote au sein de l'holobionte *S. latissima*, pour comprendre dans quelles mesures la composition du microbiote influence la croissance de l'algue.

Ainsi, je me suis attachée à répondre aux questions suivantes :

- Quelle est la composition du microbiote des populations naturelles de *Saccharina* ?
- Est-ce qu'il existe un core bactérien ?

- Comment le microbiote évolue en fonction de la condition physiologique de l'hôte, de son origine géographique ou de la saison ?
- Dans quelle mesure le microbiote est-il cultivable ?
- Quel est l'impact du microbiote sur la croissance ?
- Quel est l'impact d'une inoculation de souches bactériennes sur la communauté bactérienne de l'hôte ?
- En cas de perturbation du microbiote, quel est l'effet sur l'algue ? Par quels moyens de communications se transmet cette perturbation ?
- Est-ce qu'il existe une spécificité hôte-microbiote chez les algues brunes ?

De ces questions, trois axes ont émergé. Le 1er axe vise à spécifier le microbiote des populations naturelles par des approches de metabarcoding 16S et d'isolements bactériens. Le 2ème axe comprend la sélection de souches d'intérêt, puis leur inoculation en cocultures algues-bactéries pour déterminer leur impact sur l'hôte. Et le 3ème axe consiste à analyser les résultats obtenus suite aux cocultures en tenant compte du phénomène de quorum sensing.

Le **Chapitre I** présente un protocole d'échantillonnage simple d'utilisation sur le terrain, nécessaire pour étudier le microbiote des populations naturelles. Plusieurs techniques et leurs effets sur les données de métabarcoding 16S ont été comparées.

Le **Chapitre II** caractérise le microbiote de populations naturelles *de S. latissima*, à l'échelle de la lame, de la région, de la saison et de l'état physiologique de l'algue, grâce à des analyses de métabarcoding 16S.

Le **Chapitre III** porte sur l'étude des interactions algues-bactéries, et leur impact sur la croissance de l'algue. A partir d'isolements bactériens, des souches bactériennes d'intérêt issues de *S. latissima* et *Ectocarpus* sp. ont été sélectionnées pour réaliser des cocultures. L'impact de ces souches sur la croissance et sur la composition générale du microbiote de l'algue est discuté dans ce chapitre, en tenant compte du phénomène de quorum sensing et de son lien avec une perturbation de la croissance.

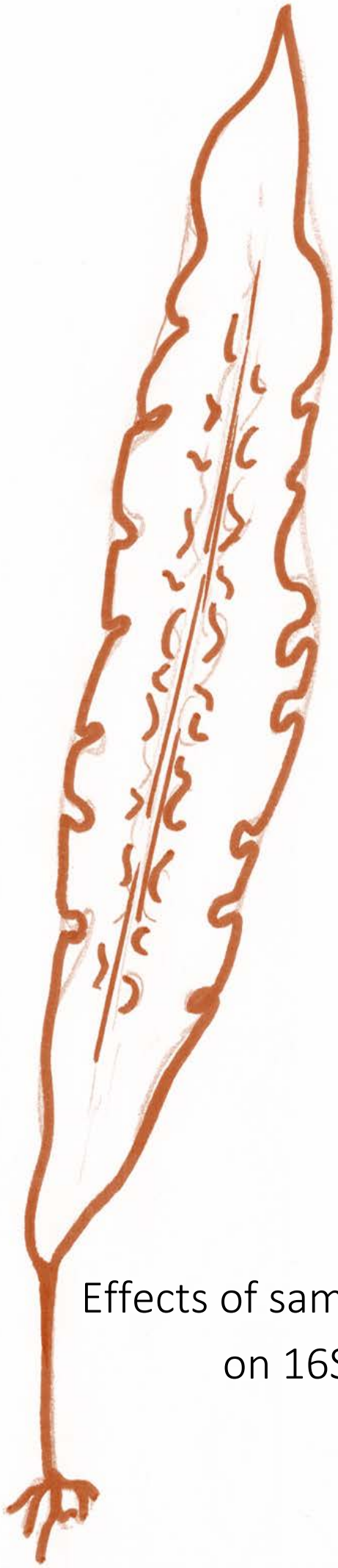

- CHAPITRE I -

Article

Effects of sampling and storage procedures on 16S amplicon sequencing results of kelp microbiomes

CHAPITRE I - Effects of sampling and storage procedures on 16S amplicon sequencing results of kelp microbiomes

Afin d'étudier le microbiote des populations naturelles d'algues, il est nécessaire d'avoir un protocole pour stocker les échantillons prélevés sur le terrain. Ce protocole doit être simple d'utilisation, en particulier quand l'échantillonnage se fait à partir d'un bateau ou loin du laboratoire d'analyses.

Une des méthodes classiquement utilisée est la flash-congélation en azote liquide avec un stockage à -80°C. Cette méthode lourde demande que la chaine du froid soit respectée jusqu'à l'utilisation des échantillons, même lors d'un envoi.

Dans cet article, nous avons testé deux méthodes alternatives : la conservation en silica-gel des tissus d'algue et le prélèvement par swab (écouvillon) puis stockage en solution de conservation.

Afin de vérifier que ces méthodes sont utilisables, nous avons étudié leurs impacts sur les résultats de métabarcoding 16S, à partir d'échantillons prélevés à l'apex et au méristème *de S. latissima* de Roscoff et comparé ces résultats avec ceux obtenus avec la méthode classique.

La composition bactérienne globale, dominée par les *Alphaproteobacteria*, *Gammaproteobacteria*, et *Bacteroidota*, a été obtenue quelle que soit la méthode, et est typique du microbiote associé aux algues brunes (Hollants et al., 2013; KleinJan et al., 2017; Parrot et al., 2019; Tourneroche et al., 2020).

L'analyse de la composition bactérienne montre une séparation nette et reproductible entre les échantillons prélevés sur les apex et ceux prélevés sur les méristèmes, quelle que soit la méthode de prélèvement utilisée. Cette séparation des échantillons était attendue, car classiquement présente chez d'autres macroalgues (cf. **Chapitre II** ; Staufenberger et al., 2008; Goecke et al., 2010; Ihua et al., 2020).

Les seules différences observées entre les méthodes sont dues à des genres rares retrouvés dans quelques échantillons de la méthode swab, et de manière non significative pour la plupart.

Ainsi, et même en prenant en compte les biais légers introduits, les trois méthodes testées (silica-gel, swab et azote liquide) sont adaptées dans le cadre de l'étude de la composition générale du microbiote de *S. latissima*.

Cet article a été soumis à *Marine Genomics* et est en cours de révision/correction.

Effects of sampling and storage procedures on 16S amplicon sequencing results of kelp microbiomes

Bertille Burgunter-Delamare [1] * id, Gwenn Tanguy [2], Erwan Legeay [2], Catherine Boyen [1,2], Simon M. Dittami [1] * id

[1] CNRS, Sorbonne Université, Integrative Biology of Marine Models (LBI2M), Station Biologique de Roscoff, 29680 Roscoff, France

[2] CNRS, Sorbonne Université, FR2424 Station Biologique de Roscoff, 29680 Roscoff, France

*Correspondence: bertille.burgunter-delamare@sb-roscoff.fr, simon.dittami@sb-roscoff.fr; +33 2 98 29 23 23

Abstract

Brown macroalgae, including the kelp *Saccharina latissima,* are of both ecological and increasing economic interest. Together with their microbiota, these organisms form a singular entity, the holobiont. Sampling campaigns are required to study the bacterial partners of algae in natural populations, but freezing samples in liquid nitrogen is complex in the field, particularly at remote locations. Here we tested two simple alternative methods for sampling the microbial diversity associated with the kelp *S. latissima*: silica gel conservation of tissue and swab samples preserved in DNA/RNA shield solution. We used these techniques to compare apex and meristem samples from Roscoff (Brittany, France) and evaluated their impact on the results of 16S rRNA metabarcoding experiments. Both methods were able to separate apex and meristem microbiomes, and the results were concordant with results obtained for flash-frozen samples. However, differences were observed for several rare genera, although they were not statistically significant for the most part. These results confirm that the silica gel technique and swabbing combined with DNA/RNA shield preservation are valid alternatives to liquid nitrogen preservation when sampling brown macroalgae in the field.

Keywords: Silica gel, swab, liquid nitrogen, brown algae, microbiome, metabarcoding, holobiont.

I. Introduction

Brown macroalgae and particularly kelp (*Laminariales*) play essential ecosystem engineering roles in coastal temperate marine environments. They contribute to primary productivity and are habitat engineers providing food and shelter to the local biodiversity (Schiel and Foster, 2006; Schiel and Lilley, 2007). In addition, species of kelps are important in many industries to produce alginates (Peteiro, 2018), human food, medicine (Smit, 2004), or food for abalone aquaculture (Roussel et al., 2019).

Macroalgal functioning has to be seen as the result of the interactions between the algal host and their associated microbiota constituting a complex system termed the algal holobiont (Egan et al., 2013). It has been shown that macroalgal health, fitness, pathogen resistance (Wiese et al., 2009), acclimation to a changing environment (Dittami et al., 2016), and metabolism (Burgunter-Delamare et al., 2020) are regulated and supported by bacterial partners (Goecke et al., 2010). Considering the biofilm composition and deciphering the interactions within the holobiont is thus essential to fully understand the biology of algae.

To study the microbiota of natural populations, especially in remote regions, we need simple sampling protocols and storage methods. Methods available involve shock-freezing in liquid nitrogen (van der Meer and Simpson, 1984; Tourneroche et al., 2020), ethanol (Hammer et al., 2015; Song et al., 2016), various preserving reagents (Hammer et al., 2015; Song et al., 2016), and silica gel (Toishi, 1959; Phillips et al., 2001; Hoarau et al., 2007; Esteban et al., 2009). These methods can be applied to both algal tissue and surface swabs (Lachnit et al., 2011; Parrot et al., 2019; Qiu et al., 2019). A few comparative studies of conservation methods in insect-, soil-, and human microbiota have established that differences introduced by storage techniques, while perceptible, did not outweigh differences classically found in the bacterial communities between species, individuals, or sample types (Lauber et al., 2010; Hammer et al., 2015; Song et al., 2016). Furthermore, a study on the red alga *Porphyra umbilicals* has shown that silica gel was as effective as flash-freezing/lyophilisation (Quigley et al., 2018) to preserve the core microbiome. Here we examine if these results were transferable also to the kelp *S. latissim*a.

The sugar kelp or sea belt *Saccharina latissima* (L.) (Phaeophyceae, Laminariales) is one of the dominant kelp-forming species of brown macroalgae in Europe and is becoming a research model for holobiont studies and others (Staufenberger et al., 2008; Wiese et al., 2009; Tourneroche et al., 2020). We compared the impact of flash-freezing of tissue in liquid

nitrogen, desiccation of tissue in silica gel, and swab sampling followed by preservation in DNA/RNA shield solution on DNA metabarcoding results of algal apex and meristem samples. Our data show that all three methods yield similar results for the vast majority of genera and that both swabs and silica gel are viable alternatives to shock-freezing of tissues in the field.

II. Material & Methods

1. Biological material

Saccharina latissima (*Phaeophyceae*) samples were collected by hand, at low tide on 22 March 2019, at Perharidy (48°43'47.0 "N 4°00'17.1 "W), Roscoff (France). Among young individuals (<1 m length), ten algae were randomly selected. The algal material was immediately placed in sterile plastic bags and rapidly transported to the laboratory in an icebox at ca. 4°C.

2. Sample preparation technics

All three techniques were carried out under a sterile hood and for each individual. Two areas of the blades were sampled: the basal meristem part and the tip (**Figure 9**). Two discs (Ø2cm) were punched out in immediate proximity for each part of the blade. One of the discs was placed in a 15ml Falcon tube containing 5ml of clean silica gel (2-6mm; VWR) and stored at 4°C for ca two weeks before use. The other disc was placed in a 2ml cryotube, shock-frozen in liquid nitrogen, and stored at -80°C until use. For the swab samples, an area of 2cm² was swabbed (Swab collection kit, Zymo Research) until a brown colouration was reached (30 s – 1 min), and the swab was placed in a collection tube filled with 1ml of DNA/RNA Shield (Zymo Research) and stored at -20°C until use.

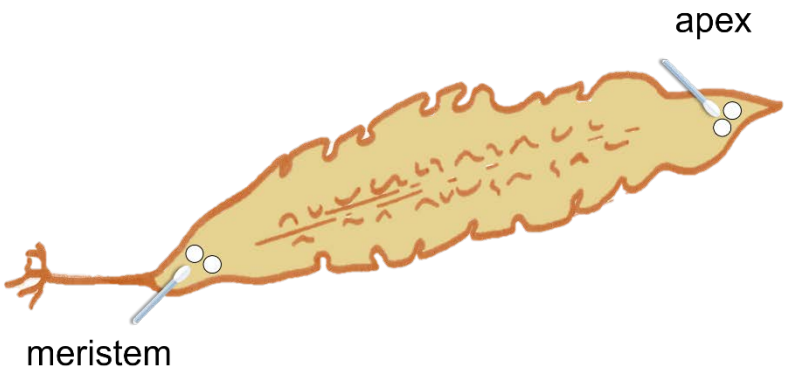

Figure 9 – Sampled parts of the thallus. Two discs (Ø2cm) were punched out in immediate proximity for each part of the blade, and an area of 2cm² was swabbed

3. DNA extraction

DNA extraction was carried out according to Bernard et al. (2017) for samples stored in silica gel and at -80°C. Briefly, samples were freeze-dried, and ½ of a disk was ground using a Qiagen TissueLyser II bead beater (3 sessions, 45 sec, 30 Hz, 3 mm stainless steel beads). Nucleic acids were then extracted using a 2% CTAB extraction buffer (100 mM Tris-HCl [pH 7.5], 1.5 M NaCl, 2% CTAB, 50 mM EDTA [pH 8], 50 mM DTT; shaker 250 rpm at room temperature). Supernatants were purified first with chloroform/isoamyl alcohol (24:1; 2 centrifugations 15 min, 10 000 rpm, 16°C), then purified onto the filter of the Nucleospin plant II kit (Macherey-Nagel, Germany). Next, DNA was eluted in 50µl of elution buffer (Macherey-Nagel). For the swab samples, DNA extraction was carried out with a ZymoBIOMICS™ DNA Miniprep Kit following the manufacturer's protocol (https://files.zymoresearch.com/protocols/_d4300t_d4300_d4304_zymobiomics_dna_miniprep_kit.pdf). One hundred µl of DNA extract was obtained. Blank extractions were also performed for each technique, and these extracts were used to identify potential contaminations introduced during the extraction and downstream processing of the samples.

4. 16S metabarcoding

The bacterial community composition associated with algal cultures was determined by 16S rDNA metabarcoding. A mock community comprising a mix of DNA from 26 cultivated bacterial strains (Thomas et al., 2019) was run parallel to the DNA extracts. For all of these samples, the V3 and V4 regions of the 16S rDNA gene were amplified using the NOCHL primers including Illumina adapters (Thomas et al., 2019), to avoid plastid DNA amplification. Then the standard Illumina protocol for metabarcoding (Illumina, 2013) was run using the Q5® High-Fidelity PCR Kit (New England BioLabs, MA, USA), the AMPure XP for PCR Purification Kit (Beckman Coulter, Brea, CA, USA), and the Nextera XT DNA Library Preparation Kit (Illumina, San Diego, CA, USA). Libraries were quantified with a Quantifluor® ds DNA System (Promega, WI, USA), and the mean fragment size was determined using a LabChip® GX Touch™ (Perkin Elmer, MA, USA). An equimolar pool of all samples was generated at a concentration of 4nM, diluted to 3 pM, spiked with 10% PhiX (Illumina), and sequenced on an Illumina MiSeq sequencer at the Genomer platform (Station Biologique de Roscoff) using a MiSeq v3 kit (2x300bp, paired-end).

5. Analyses

Sequence analysis was performed using the DADA2 1.14.0 package (Callahan et al., 2016) on R 3.6.2. Following the protocol (https://benjjneb.github.io/dada2/tutorial.html), sequences were filtered allowing for a maximum of two expected errors and reducing the read length to 291 bp for forward reads and 265 bp for reverse reads. An amplicon sequence variant (ASV) table was constructed, and chimaeras were removed. The taxonomy of the remaining ASVs was assigned using the Silva_SEED 138 database. The resulting abundance table and taxonomic classification were analyzed using Phyloseq version 1.30.0 (McMurdie and Holmes, 2013). The blank reads, organellar and eukaryote reads, rare ASVs (<0.01% of total reads), and samples with less than 7000 total reads were removed, leading to a final number of 3 to 5 replicates per condition. Non-Metric Multidimensional Scaling analyses (NMDS) were carried out using the Bray-Curtis distances derived from the ASV table using the vegan R package version 2.5-6. The Shannon H diversity index was also calculated based on the ASV table using Past version 4.02 (Hammer et al., 2001). Statistical analysis of differential abundance was carried out at the genus level using DESeq2 version 1.26.0 (Love et al., 2014), allowing for a false discovery rate (p_{adj}) of 5%. The genus level was chosen rather than the ASV level to limit the number of tests performed and thus reduce the probability of beta errors due to the correction for multiple testing. A joint analysis was performed with both methods and thallus part as factors to identify genera specifically impacted by the storage methods. Venn diagrams were generated using BioVenn (Hulsen et al., 2008), and the mean abundance of genera across storage methods was compared using linear regression on log10-transformed data in Past version 4.02. The residuals of the linear regressions were subjected to a Shapiro-Wilk test to confirm that they did not deviate significantly from a normal distribution ($p>0.05$).

III. Results

A total of 3,935,663 raw sequences were generated and, after filtering, assembled into 1,743,565 contigs. The taxonomic assignation of mock samples was consistent with the mock composition. A total of 11,106 ASVs were identified in the dataset corresponding to 571 genera. The final ASV matrix is provided as supplementary **Table S1**.

1. Comparison of apex and meristem samples with the three storage methods

Regardless of the storage method used, sequences followed the same general patterns. In all samples, they corresponded predominantly to *Alphaproteobacteria* (34.8% of reads, on average), followed by *Gammaproteobacteria* (31.5% of reads) and *Bacteroidota* (21.1% of reads), although their exact proportion varied slightly (**Figure 10**). *Planctomycetota* were significantly more abundant (t-test, $p < 0.001$) in the apex samples (5 to 8% of reads) than in the meristem ones (0.76% to 1.95% of reads). *Actinobacteriota* were less detected after desiccation in silica gel (meristem: 0.08% and apex: 0.7% of reads) compared to the samples treated with liquid nitrogen (meristem: 1.85% and apex: 1.93% of reads); and *Acidobacteriota* were almost exclusively found in the swab samples (meristem: 0.35% and apex: 0.16% of reads; <0.04% in others, t-test $p = 0.049$). Overall, as indicated by the Shannon H index in **Figure 11**, the alpha diversity was higher in apex samples than meristem samples, although this difference was statistically significant only for the liquid nitrogen and the silica gel samples. Finally, NMDS analyses confirmed a clear separation of apex and meristem samples regardless of the sampling and storage method (**Figure 12A-C**). This separation was also observed in a combined NMDS plot (**Figure 12D**). Here, separation according to the storage method was only detected at a smaller scale in the meristem samples.

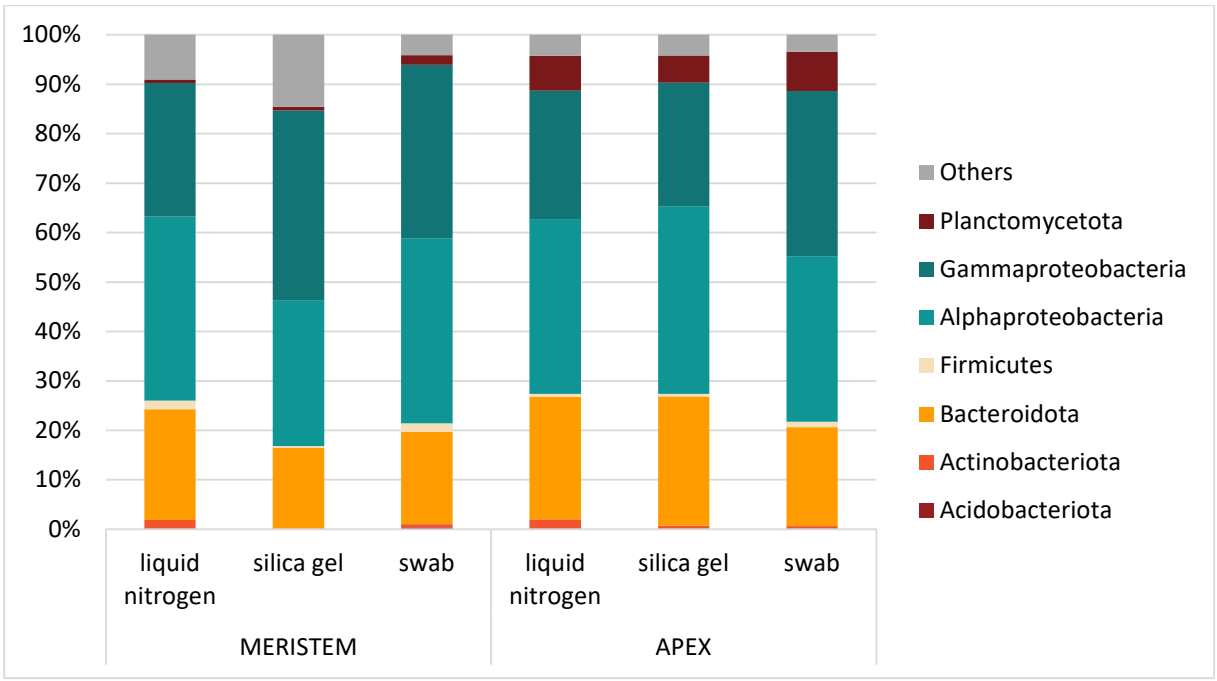

Figure 10 – Distribution of 16S rRNA gene metabarcoding sequences per phylum

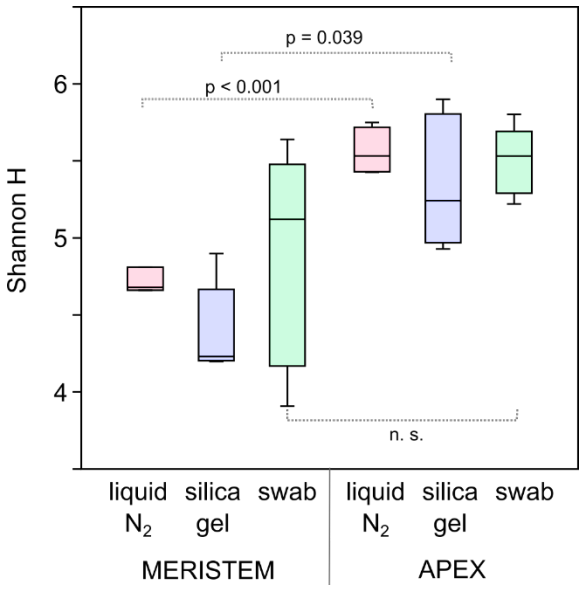

Figure 11 – Box plot of alpha-diversity (Shannon H index) across sample types. P-values correspond to the results of a two-sided t-test; n.s. = not significant (p > 0.05).

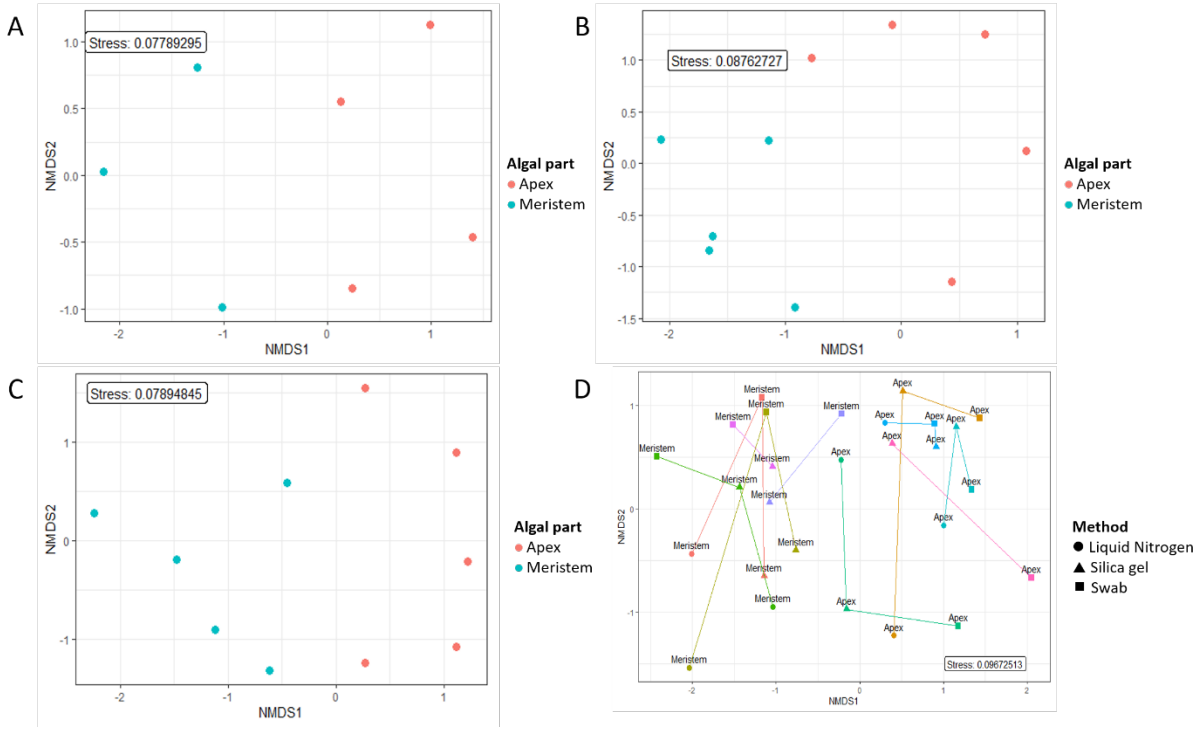

Figure 12 – NMDS analysis of the microbiome composition. Results show a clear separation of the apex and meristem samples for the (A) liquid nitrogen, (B) silica gel, and (C) swab method, as well as (D) all methods combined. The points of the same colours and connected by lines correspond to the same "parent" sample.

2. Direct comparison of storage methods

Differences were observed primarily regarding the detection of different genera depending on the storage and sampling methods (**Figure 13**). Among the 572 genera in our

dataset 158 were detected in at least one sample with all storage methods. 143 genera were detected in samples from two different storage/sampling methods, with the highest overlap occurring between liquid nitrogen and swab samples. However, most genera (271) were found only with one of the tested methods, and most of these with the swab samples. Please note, however, that as shown in **Figure 13,** these method-specific genera correspond only to a small percentage of the total reads. 96.7% of all reads were covered by the genera detected with all methods. Moreover, among these shared genera and the genera present in samples from two sampling methods, total read counts were strongly correlated across methods (**Figure 14**). It confirmes that similar read abundances were observed across the different methods for >96% of the reads. As for the method-specific genera, global DESEQ2 analysis of the relative abundance of all genera across methods and sample types confirmed only a few statistically significant differences. The genus *Profundimonas* was detected by the liquid nitrogen and swab methods (adj. *p<0.001*), and the genera *Rickettsiales_unclassified*, *Pantoea*, and *Proteobacteria_unclassified* were more abundant in the silica gel dataset compared to the swab dataset (padj=0.002, 0.005, and 0.033, respectively). The other method-specific genera did not pass the significance criteria of the DESEQ2 analysis, most likely due to their low read abundance or because they were only found in a few of the replicates.

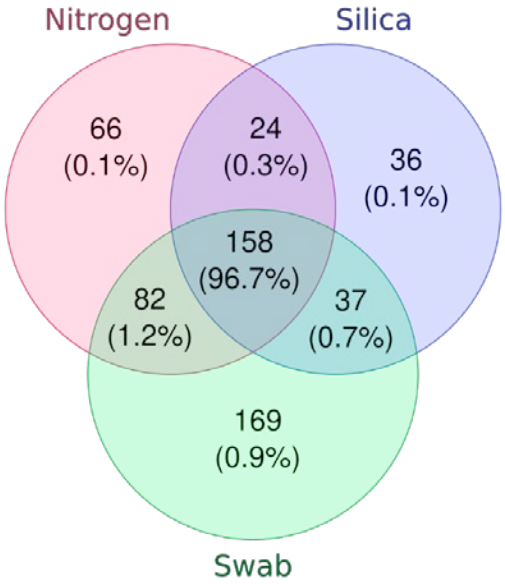

Figure 13 – Venn diagram illustrating shared genera between the liquid nitrogen (pink), silica gel (blue), and swab (green) datasets. Numbers in parentheses indicate the percentage of total reads represented by the genera in each section.

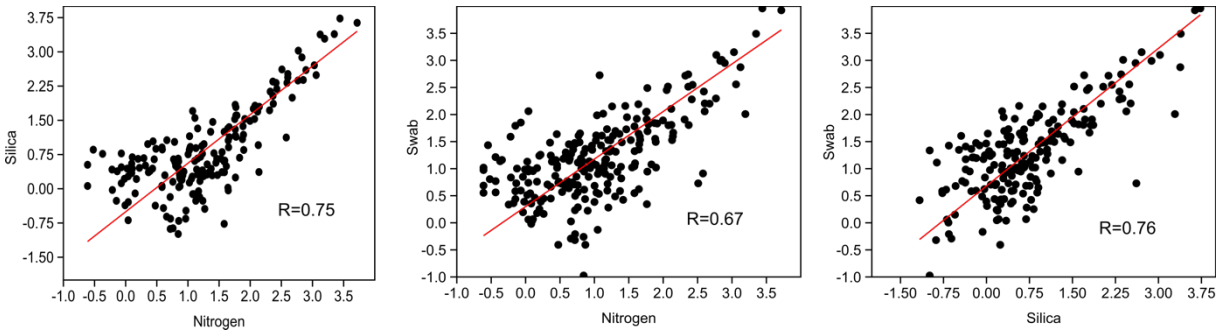

Figure 14 – Correlation of log10-transformed mean sequence abundance across the sampling protocols. Only genera shared by at least two of the protocols were considered. R=Pearson correlation coefficient, red line = linear regression, $p < 0.0001$

IV. Discussion & Conclusion

Simple sampling protocols are required to study bacterial partners in natural populations of macroalgae. In this study, we wanted to test if using silica gel and swab techniques, both of which are more convenient to put into place during field sampling campaigns, would introduce a bias in the results compared to shock-freezing in liquid nitrogen. Our results demonstrate that, regardless of the sampling and storage method, coherent results were obtained. The global bacterial composition dominated by *Alphaproteobacteria*, *Gammaproteobacteria*, and *Bacteroidota* was obtained regardless of the method employed and is typical for brown algae-associated microbiomes (Hollants et al., 2013; KleinJan et al., 2017; Parrot et al., 2019; Tourneroche et al., 2020). In the same vein, global differences in the community composition between apex and meristem persisted regardless of the sampling methods. These differences were expected, as *S. latissima* is a perennial species, and growth occurs mainly in the meristem region. The younger meristem tissues thus are typically less colonized by bacteria and, as confirmed in our study, exhibit lower bacterial diversity (Staufenberger et al., 2008; Goecke et al., 2010; Ihua et al., 2020). *Planctomycetes*, which we detected predominantly in the apex samples, are typical components of algal biofilms (Lage and Bondoso, 2014) and are, in agreement with our results, abundant also in apices of the brown alga *Fucus vesiculosus* (Parrot et al., 2019).

The main differences between the examined sampling methods were observed at the genus level, where our analyses show that almost half of the genera were only detected with one of the sampling methods. This observation may seem disconcerting at first, but these differences were driven by rare genera, which were usually detected in one or a few replicates, and for all but four genera, they were not statistically significant. Our data are thus in line with the results

obtained by Quigley et al. (2018) on the red alga *P. umbilicalis*, who found silica gel and flash freezing to yield similar patterns for the abundant core taxa that constituted >0.1% of sequences.

Why the phenomenon of method-specific detection of genera was more pronounced in the swab samples (169 specific genera vs 66 and 36, including three statistically significant) currently remains unanswered. However, the swab protocol is different from the two other protocols because of the storage method (DNA/RNA Shield solution, vs silica gel, vs shock-freezing) and the DNA extraction protocol, which, unlike the other methods, does not include the algal tissue.

Overall, we conclude that, even if caution needs to be taken when interpreting data on rare species or genera, only slight biases are introduced by the tested methods, and all three methods, flash-freezing in liquid nitrogen, drying with silica gel followed by tissue grinding, and swabbing followed by preservation in DNA/RNA shield solution, are suitable to assess the general microbiome of *S. latissima.*

Declarations

Funding: This work was funded partially by the ANR project IDEALG (ANR-10-BTBR-04) “Investissements d’Avenir, Biotechnologies-Bioressources” and the CNRS momentum call (2017). BBD was funded by a joint PhD scholarship from the Brittany region (Project HOSALA) and Sorbonne University (ED227).

Competing interests: The authors declare that they have no competing interests.

Data availability: Raw sequence data were deposited at the European Nucleotide Archive under project accession number ENA: PRJEB37561.

Authors’ contributions: Designed study: BBD, SD; Performed experiments: BBD, EL, GT; Analyzed data: BBD, SD; Wrote the manuscript: BBD, SD; Provided valuable input and corrected the manuscript: CB.

Acknowledgements

We thank François Thomas, Maéva Brunet and Nolwen Le Duff for their primers and for providing the mock community. This work benefited from access to the Station Biologique de Roscoff, an EMBRC-France and EMBRC-ERIC Site.

Supplementary Data

Table S1 - ASVs Matrix Storage Methods

Data available via link : https://doi.org/10.5281/zenodo.5752101

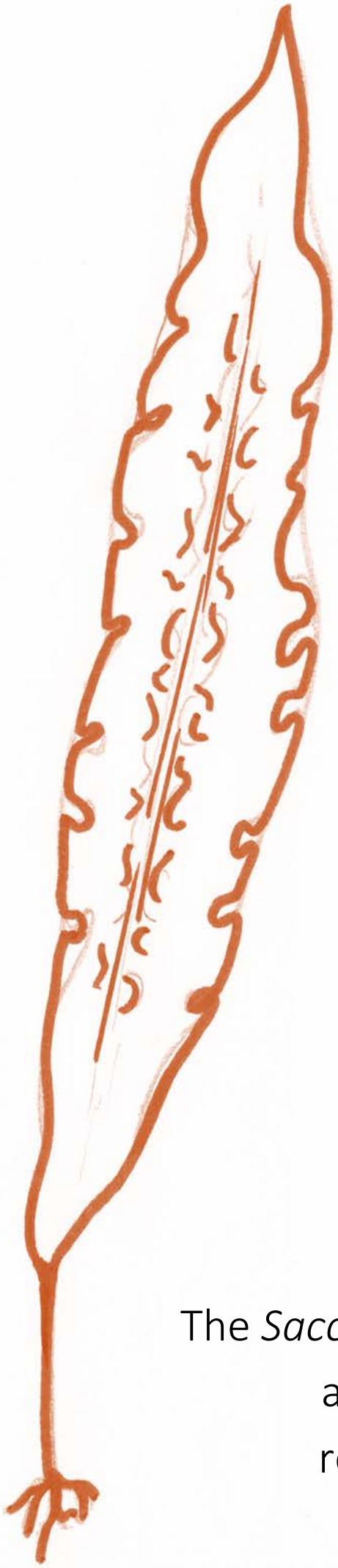

- CHAPITRE II -

Article

The *Saccharina latissima* microbiome: algal tissue matters more than region, season, and physiology

CHAPITRE II - The *Saccharina latissima* microbiome: algal tissue matters more than region, season, and physiology

Ce chapitre porte sur l'étude du microbiote bactérien présent chez les populations naturelles de *S. latissima* ; il fait l'objet d'un article en cours de soumission.

Plusieurs questions sont développées dans ce chapitre :

- La différence de composition du microbiote entre apex et méristème, classiquement observée chez d'autres macroalgues, est-elle retrouvée chez *S. latissima* ?
- Le microbiote des populations naturelles change-t-il en fonction de l'origine géographique de l'hôte ?
- Les saisons ont-elles un impact sur ce microbiote ?
- L'état physiologique de l'algue influence-t-il la composition du microbiote ?

Des collaborations m'ont permis d'avoir accès à des échantillons en provenance d'autres zones géographiques. Stein FREDRIKSEN, de l'université d'Oslo, nous a envoyé des échantillons de Skagerrak (Sud de la Norvège) ; Kai BISCHOF et Nora DIEHL, de l'Université de Brême (Allemagne), nous ont envoyé des échantillons prélevés au Svalbard (Norvège). Ces derniers échantillons n'ont pas pu être inclus dans cet article, suite à des soucis lors du séquençage. Grâce au Programme H2020 Assemble Plus, j'ai également pu échantillonner des *S. latissima* sur Helgoland (Mer du Nord, Allemagne), en juillet 2019. Le reste des prélèvements a été fait à la pointe de Perharidy (Roscoff) au cours de l'année 2019, à raison d'une date par saison.

L'analyse de la composition du microbiote a été faite par métabarcoding 16S et a révélé que les *S. latissima* ont des communautés bactériennes variables. Nous avons montré que cette différence de composition bactérienne est due à des facteurs d'importance décroissante : (i) la zone de la lame et les tissus associés (apex/méristème), (ii) la zone géographique, (iii) les saisons et (iv) l'état de l'hôte (tissus sain vs avec symptômes).

Dans l'ensemble, les *Alphaproteobacteria*, *Gammaproteobacteria* et *Bacteroidota* dominent les communautés bactériennes. Un core bactérien composé de neuf genres a été mis en évidence.

Le fait que la zone de la lame ait un impact plus fort sur la composition microbienne que les saisons ou la région, deux facteurs qui sont associés à des changements abiotiques de l'environnement, suggère que l'hôte sélectionne les bactéries qui lui sont associées.

Nos résultats font également ressortir une signature microbienne caractéristique des algues en mauvaise santé, indépendamment des symptômes présents chez l'hôte. Il se pourrait que les différents types de maladies provoquent des changements physiologiques semblables chez l'hôte, entraînant ainsi des changements microbiens similaires.

The *Saccharina latissima* microbiome: algal tissue matters more than region, season, and physiology

Bertille BURGUNTER-DELAMARE [1] * [id], Sylvie ROUSVOAL [1], Erwan LEGEAY [2], Gwenn TANGUY [2], Stein FREDRIKSEN [3], Catherine BOYEN [1,2] and Simon M. DITTAMI [1] * [id]

[1] CNRS, Sorbonne Université, Integrative Biology of Marine Models (LBI2M), Station Biologique de Roscoff, 29680 Roscoff, France

[2] CNRS, Sorbonne Université, FR2424 Station Biologique de Roscoff, 29680 Roscoff, France

[3] University of Oslo, Department of Biosciences, PO Box 1066, Blindern, N-0316 Oslo, Norway

*Correspondance: bertille.burgunter-delamare@sb-roscoff.fr, simon.dittami@sb-roscoff.fr

Abstract

Saccharina latissima is a canopy-forming species of brown algae and, as such, is considered an ecosystem engineer. Several populations of this alga are exploited worldwide, and a decrease in the abundance of *S. latissima* at its southern distributional range limits has been observed. Despite its economic and ecological interest, only a few data are available on the composition of microbiota associated with *S. latissima* and its role in algal physiology. We studied the bacterial community composition associated with *S. latissima* samples from three different locations (Brittany, Helgoland, and Skagerrak) by 16S metabarcoding analyses at different scales: algal blade part, regions, season and physiologic state.

We have shown that the difference in bacterial composition is driven by factors of decreasing importance: (i) the algal tissues (apex/meristem), (ii) the geographical area, (iii) the seasons and (iv) the algal host condition (healthy vs symptoms). Overall, *Alphaproteobacteria*, *Gammaproteobacteria* and *Bacteroidota* dominated the general bacterial communities. Almost all individuals hosted bacteria of the genus *Granulosicoccus,* accounting for 12% of the total sequences, and eight additional core genera were identified. Our results also highlight a microbial

signature characteristic for algae in poor health, dominated by the genus *Pseudoalteromonas*, and independent of the disease symptoms.

Keywords: holobiont, brown macroalgae, microbiome, metabarcoding

I. Introduction

Brown macroalgae and particularly kelps (*Laminariales*) play essential ecosystem engineering roles in coastal temperate marine environments. Depending on their genus, they are distributed across the western or eastern temperate North Pacific, the Arctic and North Atlantic Oceans (Bolton, 2010; Araújo et al., 2016). Kelps contribute to primary productivity and are habitat formers providing food and shelter to the local biodiversity (Schiel and Foster, 2006; Schiel and Lilley, 2007). In addition, species of kelps are important in many industries to produce alginates (Peteiro, 2018), human food, medicine (Smit, 2004), or food for abalone aquaculture (McHugh, 2003; Roussel et al., 2019).

Saccharina latissima (Linnaeus) is one of the dominant kelp-forming species of brown macroalgae in Europe. Its tissue growth starts from the meristematic region at the base of the blade, with the older tissue being at the apex part. These older parts can undergo erosion due to senescence and host a higher bacterial diversity, as shown in previous research in other *Laminariales*, notably *Laminaria digitata* (Corre and Prieur, 1990), *L. hyperborea* (Bengtsson et al., 2010), *L. longicruris* (Laycock, 1974), *L. pallida* (Mazure and Field, 1980), and *L. setchellii* (Lemay et al., 2021).

In recent years, a decrease in the abundance of *S. latissima* at its southern distributional range limits has been observed (Araújo et al., 2016; Smale, 2020). The exact processes driving this decline are not fully understood, but it is likely that changes in the microbiota might be at least partially linked to this process, as is the case with corals (Bourne et al., 2008; Bosch and Miller, 2016; Peixoto et al., 2017).

Indeed, macroalgal functioning needs to be seen as the result of the interactions between the algal hosts and their associated microbiota constituting a singular entity termed the algal holobiont (Egan et al., 2013). It has been shown that macroalgal health, fitness, pathogen resistance (Wiese et al., 2009), acclimation to a changing environment (Dittami et al., 2016), and metabolism (Burgunter-Delamare et al., 2020) are regulated and supported by bacterial partners (Goecke et al., 2010). Considering the biofilm composition and deciphering the interactions within the holobiont is thus essential to fully understand the biology of algae. Previous studies were made on different kelp species microbiota like *L. digitata, L. hyperborea, L. religiosa and L.*

setchellii (Vairappan et al., 2001; Bengtsson et al., 2010; Ihua et al., 2020; Lemay et al., 2021), but little is known about the *S. latissima* microbiota. Notably, Staufenberger et al. (2008) analysed the bacterial composition of *Saccharina* from two places and seasons (Baltic and North Sea; January and April 2006) using denaturing gradient gel electrophoresis (DGGE) and 16S rRNA gene clone libraries. Later, Tourneroche et al. (2020) used 16S metabarcoding and FISH to decipher the bacterial microbiota of young tissues of *S. latissima*, sampled in one place (Scotland) on the same date (July 2017).

In this study, we compared the microbiota composition of young *S. latissima* samples from several locations in the Atlantic Ocean (Brittany, Helgoland and Skagerrak) by 16S metabarcoding analyses to decipher if the microbiota is specific to the area of origin, seasonality, and algal blade part (apex/meristem). We furthermore examined the microbiota composition of healthy and diseased algae, aiming to identify possible microbial signatures characteristic of algae in poor health.

II. Material & Methods

1. Biological material & Environmental Variables

S. latissima were sampled at different sites and dates (**Table 1**). Briefly, samples were taken from three regions (Brittany, Helgoland and Skagerrak) at low tides (or diving when necessary). Among young individuals (<1m length), five healthy algae and five with physical symptoms (holes, bleaching, twisted blades) were selected for each sampling session. We focused on the "symptoms" category more than on a specific disease because it was impossible to find enough individuals with the same symptoms throughout the sampling sessions and sites. The algal material was immediately placed in sterile plastic bags and rapidly (<3h) transported to the laboratory in a cooling box at ca. 4°C.

Two parts of the blades were sampled: the basal meristem and the tip (**Figure 15**). A disc with Ø2cm punched out for each part of the blade and placed in a 15 ml Falcon tube containing 5ml of clean silica gel (2-6mm; VWR). Tubes were stored at room temperature for up to 15 days before DNA extraction.

Table 1 – Sampling dates and sites

Places	***GPS coordinates***	***Dates***	***Time***	***Types and number of samples***
Roscoff, Brittany, France	48°43'47.0 "N 4°00'17.1" W	10 October 2018 23 January 2019 18 April 2019 31 July 2019 29 October 2019	At low tide mid-day for all	Healthy + Symptoms 64 samples
Helgoland, North Sea, Germany	54°10'47.3 "N 7°54'59.4" E 54°11'27.1 "N 7°52'02.4" E	10 July 2019 11 July 2019	Diving Low tide	Healthy + Symptoms 29 samples
Skagerrak, Norway	58°15'15.5 "N 8°31'22.2" E 58°22'05.1 "N 8°44'04.7" E 58°05'39.3 "N 6°34'54.9" E	16 October 2018 18 October 2018 1 April 2019		Healthy samples 18 samples

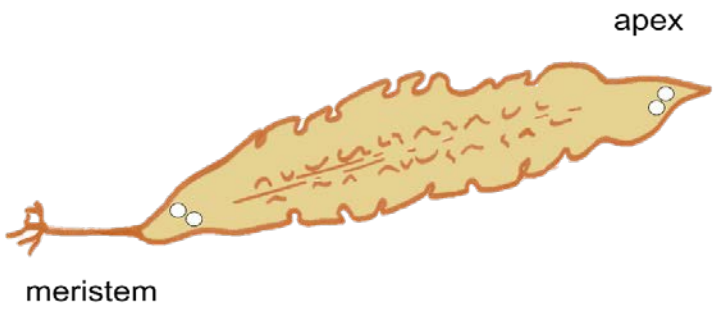

Figure 15 – Samples part of *Saccharina latissima*'s thallus. Two discs (Ø2cm) were punched out in immediate proximity for each part of the blade.

For the samples from Brittany, corresponding environmental variables (temperature, salinity and ammonium, nitrites, nitrates and phosphate concentrations) were obtained from the Service d'Observation en Milieu Littoral (SOMLIT) database (https://www.somlit.fr/mysomlit/; Astan point; approximately 3.6km North-East of the sampling point). They are available in **Figure S1**.

2. DNA extraction

DNA extraction was carried out with the silica-gel stored samples, according to the protocol described by Bernard et al. (2017). Briefly, samples were freeze-dried, and ½ of a disk was ground

using a Qiagen TissueLyser II bead beater (3 sessions, 45sec, 30Hz, 3mm stainless steel beads). Nucleic acids were then extracted using a 2% CTAB extraction buffer (100 mM Tris-HCl [pH 7.5], 1.5 M NaCl, 2% CTAB, 50 mM EDTA [pH 8], 50 mM DTT; shaker 250 rpm at room temperature). Supernatants were purified twice with one volume of chloroform/isoamyl alcohol (24:1) followed by 15min centrifugation at 10 000 rpm (16°C) and recovery of the aqueous phase. According to the manufacturer's instructions, the pre-purified DNA was purified using Nucleospin plant II columns (Macherey-Nagel, Germany). Finally, DNA was eluted in 50µl of elution buffer (Macherey-Nagel). Blank extractions were also performed, and these extracts were used to identify potential contaminations introduced during the extraction and downstream processing of the samples.

3. 16S Metabarcoding

The bacterial community composition associated with algal cultures was determined by 16S metabarcoding. A mock community comprising a mix of DNA from 26 cultivated bacterial strains (Thomas et al., 2019) and negative control were run add treated in parallel to the DNA extracts. For all of these samples, the V3 and V4 regions of the 16S rDNA gene were amplified using the NOCHL primers including Illumina adapters (Thomas et al., 2019), to avoid plastid DNA amplification. Then a standard Illumina protocol for metabarcoding (Illumina, 2013) was run using the Q5® High-Fidelity PCR Kit (New England BioLabs, MA, USA), the AMPure XP for PCR Purification Kit (Beckman Coulter, Brea, CA, USA) and the Nextera XT DNA Library Preparation Kit (Illumina, San Diego, CA, USA). Libraries were quantified with a Quantifluor® ds DNA System (Promega, WI, USA) and mean fragment size was determined using a LabChip® GX Touch™ (Perkin Elmer, MA, USA). An equimolar pool of all samples was generated at a concentration of 4 nM, diluted to 3 pM, spiked with 10% PhiX (Illumina) and sequenced on an Illumina MiSeq sequencer at the Genomer platform (Station Biologique de Roscoff) using a MiSeq v3 kit (2x300bp, paired-end). Raw Illumina reads were deposited at the European Nucleotide Archive under project accession number PRJEB47035.

4. Analyses

Sequence analysis was performed using the DADA2 1.14.0 package (Callahan et al., 2016) on R 3.6.2. Following the protocol (https://benjjneb.github.io/dada2/tutorial.html), sequences were filtered, allowing for a maximum of 2 expected errors and reducing the read length to 291 bp for forward reads and 265 bp for reverse reads. An amplicon sequence variant (ASV) table was constructed, and the chimaeras were removed. The taxonomy of the remaining ASVs was assigned using the Silva_SEED 138 database. The resulting abundance table and taxonomic classification were analysed using Phyloseq 1.30.0 (McMurdie and Holmes, 2013). The ASVs abundant in the blank samples, as wells organellar and eukaryote reads, rare ASVs (<0.01% of total reads), and samples with less than 7688 remaining reads were removed. Based on this ASV matrix, the following analyses were carried out: a Non-Metric Multidimensional Scaling analysis (NMDS) using the Bray-Curtis distances derived from the ASV table by running the vegan R package to determine the most important factor separating the samples, and this factor was then explored. The Shannon H diversity index was also calculated based on the ASV table using Past version 4.02 (Hammer et al., 2001). The bacterial core was determined at the genus level, i.e. genera present in 90% of replicates for each algal part. Statistical analysis of differential abundance was carried out at the phyla and ASV levels using DESeq2 1.26.0 (Love et al., 2014), allowing for a false discovery rate (p_{adj}) of 5%. Binomial tests followed by a Benjamini and Hochberg correction (Benjamini and Hochberg, 1995) were carried out to determine the overrepresented genera among the impacted ASVs. Then, the factor in question was eliminated from the dataset if possible (grouping of apex and meristem sample, focus on specific region), and the analyses were repeated to determine the next factor.

III. Results

1. General taxonomy

16S metabarcoding analyses were carried out for all control samples and the algal samples. A total of 4,028,372 raw sequences were generated and, after filtering, assembled into 1,658,746 merged contigs. The taxonomic assignation of mock samples was consistent with the mock composition, and a total of 18,028 ASVs were identified in the dataset. The sequences obtained

corresponded predominantly to *Alphaproteobacteria* (34,1% of total reads), followed by *Gammaproteobacteria* (29,5% of total reads) and *Bacteroidota* (26% of total reads).

2. Comparison of apex and meristem samples

Global NMDS analysis of all samples demonstrated a clear separation between the apex and meristem samples (**Figure 16A**). Overall, alpha diversity as calculated using the Shannon H index (**Figure 16B)** was higher in apex samples than meristem samples (*p-value <0.0001*). Several phyla were found to differ significantly in relative abundance between the apex and meristem samples. The *Actinobacteriota*, *Firmicutes*, and unclassified *Proteobacteria* (*p<0.0001*) were found in higher relative abundance in the meristem samples. The *Alphaproteobacteria (p=0.00016), Bacteroidota (p=0.00372)*, and *Planctomycetota (p=0.004)* phyla were relatively more abundant in the apex samples (**Figure 16C**). Through DESEQ2 analyses, a total of 50 ASVs were found to differ significantly (adjusted *p-value*< 0.05) in relative abundance between the apex and meristem samples (29 ASVs were more abundant in apex and 21 in meristem samples; **Table S2**). The taxonomic affiliation of significantly overexpressed ASVs (adjusted *p-value*< 0.05; BH correction) is shown in **Table 2**. Five genera were significantly overrepresented in the apex samples (including *Alphaproteobacteria* 70%) and three in the meristem samples (including *Gammaproteobacteria* 70%; **Table 2**). The bacterial core in the apex and meristem samples comprises the four genera *Granulosicoccus*, *Litorimonas*, *Hellea* and *Blastopirellula,* accounting for 32% of the total reads for all samples. Five additional genera were systematically present at the apical part: *Algitalea*, *Arenicella*, *Portibacter*, *Tenacibaculum*, and *Bdellovibrio* and accounted for 15% of the total reads.

3. Comparison of regions

For all the following analyses, samples were pooled as individuals to remove the apex/meristem effect. On the NMDS plot, the samples are now grouped according to their region of origin (**Figure 17A**). The alpha diversity did not differ significantly between the regions (**Figure 17B**). However, at the phylum level, the *Firmicutes* and unclassified *Proteobacteria* were underrepresented in the Norwegian samples compared to Roscoff (p=0.013 and p<0.0001) and Helgoland (p=0.004 and p<0.0001; **Figure 17C**). *Bacteroidota* and *Alphaproteobacteria* exhibited significantly higher

relative abundance in Roscoff than in Helgoland (p= 0.003 for both phyla). At the ASV level, 102

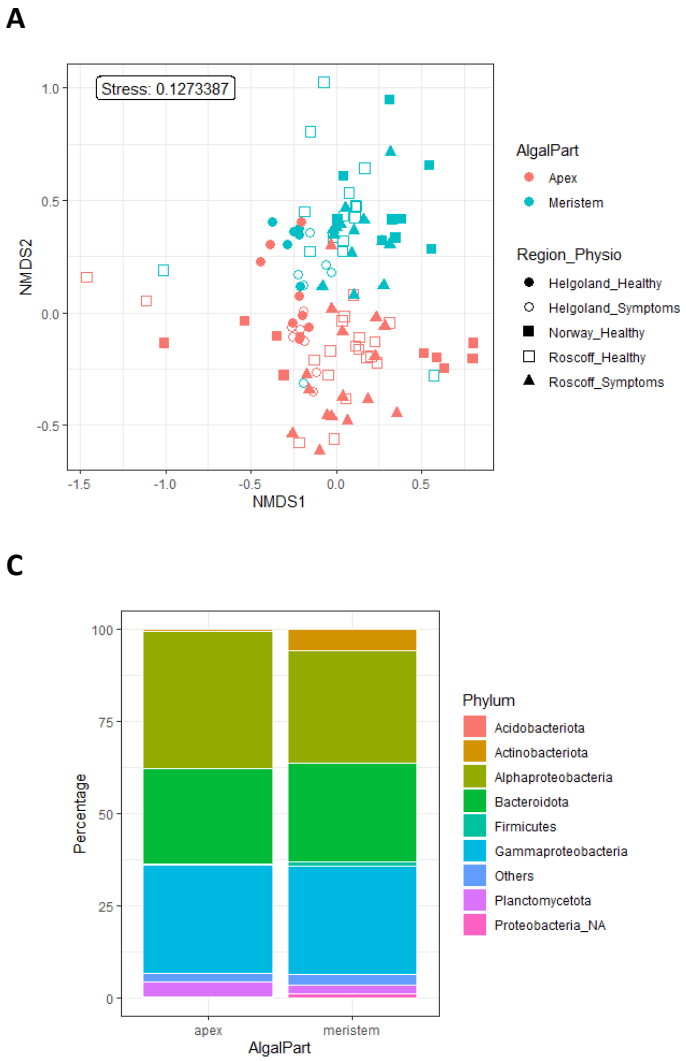

Figure 16 – Algal blade part analysis. A) NMDS analysis of the microbiome composition. Results show a clear separation of the apex and meristem samples for all the samples. B) Box plot of alpha-diversity (Shannon H index) across different sample types. *p-value* <*0.0001*. C) Comparison of microbiome composition between apex and meristem samples. Distribution of 16S rRNA gene metabarcoding sequences per phylum. *Proteobacteria_NA*: not classified as *Alpha-* or *Gammaproteobacteria*.

ASVs were represented in higher proportions in the Helgoland samples, 25 in the Roscoff samples, and 41 in the samples from Southern Norway (**Table S2**). The taxonomic affiliation of significantly overexpressed ASVs (adjusted *p-value*< 0.05; BH correction) is shown in **Table 3**, and nine genera were significantly overrepresented in Helgoland samples (including 3 *Bacteroidetes* and 3 *Gammaproteobacteria*), eight genera in Roscoff samples (*Proteobacteria* 72%) and 16 genera in the Norwegian samples (including 40% *Alphaproteobacteria*, as well as *Bacteroidetes* and *Gammaproteobacteria* ~20% each; **Table 3**).

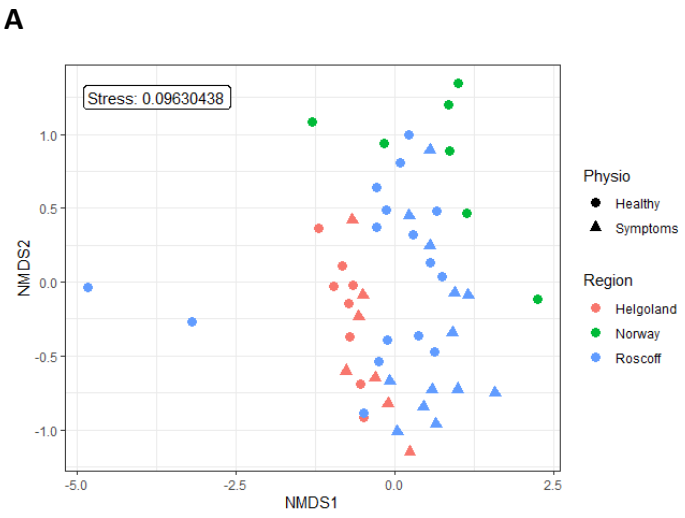

Figure 17 – Regions analysis. A) NMDS analysis of the microbiome composition. Results show a clear separation of the samples according to their origin. B) Box plot of alpha-diversity (Shannon H index) across different sample types. p-value>0.005. C) Microbiome composition of samples from Roscoff, Helgoland and Norway. Distribution of 16S rRNA gene metabarcoding sequences per phylum. *Proteobacteria_NA*: not classified as *Alpha-* or *Gammaproteobacteria*.

4. Seasonality

Only Roscoff samples were used to assess the impact of season on the microbiome because these were the only samples with four sampling points from different seasons available. The NMDS analysis shows a separation between all the season's samples. The autumn and winter samples clustered together, and the spring and summer samples were placed on the sides (**Figure 18A**), even if the alpha diversity (**Figure 18B)** did not differ significantly between the seasons. *Actinobacteria* were exclusively found in summer times. *Firmicutes* (p=0.032) were more abundant in autumn samples than in spring samples (p=0.032). *Alphaproteobacteria* were significantly more abundant in autumn than in summer (p=0.0017) and winter (p=0.014).

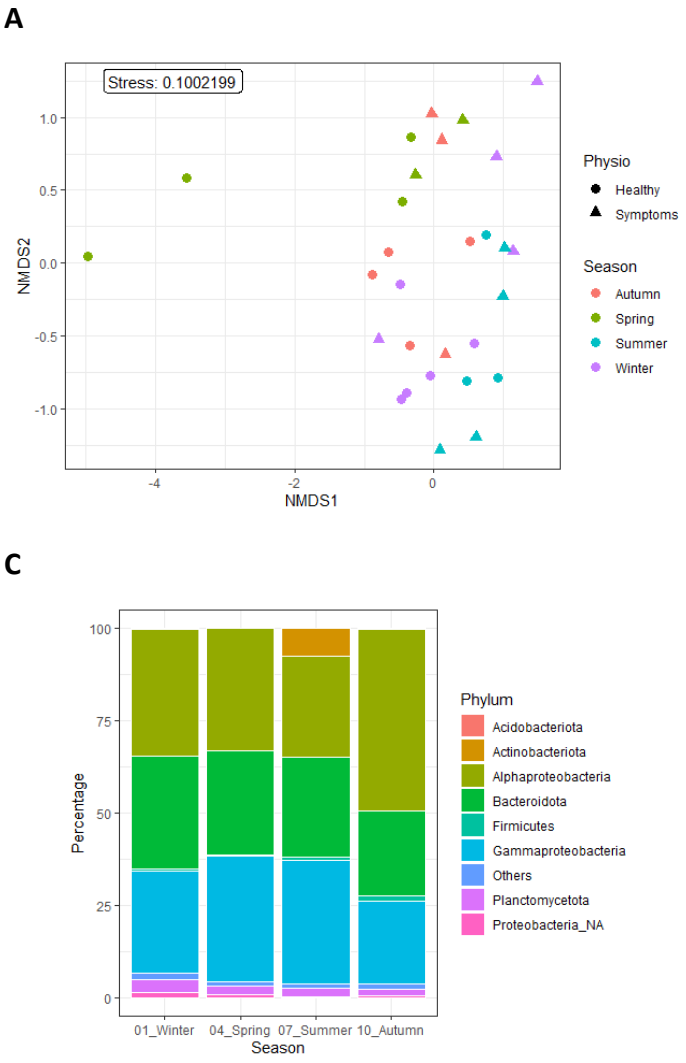

Figure 18 – Season analyses. A) NMDS analysis of the microbiome composition. Results show a separation of the samples depending on the sampling's season. B) Box plot of alpha-diversity (Shannon H index) across different sample types. P-value>0.005. C) Seasonal microbiome composition tracking in Roscoff. Distribution of 16S rRNA gene metabarcoding sequences per phylum. *Proteobacteria_NA*: not classified as *Alpha-* or *Gammaproteobacteria*.

Gammaproteobacteria were significantly more abundant in spring than in autumn (p=0.032) and winter (p=0.022; **Figure 18C**). DESeq2 analyses revealed a total of 102 ASVs that exhibited higher relative abundance in one or several seasons. 19 ASVs were most abundant in winter samples, 49 ASVs in spring samples, 17 ASVs in summer samples, and 17 ASVs in autumn samples **(Table S2)**. The taxonomic affiliation of significantly overexpressed ASVs (adjusted *p-value*< 0.05; BH correction) is shown in **Table 4**. Most of the ASVs with higher relative abundance in autumn, winter, and spring samples belonged to the *Gammaproteobacteria* (29%, 47% and 57 % of ASVs). In summer, six genera were overrepresented, and 29% of ASVs belonged to the *Alphaproteobacteria*.

5. Comparison Healthy / Symptoms

Both healthy samples and samples with symptoms were found only in Roscoff and Helgoland, and the symptoms were diverse: holes, twisted blade, bubbling in the blade (**Figure 19**). The NMDS shows no separation between the healthy individuals and those with symptoms (**Figure 20A**), although the Shannon H index indicated slightly higher alpha diversity in algal samples with symptoms than in healthy samples (*p-value=0.046;* **Figure 20B**). No phyla were found to significantly and systematically differ between healthy algae and algae with symptoms (**Figure 20C**). This observation also remains true when we distinguish samples between the different types of symptoms (**Figure 20D**), and the samples are still separated depending on the region. However, DESeq2 analyses revealed 82 ASVs that were differentially expressed: 37 exhibited higher relative abundance in samples with symptoms and 45 in the healthy ones (**Table S2**). The taxonomic affiliation of significantly overexpressed ASVs (adjusted *p-value*< 0.05; BH correction) is shown in **Table 5**: ten genera were overrepresented in the healthy samples (majority of *Bacteroidetes* and *Alphaproteobacteria*) and seven in the symptoms samples (mainly *Proteobacteria*).

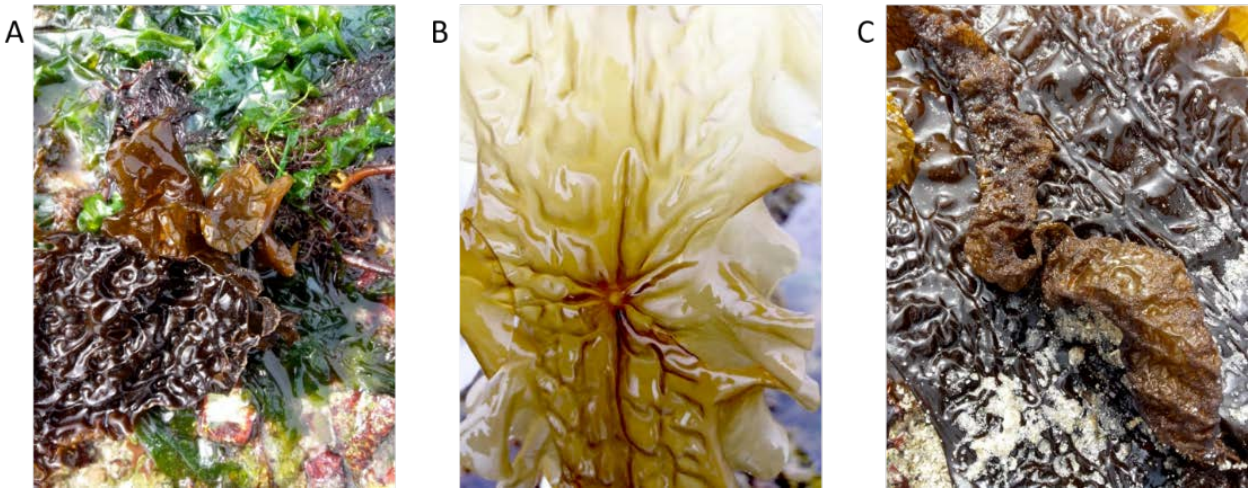

Figure 19 – Examples of symptoms observed on "diseased" *S. latissima* individuals. A) twisted blade, B) hole and C) bubbling in blade

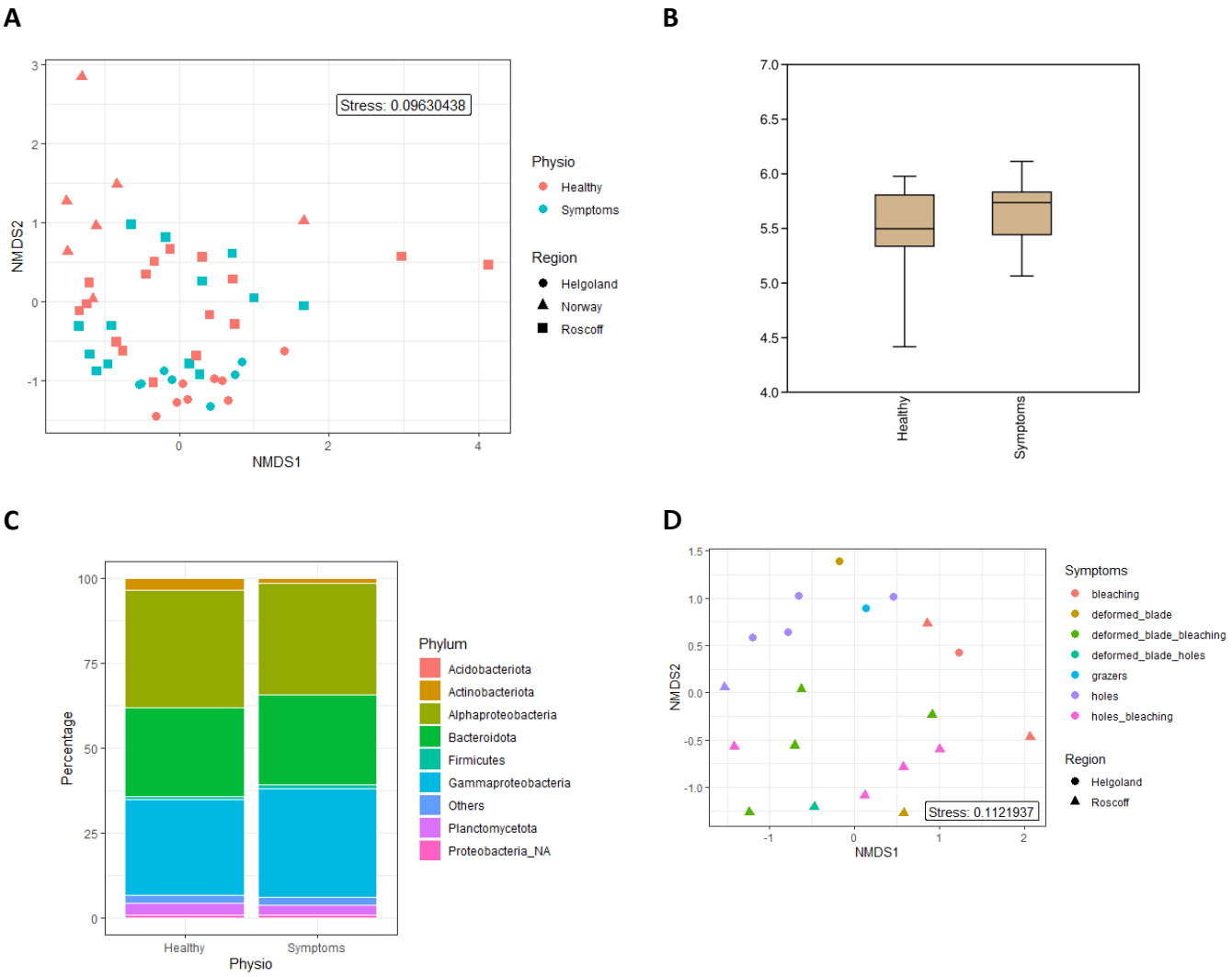

Figure 20 – Symptoms analyses. A) NMDS analysis of the microbiome composition. Results do not show a separation of the healthy and symptoms samples. B) Box plot of alpha-diversity (Shannon H index) across different sample types. *p-value=0.046*. C) Microbiome composition of healthy and symptoms samples. Distribution of 16S rRNA gene metabarcoding sequences per phylum. *Proteobacteria_NA*: not classified as Alpha- or Gammaproteobacteria. D) NMDS analysis of the microbiome composition depending on the symptoms.

IV. Discussion

Here we compared bacterial communities derived from *S. latissima* by 16S metabarcoding analysis to study the diversity and composition of the bacterial communities of this alga. The impacts of several factors on bacterial communities were examined: algal blade part, origin of the host, season, and host condition.

1. The blade part is the primary driver of samples separation

Distinct bacterial communities were demonstrated to be associated with different parts of *S. latissima* by 16S metabarcoding, and this is the primary factor of separation regardless of the other ones (region, season and physiology). Staufenberger et al. (2008) found the same type of dynamics when working on several *S. latissima* tissue from the Baltic Sea and the North Sea, sampled in winter and spring.

S. latissima's type of growth can explain this difference in bacterial communities. *S. latissima* is a perennial species, and growth occurs mainly in the meristem region. From there, the proliferating cells compose the thallus. Young algae only have short blades and no access to the surrounding sediment as they only stand up in the water column. As it grows, the thallus becomes heavier, and the apex finally bends and touches the ground (Kain, 1979; Lüning, 1991). The old blade is moved over by water currents resulting in access to nearby substrates and a broader environment. Mechanical stress is also occurring in this part, then it becomes more vulnerable to bacterial decomposition, offering new ecological niches for different bacteria. Therefore, the younger meristem tissues are typically less colonised by bacteria and exhibit lower bacterial diversity, as already found in previous studies (Staufenberger et al., 2008; Goecke et al., 2010; Ihua et al., 2020; Lemay et al., 2021). Furthermore, the synthesis or release of compounds that either has an antimicrobial effect or act as nutrients for the bacteria may vary between the different parts of the blade. This was described for phenolic substances in the kelp *L. hyperborea* and likely contributed to differences in the microbial composition (Bengtsson et al., 2012).

Our study found a higher proportion of *Planctomycetes* at the apex and *Actinobacteriota* almost exclusively in the meristem. Both phyla are classically found in brown macroalgae (Hollants et al., 2013) and on *S. latissima* [apex: Staufenberger et al. (2008); meristem: Tourneroche et al. (2020)]. *Planctomycetes* are known to contain a high number of sulfatase genes (Wegner et al., 2013), which are involved in degrading sulphated polysaccharides. They may also be involved in degrading polysaccharides from the extracellular matrix of microbial biofilms (Parrot et al., 2019), which may explain their higher relative abundance in older tissues that exhibit first signs of degradation. *Actinobacteriota*, on the other hand, is a diverse phylum that has successfully

colonised a wide range of habitats (Ul-Hassan and Wellington, 2009), but we currently do not know what features make them successful colonisers of *the S. latissima* meristem.

The bacterial core, too, reveals the shift from a low to a higher diversity as the blade grows with four genera found in both algal parts, and five addition genera found in >90% of apex samples. Those taxa were also found on the meristem part of *L. digitata* (Ihua et al., 2020) and on the blade of *L. setchellii* (Lemay et al., 2021), *T. atomaria* (Paix et al., 2021) and *U. lactuca* (Comba González et al., 2021). The genus *Granulosicoccus* (*Gammaproteobacteria*) was one of the most abundant genera (12% of total reads) and included several ASVs overexpressed in the meristem samples. This genus was also found abundantly on the youngest parts of the sister species *S. japonica* (Balakirev et al., 2012; Zhang et al., 2020) and other kelps like *L. setchellii, L. hyperborea, Nereocystis* and *Macrocystis* (Bengtsson et al., 2012; Weigel and Pfister, 2019; Lemay et al., 2021), reinforcing the idea of a strong association between *Granulosicoccus* and the kelp tissue. In the same vein, the genus *Algitalea* (*Flavobacteriaceae*; 3% of total reads) was one of the genera of the "apex" bacterial core and included several ASVs overexpressed in the apex samples. This genus belonged to the pioneer bacterial communities found on the apical parts of *T. atomaria* (Paix et al., 2020). Also, the *Flavobacterium* lineage has been recognised as necessary in the decomposition processes of organic matter during algae blooms (Riemann et al., 2000; Pinhassi et al., 2004) and thus may participate in the decay process occurring at the algal apices.

2. Regional specificities: tides, seawater, and genetics

Aside from the apex/meristem duality, the region of origin also was a decisive separation factor. Lachnit et al. (2009) has already shown this type of region-dependent separation by comparing global epibacterial communities on algae originating from the North and Baltic Seas. In this study, only *S. latissima* showed regional differences within conspecific algae (contrary to the two other studied *Phaeophyceae*). At a larger geographical scale, results on *Ulva* sp. and *Agarophyton vermiculosum* (Roth-Schulze et al., 2018; Bonthond et al., 2020) suggested that the seaweed microbiota composition, diversity and functions strongly depend on the local scale, but also shows that processes are acting at larger scales to shape this microbial community, and they need to be identified.

In our study, the regional differences were more pronounced than the seasonal differences obtained for one sampling site, suggesting that region and not just variability between samplings was the driving factor. The regional differences might be due to tidal range, wave exposure, currents, seawater temperature, or other physicochemical parameters. The tidal ranges for the three regions increase going north: 10 meters in Roscoff, 3 meters in Helgoland and less than 1 meter in Skagerrak. Increasing time exposure to abiotic factors like rain, wind, or sunlight (UV) can lead to cellular stress, and by extension, senescence. This changing environment can offer new ecological niches for different bacteria. Also, bacterial communities can be altered by physicochemical parameters such as temperature, UV light, high hydrostatic pressures, pH, and salinity by nutrient supply, interspecies competition, and viral infection (Stal and Cretoiu, 2016), and those parameters impact the microbial biogeography (Fuhrman et al., 2015). In the same vein, winter seawater temperatures are lower in the north, and this might favour psychrophilic strains over mesophilic communities, as found in a culture-based study on the surface bacteria of *L. longicruris* (Laycock, 1974).

The regional split might also be due to the genetic diversity of the algae. Using single nucleotide polymorphisms (SNPs) and microsatellites, Guzinski et al. (2016, 2020) determined that algae from Roscoff, Helgoland, and Norway are genetically different, and this might lead to the attraction of different bacterial species (Griffiths et al., 2019). Furthermore, *S. latissima* displays a unique lipidomic signature depending on its geographic origin (Monteiro et al., 2020), as the content of chemical elements (C, H, N, S), fatty acids, and lipids varies depending on the region. These molecules are common components of membranes (Harwood, 2004) and might influence the attractiveness of the algal surface for several bacterial strains.

3. Shifts in bacterial communities depending on the season

The third separation factor was seasonality. Laycock (1974) found that as the season become colder, the bacterial communities of *L. longicruris* shift from mesophilic to psychrophilic strains. When working with *L. hyperborea,* Bengtsson et al. (2010) have hypothesised that the seasonal succession in the bacterial communities might be explained by abiotic factors like seawater temperature and biotic factors like seasonal changes in the kelp substrate. However, seawater

temperature alone does not seem to have been the most important factor in our data, as the seawater was coldest in winter and spring (<12°C), but the samples from autumn and winter are grouped. Other physicochemical parameters might also play a role. Nitrogen is a quantitatively and qualitatively important element for organisms, and microorganisms can take up nitrogen in different forms such as nitrate, nitrite, ammonium, urea, organic nitrogen, and dinitrogen gas (N2), depending on the organism. Among these elements, the nitrates, nitrites, and ammonium concentrations follow seasonal variations, with nitrates being lower in summer and higher in winter and nitrites at their highest in autumn. Phosphorus is another essential nutrient for primary production in the euphotic zone. Most of the phosphorus is present in the oxidised form as free phosphate or bound to organic matter. The phosphate concentration was at its lowest in Roscoff springtime. Several ASVs overrepresented in spring belong to the *Roseobacter* lineage, and Atlantic strains of this genus are known to possess abundant high-affinity phosphorus uptake systems, constituting likely adaptations to low environmental phosphate concentrations (Newton et al., 2010).

Lastly, seasonal variations may also be due to seasonal changes in the alga's chemical composition. For instance, Schiener et al. (2015) demonstrated that in *S. latissima,* polyphenol levels are higher between May and July and decrease to be at their lowest in March. This could be interpreted as a defence against bacterial colonisation as the seawater temperature rises, the polyphenols being known for their wide range of antimicrobial properties (Zhang et al., 2006; Daglia, 2012). Also, the carbohydrates (laminarin and mannitol) content is higher in summer (Schiener et al., 2015), and these are substrates easy to degrade by the bacteria (Alderkamp et al., 2007; Jeske et al., 2013; Groisillier et al., 2015). Similarly, the iodine content is lower in summer (Nitschke et al., 2018), and the algae's production of toxic iodine compounds may control the surface biofilm and repulse microbial pathogens (Rodeheaver et al., 1982; Gobet et al., 2017).

4. Is microbiota a characteristic signature for algae in poor health?

Some bacteria affect the alga in a deleterious manner by decomposing cell material, like alginate and laminarin (Laycock, 1974; Dimitrieva and Dimitriev, 1997; Sawabe et al., 1998b; Ivanova et al., 2003) or by causing diseases like *Alteromonas* species (Vairappan et al., 2001; Peng and Li,

2013) and species of *Pseudoalteromonas* (Sawabe et al., 1998a). Ihua et al. (2019) have shown that the microbial communities (phyla level) associated with intact *Ascophyllum* differs from the rotting algae and suggested that the decay process might shape the associated bacterial community. Similarly, the microbial communities of *Ecklonia* are strongly associated with the algal conditions (stressed or not), more than with other variables (Marzinelli et al., 2015). Moreover, it has been observed that the core bacterial community characteristic of healthy algae may be lost when hosts are subjected to stress, and the microbiota of stressed individuals are more similar to each other at a given location than those on healthy hosts (Marzinelli et al., 2015).

All these data reinforce our hypothesis of microbiota as a characteristic signature for algae in poor health. In our study, the changes in bacterial communities are visible only at a lower taxa scale, and we found 82 ASVs that were differentially expressed between the healthy (45 ASVs) and symptoms samples (37 ASVs). Several of these "symptoms" ASVs (27% of ASVs) belong to the *Pseudoalteromonas* genus, and the taxonomic affiliation of ASVs is distributed among the *Proteobacteria* (57%) and the *Planctomycetes* (3%). The taxonomy of ASVs characteristic for healthy samples is more diverse at the phyla level, with several ASVs belonging to *Bacteroidetes* (22%), *Alpha-* and *Gammaproteobacteria* (20% and 11%). The fact that so many ASVs were found to differ indicates that, regardless of the type of disease, an alga that is not well will undergo characteristic changes in the microbiome. Moreover, these ASVs signatures are probably stable because they are derived from different places and times of the year, and types of symptoms, as shown with *Ecklonia* (Marzinelli et al., 2015). Although this would require additional developments, these signatures might also be helpful as bioindicators for kelp health.

V. Conclusion

In conclusion, our study provides an extensive overview of the *S. latissima* microbiome and highlights several factors driving its variability. In particular, the observation that the blade part had a more profound impact on the microbial composition than season or region, both of which are associated with changes in the abiotic environment, underlines the extent to which the algal hosts select their associated microbiota. Our discovery of microbial signatures characteristic for diseased *S. latissima* individuals that persist in our dataset independently of the disease

symptoms further supports this hypothesis. Given the variety of symptoms observed in our samples, it is unlikely that the same bacteria could be the causative agents in all cases, but rather that the different types of disease likely cause similar changes in the host, which would lead to similar microbial changes. Understanding these signatures will not only be of interest for fundamental research on the different algal diseases, in the long run, it may also help develop molecular markers of host health to survey natural populations or aquacultures.

VI. Tables

Table 2 – Taxonomic affiliations of the ASVs specific to the apex and meristem samples, compared with their occurrence in the entire dataset.

Taxa	APEX				MERISTEM				Entire dataset		
	Number of over-expressed ASVs	Total number of over-expressed ASVs	ratio	p-value	Number of over-expressed ASVs	Total number of over-expressed ASVs	ratio	p-value	Number of ASVs	Total number of ASVs	ratio
Rubidimonas	1	29	0.03448	0.02635 *	0	21	0	0.16780	157	18028	0.00871
Algitalea	6	29	0.20689	<0.00001 ***	0	21	0	0.36524	386	18028	0.02141
Robiginitomaculum	4	29	0.13793	<0.00001 ***	0	21	0	0.09976	90	18028	0.00499
Rhodobacteraceae_NA	7	29	0.24138	0.00001 ***	0	21	0	0.57562	721	18028	0.03999
Litorimonas	9	29	0.31034	<0.00001 ***	3	21	0.14286	0.00391 *	571	18028	0.03167
Maribacter	0	29	0	0.18800	3	21	0.14286	0.00001 ***	129	18028	0.00716
Granulosicoccus	0	29	0	0.79855	15	21	0.71429	<0.00001 ***	969	18028	0.05375

Table 3 – Taxonomic affiliations of the ASVs specific to Roscoff, Helgoland, or Norway samples compared with their occurrence in the entire dataset.

Taxa	Roscoff				Helgoland				Norway				Entire dataset		
	Number of over-expressed ASVs	Total number of over-expressed ASVs	ratio	p-value	Number of over-expressed ASVs	Total number of over-expressed ASVs	ratio	p-value	Number of over-expressed ASVs	Total number of over-expressed ASVs	ratio	p-value	Number of ASVs	Total number of ASVs	ratio
Tenacibaculum	1	25	0.04000	0.00023 ***	4	102	0.03922	<0.0001 ***	0	41	0	0.03575	272	18028	0,01509
Hellea	1	25	0.04000	0.00040 ***	0	102	0	0.11209	0	41	0	0.04666	187	18028	0,01037
Litorimonas	7	25	0.28000	<0.0001 ***	0	102	0	0.65477	0	41	0	0.34787	571	18028	0,03167
Parvularculaceae_NA	1	25	0.04000	0.00040 ***	0	102	0	0.11209	0	41	0	0.04666	32	18028	0,00178
Tateyamaria	2	25	0.08000	0.00058 ***	0	102	0	0.48820	0	41	0	0.23604	50	18028	0,00277
Marinicella	1	25	0.04000	0.00033 ***	0	102	0	0.10197	0	41	0	0.04231	65	18028	0,00361
Granulosicoccus	4	25	0.16000	<0.0001 ***	9	102	0.08824	<0.0001 ***	1	41	0.02439	0.00971 **	969	18028	0,05375

Saprospiraceae_NA	0	25	0	0.19641	28	102	0.27451	<0.0001 ***	3	41	0.07317	0.00045 ***	1766	18028	0,09796
Rhodobacteraceae_NA	0	25	0	0.04874	2	102	0.01961	0.00118 **	3	41	0.07317	<0.0001 ***	721	18028	0,03999
Arenicella	0	25	0	0.06708	7	102	0.06863	<0.0001 ***	3	41	0.07317	<0.0001 ***	644	18028	0,03572
Gammaproteobacteria_NA	3	25	0.12000	0.00002 ***	13	102	0.12745	<0.0001 ***	2	41	0.04878	0.00204 **	768	18028	0,04260
Sva0996_marine_group	0	25	0	0.15022	3	102	0.02941	0.00455 **	0	41	0	0.23429	117	18028	0,00649
Sporolactobacillus	0	25	0	0.14188	3	102	0.02941	0.00366 **	0	41	0	0.22193	55	18028	0,00305
Blastopirellula	0	25	0	0.07354	11	102	0.10784	<0.0001 ***	0	41	0	0.11775	274	18028	0,01520
Dokdonia	0	25	0	0.09145	0	102	0	0.32372	5	41	0.12195	<0.0001 ***	371	18028	0,02058
Marinicaulis	0	25	0	0.11761	0	102	0	0.39979	2	41	0.04878	0.00115 **	21	18028	0,00116
Micavibrionaceae_NA	0	25	0	0.04344	0	102	0	0.16574	1	41	0.02439	0.00247 **	234	18028	0,01298
Pseudahrensia	0	25	0	0.29765	0	102	0	0.76345	4	41	0.09756	0.00027 ***	91	18028	0,00505
Litoreibacter	0	25	0	0.11883	0	102	0	0.40320	3	41	0.07317	0.00006 ***	36	18028	0,00200
Sulfitobacter	0	25	0	0.10896	0	102	0	0.37542	1	41	0.02439	0.01543 *	118	18028	0,00655
Yoonia-Loktanella	0	25	0	0.06707	0	102	0	0.24670	1	41	0.02439	0.00587 **	94	18028	0,00521
Sphingorhabdus	0	25	0	0.07996	0	102	0	0.28826	1	41	0.02439	0.00833 **	55	18028	0,00305
Geminicoccaceae_NA	0	25	0	0.07354	1	102	0.00980	0.03921	1	41	0.02439	0.00705 **	20	18028	0,00111
Colwellia	0	25	0	0.02737	0	102	0	0.10705	1	41	0.02439	0.00098 ***	107	18028	0,00594
Pseudoalteromonas	0	25	0	0.12373	0	102	0	0.41662	3	41	0.07317	0.00007 ***	50	18028	0,00277

Table 4 – Taxonomic affiliations of the ASVs specific to each season from Roscoff samples, compared with their occurrence in the entire dataset

Taxa	Winter				Spring				Summer				Autumn				Entire dataset		
	Number of over-expressed ASVs	Total number of over-expressed ASVs	ratio	p-value	Number of over-expressed ASVs	Total number of over-expressed ASVs	ratio	p-value	Number of over-expressed ASVs	Total number of over-expressed ASVs	ratio	p-value	Number of over-expressed ASVs	Total number of over-expressed ASVs	ratio	p-value	Number of ASVs	Total number of ASVs	ratio
Cytophagales_NA	1	19	0.05263	0.00113 **	0	49	0	0.12007	0	17	0	0.04341	0	17	0	0.04341	47	18028	0.00261
Yoonia-Loktanella	3	19	0.15789	<0.0001 ***	0	49	0	0.22595	0	17	0	0.08502	0	17	0	0.08502	94	18028	0.00521
Gammaproteobacteria_NA	9	19	0.47368	<0.0001 ***	1	49	0.02041	0.62284	0	17	0	0.52265	0	17	0	0.52265	768	18028	0.04257
Cryomorphaceae_NA	0	19	0	0.0554	1	49	0.02041	0.00961 **	0	17	0	0.04972	0	17	0	0.04972	54	18028	0.00300
Maritimimonas	0	19	0	0.02293	1	49	0.02041	0.00169 **	0	17	0	0.02054	0	17	0	0.02054	22	18028	0.00122

NS7_marine_group	0	19	0	0.02499	1	49	0.02041	0.002 *	0	17	0	0.02239	0	17	0	0.02239	24	18028	0.00133
Octadecabacter	0	19	0	0.08394	2	49	0.04082	0.00153 **	0	17	0	0.07545	0	17	0	0.07545	83	18028	0.00460
Colwellia	0	19	0	0.10691	2	49	0.04082	0.00314 **	0	17	0	0.09622	0	17	0	0.09622	107	18028	0.00593
Roseobacter	0	19	0	0.03012	2	49	0.04082	0.00007 ***	0	17	0	0.02699	0	17	0	0.02699	29	18028	0.00161
Pseudoalteromonas	0	19	0	0.05138	2	49	0.04082	0.00036 ***	0	17	0	0.0461	0	17	0	0.0461	50	18028	0.00277
Psychromonas	0	19	0	0.07612	4	49	0.08163	<0.0001 ***	0	17	0	0.06838	0	17	0	0.06838	75	18028	0.00416
Granulosicoccus	2	19	0.10526	0.0789	20	49	0.40816	<0.0001 ***	0	17	0	0.60875	0	17	0	0.60875	969	18028	0.05371
NS9_marine_group	0	19	0	0.07811	0	49	0	0.1892	1	17	0.05882	0.00238 **	0	17	0	0.07018	77	18028	0.00427
Sva0996_marine_group	0	19	0	0.11636	0	49	0	0.27315	3	17	0.17647	<0.0001 ***	0	17	0	0.10478	117	18028	0.00649
Micavibrionales_NA	1	19	0.05263	0.0146	1	49	0.02041	0.08295	2	17	0.11765	0.00057 ***	0	17	0	0.15361	176	18028	0.00976
Pseudahrensia	0	19	0	0.09167	0	49	0	0.21961	2	17	0.11765	0.00008 ***	0	17	0	0.08243	91	18028	0.00505
Pontivivens	0	19	0	0.01569	0	49	0	0.03996	1	17	0.05882	0.00009 ***	0	17	0	0.01405	15	18028	0.00083
Saccharimonadales_NA	0	19	0	0.01049	0	49	0	0.02682	1	17	0.05882	0.00004 ***	0	17	0	0.00939 **	10	18028	0.00055
Tenacibaculum	0	19	0	0.25088	1	49	0.02041	0.16886	0	17	0	0.22775	2	17	0.11765	0.00199 **	272	18028	0.01509
Micavibrionaceae_NA	0	19	0	0.21982	0	49	0	0.4728	1	17	0.05882	0.02013	2	17	0.11765	0.0013 **	234	18028	0.01298
Erythrobacter	0	19	0	0.06136	0	49	0	0.15068	0	17	0	0.05509	1	17	0.05882	0.00146 **	60	18028	0.00332
Perspicuibacter	0	19	0	0.13117	0	49	0	0.30414	0	17	0	0.11821	1	17	0.05882	0.00687 **	133	18028	0.00737
Thalassotalea	0	19	0	0.09548	0	49	0	0.22802	0	17	0	0.08587	2	17	0.11765	0.00009 ***	95	18028	0.00527
C1-B045	0	19	0	0.03521	0	49	0	0.08829	0	17	0	0.03156	1	17	0.05882	0.00047 ***	34	18028	0.00188
Halomonas	0	19	0	0.01048	0	49	0	0.0268	0	17	0	0.00938	1	17	0.05882	0.00004 ***	10	18028	0.00055

Table 5 – Taxonomic affiliations of the ASVs specific to the healthy and symptoms samples compared with their occurrence in the entire dataset

Genera	**Healthy**				**Symptoms**				**Entire dataset**		
	Number of over-expressed ASVs	Total number of over-expressed ASVs	ratio	p-value	Number of over-expressed ASVs	Total number of over-expressed ASVs	ratio	p-value	Number of ASVs	Total number of ASVs	ratio
Saprospiraceae_NA	9	45	0.20000	0.01048 *	4	37	0.10811	0.29425	1766	18028	0.09796
Ulvibacter	1	45	0.02222	0.00650 **	0	37	0	0.09394	48	18028	0.00266
Sporolactobacillus	1	45	0.02222	0.00845 **	0	37	0	0.10690	55	18028	0.00305

Robiginitomaculum	4	45	0.08889	<0.00001 ***	0	37	0	0.16904	90	18028	0.00499
Parvularculaceae_NA	1	45	0.02222	0.00296 **	0	37	0	0.06362	32	18028	0.00178
Sulfitobacter	2	45	0.04444	0.00324 **	0	37	0	0.21570	118	18029	0.00655
Escherichia/Shigella	2	45	0.04444	0.00002 ***	0	37	0	0.03825	19	18036	0.00105
Pseudahrensia	2	45	0.04444	0.00156 **	2	37	0.05405	0.00088 ***	91	18028	0.00505
Litoreibacter	0	45	0	0.08602	2	37	0.05405	0.00006 ***	36	18028	0.00200
Planctomycetales_NA	0	45	0	0.05110	1	37	0.02703	0.00088 ***	21	18028	0.00116
Yoonia-Loktanella	0	45	0	0.20961	4	37	0.10811	<0.00001 ***	94	18030	0.00521
Colwellia	0	45	0	0.23496	3	37	0.08108	0.00007 ***	107	18032	0.00593
Pseudoalteromonas	0	45	0	0.11745	10	37	0.27027	<0.00001 ***	50	18033	0.00277
Marinicella	0	45	0	0.14995	1	37	0.02703	0.00795 **	65	18037	0.00360

VII. Declarations

Funding: This work was funded partially by ANR project IDEALG (ANR-10-BTBR-04) "Investissements d'Avenir, Biotechnologies-Bioressources", the CNRS momentum call (2017) and from the European Union's Horizon 2020 research and innovation programme under grant agreement No 730984, ASSEMBLE Plus project. BBD was funded by a joint PhD scholarship from the Brittany region (Project HOSALA) and the Sorbonne University (ED227).

Competing interests: The authors declare that they have no competing interests.

Data availability: Raw sequence data were deposited at the European Nucleotide Archive under project accession number ENA: PRJEB47035.

Code availability: not applicable

Authors' contributions: Designed study: BBD, SD; Sampling: BBD, SF, SD; Performed experiments: BBD, EL, GT; Analysed data: BBD, SD; Wrote the manuscript: BBD, SD; Provided valuable input and corrected the manuscript: CB.

VIII. Acknowledgements

We thank François Thomas, Maéva Brunet and Nolwen Le Duff for their primers and for providing the mock community; Sylvie Rousvoal for advice on sample preparation, Jonas Collén for advice and participating in the first sampling, Kai Bishof and Nora Diehl for providing samples from Svalbard, which unfortunately could not be included, and Catherine Leblanc for helpful discussions. This work benefited from access to the Station Biologique de Roscoff, an EMBRC-France and EMBRC-ERIC Site.

IX. Supplementary data

Table S2 - Taxonomic affiliations of over-expressed ASVs for each comparison (algal part, regions, seasons and symptoms)

Data available via link : https://doi.org/10.5281/zenodo.5752111

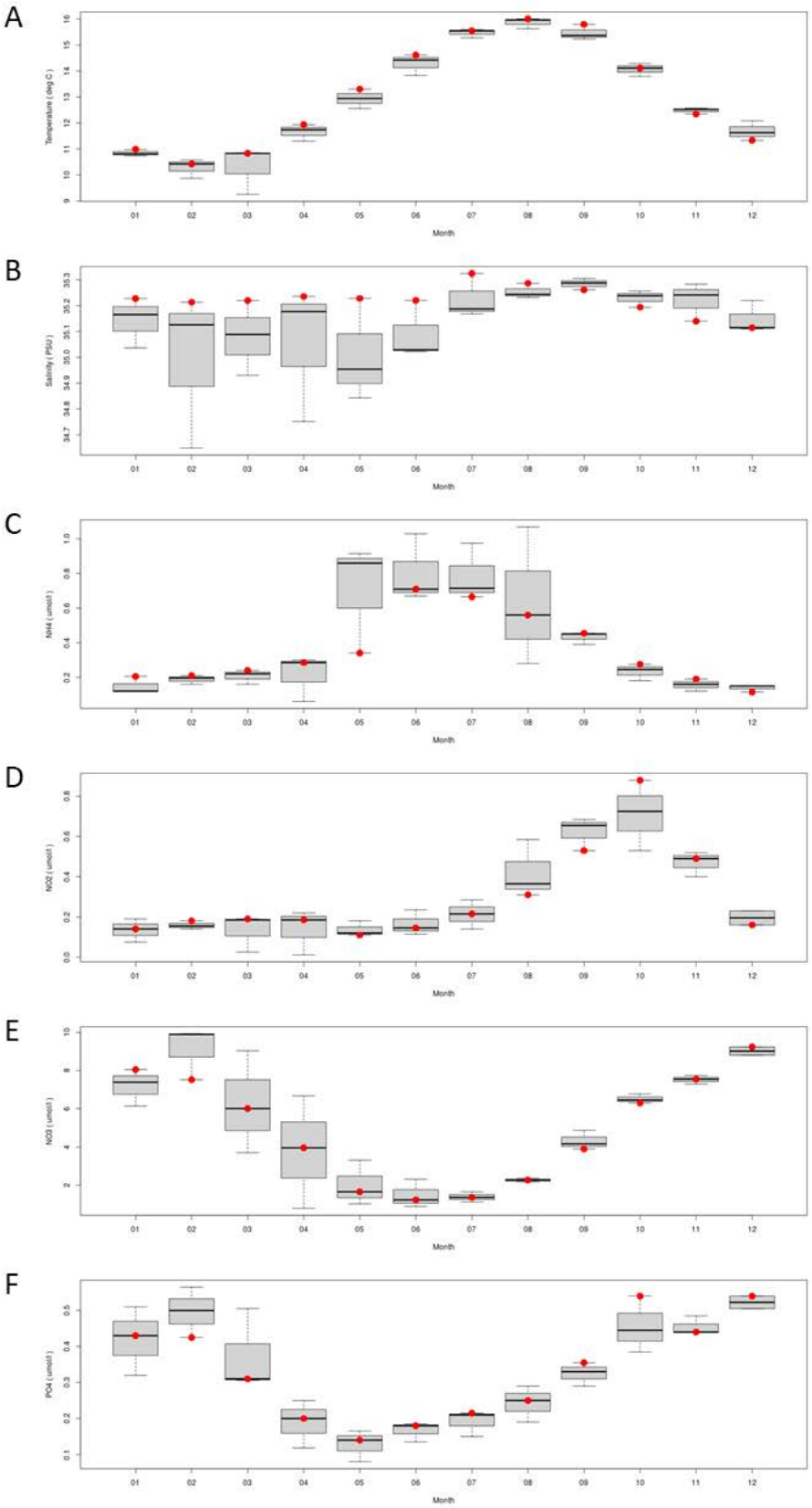

Figure S1 – Seasonal variations in A) temperature, B) salinity and C) ammonium, D) nitrites, E) nitrates, and F) phosphate concentrations. Roscoff, 2019. Legend for each month, rectangle: region inside 1st and 3rd quartiles, bold line: median value, dashed error bars: 1st and 9th deciles, red point: value for the selected year

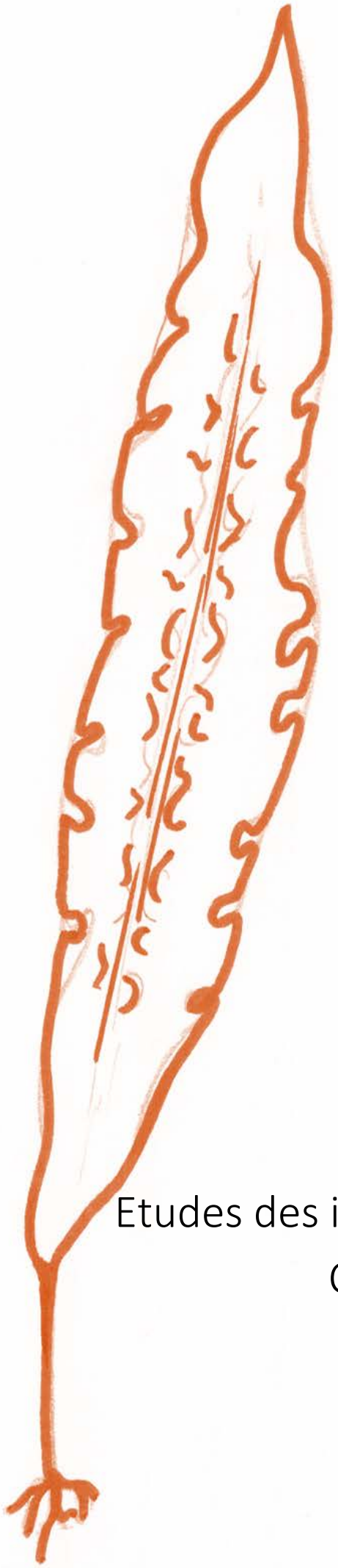

- CHAPITRE III -

Etudes des interactions algues-bactéries : Croissance & Quorum Sensing

CHAPITRE III - Etude des interactions algues-bactéries : Croissance & Quorum-Sensing

L'objectif de ce chapitre est d'aller au-delà des approches descriptives du chapitre précédent, et d'essayer de manipuler le microbiote pour comprendre son impact général, et celui de certaines souches en particulier, sur la croissance de *S. latissima*. Dans ce but, des cocultures (CC) ont été mises en place.

Ce type d'expériences et d'analyses a déjà été développé sur *Ectocarpus* au sein de l'équipe (cf. **section I** de ce chapitre), en particulier pendant la thèse d'Hetty KLEINJAN et mon stage de M2, et ces résultats ont influencé mon travail de thèse. Entre autres, nous avons montré que le microbiote est indispensable à la croissance de l'algue, modifie la morphologie d'*Ectocarpus,* et permet la production de composés spécifiques.

Pour ma thèse, les souches bactériennes nécessaires à la réalisation des cocultures ont été isolées à partir d'algues saines ou avec symptômes prélevées à Roscoff et Helgoland (cf. **Chapitre II** et **section II** de ce chapitre).

Des expériences préliminaires de cocultures croisées (*S. latissima* + souches bactériennes d'*Ectocarpus*) ont montré un effet à l'opposé de celui obtenu sur *Ectocarpus,* une des souches devenant néfaste pour l'hôte.

Par ailleurs, les cocultures de *S. latissima* et de ses souches bactériennes ont donné des résultats inattendus, certaines souches n'ayant pas l'effet escompté, et le milieu de culture utilisé impactant aussi la croissance.

Ces résultats ont été utilisés pour tester l'hypothèse sous-jacente du Quorum Sensing (QS), mode de communication bactérien concentration-dépendant. En effet, lors de sa thèse Hetty KLEINJAN a mis en évidence l'activation de voies de biosynthèse de molécules impliquées dans ce processus bactérien, en particulier au contact d'un hôte algal stressé.

Ainsi, ce chapitre a pour but de discuter de l'impact de souches bactériennes d'intérêt sur la croissance de *S. latissima* et sur la composition générale du microbiote de l'algue.

Les résultats sont ensuite discutés en tenant compte du phénomène de quorum sensing, et de son lien avec une perturbation de la croissance.

I. Contexte

1. *Ectocarpus,* microbiote et transcriptome

La thèse d'Hetty KLEINJAN « *The influence of bacteria on the adaptation to changing environments in Ectocarpus : a systems biology approach* » a vu la création de trois holobiontes avec des communautés bactériennes différentes (traitements antibiotiques différents) pour d'étudier l'adaptation d'*Ectocarpus* à un changement de salinité grâce à son microbiote. Le métatranscriptome et le métabolome de ces holobiontes ont été analysés pendant des expériences d'acclimatation (KleinJan et al., 2021). Dans les conditions de stress hyposalin, une activation de la voie de biosynthèse des AHLs (composés qui régulent le quorum-sensing ; cf. **section I. 4** de ce chapitre) est observée. En effet, les données de transcriptomique montrent qu'en condition de stress, les réactions impliquant des enzymes acyl-homoserine-lactones synthase sont fortement surexprimées chez *Hoeflea, Sulfitobacter* et *Roseovarius*. Une augmentation de l'abondance bactérienne a aussi été observée dans ces conditions, et ces résultats sont en accord avec l'hypothèse d'une dysbiose au sein de l'holobionte.

2. *Ectocarpus et l'impact de son microbiote*

Dans le cadre de cette thèse sur *Ectocarpus*, douze génomes bactériens qui représentaient le mieux la diversité du microbiome ont également été séquencés, puis les réseaux métaboliques correspondants ont été produits grâce au logiciel Pathway Tools (Karp et al., 2002). L'équipe Dyliss de l'IRISA (*DYnamics, Logics and Inference for biological Systems and Sequences*, Rennes, France) a réalisé des analyses de complémentarité des réseaux métaboliques d'*Ectocarpus* et des 12 bactéries associées, l'hypothèse de départ étant que plus les réseaux métaboliques sont complémentaires, plus il y a des possibilités d'échanges métaboliques bénéfiques, et donc que les interactions puissent être bénéfiques. Grâce aux données de complémentation, l'équipe a réussi à sélectionner des micro-communautés bactériennes parmi ces 12 bactéries qui complémentaient le réseau d'*Ectocarpus*, et j'ai testé l'impact *in vivo* de ces communautés bactériennes sur l'algue (Burgunter-Delamare et al., 2020). Les résultats obtenus montrent que les souches bactériennes ont un impact positif sur la croissance (Erreur ! Source du renvoi introuvable.), modifient la morphologie et induisent la production de composés spécifiques.

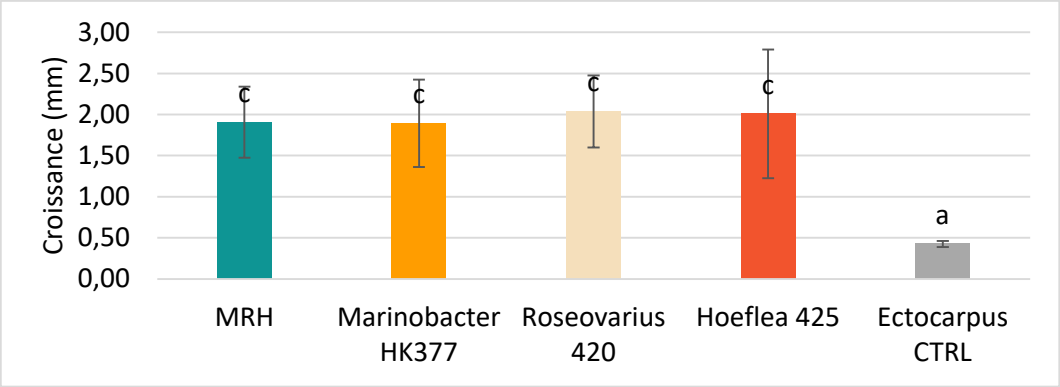

Figure 21 – Croissance Croissance en mm des algues (*Ectocarpus*) après 4 semaines de coculture, adapté de Burgunter-Delamare et al. (2020)

3. Cocultures croisées *S. latissima* et bactéries d'*Ectocarpus*

Un des mélanges testé (MRH : *Marinobacter* sp. HK377, *Roseovarius* sp. 420, *Hoeflea* sp. 425) a été choisi pour réaliser des cocultures avec *Saccharina latissima*, dans le cadre du stage de L3 d'Ulysse Flandrin, co-encadré par Sylvie Rousvoal et moi-même en 2019.

Les plantules de *S. latissima* ont été co-cultivées avec les trois souches bactériennes seules ou en mélange. A l'issue des 8 jours de cocultures, les taux de croissance des plantules inoculées avec *Marinobacter (377)*, *Roseovarius* (420) et le mélange MRH sont quasiment similaires à celui du contrôle non inoculé, alors que la croissance des plantules inoculées avec *Hoeflea* (425) est fortement diminuée (**Figure 22**).

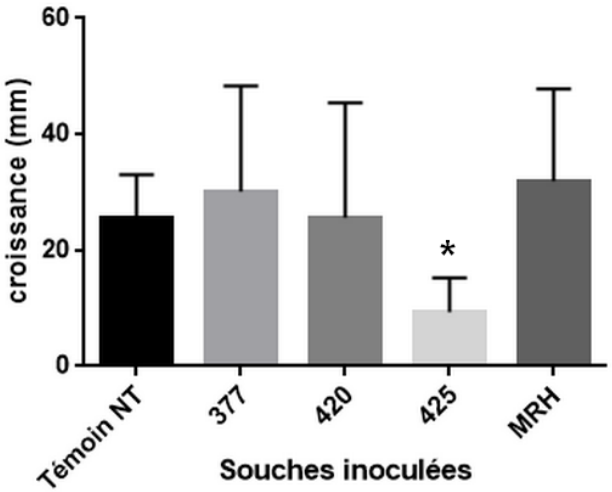

Figure 22 – Taux de croissance relatif (mm) des plantules de *S. latissima* To-T5

Cette récupération du phénotype suggère que l'effet négatif de certaines souches pourrait être inhibé ou contrebalancé au sein d'une communauté bactérienne. Une de nos hypothèses,

en partie basée sur les résultats de transcriptomique, est que cet effet récupération, et l'effet négatif en lui-même, pourraient être induits par des composés impliqués dans le phénomène de Quorum Sensing.

4. Le phénomène de Quorum-Sensing

a. Définition

Le **Quorum Sensing** (QS) est un mode de communication/perception utilisé par les bactéries, aussi bien Gram+ que Gram -, dans l'établissement d'un comportement de groupe. Il y a quatre grandes étapes dans le QS (Sifri, 2008; Verbeke et al., 2017) : 1) la synthèse de molécules signal (auto-inducteurs, AI), et 2) leur excrétion, 3) quand la concentration seuil est atteinte, des récepteurs spécifiques sont activés, et ainsi 4) l'expression de gènes est modulée.

Les gènes impliqués dans le QS sont responsables d'activités qui n'ont lieu que lorsque la densité cellulaire est élevée : formation de biofilm, bioluminescence, production d'antibiotiques, de toxines, d'exopolysaccharides et de facteurs de virulence, activités qui sont essentielles dans leur relation, bénéfique ou non, avec leur hôte (Ohtani et al., 2002; Marketon et al., 2003; Labbate et al., 2004; Quiñones et al., 2005; Suntharalingam and Cvitkovitch, 2005; Rutherford and Bassler, 2012).

b. Les molécules du QS

Diversité des molécules

Les voies de biosynthèse et les structures moléculaires du QS varient selon les bactéries, certaines molécules étant reconnues de manière interspécifique et d'autres intra-spécifique (Atkinson and Williams, 2009).

Les molécules du QS sont diverses (**Table 6**) et prennent la forme d'Acyl-Homoserine Lactones (AHL), d'auto-inducteurs de type 2 (AI-2), d'auto-inducteurs de type 3 (AI-3), Cholerae Auto-Inducteur (CAI), 3-hydroxy Palmitic Acid Methyl Ester (PAME), Pseudomonas Quinolone Signal (PQS), des DiKetoPiperazines (DKP), Diffusible Signal Factor (DSF), Butyrolactone (GBL), facteurs A/B/C/D/E, Auto-Inducing Peptides (AIP), bradyoxetine (CDF), l'acide indole-3-acétique (IAA) et l'acide tropodithietique (TDA). Ici, nous détaillerons les AHL et les AI-2 qui sont les deux types de molécules les plus étudiés.

Table 6 – Les molécules du QS

	Molécules	Bactéries impliquées	Références
Gram –	AHL	*Proteobacteria*	Galloway et al., 2011
	AI-3	*E. coli entérohémorragiques*	Sperandio et al., 2003
	CAI	*Vibrio*	Henke and Bassler, 2004
	PAME	*Ralstonia*	Flavier et al., 1997
	PQS	*Pseudomonas*	McKnight et al., 2000
	DKP	*Proteobacteria*	Holden et al., 2002
	DSF	*Proteobacteria*	Atkinson and Williams, 2009
	Facteurs A/B/C/D/E	*Myxococcus xanthus*	Konovalova et al., 2010
	CDF	*Bradyrhizobium*	Loh et al., 2002
	TDA	*Rhodobacteraceae*	Geng and Belas, 2010
Gram – et +	AI-2	*Bacteria*	Schauder et al., 2001
	IAA	*Bacteria*	Lee and Lee, 2010
Gram +	AIP	*Firmicutes*	Ji et al., 1995
	GBL	*Streptomyces*	Slattery et al., 2001

Les Acyl-Homoserine Lactones (AHLs ou AI-1)

Les Acyl-Homosérine-Lactones ou AHLs sont les autoinducteurs de type 1 (AI-1). Ces molécules sont composées d'une chaine acyle comptant de 4 à 18 carbones (Williams et al., 2007), d'une homosérine et d'un cycle lactone (Eberhard et al., 1981 ; **Figure 23**). Les AHLs sont produites et détectées principalement par des bactéries Gram - appartenant au phylum des *Proteobacteria* (Galloway et al., 2011).

Les AHLs à chaine courte (≤8 carbones, hydrophiles) diffusent à travers l'enveloppe bactérienne et les AHLs à chaine longue (> 8 carbones, hydrophobes) sont émises de manière active par la bactérie (Pearson et al., 1999). Les AHLs s'accumulent dans le milieu extérieur (Fuqua and Greenberg, 2002), mais leur récepteurs sont intracellulaires.

Les AHL sont issus d'une réaction générique qui génère une acyl-homoserine lactone par l'interaction d'une S-adenosyl-L-methionine avec une acyl-[acyl-carrier protein], relâchant une S-methyl-5'-thioadenosine et l'acyl-binding protein (**Figure 23**). L'enzyme qui catalyse cette réaction est une acyl-homoserine-lactone synthase et peut être codée par 3 familles de gènes : luxI, ainS et hdtS (Fuqua and Greenberg, 2002). On sait également que lorsque la densité cellulaire est assez élevée, les AHL accumulées se lient à des protéines DNA-binding

cytoplasmiques qui appartiennent à la famille luxR. Le complexe protéine luxR–AHL reconnait et se lie ensuite à un promoteur régulé par le QS et active alors la transcription de gènes cibles, induisant une réponse QS (Fuqua et al. 2001 ; Safari et al. 2014). Ainsi chaque AHL est synthétisée par une luxI spécifique et correspond à une protéine luxR particulière, ce qui confère un haut niveau de sélection et de complexité (Safari et al., 2014). Un grand nombre de bactéries possèdent plusieurs voies de QS luxR/luxI/AHL qui sont souvent interconnectées (Schaefer et al., 2013).

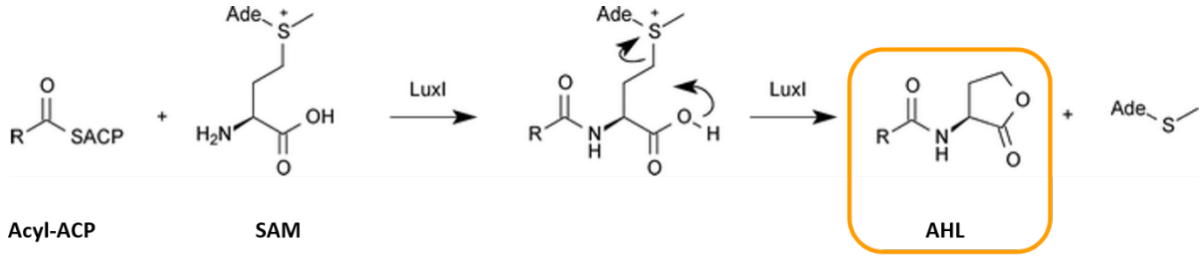

Figure 23 – Voie de biosynthèse des AHL par LuxI, d'après Dickschat (2010)

Les autoinducteurs de type 2 (AI-2)

Les autoinducteurs de type 2 ont été identifiés plus récemment et permettent une communication entre les bactéries Gram - et Gram + (Schauder et al., 2001). Les AI-2 sont produits par deux voies de biosynthèse (une chez les *Vibrio* et une chez les autres bactéries ; **Figure 24**). Les premières étapes sont communes aux deux voies. La conversion de la S-ribosyl-L-homocysteine en L-homocysteine par l'enzyme S-ribosylhomocysteine lyase (luxS) conduit aussi à la production du précurseur des AI-2 (Surette et al., 1999). Par la suite, les précurseurs des AI-2 se transforment spontanément en 2 séries de stéréo-isomères, mais les mécanismes de transformations ne sont pas connus. Il a été montré que certaines bactéries (*E. coli*) peuvent utiliser et dégrader les AI-2 produits par d'autres souches, mais le rôle de ce processus n'est pas encore bien connu. Dans sa voie de dégradation chez *E. coli*, l'AI-2 subit trois transformations enzymatiques (kinase Ec-IsrK, isomérase Ec-IsrG et thiolase Ec-IsrF) et est libéré sous forme de glycerone phosphate (DHAP ; Marques et al., 2014).

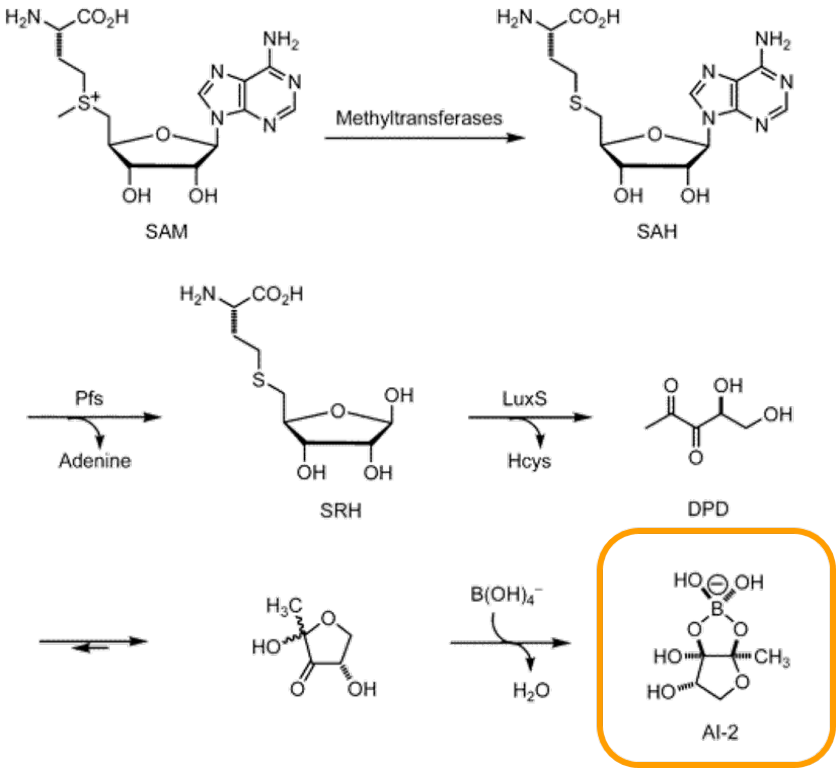

Figure 24 – Voie de biosynthèse des AI-2, d'après Zhu et al. (2004)

c. QS & bactéries associées aux macroalgues

Chez l'algue verte *Ulva*, les AHLs libérés par des bactéries du genre *Sulfitobacter* ont un impact négatif sur la germination des spores (Twigg et al., 2014), alors même que des souches du clade *Roseobacter/Sulfitobacter* sont indispensables à la croissance et la morphogenèse d'*U. mutabilis* et *U. linza* (Spoerner et al., 2012; Vesty et al., 2015). Par ailleurs, la dispersion des spores se fait selon le gradient d'AHLs émis par une colonie bactérienne, et ils s'établissent à proximité de bactéries capables de produire des AHLs (Dobretsov and Qian, 2002; Tait et al., 2005).

Chez l'algue rouge *Gracilaria* aussi, la production d'AHLs par ses bactéries épiphytes augmente significativement la libération de carpospores (Weinberger et al., 2007; Singh et al., 2015), jouant ainsi un rôle important dans sa reproduction. L'algue rouge *Delisea pulchra* interagit et contrôle son microbiote au moyen de composés de défenses, des furanones halogénées, qui ciblent les mêmes récepteurs que les AHLs, limitant ainsi la formation de biofilms (Manefield et al., 1999; Rasmussen et al., 2000) et par extension, modulent la composition du microbiote

(Harder et al., 2012). Ces furanones permettent aussi de limiter l'infection par des pathogènes responsables de blanchiment (Case et al., 2011). De plus, les *Delisea* qui présentent une inhibition du QS réduite sont bien plus colonisées par des bactéries (Steinberg and De Nys, 2002) et ont une communauté bactérienne différentes des *Delisea* avec une inhibition du QS non impactée (Fernandes et al., 2012). Par ailleurs, l'algue *Ahnfeltiopsis flabelliformis* (Rhodophyceae) possède trois inhibiteurs des AHLs, la bétonicine, la floridoside et l'acide iséthionique, qui modulent l'expression de gènes du QS chez les bactéries (Kim et al., 2007; Liu et al., 2008).

Les algues brunes *Colpomenia* sp. sont colonisées par de nombreuses bactéries, qui rentrent en compétition pour l'accès aux nutriments et au substrat. En réponse à ce problème, certaines souches bactériennes appartenant aux *Bacillaceae* (*Firmicutes*), *Pseudomonadaceae*, *Pseudoalteromonadaceae* et *Vibrionaceae* (Proteobacteria) produisent des composés inhibant le QS (AHLs) des bactéries concurrentes (Kanagasabhapathy et al., 2009). De la même manière, il a été montré que 40% des bactéries isolées chez *Fucus vesiculosus* sont capables de dégrader les AHLs (Romero et al., 2011), suggérant ainsi que l'inhibition du QS serait un phénomène courant au sein des communautés bactériennes associées aux macroalgues. Le contrôle du biofilm chez *Laminaria digitata* passe entre autre par la désactivation des AHLs grâce à des composés halogénés (Borchardt et al., 2001).

Par ailleurs, le QS médié par les AI-2 est considéré comme un processus clef au sein de l'holobionte algue brune (Tourneroche et al., 2019), les microbiotes bactériens et fongiques produisant des métabolites qui interagissent avec ces molécules.

Ainsi, le QS peut être influencé par l'hôte, les bactéries du biofilm et d'autres eucaryotes associés à l'holobionte.

5. Hypothèses de travail

A partir de ces données préliminaires, et avec l'objectif de déterminer l'impact du microbiote sur la croissance de *S. latissima*, plusieurs hypothèses ont émergé :

La 1ère hypothèse est que dans les cocultures *Saccharina* + *Hoeflea,* un événement de dysbiose au sein du microbiote de l'algue pourrait être corrélé avec un phénomène de

Quorum Sensing, et ainsi impacter indirectement la fitness de l'algue. Ce cas pourrait également s'appliquer à d'autres souches bactériennes. Cette hypothèse est aussi en lien avec celle (2ème hypothèse) d'une baisse de la croissance dans le cas d'une dysbiose.

La 3ème hypothèse est basée sur l'observation de souches bactériennes bénéfiques pour la croissance de l'algue et d'autres avec un effet négatif, et parfois la variation de l'effet d'une même bactérie selon l'hôte (plantule). Par ailleurs, certaines souches semblent sauver le phénotype algal quand elles sont en mélange avec des souches « néfastes ». Le **chapitre II** a permis de mettre en évidence des genres bactériens potentiellement spécifique à l'état physiologique de l'algue, et cette spécificité pourrait être liée à l'impact sur la croissance de l'algue.

Et finalement, la 4ème hypothèse est que l'ajout de bactéries va impacter la composition du microbiote dans son ensemble.

Des cocultures de *S. latissima* avec des souches issues de son microbiote ont donc été mises en place afin de tester ces hypothèses.

II. Sélection de souches bactériennes d'intérêt

1. Partie cultivable du microbiote de *S. latissima*

Afin de réaliser ces cocultures, il faut avoir accès à des isolats bactériens. A cet effet, et en parallèle de la caractérisation du microbiote par métabarcoding 16S, des isolements bactériens ont été faits à partir des échantillons prélevés à Roscoff (octobre 2018, janvier et avril 2019) et en Norvège (octobre 2018 et avril 2019).

a. Isolements sur boite

Lors de l'échantillonnage, des disques ont été découpés en conditions stériles, puis placés dans un tube Falcon contenant 5ml de glycérol (80% + 20% eau de mer) et stockés à -20°C jusqu'à utilisation.

Les disques ont ensuite été broyés au mortier avec 2ml du glycérol de stockage, 20µl ou 200µl de broyat ont été étalés sur boite R2A agar (9,06g de poudre R2A (Sigma Aldrich), 500ml eau de mer filtrée). Les « boites mères » (**Figure 25**) ont été incubées à température ambiante

pendant 4 semaines, et chaque semaine, chaque colonie à l'aspect visuel différent (forme, couleur, taille) a été isolée et purifiée sur boite par étalement en stries.

Figure 25 – Photos d'une « boite mère » et stries d'étalement pour purification

b. Identification des souches par séquençage du 16S bactérien

Afin d'identifier les souches bactériennes, des colonies isolées ont été placées dans des puits contenants 50µl d'eau milliQ, et chauffées à 95°C pendant 15min. L'ADN codant pour l'ARNr 16S a été amplifié à l'aide d'amorces universelles [8F 5' AGAGTTTGATCCTGGCTCAG et 1492R 5' GGTTACCTTGTTACGACTT (Weisburg et al., 1991)] et de l'enzyme GoTaq polymerase, lors d'une réaction de PCR (2 min 95°C; [1 min 95°C; 30 s 53°C; 3 min 72°C] 30 cycles; 5 min72°C). Les produits PCR ont été purifiés avec de l'ExoSAP (Affymetrix, Inc., Thermo Fisher Scientific), et séquencés par séquençage Sanger (Mix2Seq, Eurofins Genomics). Seule l'amorce sens 8F a été utilisée pour la réaction de séquençage. Grace à l'outil RDP classifier (Wang et al., 2007), et un BLAST contre les bases de données NCBI nr et Silva, les séquences ont été analysées et classées, jusqu'au niveau du genre quand c'était possible. Les séquences ont été alignées (MAFFT software version 7) et vérifiées manuellement pour déterminer les souches distinctes au sein d'un genre (>99% d'identité). Les séquences ARNr 16S uniques seront soumises prochainement à la base de données European Molecular Biology Laboratory (EMBL).

c. Distribution taxonomique des souches bactériennes

Des séquences ont été obtenues pour 317 isolats bactériens, et elles sont distribuées à travers quatre phyla, 18 ordres, 41 genres et 73 souches uniques taxonomiquement. Elles appartiennent majoritairement aux *Firmicutes* (39,1% des isolats) et aux *Gammaproteobacteria* (27,5% des isolats ; **Figure 26**). 16 des 49 genres comprennent plus

d'une souche distincte (c'est-à-dire, au moins un nucléotide différent dans la séquence 16S) : *Streptomyces* (4 souches distincts), *Bacillus* (4), *Microbacterium* (3), *Paracoccus* (3), *Pseudoalteromonas* (3), *Psychrobacter* (3), *Rhodococcus* (2), *Alkalihalobacillus* (2), *Peribacillus* (2), *Rossellomorea* (2), *Paenibacillus* (2), *Brevundimonas* (2), *Pseudovibrio* (2), *Alteromonas* (2), *Microbulbifer* (2), *Salinicola* (2 ; **Table S3**).

A la suite des séquençages, des stocks glycérol (40%) des souches ont été réalisés et stockés à -80°C.

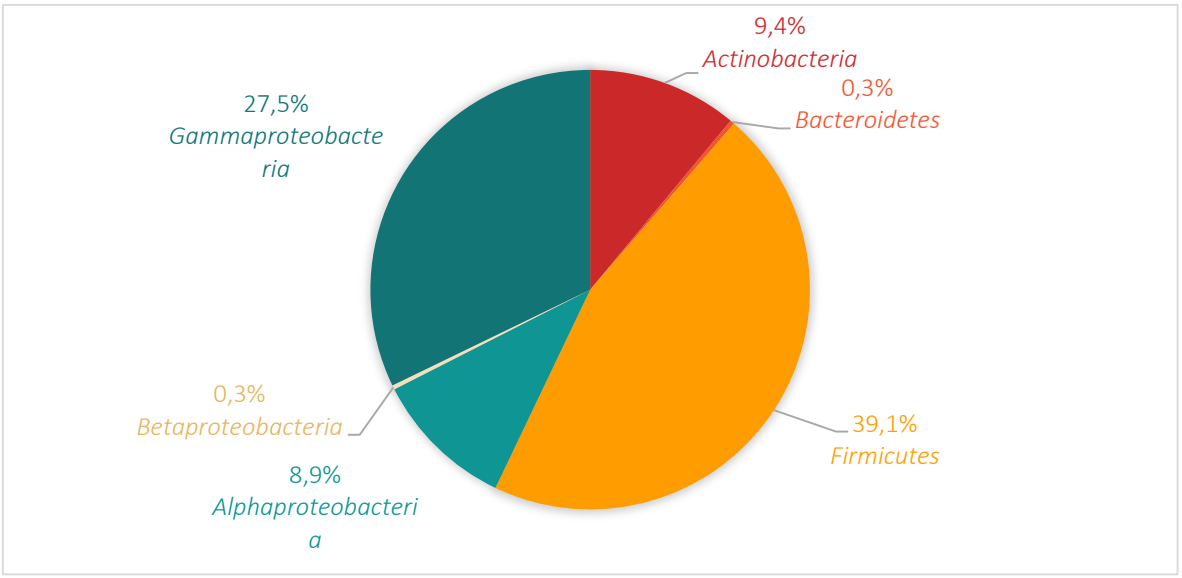

Figure 26 – Part cultivable du microbiote de *S. latissima*

d. Estimation de la portion cultivable du microbiote de S. latissima

Pour estimer la portion cultivable du microbiote de *S. latissima*, les 317 séquences des isolats bactériens ont été blastées contre le jeu de données « Métabarcoding 16S » (**cf. chap II**). Les souches cultivées couvrent 0.03% des ASVs avec 100% d'identité (0.035% des séquences), 0.11% des ASVs à 99% d'identité (0.068% des séquences) et 3.22% des genres détectés en metabarcoding.

Par ailleurs, sur les 41 genres détectés avec les isolements, 27 genres (46/69 souches) sont présents uniquement dans le jeu de données « cultivable ». Plusieurs aspects peuvent expliquer cette observation. D'un point de vue technique, les échantillons d'algues ont été stockés à -20°C en attendant leur isolement, et certaines bactéries supportent mieux la congélation que d'autres. De plus, les conditions de PCR et de séquençage ou d'analyses des

séquences ont peut-être éliminé les ASVs rares qui correspondaient à des souches isolées (Suzuki and Giovannoni, 1996; Donachie et al., 2004, 2007; Zilber-Rosenberg and Rosenberg, 2008; Skopina et al., 2016). Les bactéries peuvent être présentes en faible abondance dans le milieu naturel, mais se développer plus facilement en milieu riche (Epstein, 2009; Buerger et al., 2012; Lindh et al., 2015), changeant ainsi les ratios d'abondance entre les deux jeux de données.

Cette comparaison cultivable/métabarcoding a servi de base pour la sélection des souches des cocultures.

2. Sélection des souches

La comparaison du jeu de données cultivable avec celui du metabarcoding a permis de faire ressortir 22 genres en commun, pour lesquels une recherche bibliographique sur leur possible implication dans le quorum sensing a été faite.

Chez les bactéries marines, les genres producteurs de molécules signal appartiennent principalement aux *Alpha-* et *Gammaproteobacteria* (Dobretsov et al., 2009; Borges and Simões, 2019), mais plusieurs autres genres bactériens appartenant aux *Firmicutes*, *Bacteroidetes* et *Actinobacteria* sont capables d'inhiber ces molécules (Dong et al., 2007; Romero et al., 2011; Hmelo, 2017).

Les données de DESEQ 2 Sains/Symptômes (**cf. chapitre II**) ont également fait ressortir des genres associés à l'un ou l'autre groupe, permettant une sélection de genres possiblement négatifs, possiblement bénéfiques ou neutres pour la croissance de l'algue.

Finalement, à partir de ces données, six souches ont été sélectionnées (**Table 7**).

III. Cocultures

1. Préparation des solutions bactériennes

a. Cultures liquides

A partir des stocks glycérol, des boites R2A agar ont été ensemencées, et les 16S des colonies isolées ont été séquencés pour vérifier une possible contamination.

Des culture liquides des souches ont ensuite été faites, en inoculant 5ml de Zobell 800 avec 1 colonie pure. Les tubes ont été incubés à température ambiante pendant 4 jours, sous agitation.

Table 7 – Souches bactériennes sélectionnées pour les cocultures

Souche	Affiliation taxonomique	Genre isolé sur algue saine ou avec symptômes	DESEQ2 Spécifique sain/symptômes
Bacillus sp. 181	*Firmicutes; Bacilli; Bacillales; Bacillaceae*	Saines et Symptômes	_
Sulfitobacter sp. 214	*Alphaproteobacteria; Rhodobacterales; Rhodobacteraceae*	Symptômes	Saine
Maribacter sp. 144	*Bacteroidetes; Flavobacteriia; Flavobacteriales; Flavobacteriaceae*	Symptômes	_
Granulosicoccus sp. 302	*Gammaproteobacteria; Chromatiales; Granulosicoccaceae*	Saines et Symptômes	Saine
Pseudoalteromonas sp. 226	*Gammaproteobacteria; Alteromonadales; Pseudoalteromonadaceae*	Saines et Symptômes	Symptômes
Psychromonas sp. 235	*Gammaproteobacteria; Alteromonadales; Psychromonadaceae*	Saines	_

b. Protocole Cytométrie

Afin d'inoculer les cocultures à la même concentration finale, les concentrations des solutions bactériennes ont été déterminées par cytométrie en flux à T0. Des dilutions en série de 10^{-3} à 10^{-7} cellules/ml ont été préparées, fixées avec du glutaraldéhyde (0.25% final) et marquées au SYBER Green-I (1/50 00 de la solution commerciale).

Les échantillons ont été analysés avec un débit de 65µl/min sur un cytomètre en flux Accuri C6 PLUS (Becton-Dickinson, San Jose, CA, USA)., La fluorescence verte du Sybr Green, utilisée pour déclencher le signal, a été enregistrée ainsi que les signaux de diffusion de lumière FSC (taille) et SSC (volume) afin de délimiter les contours de la population bactérienne. Les résultats ont été analysés à l'aide du logiciel FlowingSoftware (version 2.5.1).

En fonction de la concentration de chaque solution bactérienne, un volume différent a été inoculé dans les cocultures, pour atteindre une concentration finale entre 1 et 2.10^7 cellules/ml.

2. Préparation des plantules

La veille de l'inoculation, un nombre suffisant de petites plantules (~5 mm de long ; 16 plantules / condition) a été sélectionné, placé dans une boite de pétri BP140 contenant 100ml d'eau de mer autoclavée et stockées à 13°C.

Le jour de l'inoculation, 4 plantules ont été placées par boite, avec 4 boites par condition et 100ml d'eau de mer autoclavée additionnée de PES.

Pour chaque série de cocultures, 8 plantules « contrôles avant inoculation » (4*2 plantules) ont été stockées à -80°C en prévision des analyses de métabarcoding 16S.

3. Composition des cocultures

La composition bactérienne des cocultures vise à valider ou non nos hypothèses de travail. Un groupe de cocultures est composé des cocultures réalisées en parallèle et à la même date (**Table 8**).

Les **groupes A**, **Ab** et **C** reprennent les cocultures croisées de *S. latissima* et des souches issues d'*Ectocarpus*, afin de vérifier si l'effet négatif d'*Hoeflea* et le phénomène de récupération sont toujours présents (hypothèses 1 et 2), et si les autres souches testées ont un effet particulier chez *S. latissima*.

Les **groupes B**, **D**, **E**, **F**, **G** et **H** comprennent des cocultures de *S. latissima* et des souches issues de son microbiote. Les cocultures réalisées avec une seule souche bactérienne feront ressortir l'effet positif ou négatif de la souche sur la croissance de l'algue (hypothèse 3). Le groupe B a servi de base pour la détermination des effets des souches seules et de leur répartition en mélange ou non pour les cocultures suivantes. Les cocultures « Tutti », « Sulfitobacter + 1 souche » et les mélanges de 3 souches aideront à déterminer si un couplage permet d'inhiber l'effet négatif d'une souche (hypothèse 3). Les mélanges sont généralement composés d'une souche positive et d'une souche négative ou de deux souches positives et d'une négative, caractérisées comme telle en fonction de l'effet observé lors du groupe B ou des cocultures croisées. Certains mélanges sont formés de souches issues d'*Ectocarpus* et de *Saccharina*, afin de déterminer si l'effet récupération est spécifique d'une certaine souche ou non.

Les groupes de cocultures D à H ont été adaptés en fonction des résultats des groupes antérieurs. En particulier, le groupe G est équivalent au groupe F, pour lequel nous nous

sommes rendus compte pendant l'incubation que le milieu Zobell était contaminé. De même, les groupe E et F sont identiques car les solutions bactériennes du groupe E n'étaient pas pures.

Les **groupes F** et **G** comprennent aussi des contrôles Zobell (F_Zb_act, F_Zb_max et G_Zb), qui reprennent les volumes maximums de Zobell inoculés depuis le début des cocultures (F_Zb_max), au moment de l'inoculation du groupe F (F_Zb_act) et du groupe G (G_Zb).

Le **groupe H** comprend des cocultures dont les résultats précédents étaient visibles, mais les solutions bactériennes utilisées ici ont été nettoyées avec une solution saline avant l'inoculation pour éliminer les traces du milieu Zobell.

En parallèle et pour chaque groupe de cocultures (**Table 8**), des cocultures bactériennes en milieu Zobell (5ml) ont aussi été faites, à la même concentration finale que les cocultures algues-bactéries. Ces cocultures ont été mises en place pour déterminer la production de molécules du QS par les bactéries en elles-mêmes (sans la présence de l'hôte algue).

4. Incubation

Après inoculation, les cocultures ont été incubées pendant 5 jours à 13°C, sous agitation douce, et un cycle jour/nuit 12h/12h.

Un suivi de la survie pendant 1 semaine post-incubation a été fait, avec un transfert des plantules dans 100ml de NSW + PES (*Natural Seawater* + *Provasoli Enrichissement SeaWater*) et dans les mêmes conditions de lumière et de température que l'incubation T0-T5.

Les cocultures bactéries seules ont été centrifugées (10min, 10 000g), filtrées (1ml, 0.22µm), et stockées à -80°C.

Table 8 – Composition bactérienne des cocultures et concentration finale après inoculation

Groupe	Composition		Concentration finale dans le milieu
	Souche seule	Mélanges	
GROUPE A	– *Marinobacter* HK377 – *Roseovarius* 420 – *Hoeflea* 425	– *Marinobacter + Hoeflea* – *Roseovarius + Hoeflea* – *Marinobacter + Roseovarius + Hoeflea*	2.10^7 cellules/ml
GROUPE Ab antibiotiques	– *Marinobacter* HK377 – *Hoeflea* 425	– *Marinobacter + Hoeflea*	2.10^7 cellules/ml
GROUPE B	– *Bacillus* 181 – *Maribacter* 144 – *Sulfitobacter* 214 – *Pseudoalteromonas* 226 – *Psychromonas* 235 – *Granulosicoccus* 302	– *Bacillus + Maribacter + Sulfitobacter + Pseudoalteromonas + Psychromonas + Granulosicoccus (=Tutti)* – *Hoeflea + Bacillus + Granulosicoccus*	2.10^7 cellules/ml
GROUPE C	– *Marinobacter* HK377 – *Roseovarius* 420 – *Hoeflea* 425 – *Bosea* 5a – *Imperialibacter* R9	– *Marinobacter + Roseovarius + Bosea* – *Marinobacter + Roseovarius + Hoeflea* – *Roseovarius + Imperialibacter + Hoeflea*	2.10^7 cellules/ml
GROUPE D	– *Bacillus* 181 – *Maribacter* 144 – *Sulfitobacter* 214 – *Pseudoalteromonas* 226 – *Psychromonas* 235 – *Granulosicoccus* 302	– *Tutti* – *Sulfitobacter +* 1 souche	2.10^7 cellules/ml
GROUPE E	– *Bacillus* 181 – *Maribacter* 144 – *Sulfitobacter* 214 – *Pseudoalteromonas* 226 – *Psychromonas* 235 – *Granulosicoccus* 302	– *Marinobacter + Roseovarius + Hoeflea* – *Sulfitobacter + Bacillus + Maribacter* – *Marinobacter + Sulfitobacter* – *Marinobacter + Roseovarius* – *Hoeflea + Bacillus* – *Hoeflea + Marinobacter*	2.10^7 cellules/ml

GROUPE F	– *Bacillus* 181 – *Maribacter* 144 – *Sulfitobacter* 214 – *Pseudoalteromonas* 226 – *Psychromonas* 235 – *Granulosicoccus* 302 – *Marinobacter* HK377	– *Tutti* – *Sulfitobacter* + 1 souche – *Marinobacter* + *Sulfitobacter* – *Sulfitobacter* + *Bacillus* + *Maribacter*	2.10^7 cellules/ml
GROUPE G	– *Bacillus* 181 – *Maribacter* 144 – *Sulfitobacter* 214 – *Pseudoalteromonas* 226 – *Psychromonas* 235 – *Granulosicoccus* 302 – *Marinobacter* HK377	– *Tutti* – *Sulfitobacter* + 1 souche – *Marinobacter* + *Sulfitobacter* – *Sulfitobacter* + *Bacillus* + *Maribacter*	1.10^7 cellules/ml
GROUPE H	– *Sulfitobacter* 214 – *Bacillus* 181 – *Maribacter* 144 – *Marinobacter* HK377	– *Marinobacter* + *Sulfitobacter* – *Sulfitobacter* + *Bacillus* – *Sulfitobacter* + *Maribacter*	$2{,}96.10^5$ cellules/ml

IV. Étude de l'impact sur la croissance de l'algue

1. Méthodes

a. Suivi de la croissance relative journalière

Le suivi de la croissance relative journalière a été fait à 3 points : T0, T5 et T1week. Chaque plantule a été étalée entre deux lames millimétrées et prise en photo avec une loupe binoculaire. Chaque photo a ensuite été analysée sur le logiciel Fiji-ImageJ (win64) et la longueur du thalle et l'aire de l'algue obtenues (Fonctions « Threshold », puis « Analyse Particles » ; **Figure 27**). La croissance relative pour T0-T5 et T5-T1week a été calculée.

La normalité des données a été vérifiée avec un test de Shapiro. Les données ont été analysées par ANOVA ou par un test de Kruskal-Wallis. Les différences entre traitements ont été acceptées comme significatives pour une p-value inférieure au seuil de 0,05. Un test post hoc de Tukey a également été fait à l'aide du package Multcomp 1.4-17 du logiciel R.

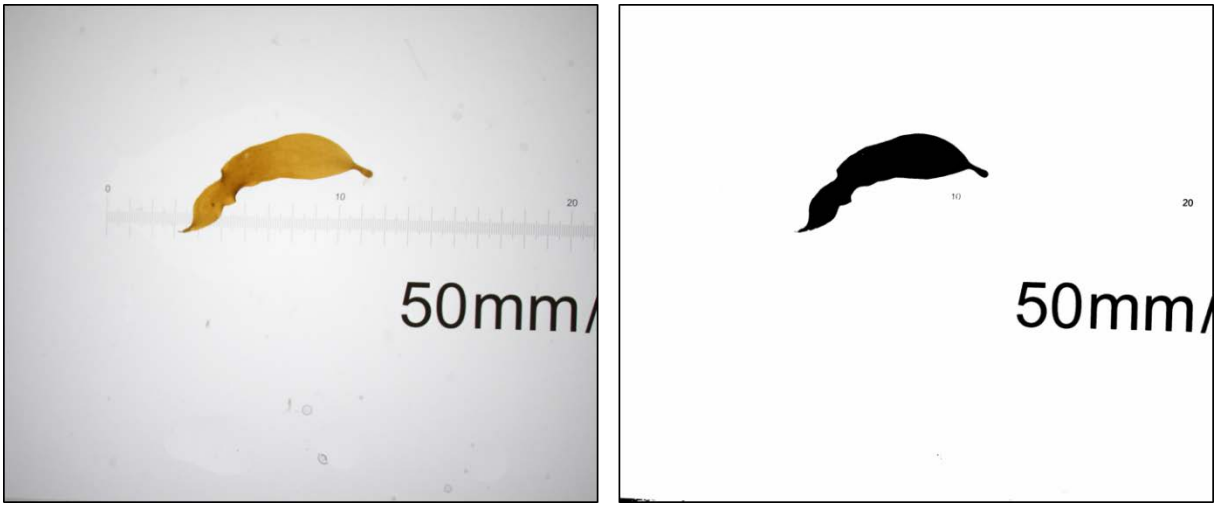

Figure 27 – Photo d'une plantule de *S. latissima* sur lame millimétré (à gauche) et sa conversion pour l'analyse de la surface (à droite)

b. Suivi de la photosynthèse

Le rendement maximal du photosystème II (Fv/Fm) a été mesuré à T0, T5 et T1week à l'aide d'un JuniorPAM (Walz, Effeltrich, Allemagne). Les plantules ont été mises à l'obscurité pendant 10 minutes avant la mesure.

2. Résultats & Discussion

a. Suivi de la photosynthèse

Les mesures du PAM n'ont révélé aucun impact significatif des inoculations sur le rendement du photosystème II.

b. Suivi de la croissance relative journalière

Les taux relatifs de croissance journalière (T0-T5 et T5-T1week) des cocultures sont présentés en **Figure 28**.

Pour le **groupe A**, il n'y a pas de différences significatives entre les différentes cocultures que ce soit pour la croissance pendant le traitement ou après une semaine de repos. Les résultats sont différents de ceux obtenus lors des manips préliminaires. Un stress de l'algue par ajout d'antibiotiques et culture en eau de mer artificielle (ASW) a été réalisé pour le **Groupe Ab**. Ces conditions de stress permettent de recréer la tendance négative de *Hoeflea* (H425). De même, la combinaison ATB+ASW ne favorise pas la croissance de l'algue.

Le **Groupe C** comprend deux autres souches issues d'*Ectocarpus, Imperialibacter* et *Bosea,* qui réduisent significativement la croissance des plantules. Ces résultats sont différents de ceux obtenus chez *Ectocarpus*. Les taux de croissance négatifs sont dû à la mortalité des tissus algaux : les plantules se délitent. Cependant, leur inoculation en mélange avec deux autres souches ne bloque pas la croissance des plantules.

Il n'y a pas de différences significatives entre les différentes cocultures du **Groupe B,** que ce soit pour la croissance pendant le traitement ou après une semaine de repos. A T5, les algues cultivées avec *Sulfitobacter* 214 semblent se déliter légèrement, cette souche est alors déclarée comme « néfaste » pour l'algue et sera utilisée comme telle pour la suite des cocultures.

Pour le **groupe D,** sur la période T0-T5, on observe une réduction de la croissance pour toutes les cocultures testées sauf pour *Maribacter* 144 et le mélange *Sulfitobacter* 214 et *Maribacter* 144 (SMb). Mb144 est alors considérée pour la suite des cocultures comme une souche bénéfique pour l'algue et qui participe possiblement à l'effet « récupération ». Pour la période T5-T1week, la baisse de la croissance se maintient. Les plantules inoculées avec le mélange *Sulfitobacter* 214 et *Pseudoalteromonas* 226 (SPa) voient leur croissance fortement perturbée pendant le traitement, mais le transfert en NSW lève le blocage. Par ailleurs, le groupe D présente une mortalité importante, avec 31% des plantules qui ne survivent pas au traitement, 56% qui sont impactées négativement (taches vertes, décoloration) et seulement 13% des plantules qui survivent sans dommages.

Dans le **groupe E**, il n'y a pas de différences significatives entre les différentes cocultures et le contrôle non inoculé, que ce soit pour la croissance pendant le traitement ou après une semaine de repos.

Le **groupe F** montre une baisse de croissance significative uniquement pour les cocultures avec un grand volume de Zobell par rapport au contrôle non inoculé.

Le **groupe G** présentent des résultats différents du groupe F, même si les types de cocultures sont identiques. On observe une baisse de la croissance avec les souches S214, Ba181, G302, et le mélange MS. Le milieu Zobell réduit encore de manière significative la croissance de l'algue. La baisse de croissance persiste après une semaine en NSW pour les cocultures Ba181, G302 et Zobell. Le mélange SG voit sa croissance diminuer significativement après son

transfert en NSW (T5-T1week). Le mélange MS permet une récupération de la croissance de l'algue suite au transfert en NSW.

Enfin, pour le **groupe H**, il n'y a pas de différences significatives entre les différentes cocultures que ce soit pour la croissance pendant le traitement ou après une semaine de repos.

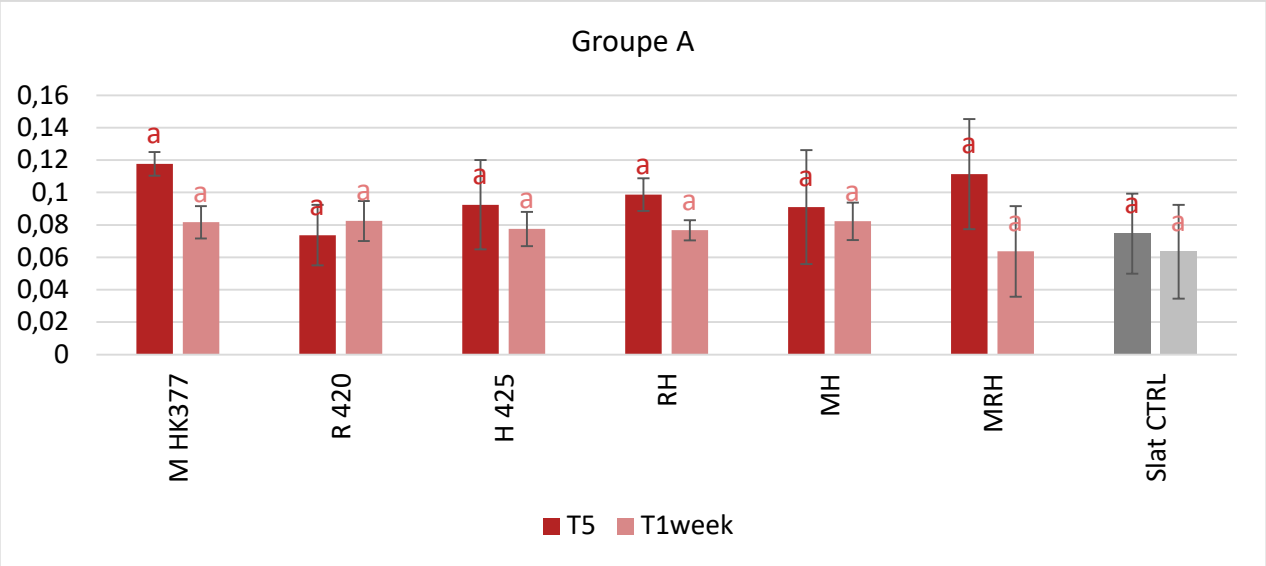

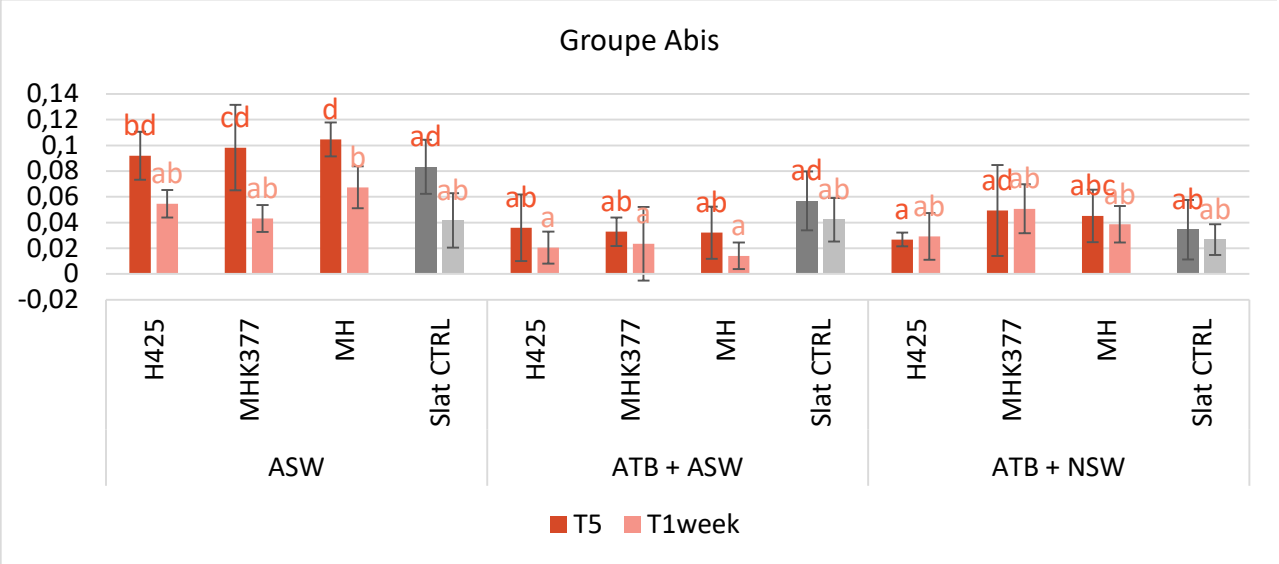

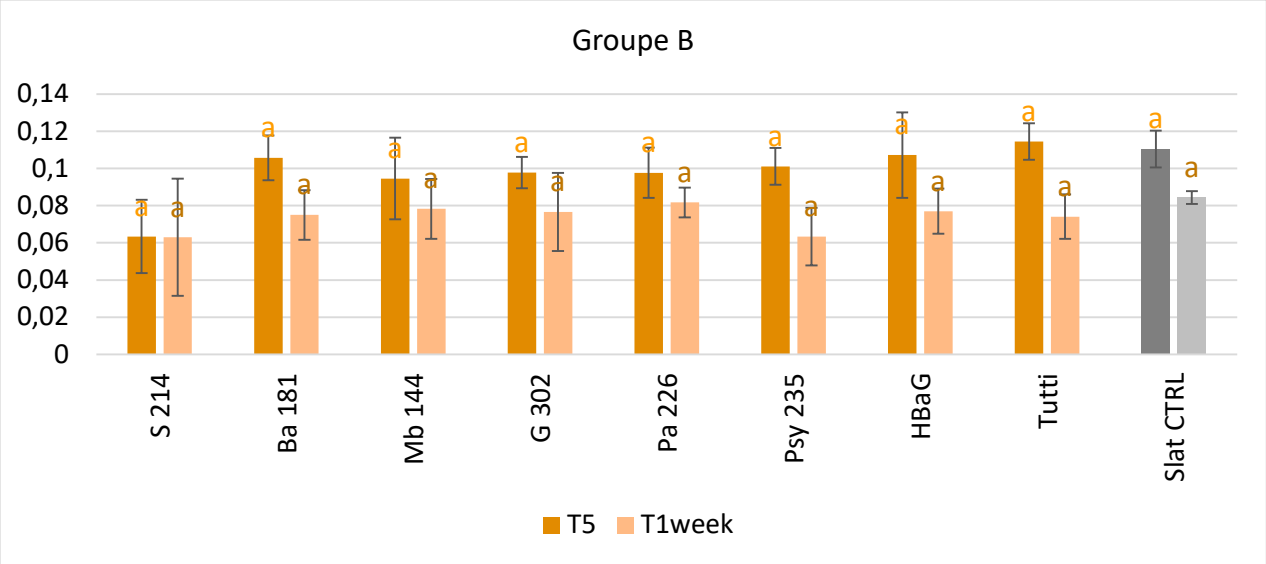
Groupe B
0,14
0,12
0,1
0,08
0,06
0,04
0,02
0
S 214
Ba 181
Mb 144
G 302
Pa 226
Psy 235
HBaG
Tutti
Slat CTRL
T5
T1week

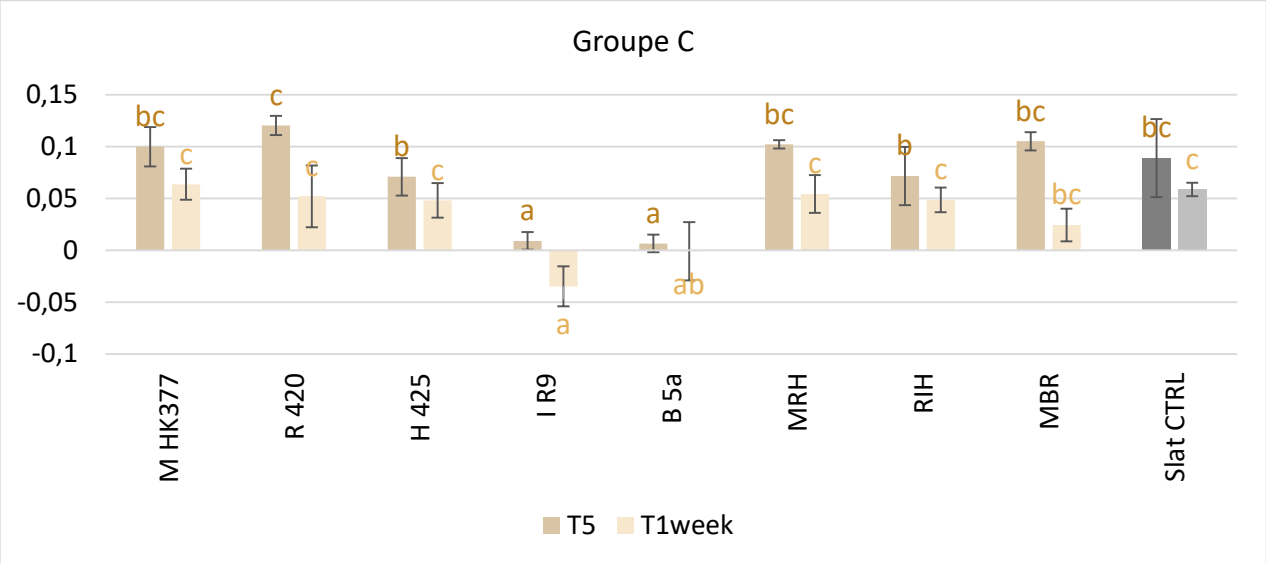
Groupe C
0,15
0,1
0,05
0
-0,05
-0,1
M HK377
R 420
H 425
I R9
B 5a
MRH
RIH
MBR
Slat CTRL
T5
T1week

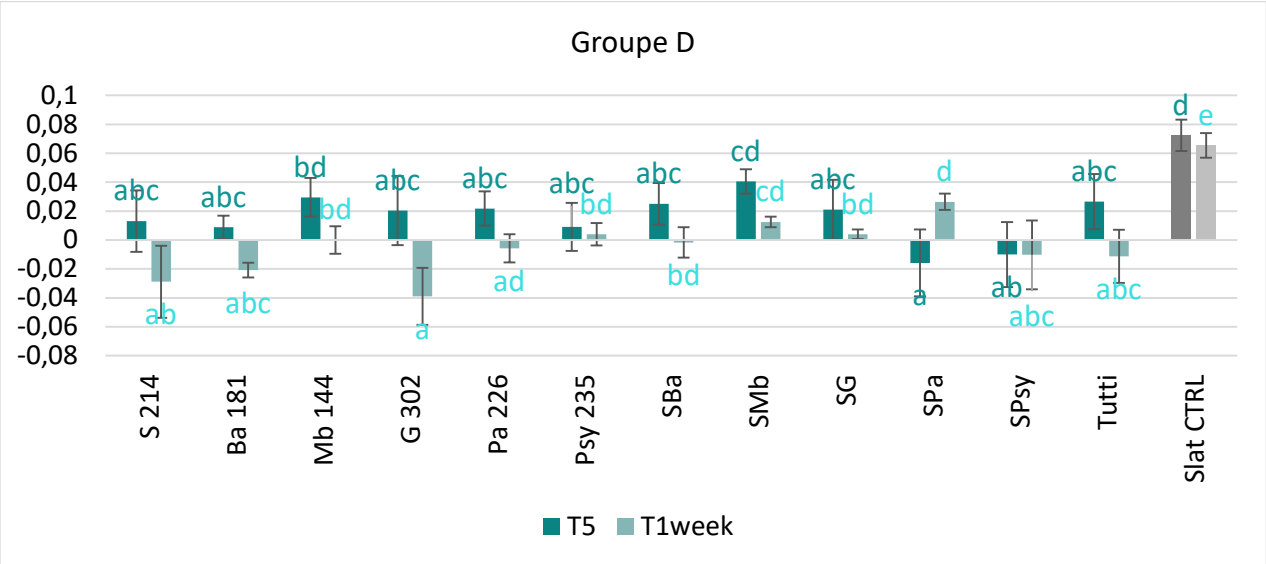
Groupe D
0,1
0,08
0,06
0,04
0,02
0
-0,02
-0,04
-0,06
-0,08
S 214
Ba 181
Mb 144
G 302
Pa 226
Psy 235
SBa
SMb
SG
SPa
SPsy
Tutti
Slat CTRL
T5
T1week

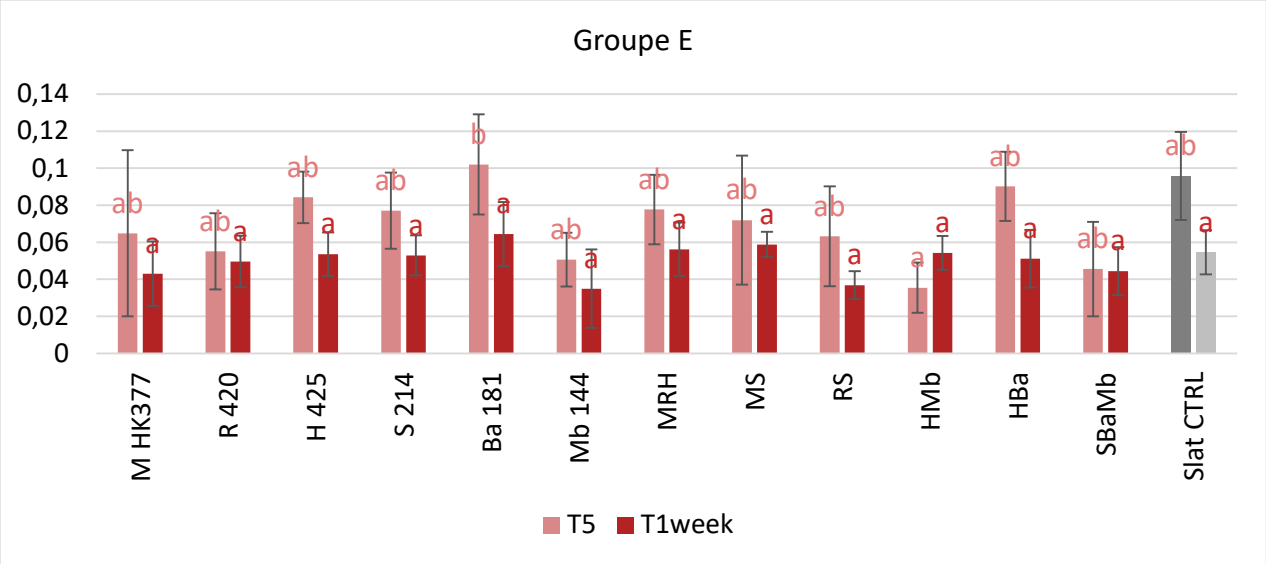
Groupe E
0,14
0,12
0,1
0,08
0,06
0,04
0,02
0
M HK377
R 420
H 425
S 214
Ba 181
Mb 144
MRH
MS
RS
HMb
HBa
SBaMb
Slat CTRL
T5
T1week

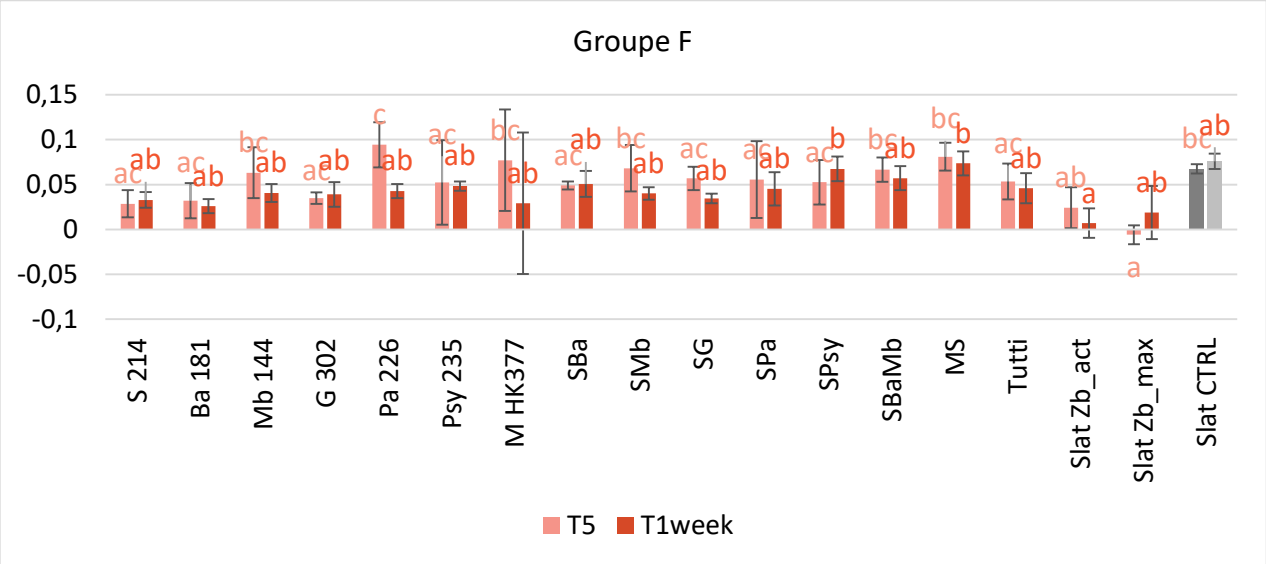
Groupe F
0,15
0,1
0,05
0
-0,05
-0,1
S 214
Ba 181
Mb 144
G 302
Pa 226
Psy 235
M HK377
SBa
SMb
SG
SPa
SPsy
SBaMb
MS
Tutti
Slat Zb_act
Slat Zb_max
Slat CTRL
T5
T1week

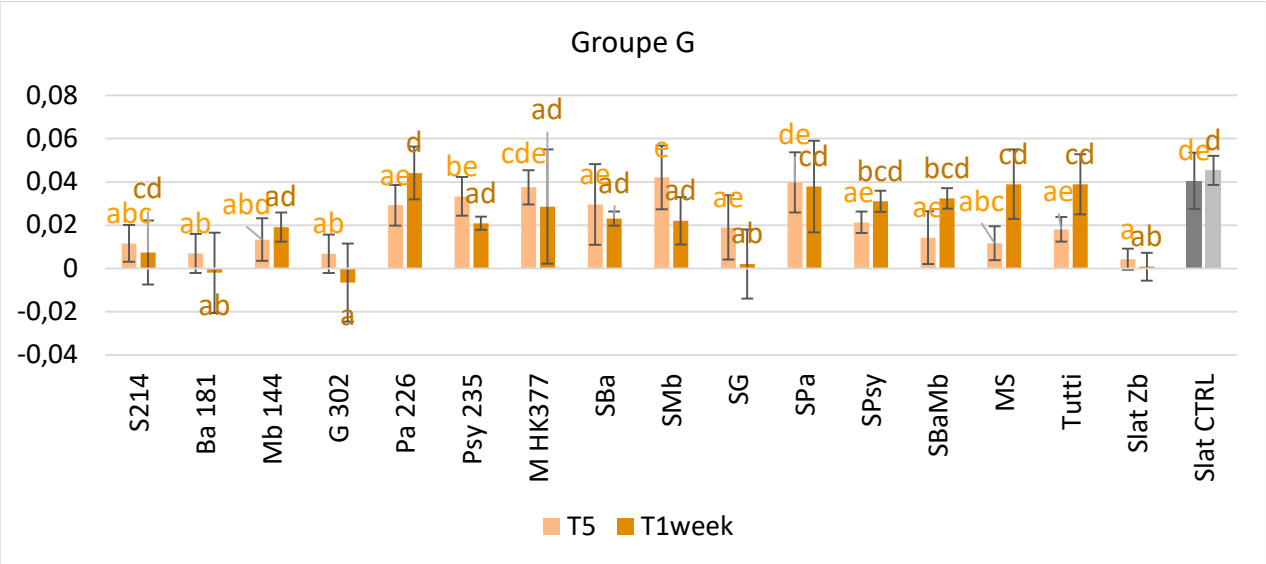
Groupe G
0,08
0,06
0,04
0,02
0
-0,02
-0,04
S214
Ba 181
Mb 144
G 302
Pa 226
Psy 235
M HK377
SBa
SMb
SG
SPa
SPsy
SBaMb
MS
Tutti
Slat Zb
Slat CTRL
T5
T1week

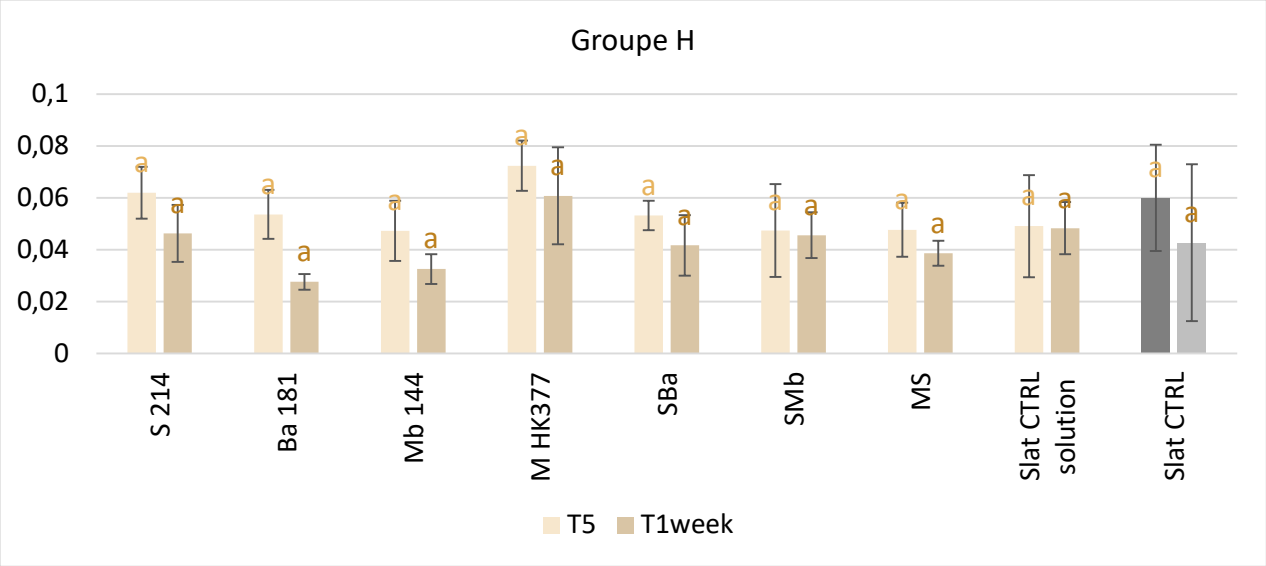

Figure 28 – Croissance relative journalière des plantules de *S. latissima* entre To-T5 (T5) et T5-T1week (T1week). Les lettres du test post hoc sont distinctes entre les deux séries. Zb : Zobell. Tutti : mélange des souches du groupe de coculture. Slat CTRL : plantules non inoculées. **Cf Table 8.**

Certaines souches protègent la croissance et d'autres la perturbent sur le long terme. Dans certains cas, on peut observer un effet récupération de la croissance lorsque des souches qui sont néfastes inoculées seules sont inoculées en mélange. En effet, *Maribacter* sp. ne bloque pas la croissance des plantules, voire permet son maintien dans les groupes où la croissance est fortement impactée. Il se peut que cette protection de la croissance soit due à de composés spécifiques produits par cette souche bactérienne. En effet, chez *Ulva mutabilis* par exemple, les souches de *Maribacter* sont connues pour libérer des composés morphogènes qui impactent le positivement le développement du rhizoïde et des parois cellulaires (Weiss et al., 2017). Cette sauvegarde de la croissance par *Maribacter* est aussi visible lorsqu'elle est co-inoculée avec une autre souche ayant un impact négatif, comme *Sulfitobacter.*

Le milieu Zobell en lui-même a un impact négatif sur la croissance des plantules, même à forte dilution (~3µl/ml), impact absent lorsque les plantules ont été inoculées avec des solutions bactériennes salines. Cet impact négatif pourrait être due à une perturbation du microbiote déjà en place, entrainant ainsi une dysbiose.

Ainsi, le lien entre la concentration en Zobell et la croissance des plantules a été examiné. On observe effectivement une corrélation entre une augmentation de la concentration en Zobell et une baisse de la croissance (**Figure 29**).

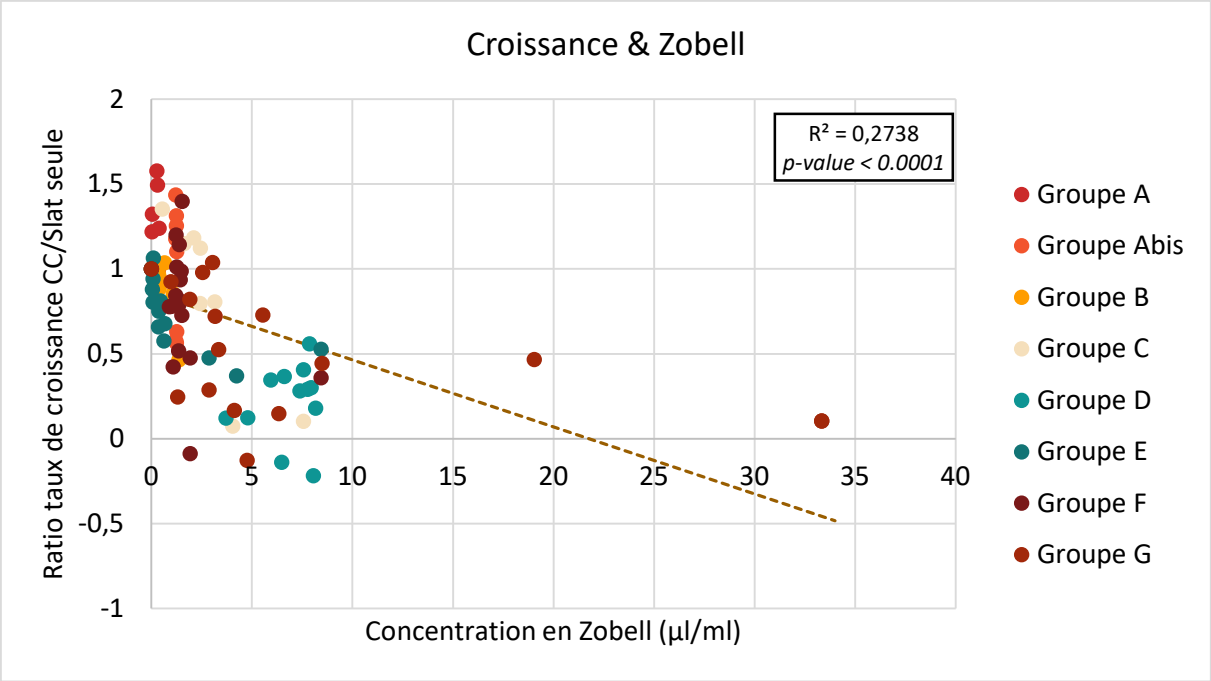

Figure 29 – Taux de croissance et concentration en Zobell. On considère le taux de croissance par rapport au contrôle comme très faible : -0.3-0.2, faible : 0.2-0.5, moyen :0.5-1 et élevé >1. On considère la concentration en Zobell comme très faible : <1 µl/ml, faible : 1-1.75 µl/ml, moyenne : 1.75-3.5 µl/ml, élevée : 3.5-5 µl/ml et très élevée : >5 µl/ml.

V. Corrélation QS & Croissance

Une de nos hypothèses est que cette baisse de croissance pourrait être la conséquence d'une dysbiose, et donc potentiellement liée au phénomène de QS. Pour tester cette hypothèse, nous avons utilisé des biosenseurs permettant de détecter les composés de QS (type AI-1 et AI-2) dans les surnageants des cultures bactériennes ainsi que les cocultures.

1. Méthodes

a. Obtention des surnageants

Au T5, 50ml du milieu de culture des cocultures algues-bactéries ont été collectés et stockés à -20°C. Les CC bactéries seules ont été traitées immédiatement.

Pour obtenir les surnageants, les échantillons ont été centrifugés pendant 10min à 10,000g et 1ml de surnageant filtré (0.22µm) récupéré pour analyse.

b. Protocole de détection des AHL

Les AHLs sont détectées à l'aide de biosenseurs (bactéries modifiées) basés sur des souches de *Pseudomonas putida* et *Escherichia coli* (Andersen et al., 2001; Riedel et al., 2001; Steindler and Venturi, 2007). *P. putida* F117 (pRK-C12 ; Kmr ; ppuI::npt) est utilisée pour la détection

des AHLs à chaîne longue (Andersen et al., 2001) et *E. coli* MT102 (pJBA132) pour la détection des AHLs à chaîne courte (Riedel et al., 2001). Le protocole suivi est adapté de Doberva et al. (2017).

Une culture liquide de MT102 et F117 à partir de colonies isolées a été faite en milieu Luria-Bertani (LB), pendant la nuit, sous agitation continue (200 tr/min), à 30 °C et avec traitement antibiotique (tétracycline 25 µg/ml et gentamicine 20 µg/ml, respectivement). A partir de ces cultures liquides, des cultures fraiches ont été faites (1ml de MT102 + 125 µL de tétracycline + 49ml de LB ; 2 ml de F117 + 48ml de LB), et distribuées en microplaque 96 puits (150µl par puits). 50µl des surnageants de cultures à tester ont été rajouté dans chaque puits en triplicat. Les contrôles positifs consistent en des solutions (2µM) préparées à partir de poudre d'AHL, C6-HSL pour *E. coli* MT102 et C10-HSL pour *P. putida* F117 (Fluka Chemie AG, Buchs, Suisse). Quatre contrôles négatifs ont été également faits : les milieux de cultures Zobell800 et LB seuls (200µl) et en mélange avec les biosenseurs (50µl). Les microplaques ont été incubées pendant 24h à 25°C, sans agitation et à l'obscurité. La mesure de la fluorescence GFP a été faite avec une excitation à 485 nm et une détection à 535 nm. La DO630nm a également été mesurée pour déterminer la croissance cellulaire. Ces mesures ont été faites sur le lecteur de plaque Spark® (TECAN, Suisse) de la plateforme Genomer de la Station Biologique de Roscoff.

c. Protocole de détection des AI-2

Pour la détection des AI-2, le biosenseur *Vibrio campbellii* MM32 (luxN::Cm, luxS::Tn5Kan) a été utilisé (Bassler et al., 1993; Freeman and Bassler, 1999) et le protocole est adapté de (Miller et al., 2004).

Une culture liquide de MM32 a été faite en milieu MB (Marine Broth) additionné de Kanamycine (50 µg/ml) et de Chloramphénicol (10 µg/ml) et incubée pendant 24h à 25 °C, sous agitation (~160 rpm). Une culture fraîche de MM32 (100µl MM32 + 50 µL Kanamycine + 25 µL chloramphénicol + 50ml de MB) a été répartie en microplaque 96 puits (180µl par puits). Les surnageants à tester ont été déposés en triplicat (20µlpar puits). Un surnageant de souche bactérienne positive (Mola424)[1] a été utilisé comme contrôle positif. Les milieux de cultures Zobell800 et MB seuls (200µl) et en mélange avec les biosenseurs (20µl) ont servi de contrôle

[1] En provenance de l'équipe de Soizic Prado, MNHM

négatif. Les plaques ont été mise à incuber à 25°C pendant 24h à l'obscurité. La luminescence et la croissance cellulaire (DO630nm) ont été mesurée sur un lecteur de plaque EnVision® 2105 (Perkin Elmer, Waltham, MA, USA) sur la plateforme KISSf de la Station Biologique.

Le pourcentage d'induction du biosenseur a été calculé comme %induction= 100*[($lumi_{échantillon}$ – $lumi_{BSnégatif}$) / $lumi_{BSpositif}$], avec $lumi_{échantillon}$ la luminescence mesurée de l'échantillon, $lumi_{BSnégatif}$ la luminescence mesurée du contrôle négatif biosenseur (MM32+MB) et $lumi_{BSpositif}$ la luminescence mesurée du contrôle positif biosenseur (MM32+424).

2. Le QS dans les cocultures

a. Zobell

Les surnageants de cocultures Zobell déclenchent la bioluminescence de MM32, mais n'ont pas d'effet sur l'induction de F117 et ont un niveau d'induction identique à celui du contrôle chez MT102 (**Figure 30**). Les surnageants issus de ces cocultures sont donc enrichis en AI-2.

Par ailleurs, l'analyse de la production de molécules du QS par les souches bactériennes en elle-même ne montre aucune production d'AHL (**Figure 31**).

L'hypothèse d'une production d'AI-2 dans les cocultures avec faible taux de croissance de l'algue est donc émise. La détection des AI-2 par MM32 a donc été choisi comme méthode d'analyse pour la suite des expérimentations.

b. Cocultures

Les échantillons à tester en biosenseurs ont été sélectionnés après analyse de leur croissance et de leur concentration en Zobell. Deux échantillons par sous-cluster « concentration X croissance » (**Figure 29**) ont été choisis ainsi que les points aberrants. Les cocultures G302, Ba181 et Psy235 ont aussi été choisies parce que ces souches ont été considérée comme bénéfique, neutre et néfaste pour l'hôte, respectivement. Un total de 48 échantillons a ainsi été sélectionnés.

Induction du QS

On observe une induction forte du QS (>50% induction de MM32) dans les cocultures bactéries seules pour quasiment toutes les cocultures (

Figure 32). Cette production de composées suite à une incubation en milieu riche est en accord avec la littérature.

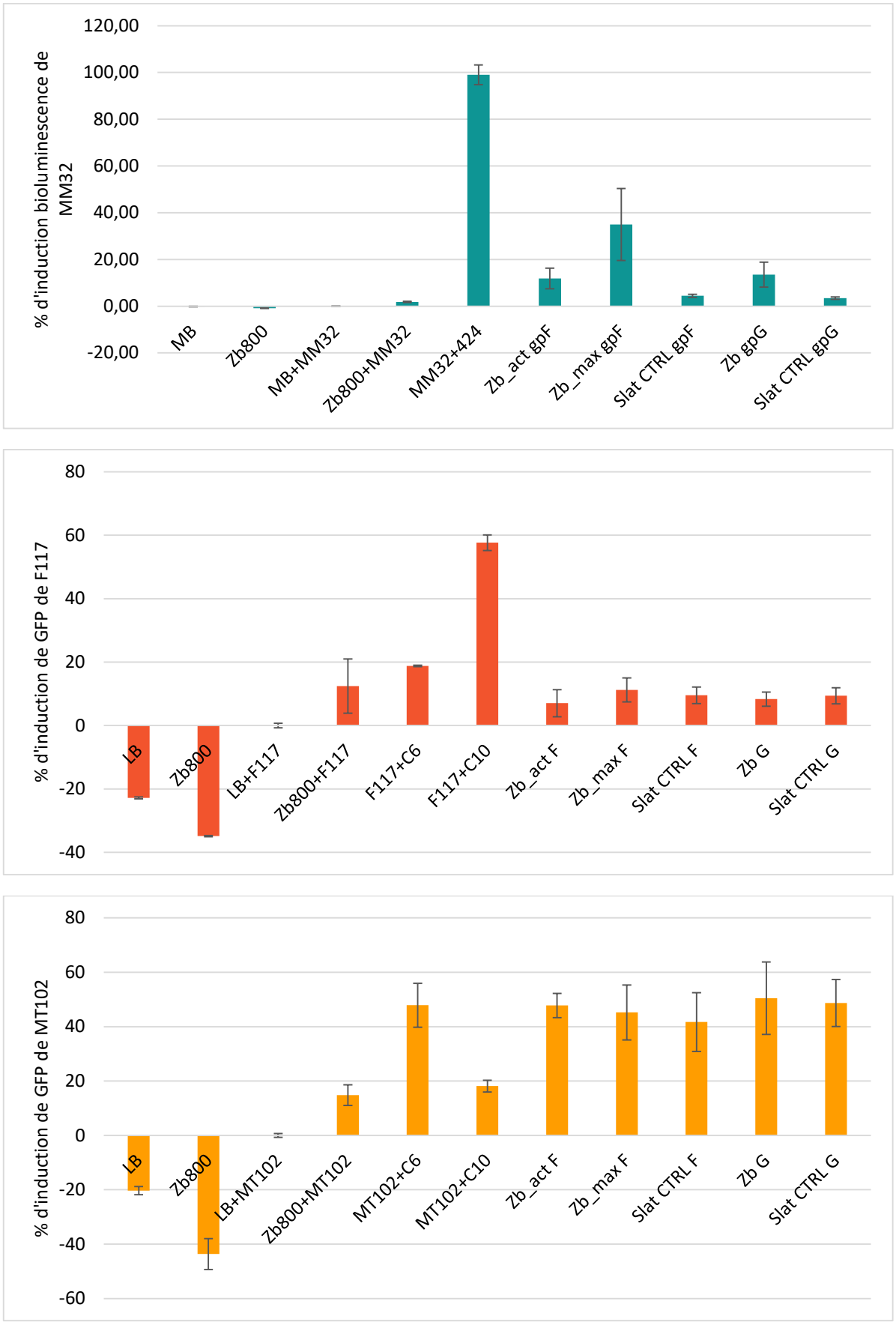

Figure 30 – Induction des biosenseurs par les différents surnageants de cocultures.

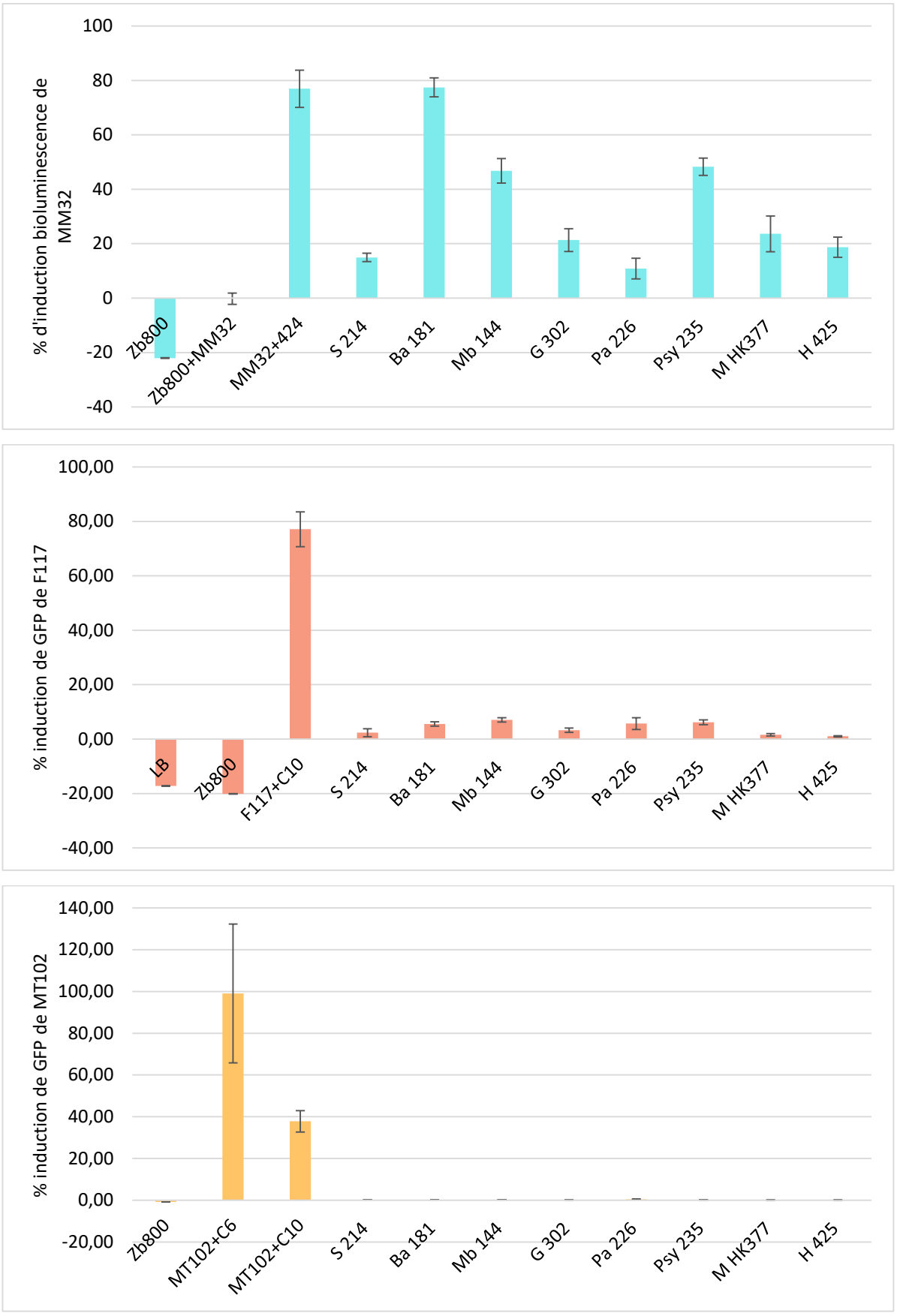

Figure 31 – Induction des biosenseurs par les différentes souches bactériennes

La

Figure 33 présente le niveau d'induction de MM32 dans les cocultures algues-bactéries. Il y a différents niveaux d'induction, allant d'une induction moyenne (>20% ; 11 cocultures) à forte (>50% ; 2 cocultures ; **Table 9**). Le groupe H, qui n'a pas reçu de Zobell, présente un niveau d'induction équivalent au niveau basal du biosenseur seul.

Table 9 – Cocultures algues-bactéries & induction du QS. Les taux de croissance sont ceux de la section IV.2 Figure 8 de ce chapitre. Pour la concentration en Zobell, très faible : <1 µl/ml, faible : 1-1.75 µl/ml, moyenne : 1.75-3.5 µl/ml, élevée : 3.5-5 µl/ml et très élevée : >5 µl/ml.

Induction de MM32	Cocultures	Taux de croissance par rapport au contrôle non inoculé	Concentration en Zobell
Moyenne >20%	B_Psy235	Non significatif	Très faible
	C_B5a	Très faible	Elevée
	C_ImpR9	Très faible	Très élevée
	D_G302	Faible	Très élevée
	D_Psy235	Faible	Elevée
	D_SMb	Non significatif	Très élevée
	D_Tutti	Faible	Très élevée
	E_SBaMb	Faible mais non significatif	Moyenne
	F_Ba181	Faible	Moyenne
	F_Psy235	Faible	Faible
	F_Zb_max	Très faible	Moyenne
Forte >50%	D_SPsy	Très faible	Très élevée
	E_Mb144	Faible mais non significatif	Très élevée

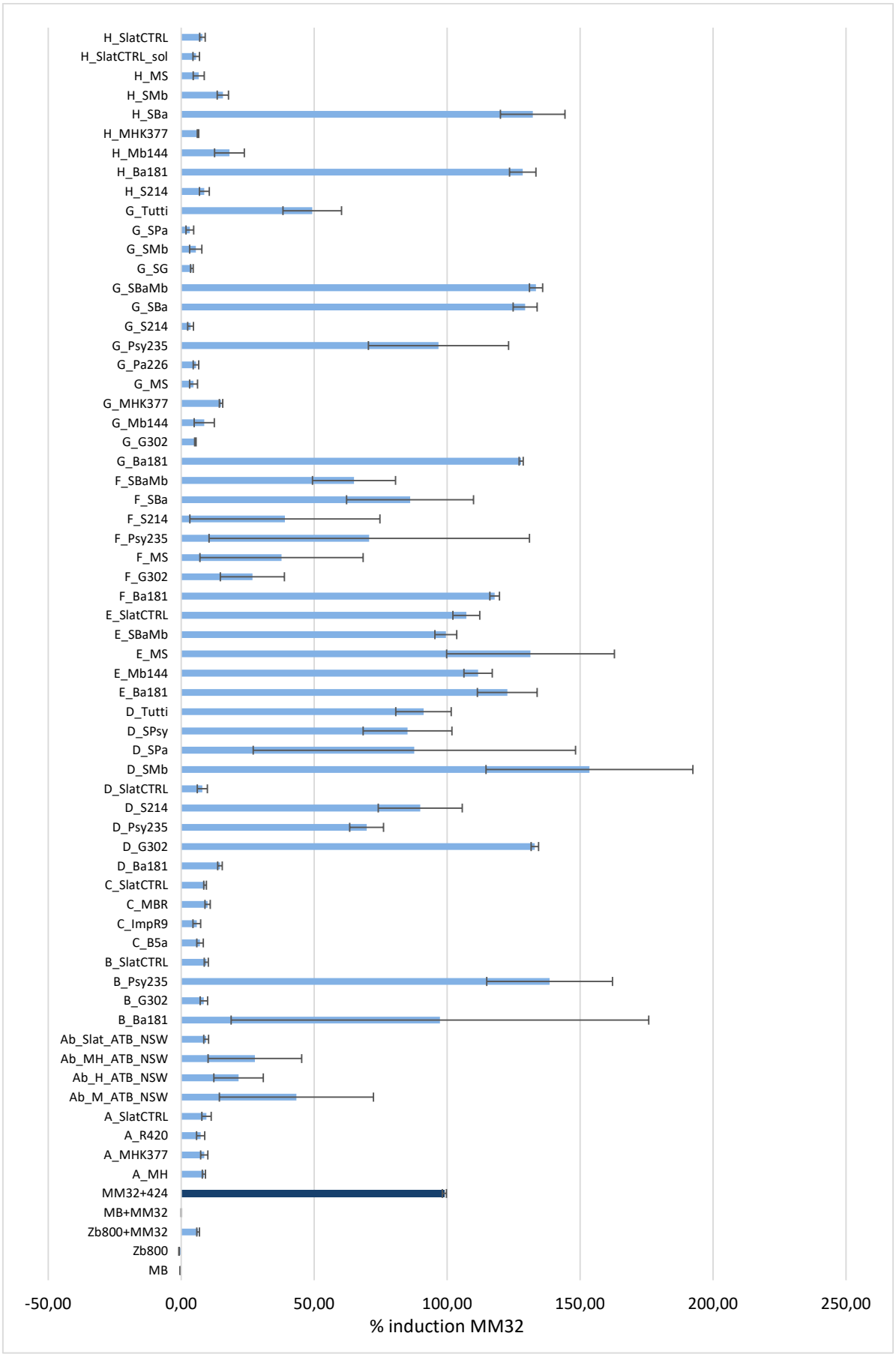

Figure 32 – Induction de MM32 par les surnageants de cocultures bactéries et algues + bactéries

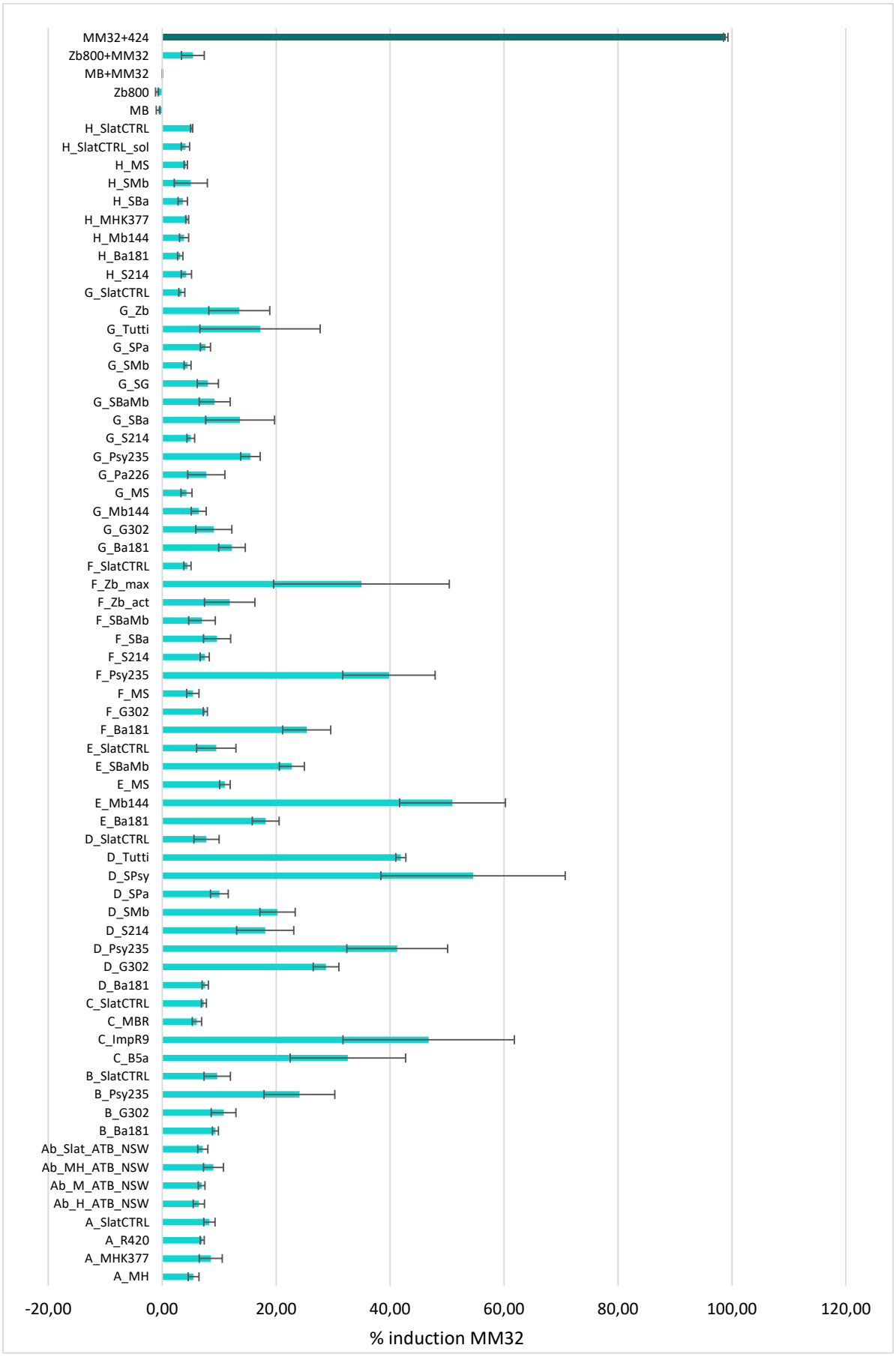

Figure 33 – Induction de MM32 dans CC algues-bactéries

QS & Zobell

De manière générale, il existe une légère corrélation entre l'induction de MM32 et le volume de Zobell inoculé dans la coculture (Spearman's rs *p-value= 0,0089* ; **Figure 34**). En effet, plus la concentration en Zobell augmente, plus la présence d'AI-2 est forte, même s'il existe certains points aberrants.

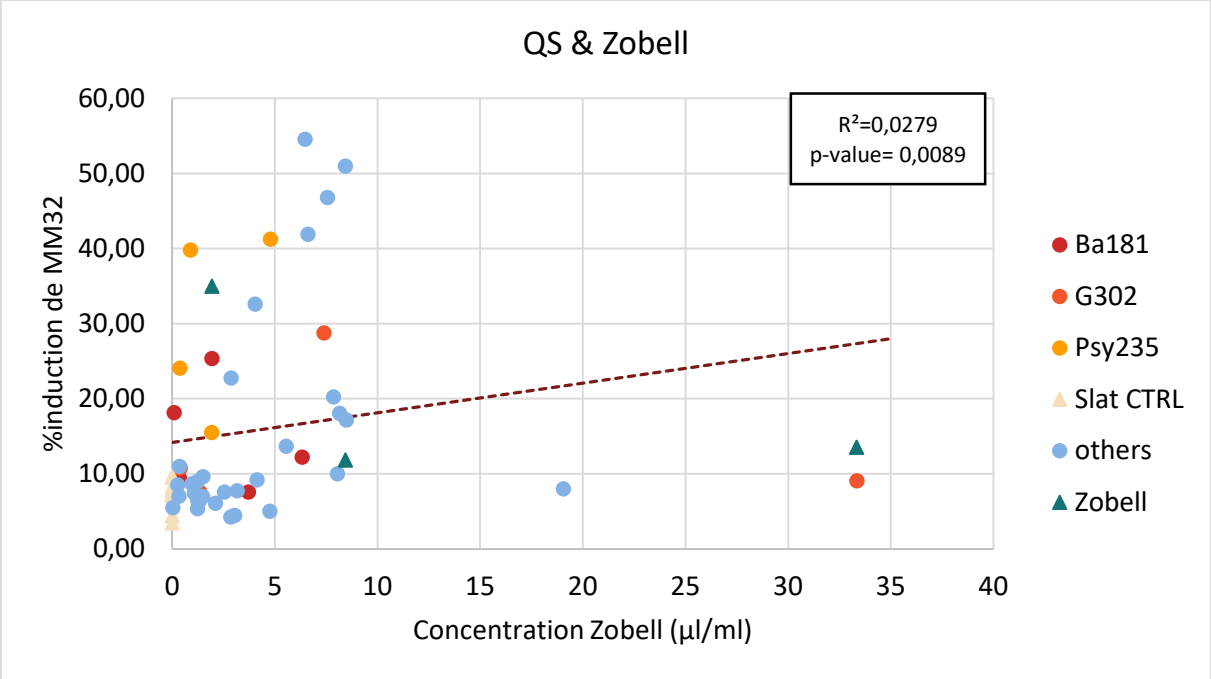

Figure 34 – Induction de MM32 en fonction de la concentration en Zobell

3. Corrélation Croissance des algues et QS

Il existe une corrélation entre une baisse de la croissance et une augmentation du QS dans les cocultures testées (*p-value= 0.00429* ; **Figure 35**).

Cependant, il reste des cocultures où la faible croissance n'est pas en lien avec la présence d'AI-2. Il se pourrait que d'autres molécules du QS, les AHLs, rentrent en jeu. L'induction des biosenseurs F117 et MT102 par les surnageants de ces cocultures a été testée, mais les résultats sont négatifs pour les deux (**Figure 36**).

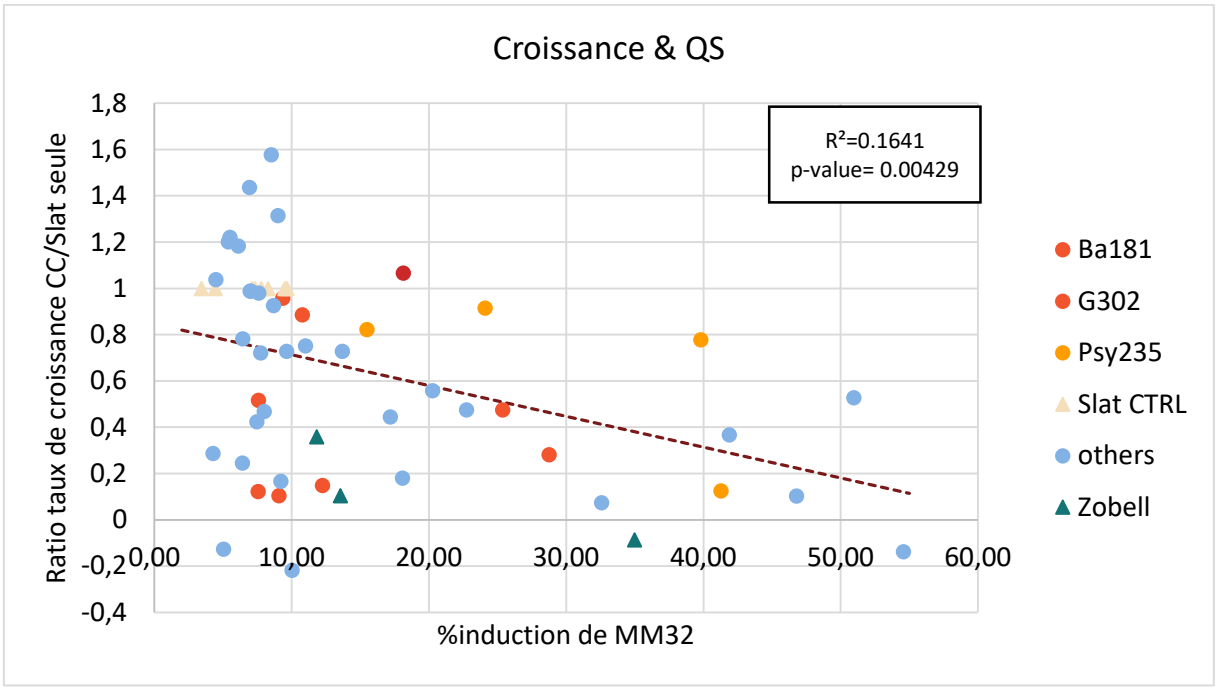

Figure 35 – Taux de croissance en fonction de l'induction de MM32

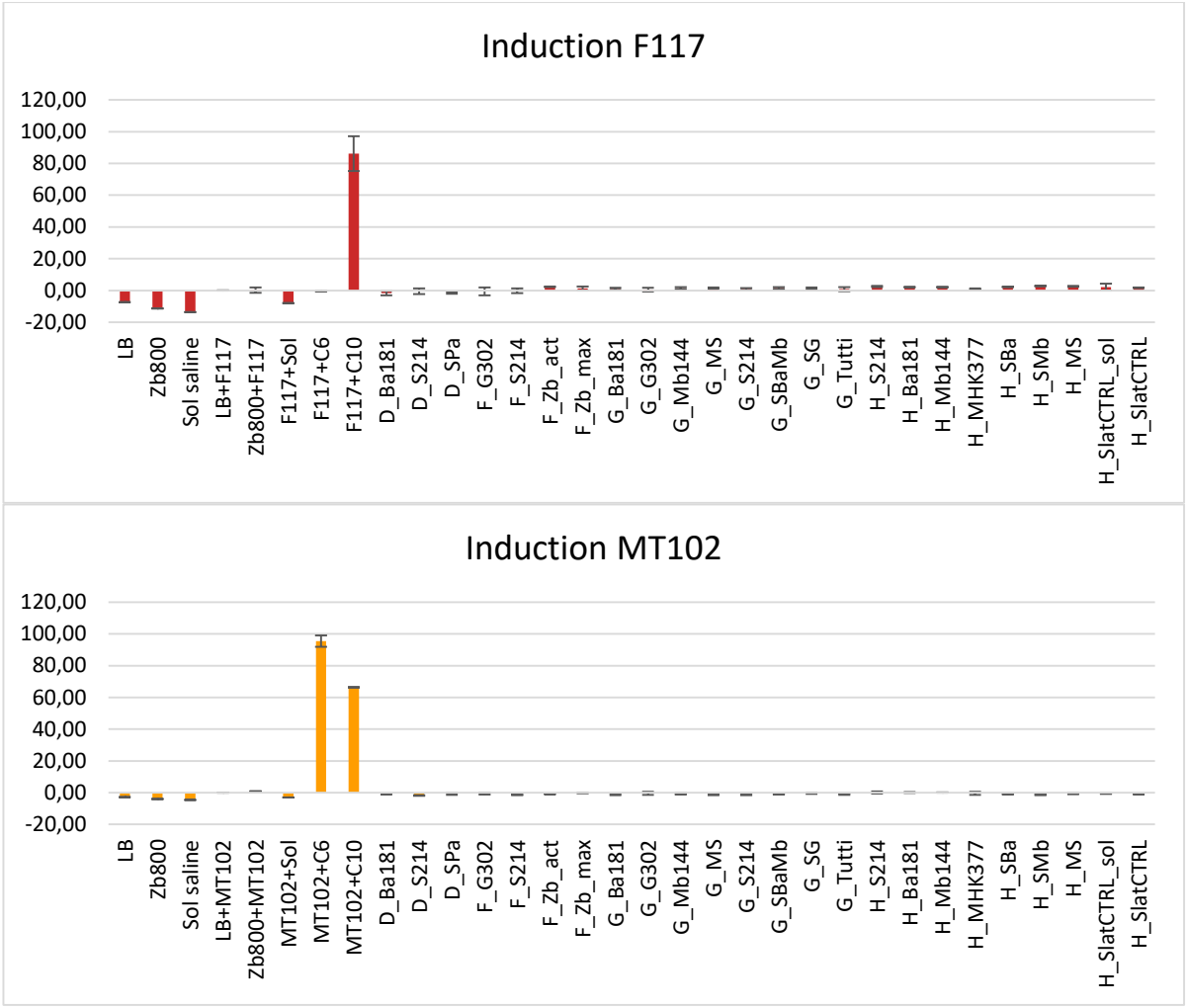

Figure 36 – Induction des biosenseurs AHL par les cocultures

L'étude de la composition bactérienne de ces cocultures est en cours et des résultats préliminaires sont présentés en section suivante. La composition bactérienne pourrait apporter des explications quant à cette faible croissance, mais également sur une possible corrélation entre la production des AI-2 et la présence de certains genres bactériens, ou sur la présence des souches inoculées sur le long terme. Cette analyse pourrait également expliquer certaines différences entre les groupes de cocultures.

VI. Etude de l'impact de l'inoculation sur la composition de la communauté bactérienne

1. Matériel & Méthodes

a. Echantillons

Les échantillons testés avec les biosenseurs ont également été utilisés pour les analyses de métabarcoding 16S. Pour chaque coculture, 3 des 4 tubes stockés à-80°C ont été sélectionnés au hasard. Les plantules contrôles prélevées avant inoculation « CTRL_anté » et les plantules non inoculées « SlatCTRL » ont également été analysées.

b. Extraction ADN

Les plantules stockées à -80°C ont été lyophilisées puis broyées (deux sessions, 30Hz, 45sec) au TissueLyserII (Qiagen, Hilden, Allemagne). Les extractions ont été faites sur les poudres avec le kit NucleoSpin® 96 Plant II – centrifuge processing (Macherey-Nagel), en suivant le protocole du fabricant.

c. Métabarcoding 16S

La composition de la communauté bactérienne associée avec les cultures d'algues a été déterminée par metabarcoding 16S. Une communauté mock comprenant un mélange d'ADN de 26 souches bactériennes (Thomas et al., 2019) et des contrôles négatifs a été traitée en parallèle des extraits d'ADN. Pour tous les échantillons, les régions V3 et V4 de l'ARNr 16S ont été amplifiées à l'aide des amorces NOCHL, comprenant des adaptateurs Illumina (Thomas et coll., 2019), afin d'éviter l'amplification de chloroplastes. Ensuite, un protocole Illumina standard pour le metabarcoding (Illumina, 2013) a été suivi : PCR Q5® High-Fidelity PCR Kit (New England BioLabs, MA, USA), kit de purification de produits PCR AMPure XP for PCR

Purification Kit (Beckman Coulter, Brea, CA, USA) et kit de préparation de librairies d'ADN Nextera XT DNA Library Preparation Kit (Illumina, San Diego, CA, USA).

Les librairies ont été quantifiées au Quantifluor® ds DNA System (Promega, WI, USA) et la taille moyenne des fragments a été déterminée à l'aide du LabChip® GX Touch™ (Perkin Elmer, MA, USA). Un pool équimolaire de tous les échantillons a été généré à une concentration de 4 nM, dilué à 3 pM, dopé à 10 % PhiX (Illumina) et séquencé sur un séquenceur Illumina MiSeq à l'aide d'un kit MiSeq v3 (2x300bp, à extrémité appariée) sur la plateforme Genomer de la Station Biologique.

d. Analyses

L'analyse des séquences a été faite avec le package DADA2 1.14.0 (Callahan et al., 2016) sur R 3.6.2. Les séquences ont été filtrées en suivant le protocole de Benjamin Callahan (https://benjjneb.github.io/dada2/tutorial.html), en admettant un maximum de 2 erreurs attendues et en réduisant la longueurs des reads à 291 pb (forward) et 250 pb (reverse). Une table des ASVs (*Amplicon Sequence Variant*) a été construite et les chimères supprimées. La taxonomie des ASVs restants a été assignée en utilisant la base de données Silva_SEED 138, et la table d'abondance et la classification taxonomique résultantes ont étés analysés avec Phyloseq 1.30.0 (McMurdie and Holmes, 2013). Les ASVs qui étaient abondants dans les contrôles négatifs, ou appartenant à des organites ou des eucaryotes, les ASVs rares (<0.01% des reads totaux), et les échantillons contenants moins de 7688 reads restants ont été enlevés. A partir de cette matrice des ASVs, une NMDS avec les distances de Bray-Curtis a été calculée avec le package R vegan.

2. Résultats

L'analyse multidimensionnelle non-métrique (NMDS) sur les données d'abondance montre une séparation en fonction du groupe de coculture plutôt qu'en fonction du type d'échantillon (**Figure 37**). Les échantillons Zobell (symbole +) mappent du même côté.

Les NMDS spécifiques à chaque groupe de cocultures sont présentées en **Figure 38**. Un changement dans la composition de la communauté bactérienne associée suite au transfert à T0 est visible pour tous les groupes. Il n'y a pas de regroupement des échantillons en fonction de la croissance.

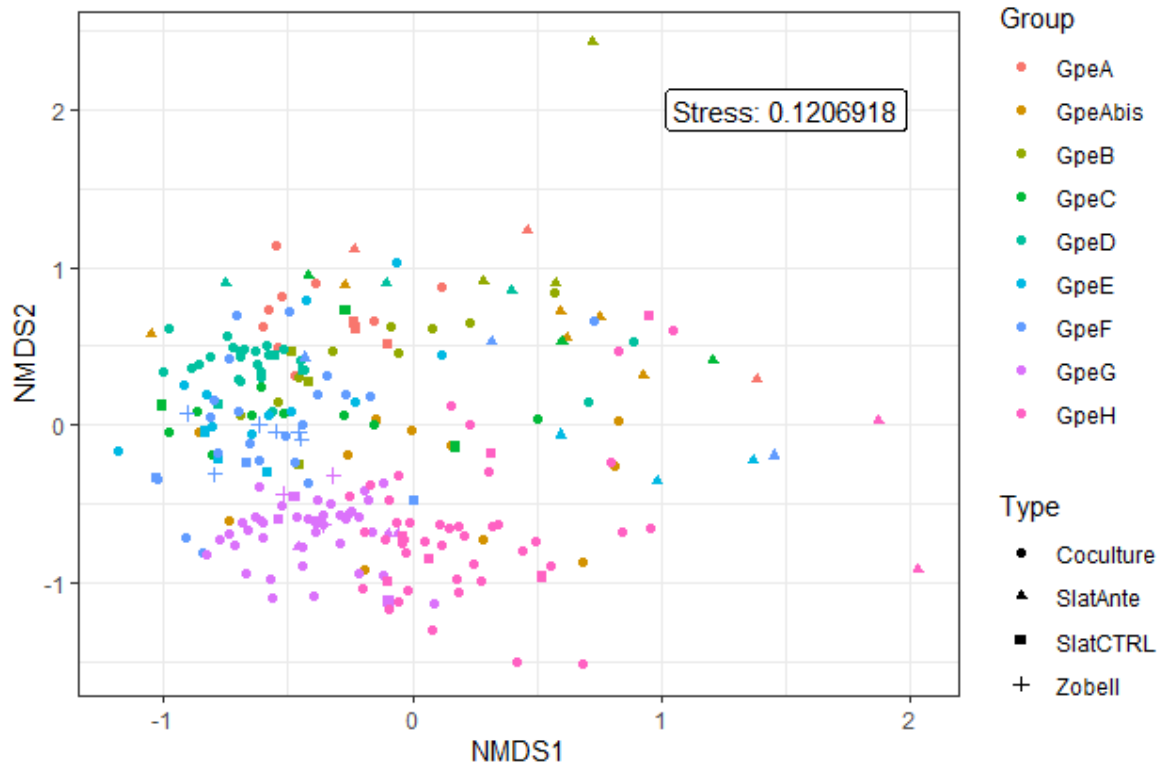

Figure 37 – NMDS générale sur les données d'abondance pour tous les groupes de cocultures

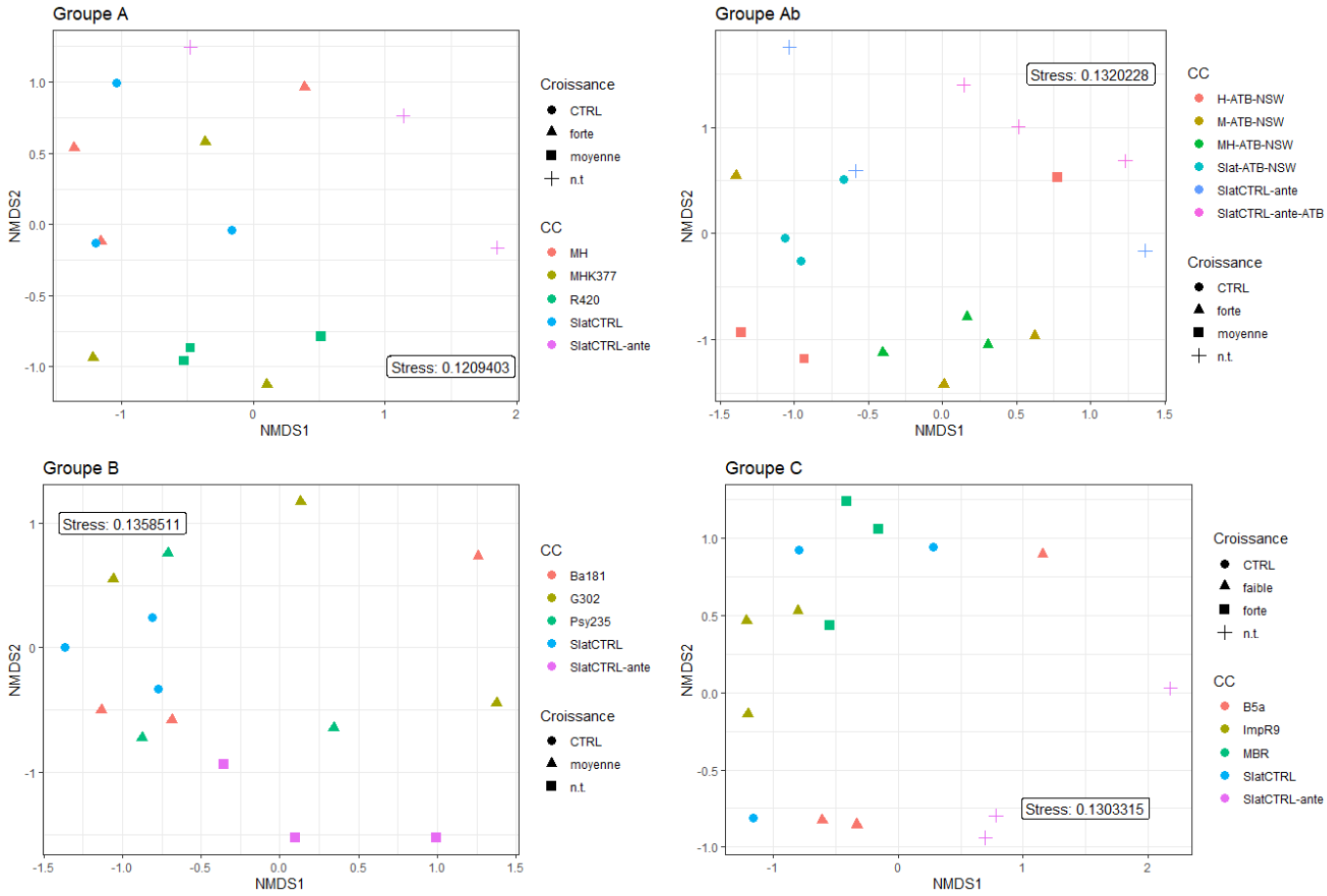

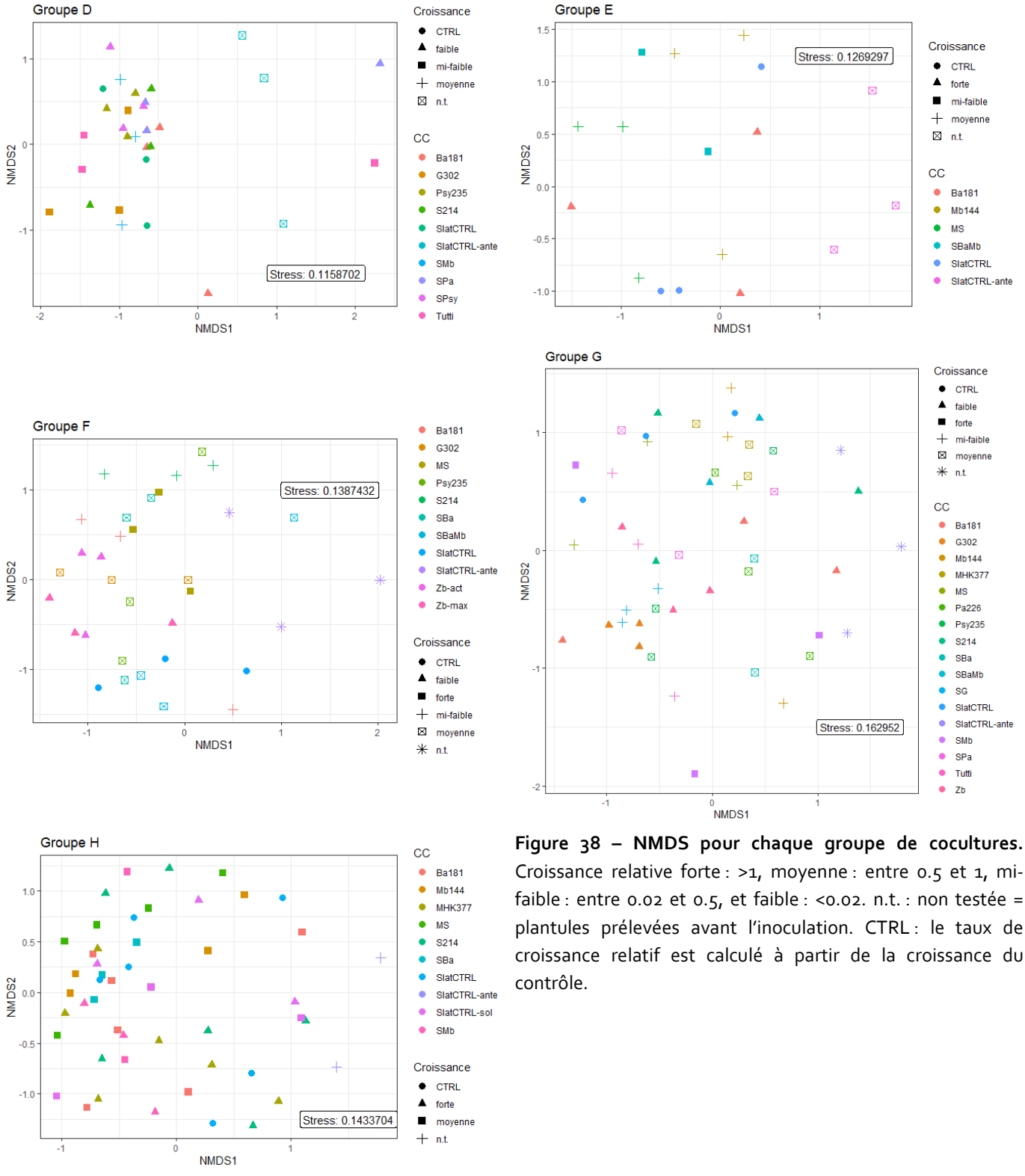

Figure 38 – NMDS pour chaque groupe de cocultures. Croissance relative forte : >1, moyenne : entre 0.5 et 1, mi-faible : entre 0.02 et 0.5, et faible : <0.02. n.t. : non testée = plantules prélevées avant l'inoculation. CTRL : le taux de croissance relatif est calculé à partir de la croissance du contrôle.

VII. Discussion

Nous avons observé une forte variabilité dans les résultats d'une coculture à l'autre, et cette problématique de répétabilité peut résulter de plusieurs facteurs : l'état général des plantules

au moment de l'inoculation, la modification de la composition du milieu de culture ou la composition de leur microbiote de départ.

Les résultats préliminaires sur *S. latissima* avec les souches d'*Ectocarpus* ne sont pas forcément reproductibles, puisqu'il faut stresser les plantules pour qu'une tendance négative d'*Hoeflea* soit observée. Par ailleurs, certaines souches positives chez *Ectocarpus* n'ont pas le même effet sur *S. latissima*. En effet, *Imperialibacter* et *Bosea* ont un effet très négatif sur la croissance alors qu'elles la favorisaient chez *Ectocarpus* (Burgunter-Delamare et al., 2020). Ainsi, la proximité phylogénétique des hôtes ne garantit en rien la redondance de l'effet positif.

De manière générale, l'inoculation de bactéries impacte la composition du microbiote dans son ensemble, ce qui avait été montré avec *Ectocarpus*. Par ailleurs, le regroupement des échantillons se fait en fonction de leur groupe de coculture plutôt qu'en fonction du type de coculture ou de leur croissance, renforçant ainsi l'idée que deux plantules ne réagiront pas de la même manière face à l'inoculation. La composition du microbiote de l'algue de départ peut donc être un facteur extrêmement important qui va modérer l'impact des souches inoculées sur leur hôte.

Un facteur corrélé avec la baisse de croissance est le phénomène de quorum sensing et notamment la production d'AI-2 dans les cocultures, qui pourrait entrainer une dysbiose. Cette dysbiose pourrait être favorisée par les nutriments présents dans le milieu Zobell, ce qui permettrai une prolifération bactérienne (en nombre de bactéries totales ou en groupes bactériens spécifiques), et ainsi d'atteindre la concentration seuil de déclenchement du QS. Les bactéries impliquées pourraient alors activer des voies de biosynthèse différentes, la production de facteur de virulences ou rediriger des molécules nécessaires à la croissance de l'algue (Stubbendieck and Straight, 2016).

Dans l'objectif de découvrir un impact spécifique d'une souche sur les plantules de *S. latissima*, il faudrait réaliser d'autres séries de réplicats et analyser la fréquence d'observation d'un effet sur la croissance pour cette souche. Ces analyses couplées à l'étude plus approfondie du jeu de données de métabarcoding pourraient mettre en lumière une composition bactérienne particulière en fonction du type d'échantillon et une évolution caractéristique dans la composition de la communauté.

Des analyses statistiques plus poussées sur la composition bactérienne des échantillons Zobell pourrait nous aider à comprendre quels groupes bactériens sont responsables du QS et de la baisse de croissance au sein de ces cocultures. L'élargissement de ces analyses aux autre cocultures serait aussi une approche pertinente.

Pour aller plus loin, des résultats non publiés au sein de l'équipe ont montré sur les plantules de *Laminaria digitata* possèdent un microbiote très proche de celui du méristème des sporophytes matures. Il serait intéressant de regarder si le même type de constatation peut être faite chez *Saccharina latissima*, auquel cas il serait judicieux d'inoculer les plantules avec des bactéries essentiellement présentes au niveau des méristèmes pour en mesurer les effets. En effet, l'ajout de bactéries présentes chez les apex pourrait ne pas avoir d'effet, ces souches étant hors de leur niche, ou entrainer un déséquilibre « involontaire » du système.

VIII. Données Supplémentaires

Table S3 - Affiliation taxonomique des souches bactériennes isolées de *S. latissima* et nombre d'isolats bactériens correspondants

						Roscoff							Norvège		
						Octobre 2018		Janvier 2019		Avril 2019		Juillet 2019	Octobre 2018	Avril 2019	
						Sain	Symptômes	Sain	Symptômes	Sain	Symptômes	Symptômes			
Phylum	**Classe**	**Ordre**	**Famille**	**Genre**	**Souche**										Total isolats / souche unique
Actinobacteria	*Actinomycetia*	*Corynebacteriales*	*Nocardiaceae*	*Rhodococcus*	SL-BBDNW59									1	1
Actinobacteria	*Actinomycetia*	*Corynebacteriales*	*Nocardiaceae*	*Rhodococcus*	SL-BBDNW64									2	2
Actinobacteria	*Actinomycetia*	*Glycomycetales*	*Glycomycetaceae*	*Glycomyces*	SL-BBD168				1						1
Actinobacteria	*Actinomycetia*	*Micrococcales*	*Demequinaceae*	*Demequina*	SL-BBD127		1								1
Actinobacteria	*Actinomycetia*	*Micrococcales*	*Microbacteriaceae*	*Agrococcus*	SL-BBD152		1								1
Actinobacteria	*Actinomycetia*	*Micrococcales*	*Microbacteriaceae*	*Microbacterium*	SL-BBD207					1					1
Actinobacteria	*Actinomycetia*	*Micrococcales*	*Microbacteriaceae*	*Microbacterium*	SL-BBD209						1				1
Actinobacteria	*Actinomycetia*	*Micrococcales*	*Microbacteriaceae*	*Microbacterium*	SL-BBD252		2		2						4
Actinobacteria	*Actinomycetia*	*Micrococcales*	*Microbacteriaceae*	*Salinibacterium*	SL-BBD143		4		1	1					6
Actinobacteria	*Actinomycetia*	*Micrococcales*	*Micrococcaceae*	*Kocuria*	SL-BBD151	1									1
Actinobacteria	*Actinomycetia*	*Micrococcales*	*Promicromonosporaceae*	*Isoptericola*	SL-BBD260				1						1
Actinobacteria	*Actinomycetia*	*Propionibacteriales*	*Nocardioidaceae*	*Nocardioides*	SL-BBD155	1									1
Actinobacteria	*Actinomycetia*	*Propionibacteriales*	*Propionibacteriaceae*	*Desertihabitans*	SL-BBD146				4		4				8
Actinobacteria	*Actinomycetia*	*Streptomycetales*	*Streptomycetaceae*	*[Kitasatospora]*	SL-BBD124		1								1
Actinobacteria	*Actinomycetia*	*Streptomycetales*	*Streptomycetaceae*	*Streptomyces*	SL-BBD094		1								1
Actinobacteria	*Actinomycetia*	*Streptomycetales*	*Streptomycetaceae*	*Streptomyces*	SL-BBD128		2								2
Actinobacteria	*Actinomycetia*	*Streptomycetales*	*Streptomycetaceae*	*Streptomyces*	SL-BBD139	1									1
Actinobacteria	*Actinomycetia*	*Streptomycetales*	*Streptomycetaceae*	*Streptomyces*	SL-BBD262			1							1
Bacteroidetes	*Flavobacteriia*	*Flavobacteriales*	*Flavobacteriaceae*	*Maribacter*	SL-BBD144		1								1
Firmicutes	*Bacilli*	*Bacillales*	*Bacillaceae*	*Alkalihalobacillus*	SL-BBD071	5	4				2				11
Firmicutes	*Bacilli*	*Bacillales*	*Bacillaceae*	*Alkalihalobacillus*	SL-BBD171	23	26	14	18	2	4	3			90
Firmicutes	*Bacilli*	*Bacillales*	*Bacillaceae*	*Bacillus*	SL-BBD076	1									1
Firmicutes	*Bacilli*	*Bacillales*	*Bacillaceae*	*Bacillus*	SL-BBD081	2	3								5
Firmicutes	*Bacilli*	*Bacillales*	*Bacillaceae*	*Bacillus*	SL-BBD309							1			1
Firmicutes	*Bacilli*	*Bacillales*	*Bacillaceae*	*Bacillus*	SL-BBDNW41			1						1	2
Firmicutes	*Bacilli*	*Bacillales*	*Bacillaceae*	*Halobacillus*	SL-BBD283			2							2

Firmicutes	*Bacilli*	*Bacillales*	*Bacillaceae*	*Peribacillus*	SL-BBD181	1	1	1	4						7
Firmicutes	*Bacilli*	*Bacillales*	*Bacillaceae*	*Peribacillus*	SL-BBD085	1									1
Firmicutes	*Bacilli*	*Bacillales*	*Bacillaceae*	*Priestia*	SL-BBD212	2	5		2						9
Firmicutes	*Bacilli*	*Bacillales*	*Bacillaceae*	*Rossellomorea*	SL-BBD093		1								1
Firmicutes	*Bacilli*	*Bacillales*	*Bacillaceae*	*Rossellomorea*	SL-BBD107		1		6						7
Firmicutes	*Bacilli*	*Bacillales*	*Bacillaceae*	*Virgibacillus*	SL-BBD153		1								1
Firmicutes	*Bacilli*	*Bacillales*	*Paenibacillaceae*	*Paenibacillus*	SL-BBDNW60									2	2
Firmicutes	*Bacilli*	*Bacillales*	*Paenibacillaceae*	*Paenibacillus*	SL-BBDNW63									1	1
Firmicutes	*Bacilli*	*Bacillales*	*Planococcaceae*	*Jeotgalibacillus*	SL-BBDNW17A								1		1
Firmicutes	*Bacilli*	*Bacillales*	*Planococcaceae*	*Paenisporosarcina*	SL-BBD135		1								1
Firmicutes	*Bacilli*	*Bacillales*	*Planococcaceae*	*Sporosarcina*	SL-BBD267				1						1
Firmicutes	*Bacilli*	*Bacillales*	*Staphylococcaceae*	*Staphylococcus*	SL-BBD130		1								1
Proteobacteria	*Alphaproteobacteria*	*Caulobacterales*	*Caulobacteraceae*	*Brevundimonas*	SL-BBD256			1							1
Proteobacteria	*Alphaproteobacteria*	*Caulobacterales*	*Caulobacteraceae*	*Brevundimonas*	SL-BBD269			1							1
Proteobacteria	*Alphaproteobacteria*	*Hyphomicrobiales*	*Amorphaceae*	*Amorphus*	SL-BBD156		1								1
Proteobacteria	*Alphaproteobacteria*	*Hyphomicrobiales*	*Rhizobiaceae*	*Rhizobium*	SL-BBD200			2			1				3
Proteobacteria	*Alphaproteobacteria*	*Hyphomicrobiales*	*Stappiaceae*	*Labrenzia*	SL-BBD111		1								1
Proteobacteria	*Alphaproteobacteria*	*Hyphomicrobiales*	*Stappiaceae*	*Pseudovibrio*	SL-BBD005		4								4
Proteobacteria	*Alphaproteobacteria*	*Hyphomicrobiales*	*Stappiaceae*	*Pseudovibrio*	SL-BBD164		3								3
Proteobacteria	*Alphaproteobacteria*	*Hyphomicrobiales*	*Stappiaceae*	*Roseibium*	SL-BBD299		1				1				2
Proteobacteria	*Alphaproteobacteria*	*Rhodobacterales*	*Rhodobacteraceae*	*Cereibacter*	SL-BBD184				1						1
Proteobacteria	*Alphaproteobacteria*	*Rhodobacterales*	*Rhodobacteraceae*	*Paracoccus*	SL-BBD013B		1								1
Proteobacteria	*Alphaproteobacteria*	*Rhodobacterales*	*Rhodobacteraceae*	*Paracoccus*	SL-BBD201			4		1					5
Proteobacteria	*Alphaproteobacteria*	*Rhodobacterales*	*Rhodobacteraceae*	*Paracoccus*	SL-BBD293						1				1
Proteobacteria	*Alphaproteobacteria*	*Rhodobacterales*	*Rhodobacteraceae*	*Sulfitobacter*	SL-BBD214						1				1
Proteobacteria	*Alphaproteobacteria*	*Sphingomonadales*	*Erythrobacteraceae*	*Altericroceibacterium*	SL-BBD086	1									1
Proteobacteria	*Alphaproteobacteria*	*Sphingomonadales*	*Sphingomonadaceae*	*Sphingobium*	SL-BBD292				1						1
Proteobacteria	*Alphaproteobacteria*	*Sphingomonadales*	*Sphingomonadaceae*	*Sphingomonas*	SL-BBD300		2	2		1				1	6
Proteobacteria	*Betaproteobacteria*	*Burkholderiales*	*Burkholderiaceae*	*Ralstonia*	SL-BBDNW28								1		1
Proteobacteria	*Gammaproteobacteria*	*Alteromonadales*	*Alteromonadaceae*	*Alteromonas*	SL-BBD219						1				1
Proteobacteria	*Gammaproteobacteria*	*Alteromonadales*	*Alteromonadaceae*	*Alteromonas*	SL-BBD243A					1	1				2
Proteobacteria	*Gammaproteobacteria*	*Alteromonadales*	*Pseudoalteromonadaceae*	*Pseudoalteromonas*	SL-BBD226					2	2				4
Proteobacteria	*Gammaproteobacteria*	*Alteromonadales*	*Pseudoalteromonadaceae*	*Pseudoalteromonas*	SL-BBD275					4	3				7

Proteobacteria	*Gammaproteobacteria*	*Alteromonadales*	*Pseudoalteromonadaceae*	*Pseudoalteromonas*	SL-BBD303					1	3				4
Proteobacteria	*Gammaproteobacteria*	*Alteromonadales*	*Psychromonadaceae*	*Psychromonas*	SL-BBD235					3					3
Proteobacteria	*Gammaproteobacteria*	*Cellvibrionales*	*Microbulbiferaceae*	*Microbulbifer*	SL-BBD065	11	14	2					1		28
Proteobacteria	*Gammaproteobacteria*	*Cellvibrionales*	*Microbulbiferaceae*	*Microbulbifer*	SL-BBD161	1									1
Proteobacteria	*Gammaproteobacteria*	*Chromatiales*	*Granulosicoccaceae*	*Granulosicoccus*	SL-BBD302					1	1				2
Proteobacteria	*Gammaproteobacteria*	*Oceanospirillales*	*Halomonadaceae*	*Chromohalobacter*	SL-BBDNW09								1		1
Proteobacteria	*Gammaproteobacteria*	*Oceanospirillales*	*Halomonadaceae*	*Cobetia*	SL-BBDNW29	2	4			2	6	3	3		20
Proteobacteria	*Gammaproteobacteria*	*Oceanospirillales*	*Halomonadaceae*	*Salinicola*	SL-BBDNW24								3		3
Proteobacteria	*Gammaproteobacteria*	*Oceanospirillales*	*Halomonadaceae*	*Salinicola*	SL-BBDNW26B								5	1	6
Proteobacteria	*Gammaproteobacteria*	*Pseudomonadales*	*Moraxellaceae*	*Psychrobacter*	SL-BBD102		2								2
Proteobacteria	*Gammaproteobacteria*	*Pseudomonadales*	*Moraxellaceae*	*Psychrobacter*	SL-BBD123		4				3				7
Proteobacteria	*Gammaproteobacteria*	*Pseudomonadales*	*Moraxellaceae*	*Psychrobacter*	SL-BBD249A						6				6
Proteobacteria	*Gammaproteobacteria*	*Pseudomonadales*	*Pseudomonadaceae*	*Pseudomonas*	SL-BBDNW40									1	1
Proteobacteria	*Gammaproteobacteria*	*Xanthomonadales*	*Xanthomonadaceae*	*Stenotrophomonas*	SL-BBD066		1							3	4
				Total isolats / zone		53	95	31	42	20	41	7	15	13	**317**

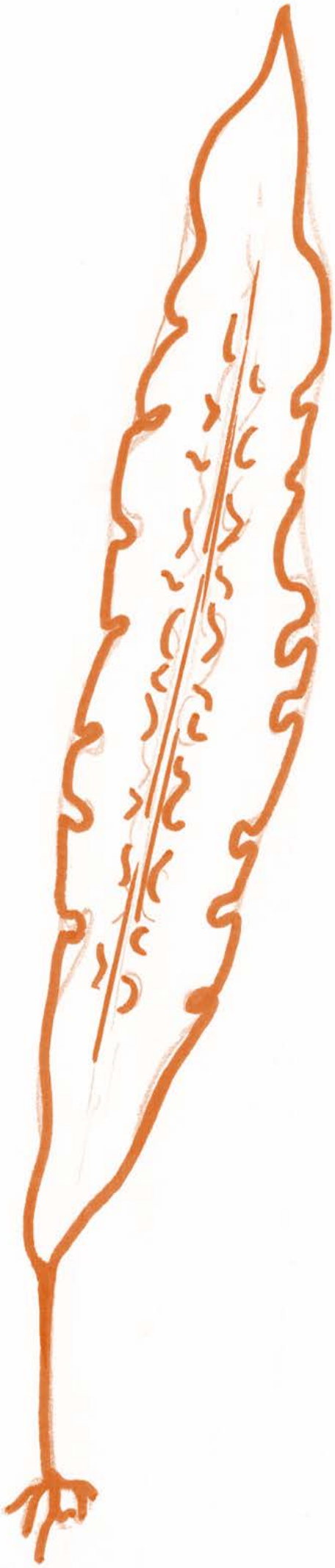

- CONCLUSION & PERSPECTIVES -

CONCLUSION & PERSPECTIVES

Ma thèse sur *S. latissima* et son microbiote avait pour but de le caractériser et d'étudier leurs interactions pour comprendre dans quelles mesures la composition du microbiote influence la croissance de l'algue.

Pour commencer, la notion d'holobionte n'est valable qu'en présence d'une association longue et durable entre les deux partenaires, ce qui est le cas ici, avec la présence d'un core de genres bactériens apex/méristème présent chez tous les individus, peu importe l'origine des échantillons (**Figure 39**).

Je me suis demandé quelle était la composition du microbiote des populations naturelles de *S. latissima,* et si le microbiote évoluait en fonction de paramètres particulier comme la condition physiologique de l'hôte, son origine géographique ou la saison. Mon travail montre que ces facteurs influencent effectivement la composition du microbiote, avec une importance décroissante : les tissus algaux, l'origine géographique, la saisonnalité et l'état physiologique de l'algue (**Chapitre II**).

Je trouve particulièrement intéressant que le facteur hôte soit le plus déterminant, et ce, quel que soit l'environnement : cette régulation fine de la composition par l'hôte surpasse l'accumulation de facteurs extérieurs dont un impact puissant pourrait être attendu. Une caractérisation du métabolome associée à ces tissus et à cette sélection pourrait permettre de comprendre les mécanismes moléculaires en jeu. Cette analyse pourrait aussi mettre en évidence les mécanismes de défense mis en place par l'hôte dans le cas d'une dysbiose.

L'isolement de la part cultivable de ce microbiote a permis de créer par la suite des systèmes holobionte simplifiés, avec pour objectif d'étudier l'impact de ces souches sur la croissance de l'hôte.

Mon travail montre que la perturbation du microbiote (par inoculation ou par antibiotiques) impacte fortement l'hôte et la communauté bactérienne associée dans son ensemble, et que les effets sont variables d'un groupe de plantule à l'autre (**Chapitre III**). En effet, la composition du microbiote initial joue un rôle important dans la réponse de l'hôte à l'inoculation. Certains composants bactériens pourraient protéger l'holobionte d'une dysbiose en limitant le développement de bactéries néfastes. Cette protection passerait par le blocage du phénomène de quorum sensing, limitant l'apparition de phénomène de

virulence par exemple. L'activation du QS dans les cocultures montrant une dysbiose (**Figure 39**) est également une piste à poursuivre et l'analyse de la composition des communautés bactériennes est nécessaire pour comprendre quels genres bactériens en sont responsables. Ces analyses sont en cours de réalisation.

L'holobionte est un système complexe et son étude *in vivo* passe par la simplification de ce système. La plupart des études portant sur l'impact du microbiote sur son hôte passent par une étape de nettoyage ou d'éradication du microbiote initial, et par une inoculation ensuite d'une ou plusieurs souches bactériennes. Cependant, la perturbation du microbiote perturbe aussi l'hôte, et de ce fait, l'effet observé n'est pas nécessairement celui de la souche inoculée, mais la résultante de la dysbiose. Cette constatation est d'autant plus vraie pour l'analyse de l'impact de souches avec un effet considéré comme négatif pour l'hôte.

L'utilisation de souches d'algues acclimatées en laboratoire avec un microbiote réduit pourrait être un moyen de tester des souches bactériennes d'intérêt (avec des ajouts successifs) et la réalisation de nombreux réplicats pour connaitre l'effet réel de ces souches. Seulement, cette technique ne permet que d'approcher de la réalité, l'holobionte étant un système complexe. En effet, l'hyper-simplification du système (une algue + quelques souches bactériennes) ne prend pas en compte les interactions bactéries-bactéries qui ont également lieu au sein de l'holobionte.

Par ailleurs, l'obtention de souches axéniques chez *Saccharina latissima* et *Ectocarpus* est extrêmement difficile, voire impossible (l'algue meurt sans son microbiote) : ce phénomène ne semble pas se retrouver chez l'algue verte *Ulva* sp. En effet, l'étude des interactions hôte-microbiote chez *Ulva* sp. faite avec des *Ulva* asymbiotiques, a montré que l'association avec deux souches bactériennes (*Roseovarius* sp. et *Maribacter* sp.) était indispensable pour la croissance et le développement morphologique de l'algue. Pour moi, il serait intéressant de comparer les réseaux métaboliques de ces trois algues, pour comprendre dans quelles mesures elles sont dépendantes de leurs microbiotes pour des fonctions essentielles à leur survie. Il se pourrait que ces algues brunes soient très dépendantes de leurs partenaires bactériens pour remplir certaines fonctions vitales, expliquant ainsi la difficulté à obtenir des algues axéniques viables.

L'obtention du réseau métabolique de l'algue fait partie des outils développés sur *Ectocarpus*, et je pense que sa transposition sur *Saccharina latissima* serait une approche intéressante pour l'analyse des interactions algue-bactéries, et la complémentation métabolique qui en découle. Ce type de comparaison pourrait apporter des réponses quant à l'effet bénéfique, néfaste ou neutre d'une souche en fonction de l'hôte avec lequel elle est cultivée. En effet, les différences dans l'impact sur l'hôte pourraient être dues à une redondance dans les réactions métaboliques déjà présentes chez l'algue, ou à une complémentation incomplète, ou en inadéquation avec les besoins de l'hôte. Cela permettrait également d'aborder la spécificité hôte-microbiote chez les algues brunes.

De même, les différences observées entre *Ectocarpus* et *Saccharina* pourraient s'expliquer par la complexité de ces systèmes holobionte. Une étude du microbiote des populations naturelles d'*Ectocarpus* et de *Saccharina,* prélevées au même endroit et au même moment, serait intéressante pour réaliser une comparaison complète des microbiotes. Les données sur le microbiote d'*Ectocarpus* proviennent principalement de souches de laboratoire et il est probable que les populations naturelles possèdent des communautés associées plus diverses, le microbiote étant une signature caractéristique et unique de l'hôte.

Finalement, mon travail a montré l'importance du microbiote pour l'hôte *Saccharina latissima* et que sa perturbation entraine des effets négatifs sur la croissance. La poursuite et l'approfondissement de ces recherches sur les populations naturelles pourraient également apporter des réponses nécessaires sur le déclin et la possible sauvegarde des populations naturelles.

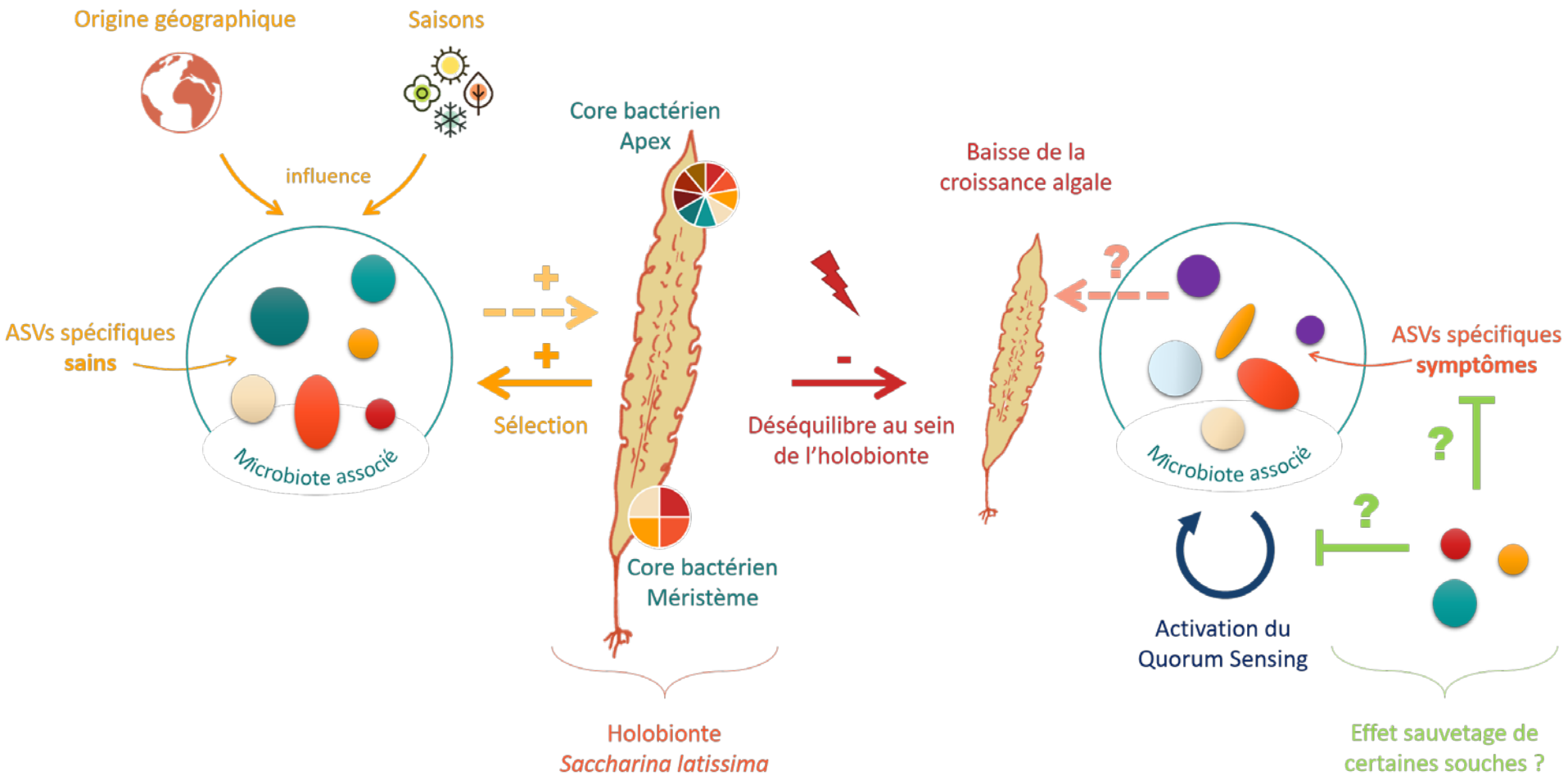

Figure 39 – Schéma récapitulatif des principaux résultats de thèse. L'épaisseur des flèches caractérisent l'importance des facteurs d'influence.

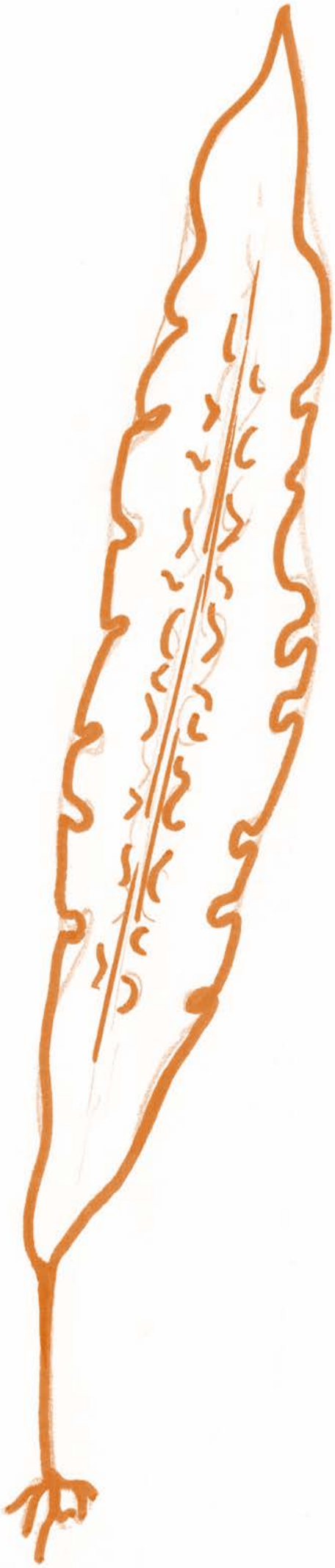

- REFERENCES BIBLIOGRAPHIQUES -

REFERENCES BIBLIOGRAPHIQUES

Alderkamp, A.-C., Van Rijssel, M., and Bolhuis, H. (2007). Characterization of marine bacteria and the activity of their enzyme systems involved in degradation of the algal storage glucan laminarin: *FEMS Microbiol. Ecol.* 59, 108–117. doi:10.1111/j.1574-6941.2006.00219.x.

Alsufyani, T., Califano, G., Deicke, M., Grueneberg, J., Weiss, A., Engelen, A. H., et al. (2020). Macroalgal–bacterial interactions: identification and role of thallusin in morphogenesis of the seaweed *Ulva* (Chlorophyta). *J. Exp. Bot.* 71, 3340–3349. doi:10.1093/jxb/eraa066.

Amsler, C. D., and Neushul, M. (1989). Chemotactic effects of nutrients on spores of the kelps *Macrocytis pyrifera* and *Pterygophora california*. *Mar. Biol.* 102, 557–564. doi:10.1007/BF00438358.

Andersen, J. B., Heydorn, A., Hentzer, M., Eberl, L., Geisenberger, O., Christensen, B. B., et al. (2001). *gfp* -based *n* -acyl homoserine-lactone sensor systems for detection of bacterial communication. *Appl. Environ. Microbiol.* 67, 575–585. doi:10.1128/AEM.67.2.575-585.2001.

Araújo, R. M., Assis, J., Aguillar, R., Airoldi, L., Bárbara, I., Bartsch, I., et al. (2016). Status, trends and drivers of kelp forests in Europe: an expert assessment. *Biodivers. Conserv.* 25, 1319–1348. doi:10.1007/s10531-016-1141-7.

Atkinson, S., and Williams, P. (2009). Quorum sensing and social networking in the microbial world. *J. R. Soc. Interface* 6, 959–978. doi:10.1098/rsif.2009.0203.

Badri, D. V., Zolla, G., Bakker, M. G., Manter, D. K., and Vivanco, J. M. (2013). Potential impact of soil microbiomes on the leaf metabolome and on herbivore feeding behavior. *New Phytol.* 198, 264–273. doi:10.1111/nph.12124.

Balakirev, E. S., Krupnova, T. N., and Ayala, F. J. (2012). Symbiotic associations in the phenotypically-diverse brown alga *Saccharina japonica*. *PLoS ONE* 7, e39587. doi:10.1371/journal.pone.0039587.

Bang, C., and Schmitz, R. A. (2018). *Archaea*: forgotten players in the microbiome. *Emerg. Top. Life Sci.* 2, 459–468. doi:10.1042/ETLS20180035.

Bartsch, I., Wiencke, C., Bischof, K., Buchholz, C. M., Buck, B. H., Eggert, A., et al. (2008). The genus *Laminaria sensu lato* : recent insights and developments. *Eur. J. Phycol.* 43, 1–86. doi:10.1080/09670260701711376.

Bassler, B. L., Wright, M., Showalter, R. E., and Silverman, M. R. (1993). Intercellular signalling in *Vibrio harveyi*: sequence and function of genes regulating expression of luminescence. *Mol. Microbiol.* 9, 773–786. doi:10.1111/j.1365-2958.1993.tb01737.x.

Beattie, D. T., Lachnit, T., Dinsdale, E. A., Thomas, T., and Steinberg, P. D. (2018). Novel ssDNA viruses detected in the virome of bleached, habitat-forming kelp *Ecklonia radiata*. *Front. Mar. Sci.* 4, 441. doi:10.3389/fmars.2017.00441.

Bekkby, T., and Moy, F. E. (2011). Developing spatial models of sugar kelp (*Saccharina latissima*) potential distribution under natural conditions and areas of its disappearance in Skagerrak. *Estuar. Coast. Shelf Sci.* 95, 477–483. doi:10.1016/j.ecss.2011.10.029.

Bengtsson, M. M., Sjøtun, K., Lanzén, A., and Øvreås, L. (2012). Bacterial diversity in relation to secondary production and succession on surfaces of the kelp *Laminaria hyperborea*. *ISME J.* 6, 2188–2198. doi:10.1038/ismej.2012.67.

Bengtsson, M., Sjøtun, K., and Øvreås, L. (2010). Seasonal dynamics of bacterial biofilms on the kelp *Laminaria hyperborea*. *Aquat. Microb. Ecol.* 60, 71–83. doi:10.3354/ame01409.

Benjamini, Y., and Hochberg, Y. (1995). Controlling the false discovery rate: a practical and powerful approach to multiple testing. *J. R. Stat. Soc. Ser. B Methodol.* 57, 289–300. doi:10.1111/j.2517-6161.1995.tb02031.x.

Berg, G., and Smalla, K. (2009). Plant species and soil type cooperatively shape the structure and function of microbial communities in the rhizosphere. *FEMS Microbiol. Ecol.* 68, 1–13. doi:10.1111/j.1574-6941.2009.00654.x.

Berkelmans, R., and van Oppen, M. J. H. (2006). The role of zooxanthellae in the thermal tolerance of corals: a 'nugget of hope' for coral reefs in an era of climate change. *Proc. R. Soc. B Biol. Sci.* 273, 2305–2312. doi:10.1098/rspb.2006.3567.

Bernard, M., Rousvoal, S., Jacquemin, B., Ballenghien, M., Peters, A. F., and Leblanc, C. (2017). qPCR-based relative quantification of the brown algal endophyte *Laminarionema elsbetiae* in *Saccharina latissima*: variation and dynamics of host - endophyte interactions. *J. Appl. Phycol.* 30, 2901–2911. doi:10.1007/s10811-017-1367-0.

Blunden, G. (1991). Agricultural uses of seaweeds and seaweed extracts. *Seaweed Resour. Eur.*, 65–81.

Boccardo, G., Lisa, V., Luisoni, E., and Milne, R. G. (1987). "Cryptic plant viruses," in *Advances in Virus Research* (Elsevier), 171–214. doi:10.1016/S0065-3527(08)60477-7.

Bold, H. C., and Wynne, M. J. (1985). *Introduction to the algae: structure and reproduction*. 2nd ed. Englewood Cliffs, N.J: Prentice-Hall.

Bolton, J. J. (2010). The biogeography of kelps (*Laminariales, Phaeophyceae*): a global analysis with new insights from recent advances in molecular phylogenetics. *Helgol. Mar. Res.* 64, 263–279. doi:10.1007/s10152-010-0211-6.

Bonthond, G., Bayer, T., Krueger-Hadfield, S. A., Barboza, F. R., Nakaoka, M., Valero, M., et al. (2020). How do microbiota associated with an invasive seaweed vary across scales? *Mol. Ecol.* 29, 2094–2108. doi:10.1111/mec.15470.

Bonthond, G., Bayer, T., Krueger-Hadfield, S. A., Stärck, N., Wang, G., Nakaoka, M., et al. (2021). The role of host promiscuity in the invasion process of a seaweed holobiont. *ISME J.* 15, 1668–1679. doi:10.1038/s41396-020-00878-7.

Borchardt, S. A., Allain, E. J., Michels, J. J., Stearns, G. W., Kelly, R. F., and McCoy, W. F. (2001). Reaction of acylated homoserine lactone bacterial signaling molecules with oxidized halogen antimicrobials. *Appl. Environ. Microbiol.* 67, 3174–3179. doi:10.1128/AEM.67.7.3174-3179.2001.

Bordenstein, S. R., and Theis, K. R. (2015). Host biology in light of the microbiome: ten principles of holobionts and hologenomes. *PLOS Biol.* 13, e1002226. doi:10.1371/journal.pbio.1002226.

Borges, A., and Simões, M. (2019). Quorum sensing inhibition by marine bacteria. *Mar. Drugs* 17, 427. doi:10.3390/md17070427.

Borrel, G., Brugère, J.-F., Gribaldo, S., Schmitz, R. A., and Moissl-Eichinger, C. (2020). The host-associated archaeome. *Nat. Rev. Microbiol.* doi:10.1038/s41579-020-0407-y.

Bosch, T. C. G., and Miller, D. J. (2016). "Bleaching as an obvious dysbiosis in corals," in *The Holobiont Imperative* (Vienna: Springer Vienna), 113–125. doi:10.1007/978-3-7091-1896-2_9.

Bourne, D., Iida, Y., Uthicke, S., and Smith-Keune, C. (2008). Changes in coral-associated microbial communities during a bleaching event. *ISME J.* 2, 350–363. doi:10.1038/ismej.2007.112.

Brazelton, J. N., Pfeufer, E. E., Sweat, T. A., Gardener, B. B. M., and Coenen, C. (2008). 2,4-diacetylphloroglucinol alters plant root development. *Mol. Plant. Microbe Interact.* 21, 1349–1358. doi:10.1094/MPMI-21-10-1349.

Bringloe, T. T., Starko, S., Wade, R. M., Vieira, C., Kawai, H., De Clerck, O., et al. (2020). Phylogeny and evolution of the brown algae. *Crit. Rev. Plant Sci.* 39, 281–321. doi:10.1080/07352689.2020.1787679.

Buerger, S., Spoering, A., Gavrish, E., Leslin, C., Ling, L., and Epstein, S. S. (2012). Microbial scout hypothesis, stochastic exit from dormancy, and the nature of slow growers. *Appl. Environ. Microbiol.* 78, 3221–3228. doi:10.1128/AEM.07307-11.

Bulgarelli, D., Rott, M., Schlaeppi, K., Ver Loren van Themaat, E., Ahmadinejad, N., Assenza, F., et al. (2012). Revealing structure and assembly cues for *Arabidopsis* root-inhabiting bacterial microbiota. *Nature* 488, 91–95. doi:10.1038/nature11336.

Bulleri, F., Benedetti-Cecchi, L., Acunto, S., Cinelli, F., and Hawkins, S. J. (2002). The influence of canopy algae on vertical patterns of distribution of low-shore assemblages on rocky coasts in the northwest Mediterranean. *J. Exp. Mar. Biol. Ecol.* 267, 89–106. doi:10.1016/S0022-0981(01)00361-6.

Burgess, S. C., Baskett, M. L., Grosberg, R. K., Morgan, S. G., and Strathmann, R. R. (2016). When is dispersal for dispersal? Unifying marine and terrestrial perspectives. *Biol. Rev.* 91, 867–882. doi:10.1111/brv.12198.

Burgunter-Delamare, B., KleinJan, H., Frioux, C., Fremy, E., Wagner, M., Corre, E., et al. (2020). Metabolic complementarity between a brown alga and associated cultivable bacteria

provide indications of beneficial interactions. *Front. Mar. Sci.* 7, 85. doi:10.3389/fmars.2020.00085.

Burki, F., Roger, A. J., Brown, M. W., and Simpson, A. G. B. (2020). The new tree of Eukaryotes. *Trends Ecol. Evol.* 35, 43–55. doi:10.1016/j.tree.2019.08.008.

Califano, G., Kwantes, M., Abreu, M. H., Costa, R., and Wichard, T. (2020). Cultivating the Macroalgal Holobiont: Effects of Integrated Multi-Trophic Aquaculture on the Microbiome of Ulva rigida (Chlorophyta). *Front. Mar. Sci.* 7, 52. doi:10.3389/fmars.2020.00052.

Callahan, B. J., McMurdie, P. J., Rosen, M. J., Han, A. W., Johnson, A. J. A., and Holmes, S. P. (2016). DADA2: High-resolution sample inference from Illumina amplicon data. *Nat. Methods* 13, 581–583. doi:10.1038/nmeth.3869.

Cardini, U., Bednarz, V. N., Naumann, M. S., van Hoytema, N., Rix, L., Foster, R. A., et al. (2015). Functional significance of dinitrogen fixation in sustaining coral productivity under oligotrophic conditions. *Proc. R. Soc. B Biol. Sci.* 282, 20152257. doi:10.1098/rspb.2015.2257.

Case, R. J., Longford, S. R., Campbell, A. H., Low, A., Tujula, N., Steinberg, P. D., et al. (2011). Temperature induced bacterial virulence and bleaching disease in a chemically defended marine macroalga: Temperature, disease and algal chemical defense. *Environ. Microbiol.* 13, 529–537. doi:10.1111/j.1462-2920.2010.02356.x.

Chamam, A., Sanguin, H., Bellvert, F., Meiffren, G., Comte, G., Wisniewski-Dyé, F., et al. (2013). Plant secondary metabolite profiling evidences strain-dependent effect in the *Azospirillum–Oryza sativa* association. *Phytochemistry* 87, 65–77. doi:10.1016/j.phytochem.2012.11.009.

Chamam, A., Wisniewski-Dyé, F., Comte, G., Bertrand, C., and Prigent-Combaret, C. (2015). Differential responses of *Oryza sativa* secondary metabolism to biotic interactions with cooperative, commensal and phytopathogenic bacteria. *Planta* 242, 1439–1452. doi:10.1007/s00425-015-2382-5.

Christie, H., Norderhaug, K., and Fredriksen, S. (2009). Macrophytes as habitat for fauna. *Mar. Ecol. Prog. Ser.* 396, 221–233. doi:10.3354/meps08351.

Chung, I. K., Oak, J. H., Lee, J. A., Shin, J. A., Kim, J. G., and Park, K.-S. (2013). Installing kelp forests/seaweed beds for mitigation and adaptation against global warming: Korean Project Overview. *ICES J. Mar. Sci.* 70, 1038–1044. doi:10.1093/icesjms/fss206.

Cock, J. M., Sterck, L., Rouzé, P., Scornet, D., Allen, A. E., Amoutzias, G., et al. (2010). The *Ectocarpus* genome and the independent evolution of multicellularity in brown algae. *Nature* 465, 617–621. doi:10.1038/nature09016.

Coelho, S. M., Scornet, D., Rousvoal, S., Peters, N. T., Dartevelle, L., Peters, A. F., et al. (2012). *Ectocarpus*: a model organism for the brown algae. *Cold Spring Harb. Protoc.* 2012, pdb.emo065821-pdb.emo065821. doi:10.1101/pdb.emo065821.

Comba González, N. B., Niño Corredor, A. N., López Kleine, L., and Montoya Castaño, D. (2021). Temporal changes of the epiphytic bacteria community from the marine macroalga *Ulva lactuca* (Santa Marta, Colombian-Caribbean). *Curr. Microbiol.* 78, 534–543. doi:10.1007/s00284-020-02302-x.

Corre, S., and Prieur, D. (1990). Density and morphology of epiphytic bacteria on the kelp *Laminaria digitata*. *Bot. Mar.* 33. doi:10.1515/botm.1990.33.6.515.

Couillerot, O., Prigent-Combaret, C., Caballero-Mellado, J., and Moënne-Loccoz, Y. (2009). *Pseudomonas fluorescens* and closely-related fluorescent pseudomonads as biocontrol agents of soil-borne phytopathogens. *Lett. Appl. Microbiol.* 48, 505–512. doi:10.1111/j.1472-765X.2009.02566.x.

Daglia, M. (2012). Polyphenols as antimicrobial agents. *Curr. Opin. Biotechnol.* 23, 174–181. doi:10.1016/j.copbio.2011.08.007.

Dang, H., and Lovell, C. R. (2000). Bacterial primary colonization and early succession on surfaces in marine waters as determined by amplified rRNA gene restriction analysis and sequence analysis of 16s rRNA genes. *Appl. Environ. Microbiol.* 66, 467–475. doi:10.1128/AEM.66.2.467-475.2000.

Dayton, P. K. (1985). Ecology of kelp communities. *Annu. Rev. Ecol. Syst.* 16, 215–245.

De Bary, A. (1879). *Die erscheinung der symbiose: Vortrag gehalten auf der versammlung deutscher naturforscher und aerzte zu cassel*. Trübner doi:10.1515/9783111471839.

de Vargas, C., Audic, S., Henry, N., Decelle, J., Mahé, F., Logares, R., et al. (2015). Eukaryotic plankton diversity in the sunlit ocean. *Science* 348, 1261605. doi:10.1126/science.1261605.

DeLong, E. F. (1992). Archaea in coastal marine environments. *Proc. Natl. Acad. Sci.* 89, 5685–5689. doi:10.1073/pnas.89.12.5685.

DeLong, E. F., and Karl, D. M. (2005). Genomic perspectives in microbial oceanography. *Nature* 437, 336–342. doi:10.1038/nature04157.

Dimitrieva, G. Y., and Dimitriev, S. M. (1997). Symbiotic microflora of brown algae of the genus *Laminaria* as a bioindicator of the ecological condition of coastal laminarian biocenoses. *Oceanogr. Lit. Rev.* 11, 1330.

Dittami, S. M., Arboleda, E., Auguet, J.-C., Bigalke, A., Briand, E., Cárdenas, P., et al. (2021). A community perspective on the concept of marine holobionts: current status, challenges, and future directions. *PeerJ* 9, e10911. doi:10.7717/peerj.10911.

Dittami, S. M., Duboscq-Bidot, L., Perennou, M., Gobet, A., Corre, E., Boyen, C., et al. (2016). Host-microbe interactions as a driver of acclimation to salinity gradients in brown algal cultures. *ISME J.* 10, 51–63. doi:10.1038/ismej.2015.104.

Dittami, S. M., Eveillard, D., and Tonon, T. (2014). A metabolic approach to study algal-bacterial interactions in changing environments. *Mol. Ecol.* 23, 1656–1660. doi:10.1111/mec.12670.

Doberva, M., Stien, D., Sorres, J., Hue, N., Sanchez-Ferandin, S., Eparvier, V., et al. (2017). Large diversity and original structures of acyl-homoserine lactones in strain MOLA 401, a marine *Rhodobacteraceae* bacterium. *Front. Microbiol.* 8, 1152. doi:10.3389/fmicb.2017.01152.

Dobretsov, S., Teplitski, M., and Paul, V. (2009). Mini-review: quorum sensing in the marine environment and its relationship to biofouling. *Biofouling* 25, 413–427. doi:10.1080/08927010902853516.

Dobretsov, S. V., and Qian, P.-Y. (2002). Effect of bacteria associated with the green alga *Ulva reticulate* on marine micro- and macrofouling. *Biofouling* 18, 217–228. doi:10.1080/08927010290013026.

Donachie, S. P., Foster, J. S., and Brown, M. V. (2007). Culture clash: challenging the dogma of microbial diversity. *ISME J.* 1, 97–99. doi:10.1038/ismej.2007.22.

Donachie, S. P., Hou, S., Lee, K. S., Riley, C. W., Pikina, A., Belisle, C., et al. (2004). The Hawaiian Archipelago: a microbial diversity hotspot. *Microb. Ecol.* 48, 509–520. doi:10.1007/s00248-004-0217-1.

Dong, Y.-H., Wang, L.-H., and Zhang, L.-H. (2007). Quorum-quenching microbial infections: mechanisms and implications. *Philos. Trans. R. Soc. B Biol. Sci.* 362, 1201–1211. doi:10.1098/rstb.2007.2045.

Drogue, B., Sanguin, H., Chamam, A., Mozar, M., Llauro, C., Panaud, O., et al. (2014). Plant root transcriptome profiling reveals a strain-dependent response during *Azospirillum*-rice cooperation. *Front. Plant Sci.* 5. doi:10.3389/fpls.2014.00607.

Duarte, C. M., Losada, I. J., Hendriks, I. E., Mazarrasa, I., and Marbà, N. (2013). The role of coastal plant communities for climate change mitigation and adaptation. *Nat. Clim. Change* 3, 961–968. doi:10.1038/nclimate1970.

Dworjanyn, S., de Nys, R., and Steinberg, P. (2006). Chemically mediated antifouling in the red alga *Delisea pulchra*. *Mar. Ecol. Prog. Ser.* 318, 153–163. doi:10.3354/meps318153.

Eberhard, A., Burlingame, A. L., Eberhard, C., Kenyon, G. L., Nealson, K. H., and Oppenheimer, N. J. (1981). Structural identification of autoinducer of *Photobacterium fischeri* luciferase. *Biochemistry* 20, 2444–2449. doi:10.1021/bi00512a013.

Egan, S., Harder, T., Burke, C., Steinberg, P., Kjelleberg, S., and Thomas, T. (2013). The seaweed holobiont: understanding seaweed–bacteria interactions. *FEMS Microbiol. Rev.* 37, 462–476. doi:10.1111/1574-6976.12011.

Epstein, S. S. (2009). Microbial awakenings. *Nature* 457, 1083–1083. doi:10.1038/4571083a.

Esteban, R., Balaguer, L., Manrique, E., Rubio de Casas, R., Ochoa, R., Fleck, I., et al. (2009). Alternative methods for sampling and preservation of photosynthetic pigments and tocopherols in plant material from remote locations. *Photosynth. Res.* 101, 77–88. doi:10.1007/s11120-009-9468-5.

Eymann, C., Lassek, C., Wegner, U., Bernhardt, J., Fritsch, O. A., Fuchs, S., et al. (2017). Symbiotic interplay of fungi, algae, and bacteria within the lung lichen *Lobaria*

pulmonaria L. Hoffm. as assessed by state-of-the-art metaproteomics. *J. Proteome Res.* 16, 2160–2173. doi:10.1021/acs.jproteome.6b00974.

Fernandes, N., Steinberg, P., Rusch, D., Kjelleberg, S., and Thomas, T. (2012). Community structure and functional gene profile of bacteria on healthy and diseased thalli of the red seaweed *Delisea pulchra*. *PLoS ONE* 7, e50854. doi:10.1371/journal.pone.0050854.

Fettweis, J. M., Serrano, M. G., Brooks, J. P., Edwards, D. J., Girerd, P. H., Parikh, H. I., et al. (2019). The vaginal microbiome and preterm birth. *Nat. Med.* 25, 1012–1021. doi:10.1038/s41591-019-0450-2.

Fiore, C. L., Jarett, J. K., Olson, N. D., and Lesser, M. P. (2010). Nitrogen fixation and nitrogen transformations in marine symbioses. *Trends Microbiol.* 18, 455–463. doi:10.1016/j.tim.2010.07.001.

Flavier, A. B., Ganova-Raeva, L. M., Schell, M. A., and Denny, T. P. (1997). Hierarchical autoinduction in *Ralstonia solanacearum*: control of acyl-homoserine lactone production by a novel autoregulatory system responsive to 3-hydroxypalmitic acid methyl ester. *J. Bacteriol.* 179, 7089–7097. doi:10.1128/jb.179.22.7089-7097.1997.

Fleurence, J. (1999). Seaweed proteins. *Trends Food Sci. Technol.* 10, 25–28. doi:10.1016/S0924-2244(99)00015-1.

Freeman, J. A., and Bassler, B. L. (1999). A genetic analysis of the function of LuxO, a two-component response regulator involved in quorum sensing in Vibrio harveyi. *Mol. Microbiol.* 31, 665–677. doi:10.1046/j.1365-2958.1999.01208.x.

Fuhrman, J. A., Cram, J. A., and Needham, D. M. (2015). Marine microbial community dynamics and their ecological interpretation. *Nat. Rev. Microbiol.* 13, 133–146. doi:10.1038/nrmicro3417.

Fuqua, C., and Greenberg, E. P. (2002). Listening in on bacteria: acyl-homoserine lactone signalling. *Nat. Rev. Mol. Cell Biol.* 3, 685–695. doi:10.1038/nrm907.

Fuqua, C., Parsek, M. R., and Greenberg, E. P. (2001). Regulation of gene expression by cell-to-cell communication: acyl-homoserine lactone quorum sensing. *Annu. Rev. Genet.* 35, 439–468. doi:10.1146/annurev.genet.35.102401.090913.

Galloway, W. R. J. D., Hodgkinson, J. T., Bowden, S. D., Welch, M., and Spring, D. R. (2011). Quorum sensing in gram-negative bacteria: small-molecule modulation of AHL and AI-2 quorum sensing pathways. *Chem. Rev.* 111, 28–67. doi:10.1021/cr100109t.

Garbary, D. J., and Deckert, R. J. (2001). “Three part harmony — *Ascophyllum* and its symbionts,” in *Symbiosis* Cellular Origin, Life in Extreme Habitats and Astrobiology., ed. J. Seckbach (Dordrecht: Kluwer Academic Publishers), 309–321. doi:10.1007/0-306-48173-1_19.

Garbary, D. J., and London, J. F. (1995). The *Ascophyllum / Polysiphonia / Mycosphaerella* symbiosis V. fungal infection protects *A. nosodum* from desiccation. *Bot. Mar.* 38. doi:10.1515/botm.1995.38.1-6.529.

Gärdes, A., Iversen, M. H., Grossart, H.-P., Passow, U., and Ullrich, M. S. (2011). Diatom-associated bacteria are required for aggregation of *Thalassiosira weissflogii*. *ISME J.* 5, 436–445. doi:10.1038/ismej.2010.145.

Geng, H., and Belas, R. (2010). Expression of tropodithietic acid biosynthesis is controlled by a novel autoinducer. *J. Bacteriol.* 192, 4377–4387. doi:10.1128/JB.00410-10.

Gobet, A., Corre, E., Correc, G., Delage, L., Dittami, S., KleinJan, H., et al. (2017). Characterization of the epiphytic bacterial community associated with the kelp *Laminaria digitate*. *Phycologia* 56, 64.

Goecke, F., Labes, A., Wiese, J., and Imhoff, J. (2010). Chemical interactions between marine macroalgae and bacteria. *Mar. Ecol. Prog. Ser.* 409, 267–299. doi:10.3354/meps08607.

Gopal, M., and Gupta, A. (2016). Microbiome selection could spur next-generation plant breeding strategies. *Front. Microbiol.* 7. doi:10.3389/fmicb.2016.01971.

Graham, M. H., Kinlan, B. P., Druehl, L. D., Garske, L. E., and Banks, S. (2007). Deep-water kelp refugia as potential hotspots of tropical marine diversity and productivity. *Proc. Natl. Acad. Sci.* 104, 16576–16580. doi:10.1073/pnas.0704778104.

Grasis, J. A., Lachnit, T., Anton-Erxleben, F., Lim, Y. W., Schmieder, R., Fraune, S., et al. (2014). Species-specific viromes in the ancestral holobiont *Hydra*. *PLoS ONE* 9, e109952. doi:10.1371/journal.pone.0109952.

Gregory, A. C., Zayed, A. A., Conceição-Neto, N., Temperton, B., Bolduc, B., Alberti, A., et al. (2019). Marine DNA viral macro- and microdiversity from pole to pole. *Cell* 177, 1109-1123.e14. doi:10.1016/j.cell.2019.03.040.

Griffiths, S. M., Antwis, R. E., Lenzi, L., Lucaci, A., Behringer, D. C., Butler, M. J., et al. (2019). Host genetics and geography influence microbiome composition in the sponge *Ircinia campana*. *J. Anim. Ecol.* 88, 1684–1695. doi:10.1111/1365-2656.13065.

Grimm, M., Grube, M., Schiefelbein, U., Zühlke, D., Bernhardt, J., and Riedel, K. (2021). The lichens' microbiota, still a mystery? *Front. Microbiol.* 12, 623839. doi:10.3389/fmicb.2021.623839.

Groisillier, A., Labourel, A., Michel, G., and Tonon, T. (2015). The mannitol utilization system of the marine bacterium *Zobellia galactanivorans*. *Appl. Environ. Microbiol.* 81, 1799–1812. doi:10.1128/AEM.02808-14.

Guzinski, J., Mauger, S., Cock, J. M., and Valero, M. (2016). Characterization of newly developed expressed sequence tag-derived microsatellite markers revealed low genetic diversity within and low connectivity between European *Saccharina latissima* populations. *J. Appl. Phycol.* 28, 3057–3070. doi:10.1007/s10811-016-0806-7.

Guzinski, J., Ruggeri, P., Ballenghien, M., Mauger, S., Jacquemin, B., Jollivet, C., et al. (2020). Seascape genomics of the sugar kelp *Saccharina latissima* along the North Eastern Atlantic Latitudinal Gradient. *Genes* 11, 1503. doi:10.3390/genes11121503.

Hammer, Ø., Harper, D. A., and Ryan, P. D. (2001). PAST: Paleontological statistics software package for education and data analysis. *Palaeontol. Electron.* 4, 9.

Hammer, T. J., Dickerson, J. C., and Fierer, N. (2015). Evidence-based recommendations on storing and handling specimens for analyses of insect microbiota. *PeerJ* 3, e1190. doi:10.7717/peerj.1190.

Handå, A., Forbord, S., Wang, X., Broch, O. J., Dahle, S. W., Størseth, T. R., et al. (2013). Seasonal- and depth-dependent growth of cultivated kelp (*Saccharina latissima*) in close proximity to salmon (*Salmo salar*) aquaculture in Norway. *Aquaculture* 414–415, 191–201. doi:10.1016/j.aquaculture.2013.08.006.

Harder, T., Campbell, A. H., Egan, S., and Steinberg, P. D. (2012). Chemical mediation of ternary interactions between marine holobionts and their environment as exemplified by the red alga *Delisea pulchra*. *J. Chem. Ecol.* 38, 442–450. doi:10.1007/s10886-012-0119-5.

Hartmann, A., Rothballer, M., and Schmid, M. (2008). Lorenz Hiltner, a pioneer in rhizosphere microbial ecology and soil bacteriology research. *Plant Soil* 312, 7–14. doi:10.1007/s11104-007-9514-z.

Hartmann, A., Schmid, M., Tuinen, D. van, and Berg, G. (2009). Plant-driven selection of microbes. *Plant Soil* 321, 235–257. doi:10.1007/s11104-008-9814-y.

Hartstra, A. V., Bouter, K. E. C., Bäckhed, F., and Nieuwdorp, M. (2015). Insights into the role of the microbiome in obesity and type 2 diabetes. *Diabetes Care* 38, 159–165. doi:10.2337/dc14-0769.

Harwood, J. L. (2004). “Membrane lipids in algae,” in *Lipids in Photosynthesis: Structure, Function and Genetics* Advances in Photosynthesis and Respiration., eds. S. Paul-André and M. Norio (Dordrecht: Kluwer Academic Publishers), 53–64. doi:10.1007/0-306-48087-5_3.

Henke, J. M., and Bassler, B. L. (2004). Three parallel quorum-sensing systems regulate gene expression in *Vibrio harveyi*. *J. Bacteriol.* 186, 6902–6914. doi:10.1128/JB.186.20.6902-6914.2004.

Hiltner, L. (1904). Uber nevere Erfahrungen und Probleme auf dem Gebiet der Boden Bakteriologie und unter besonderer Beurchsichtigung der Grundungung und Broche. *Arb. Deut Landw Ges Berl.* 98, 59–78.

Hirsch, P. R., and Mauchline, T. H. (2012). Who’s who in the plant root microbiome? *Nat. Biotechnol.* 30, 961–962. doi:10.1038/nbt.2387.

Hmelo, L. R. (2017). Quorum sensing in marine microbial environments. *Annu. Rev. Mar. Sci.* 9, 257–281. doi:10.1146/annurev-marine-010816-060656.

Hoarau, G., Coyer, J. A., Stam, W. T., and Olsen, J. L. (2007). A fast and inexpensive DNA extraction/purification protocol for brown macroalgae. *Mol. Ecol. Notes* 7, 191–193. doi:10.1111/j.1471-8286.2006.01587.x.

Holden, M. T. G., Ram Chhabra, S., De Nys, R., Stead, P., Bainton, N. J., Hill, P. J., et al. (2002). Quorum-sensing cross talk: isolation and chemical characterization of cyclic dipeptides from *Pseudomonas aeruginosa* and other Gram-negative bacteria. *Mol. Microbiol.* 33, 1254–1266. doi:10.1046/j.1365-2958.1999.01577.x.

Hollants, J., Leliaert, F., De Clerck, O., and Willems, A. (2013). What we can learn from sushi: a review on seaweed–bacterial associations. *FEMS Microbiol. Ecol.* 83, 1–16. doi:10.1111/j.1574-6941.2012.01446.x.

Hou, X., Chai, C., Qian, Q., Yan, X., and Fan, X. (1997). Determination of chemical species of iodine in some seaweeds. *Sci. Total Environ.* 204, 215–221. doi:10.1016/S0048-9697(97)00182-4.

Hulsen, T., de Vlieg, J., and Alkema, W. (2008). BioVenn – a web application for the comparison and visualization of biological lists using area-proportional Venn diagrams. *BMC Genomics* 9, 488. doi:10.1186/1471-2164-9-488.

Ihua, M., Guihéneuf, F., Mohammed, H., Margassery, L., Jackson, S., Stengel, D., et al. (2019). Microbial population changes in decaying *Ascophyllum nodosum* result in macroalgal-polysaccharide-degrading bacteria with potential applicability in enzyme-assisted extraction technologies. *Mar. Drugs* 17, 200. doi:10.3390/md17040200.

Ihua, M. W., FitzGerald, J. A., Guihéneuf, F., Jackson, S. A., Claesson, M. J., Stengel, D. B., et al. (2020). Diversity of bacteria populations associated with different thallus regions of the brown alga *Laminaria digitata*. *PLOS ONE* 15, e0242675. doi:10.1371/journal.pone.0242675.

Illumina (2013). 16S Metagenomic sequencing library preparation. *Prep. 16S Ribosomal RNA Gene Amplicons Illumina MiSeq Syst.*, 1–28.

Indergaard, M., and Ostgaard, K. (1991). "Polysaccharides for food and pharmaceutical uses," in *Seaweed Resources in Europe. Uses and Potential*, eds. M. D. Guiry and G. Blunden (John Wiley & Sons), 169–183.

Ivanova, E. P., Bakunina, I. Yu., Nedashkovskaya, O. I., Gorshkova, N. M., Alexeeva, Y. V., Zelepuga, E. A., et al. (2003). Ecophysiological variabilities in ectohydrolytic enzyme activities of some *Pseudoalteromonas* species, *P. citrea, P. issachenkonii*, and *P. nigrifaciens*. *Curr. Microbiol.* 46, 6–10. doi:10.1007/s00284-002-3794-6.

Jackson, G. A. (1983). The physical and chemical environment of a kelp community. *Eff. Waste Dispos. Kelp Communities South. Calif. Coast. Water Res. Proj. Long Beach*, 11–37.

Jackson, G., Roberts, R. T., and Wainwright, T. (1980). Mechanism of beer foam stabilization by propylene glycol alginate. *J. Inst. Brew.* 86, 34–37. doi:10.1002/j.2050-0416.1980.tb03953.x.

Jeske, O., Jogler, M., Petersen, J., Sikorski, J., and Jogler, C. (2013). From genome mining to phenotypic microarrays: *Planctomycetes* as source for novel bioactive molecules. *Antonie Van Leeuwenhoek* 104, 551–567. doi:10.1007/s10482-013-0007-1.

Ji, G., Beavis, R. C., and Novick, R. P. (1995). Cell density control of staphylococcal virulence mediated by an octapeptide pheromone. *Proc. Natl. Acad. Sci.* 92, 12055–12059. doi:10.1073/pnas.92.26.12055.

Jones, E. B. G. ed. (2012). *Marine fungi and fungal-like organisms*. Berlin: De Gruyter.

Kain, J. M. (1979). A view of the genus *Laminaria*. *Oceanogr. Mar. Biol. Annu. Rev.* 17, 101–161.

Kain, J. M., and Dawes, C. P. (1987). "Useful European seaweeds: past hopes and present cultivation," in *Twelfth International Seaweed Symposium*, eds. M. A. Ragan and C. J. Bird (Dordrecht: Springer Netherlands), 173–181. doi:10.1007/978-94-009-4057-4_24.

Kanagasabhapathy, M., Yamazaki, G., Ishida, A., Sasaki, H., and Nagata, S. (2009). Presence of quorum-sensing inhibitor-like compounds from bacteria isolated from the brown alga *Colpomenia sinuosa*. *Lett. Appl. Microbiol.* 49, 573–579. doi:10.1111/j.1472-765X.2009.02712.x.

Karimi, E., Slaby, B. M., Soares, A. R., Blom, J., Hentschel, U., and Costa, R. (2018). Metagenomic binning reveals versatile nutrient cycling and distinct adaptive features in alphaproteobacterial symbionts of marine sponges. *FEMS Microbiol. Ecol.* 94. doi:10.1093/femsec/fiy074.

Karner, M. B., DeLong, E. F., and Karl, D. M. (2001). Archaeal dominance in the mesopelagic zone of the Pacific Ocean. *Nature* 409, 507–510. doi:10.1038/35054051.

Karp, P. D., Paley, S., and Romero, P. (2002). The Pathway Tools software. *Bioinforma. Oxf. Engl.* 18 Suppl 1, S225–S232. doi:10.1093/bioinformatics/18.suppl_1.S225.

Kim, J. S., Kim, Y. H., Seo, Y. W., and Park, S. (2007). Quorum sensing inhibitors from the red alga *Ahnfeltiopsis flabelliformis*. *Biotechnol. Bioprocess Eng.* 12, 308–311. doi:10.1007/BF02931109.

Kimbrel, J. A., Samo, T. J., Ward, C., Nilson, D., Thelen, M. P., Siccardi, A., et al. (2019). Host selection and stochastic effects influence bacterial community assembly on the microalgal phycosphere. *Algal Res.* 40, 101489. doi:10.1016/j.algal.2019.101489.

Kinlan, B. P., and Gaines, S. D. (2003). Propagule dispersal in marine and terrestrial environments: a community perspective. *Ecology* 84, 2007–2020. doi:10.1890/01-0622.

Kjelleberg, S., and Steinberg, P. (1999). Surface warfare in the sea. *Mar Biol* 133, 727–736.

KleinJan, H., Caliafano, G., Aite, M., Fremy, E., Frioux, C., Karimi, E., et al. (2021). Changing microbial activities during low salinity acclimation in the brown alga *Ectocarpus subulatus*. Ecology doi:10.1101/2021.04.13.439635.

KleinJan, H., Jeanthon, C., Boyen, C., and Dittami, S. M. (2017). Exploring the cultivable *Ectocarpus* microbiome. *Front. Microbiol.* 8, 2456. doi:10.3389/fmicb.2017.02456.

Kohlmeyer, J., and Demoulin, V. (1981). Parasitic and symbiotic fungi on marine algae. *Bot. Mar.* 24. doi:10.1515/botm.1981.24.1.9.

Konovalova, A., Petters, T., and Søgaard-Andersen, L. (2010). Extracellular biology of *Myxococcus xanthus*. *FEMS Microbiol. Rev.* 34, 89–106. doi:10.1111/j.1574-6976.2009.00194.x.

Kostic, A. D., Xavier, R. J., and Gevers, D. (2014). The microbiome in Inflammatory Bowel Disease: current status and the future ahead. *Gastroenterology* 146, 1489–1499. doi:10.1053/j.gastro.2014.02.009.

Kumar, V., Zozaya-Valdes, E., Kjelleberg, S., Thomas, T., and Egan, S. (2016). Multiple opportunistic pathogens can cause a bleaching disease in the red seaweed *Delisea pulchra*. *Environ. Microbiol.* 18, 3962–3975. doi:10.1111/1462-2920.13403.

Labbate, M., Queck, S. Y., Koh, K. S., Rice, S. A., Givskov, M., and Kjelleberg, S. (2004). Quorum sensing-controlled biofilm development in *Serratia liquefaciens* MG1. *J. Bacteriol.* 186, 692–698. doi:10.1128/JB.186.3.692-698.2004.

Lachnit, T., Blümel, M., Imhoff, J., and Wahl, M. (2009). Specific epibacterial communities on macroalgae: phylogeny matters more than habitat. *Aquat. Biol.* 5, 181–186. doi:10.3354/ab00149.

Lachnit, T., Meske, D., Wahl, M., Harder, T., and Schmitz, R. (2011). Epibacterial community patterns on marine macroalgae are host-specific but temporally variable. *Environ. Microbiol.* 13, 655–665. doi:10.1111/j.1462-2920.2010.02371.x.

Lachnit, T., Thomas, T., and Steinberg, P. (2016). Expanding our understanding of the seaweed holobiont: RNA viruses of the red alga *Delisea pulchra*. *Front. Microbiol.* 6. doi:10.3389/fmicb.2015.01489.

Lage, O. M., and Bondoso, J. (2014). *Planctomycetes* and macroalgae, a striking association. *Front. Microbiol.* 5. doi:10.3389/fmicb.2014.00267.

Lauber, C. L., Zhou, N., Gordon, J. I., Knight, R., and Fierer, N. (2010). Effect of storage conditions on the assessment of bacterial community structure in soil and human-associated samples: Influence of short-term storage conditions on microbiota. *FEMS Microbiol. Lett.* 307, 80–86. doi:10.1111/j.1574-6968.2010.01965.x.

Laycock, R. A. (1974). The detrital food chain based on seaweeds. I. Bacteria associated with the surface of *Laminaria* fronds. *Mar. Biol.* 25, 223–231. doi:10.1007/BF00394968.

Layton, C., Shelamoff, V., Cameron, M. J., Tatsumi, M., Wright, J. T., and Johnson, C. R. (2019). Resilience and stability of kelp forests: The importance of patch dynamics and environment-engineer feedbacks. *PLOS ONE* 14, e0210220. doi:10.1371/journal.pone.0210220.

Lebeis, S. L., Paredes, S. H., Lundberg, D. S., Breakfield, N., Gehring, J., McDonald, M., et al. (2015). Salicylic acid modulates colonization of the root microbiome by specific bacterial taxa. *Science* 349, 860–864. doi:10.1126/science.aaa8764.

Lee, J.-H., and Lee, J. (2010). Indole as an intercellular signal in microbial communities. *FEMS Microbiol. Rev.* 34, 426–444. doi:10.1111/j.1574-6976.2009.00204.x.

Lemay, M. A., Davis, K. M., Martone, P. T., and Parfrey, L. W. (2021). Kelp-associated microbiota are structured by host anatomy. *J. Phycol.* 57, 1119–1130. doi:10.1111/jpy.13169.

Ley, R. E., Hamady, M., Lozupone, C., Turnbaugh, P. J., Ramey, R. R., Bircher, J. S., et al. (2008). Evolution of mammals and their gut microbes. *Science* 320, 1647–1651. doi:10.1126/science.1155725.

Li, B.-J., Shi, Y.-Y., Yang, G.-P., Che, S., Xiao-Jie, L., and Yi-Zhou, C. (2008). Microsatellite DNA variation of the gametophyte clones isolated from introduced *Laminaria japonica* (Phaeophyta) and *L. longissima* of China and varieties derived from them. *J. Integr. Plant Biol.* 50, 352–359. doi:10.1111/j.1744-7909.2007.00622.x.

Li, J., Majzoub, M. E., Marzinelli, E. M., Dai, Z., Thomas, T., and Egan, S. (2021a). Bacterial controlled mitigation of dysbiosis in a seaweed disease. *ISME J.* doi:10.1038/s41396-021-01070-1.

Li, J., Weinberger, F., Saha, M., Majzoub, M. E., and Egan, S. (2021b). Cross-host protection of marine bacteria against macroalgal disease. *Microb. Ecol.* doi:10.1007/s00248-021-01909-2.

Lindh, M. V., Figueroa, D., SjÃ¶stedt, J., Baltar, F., Lundin, D., Andersson, A., et al. (2015). Transplant experiments uncover Baltic Sea basin-specific responses in bacterioplankton community composition and metabolic activities. *Front. Microbiol.* 6. doi:10.3389/fmicb.2015.00223.

Little, B. J., and Zsolnay, A. (1985). Chemical fingerprinting of adsorbed organic materials on metal surfaces. *J. Colloid Interface Sci.* 104, 79–86. doi:10.1016/0021-9797(85)90011-6.

Liu, H. B., Koh, K. P., Kim, J. S., Seo, Y., and Park, S. (2008). The effects of betonicine, floridoside, and isethionic acid from the red alga *Ahnfeltiopsis flabelliformis* on quorum-sensing activity. *Biotechnol. Bioprocess Eng.* 13, 458–463. doi:10.1007/s12257-008-0145-x.

Lloyd-Price, J., Arze, C., Ananthakrishnan, A. N., Schirmer, M., Avila-Pacheco, J., Poon, T. W., et al. (2019). Multi-omics of the gut microbial ecosystem in inflammatory bowel diseases. *Nature* 569, 655–662. doi:10.1038/s41586-019-1237-9.

Loh, J., Carlson, R. W., York, W. S., and Stacey, G. (2002). Bradyoxetin, a unique chemical signal involved in symbiotic gene regulation. *Proc. Natl. Acad. Sci.* 99, 14446–14451. doi:10.1073/pnas.222336799.

Longford, S. R., Campbell, A. H., Nielsen, S., Case, R. J., Kjelleberg, S., and Steinberg, P. D. (2019). Interactions within the microbiome alter microbial interactions with host chemical defences and affect disease in a marine holobiont. *Sci. Rep.* 9. doi:10.1038/s41598-018-37062-z.

Longford, S., Tujula, N., Crocetti, G., Holmes, A., Holmström, C., Kjelleberg, S., et al. (2007). Comparisons of diversity of bacterial communities associated with three sessile marine eukaryotes. *Aquat. Microb. Ecol.* 48, 217–229. doi:10.3354/ame048217.

Love, M. I., Huber, W., and Anders, S. (2014). Moderated estimation of fold change and dispersion for RNA-seq data with DESeq2. *Genome Biol.* 15, 550. doi:10.1186/s13059-014-0550-8.

Lüning, K. (1979). Growth strategies of three *Laminaria* species (Phaeophyceae) inhabiting different depth zones in the sublittoral region of Helgoland (North Sea). *Mar. Ecol. Prog. Ser.* 1, 195e207.

Lüning, K. (1991). *Seaweeds: their environment, biogeography, and ecophysiology*. New York, NY: Wiley.

Manefield, M., de Nys, R., Naresh, K., Roger, R., Givskov, M., Peter, S., et al. (1999). Evidence that halogenated furanones from *Delisea pulchra* inhibit acylated homoserine lactone (AHL)-mediated gene expression by displacing the AHL signal from its receptor protein. *Microbiology* 145, 283–291. doi:10.1099/13500872-145-2-283.

Mann, K. H. (1973). Seaweeds: their productivity and strategy for growth. *Science* 182, 975–981.

Margulis, L. (1991). "Symbiogenesis and Symbionticism," in *Symbiosis as a source of evolutionary innovation*, ed. R. Fester (Cambridge, Mass: MIT Press), 1–14.

Marketon, M. M., Glenn, S. A., Eberhard, A., and González, J. E. (2003). Quorum sensing controls exopolysaccharide production in *Sinorhizobium meliloti*. *J. Bacteriol.* 185, 325–331. doi:10.1128/JB.185.1.325-331.2003.

Marques, J. C., Oh, I. K., Ly, D. C., Lamosa, P., Ventura, M. R., Miller, S. T., et al. (2014). LsrF, a coenzyme A-dependent thiolase, catalyzes the terminal step in processing the quorum sensing signal autoinducer-2. *Proc. Natl. Acad. Sci.* 111, 14235–14240. doi:10.1073/pnas.1408691111.

Marzinelli, E. M., Campbell, A. H., Zozaya Valdes, E., Vergés, A., Nielsen, S., Wernberg, T., et al. (2015). Continental-scale variation in seaweed host-associated bacterial communities is a function of host condition, not geography. *Environ. Microbiol.* 17, 4078–4088. doi:10.1111/1462-2920.12972.

Marzinelli, E. M., Qiu, Z., Dafforn, K. A., Johnston, E. L., Steinberg, P. D., and Mayer-Pinto, M. (2018). Coastal urbanisation affects microbial communities on a dominant marine holobiont. *Npj Biofilms Microbiomes* 4, 1. doi:10.1038/s41522-017-0044-z.

Matsuo, Y., Imagawa, H., Nishizawa, M., and Shizuri, Y. (2005). Isolation of an algal morphogenesis inducer from a marine bacterium. *Science* 307, 1598–1598. doi:10.1126/science.1105486.

Mayer, A. M. S., and Hamann, M. T. (2002). Marine pharmacology in 1999: compounds with antibacterial, anticoagulant, antifungal, anthelmintic, anti-inflammatory, antiplatelet, antiprotozoal and antiviral activities affecting the cardiovascular, endocrine, immune and nervous systems, and other miscellaneous mechanisms of action. *Comp. Biochem. Physiol. Part C Toxicol. Pharmacol.* 132, 315–339. doi:10.1016/S1532-0456(02)00094-7.

Mayer, A. M. S., and Hamann, M. T. (2005). Marine pharmacology in 2001–2002: Marine compounds with anthelmintic, antibacterial, anticoagulant, antidiabetic, antifungal, anti-inflammatory, antimalarial, antiplatelet, antiprotozoal, antituberculosis, and antiviral activities; affecting the cardiovascular, immune and nervous systems and

other miscellaneous mechanisms of action. *Comp. Biochem. Physiol. Part C Toxicol. Pharmacol.* 140, 265–286. doi:10.1016/j.cca.2005.04.004.

Mazure, H. G. F., and Field, J. G. (1980). Density and ecological importance of bacteria on kelp fronds in an upwelling region. *J. Exp. Mar. Biol. Ecol.* 43, 173–182. doi:10.1016/0022-0981(80)90024-6.

McHugh, D. J. (2003). *A guide to the seaweed industry*. Rome: Food and Agriculture Organization of the United Nations Available at: https://www.fao.org/3/y4765e/y4765e.pdf.

McKeown, D. A., Stevens, K., Peters, A. F., Bond, P., Harper, G. M., Brownlee, C., et al. (2017). Phaeoviruses discovered in kelp (*Laminariales*). *ISME J.* 11, 2869–2873. doi:10.1038/ismej.2017.130.

McKnight, S. L., Iglewski, B. H., and Pesci, E. C. (2000). The *Pseudomonas* quinolone signal regulates *rhl* quorum sensing in *Pseudomonas aeruginosa*. *J. Bacteriol.* 182, 2702–2708. doi:10.1128/JB.182.10.2702-2708.2000.

McMurdie, P. J., and Holmes, S. (2013). phyloseq: an R package for reproducible interactive analysis and graphics of microbiome census data. *PLoS ONE* 8, e61217. doi:10.1371/journal.pone.0061217.

Meyer-Abich, A. (1943). I. Das Typologische Grundgesetz und Seine Folgerungen Für Phylogenie und Entwicklungsphysiologie. *Acta Biotheor.* 7, 1–80.

Middelboe, M., and Brussaard, C. (2017). Marine viruses: key players in marine ecosystems. *Viruses* 9, 302. doi:10.3390/v9100302.

Miller, S. T., Xavier, K. B., Campagna, S. R., Taga, M. E., Semmelhack, M. F., Bassler, B. L., et al. (2004). *Salmonella typhimurium* recognizes a chemically distinct form of the bacterial quorum-sensing signal AI-2. *Mol. Cell* 15, 677–687. doi:10.1016/j.molcel.2004.07.020.

Mills, E., Shechtman, K., Loya, Y., and Rosenberg, E. (2013). Bacteria appear to play important roles in both causing and preventing the bleaching of the coral Oculina patagonica. *Mar. Ecol. Prog. Ser.* 489, 155–162. doi:10.3354/meps10391.

Mitchell, M. E. (2007). Signposts to symbiosis: A review of early attempts to establish the constitution of lichens. *Huntia* 13, 101–120.

Mitra, A., Flynn, K. J., Burkholder, J. M., Berge, T., Calbet, A., Raven, J. A., et al. (2014). The role of mixotrophic protists in the biological carbon pump. *Biogeosciences* 11, 995–1005. doi:10.5194/bg-11-995-2014.

Monteiro, J. P., Rey, F., Melo, T., Moreira, A. S. P., Arbona, J.-F., Skjermo, J., et al. (2020). The unique lipidomic signatures of *Saccharina latissima* can be used to pinpoint their geographic origin. *Biomolecules* 10, 107. doi:10.3390/biom10010107.

Morgan, X. C., Tickle, T. L., Sokol, H., Gevers, D., Devaney, K. L., Ward, D. V., et al. (2012). Dysfunction of the intestinal microbiome in inflammatory bowel disease and treatment. *Genome Biol.* 13, R79. doi:10.1186/gb-2012-13-9-r79.

Morris, R. L., Graham, T. D. J., Kelvin, J., Ghisalberti, M., and Swearer, S. E. (2019). Kelp beds as coastal protection: wave attenuation of *Ecklonia radiata* in a shallow coastal bay. *Ann. Bot.*, mcz127. doi:10.1093/aob/mcz127.

Müller, D. G. (1996). Host-virus interactions in marine brown algae. *Hydrobiologia* 326–327, 21–28. doi:10.1007/BF00047783.

Müller, D. G., Kapp, M., and Knippers, R. (1998). "Viruses in Marine Brown Algae," in *Advances in Virus Research* (Elsevier), 49–67. doi:10.1016/S0065-3527(08)60805-2.

Müller, D. G., Kawai, H., Stache, B., and Lanka, S. (1990). A virus infection in the marine brown alga *Ectocarpus siliculosus* (*Phaeophyceae*). *Bot. Acta* 103, 72–82. doi:10.1111/j.1438-8677.1990.tb00129.x.

Newton, R. J., Griffin, L. E., Bowles, K. M., Meile, C., Gifford, S., Givens, C. E., et al. (2010). Genome characteristics of a generalist marine bacterial lineage. *ISME J.* 4, 784–798. doi:10.1038/ismej.2009.150.

NIH Human Microbiome Portfolio Analysis Team (2019). A review of 10 years of human microbiome research activities at the US National Institutes of Health, Fiscal Years 2007-2016. *Microbiome* 7, 31. doi:10.1186/s40168-019-0620-y.

Nitschke, U., Walsh, P., McDaid, J., and Stengel, D. B. (2018). Variability in iodine in temperate seaweeds and iodine accumulation kinetics of *Fucus vesiculosus* and *Laminaria digitata* (Phaeophyceae, Ochrophyta). *J. Phycol.* 54, 114–125. doi:10.1111/jpy.12606.

Ohtani, K., Hayashi, H., and Shimizu, T. (2002). The luxS gene is involved in cell-cell signalling for toxin production in *Clostridium perfringens*. *Mol. Microbiol.* 44, 171–179. doi:10.1046/j.1365-2958.2002.02863.x.

Overmann, J., and Lepleux, C. (2016). "Marine bacteria and archaea: diversity, adaptations, and culturability," in *The Marine Microbiome*, eds. L. J. Stal and M. S. Cretoiu (Cham: Springer International Publishing), 21–55. doi:10.1007/978-3-319-33000-6_2.

Paix, B., Carriot, N., Barry-Martinet, R., Greff, S., Misson, B., Briand, J.-F., et al. (2020). A multi-omics analysis suggests links between the differentiated surface metabolome and epiphytic microbiota along the thallus of a Mediterranean seaweed holobiont. *Front. Microbiol.* 11, 494. doi:10.3389/fmicb.2020.00494.

Paix, B., Layglon, N., Le Poupon, C., D'Onofrio, S., Misson, B., Garnier, C., et al. (2021). Integration of spatio-temporal variations of surface metabolomes and epibacterial communities highlights the importance of copper stress as a major factor shaping host-microbiota interactions within a Mediterranean seaweed holobiont. *Microbiome* 9, 201. doi:10.1186/s40168-021-01124-8.

Parke, M. (1948). Studies on British *Laminariaceae*. I. Growth in *Laminaria Saccharina* (L.) Lamour. *J. Mar. Biol. Assoc. U. K.* 27, 651–709. doi:10.1017/S0025315400056071.

Parrot, D., Blümel, M., Utermann, C., Chianese, G., Krause, S., Kovalev, A., et al. (2019). Mapping the surface microbiome and metabolome of brown seaweed *Fucus*

vesiculosus by amplicon sequencing, integrated metabolomics and imaging techniques. *Sci. Rep.* 9, 1061. doi:10.1038/s41598-018-37914-8.

Passow, U., Shipe, R. F., Murray, A., Pak, D. K., Brzezinski, M. A., and Alldredge, A. L. (2001). The origin of transparent exopolymer particles (TEP) and their role in the sedimentation of particulate matter. *Cont. Shelf Res.* 21, 327–346. doi:10.1016/S0278-4343(00)00101-1.

Pearson, J. P., Van Delden, C., and Iglewski, B. H. (1999). Active efflux and diffusion are involved in transport of *Pseudomonas aeruginosa* cell-to-cell signals. *J. Bacteriol.* 181, 1203–1210. doi:10.1128/JB.181.4.1203-1210.1999.

Pedersén, M. (1968). *Ectocarpus fasciculatus*: Marine brown alga requiring kinetin. *Nature* 218, 776–776. doi:10.1038/218776a0.

Pedersén, M. (1969a). Marine brown algae requiring vitamin B12. *Physiol. Plant.* 22, 977–983. doi:10.1111/j.1399-3054.1969.tb07455.x.

Pedersén, M. (1969b). The demand for iodine and bromine of three marine brown algae grown in bacteria-free cultures. *Physiol. Plant.* 22, 680–685. doi:10.1111/j.1399-3054.1969.tb07423.x.

Pedersén, M. (1973). Identification of a cytokinin, 6-(3 Methyl-2-butenylamino) purine, in sea water and the effect of cytokinins on brown algae. *Physiol. Plant.* 28, 101–105. doi:10.1111/j.1399-3054.1973.tb01158.x.

Peixoto, R. S., Rosado, P. M., Leite, D. C. de A., Rosado, A. S., and Bourne, D. G. (2017). Beneficial Microorganisms for Corals (BMC): Proposed Mechanisms for Coral Health and Resilience. *Front. Microbiol.* 8. doi:10.3389/fmicb.2017.00341.

Peng, Y., and Li, W. (2013). A bacterial pathogen infecting gametophytes of *Saccharina japonica* (*Laminariales, Phaeophyceae*). *Chin. J. Oceanol. Limnol.* 31, 366–373. doi:10.1007/s00343-013-2136-9.

Peteiro, C. (2018). “Alginate production from marine macroalgae, with emphasis on kelp farming,” in *Alginates and their biomedical applications* Springer Series in Biomaterials Science and Engineering., eds. B. H. A. Rehm and M. F. Moradali (Singapore: Springer Singapore), 27–66. doi:10.1007/978-981-10-6910-9_2.

Peters, A. F., Marie, D., Scornet, D., Kloareg, B., and Mark Cock, J. (2004). Proposal of *Ectocarpus siliculosus* (Ectocarpales, Phaeophyceae) as a model organism for brown algal genetics and genomics. *J. Phycol.* 40, 1079–1088. doi:10.1111/j.1529-8817.2004.04058.x.

Peters, A. F., Scornet, D., Ratin, M., Charrier, B., Monnier, A., Merrien, Y., et al. (2008). Life-cycle-generation-specific developmental processes are modified in the *immediate upright* mutant of the brown alga *Ectocarpus siliculosus*. *Development* 135, 1503–1512. doi:10.1242/dev.016303.

Phillips, N., Smith, C. M., and Morden, C. W. (2001). An effective DNA extraction protocol for brown algae. *Phycol. Res.* 49, 97–102. doi:10.1111/j.1440-1835.2001.tb00239.x.

Pinhassi, J., Sala, M. M., Havskum, H., Peters, F., Guadayol, Ò., Malits, A., et al. (2004). Changes in bacterioplankton composition under different phytoplankton regimens. *Appl. Environ. Microbiol.* 70, 6753–6766. doi:10.1128/AEM.70.11.6753-6766.2004.

Pita, L., Rix, L., Slaby, B. M., Franke, A., and Hentschel, U. (2018). The sponge holobiont in a changing ocean: from microbes to ecosystems. *Microbiome* 6, 46. doi:10.1186/s40168-018-0428-1.

Potin, P., Bouarab, K., Salaün, J.-P., Pohnert, G., and Kloareg, B. (2002). Biotic interactions of marine algae. *Curr. Opin. Plant Biol.* 5, 308–317. doi:10.1016/S1369-5266(02)00273-X.

Prigent, S., Collet, G., Dittami, S. M., Delage, L., Ethis de Corny, F., Dameron, O., et al. (2014). The genome-scale metabolic network of *Ectocarpus siliculosus* (EctoGEM): a resource to study brown algal physiology and beyond. *Plant J.* 80, 367–381. doi:10.1111/tpj.12627.

Prigent, S., Frioux, C., Dittami, S. M., Thiele, S., Larhlimi, A., Collet, G., et al. (2017). Meneco, a topology-based gap-filling tool applicable to degraded genome-wide metabolic networks. *PLOS Comput. Biol.* 13, e1005276. doi:10.1371/journal.pcbi.1005276.

Provasoli, L. (1958). Effect of plant hormones on *Ulva*. *Biol. Bull.* 114, 375–384. doi:10.2307/1538992.

Qian, P.-Y., Lau, S. C. K., Dahms, H.-U., Dobretsov, S., and Harder, T. (2007). Marine biofilms as mediators of colonization by marine macroorganisms: implications for antifouling and aquaculture. *Mar. Biotechnol.* 9, 399–410. doi:10.1007/s10126-007-9001-9.

Qiu, Z., Coleman, M. A., Provost, E., Campbell, A. H., Kelaher, B. P., Dalton, S. J., et al. (2019). Future climate change is predicted to affect the microbiome and condition of habitat-forming kelp. *Proc. R. Soc. B Biol. Sci.* 286, 20181887. doi:10.1098/rspb.2018.1887.

Quigley, C. T., Morrison, H. G., Mendonça, I. R., and Brawley, S. H. (2018). A common garden experiment with *Porphyra umbilicalis* (Rhodophyta) evaluates methods to study spatial differences in the macroalgal microbiome. *J. Phycol.* 54, 653–664. doi:10.1111/jpy.12763.

Quiñones, B., Dulla, G., and Lindow, S. E. (2005). Quorum sensing regulates exopolysaccharide production, motility, and virulence in *Pseudomonas syringae*. *Mol. Plant-Microbe Interactions®* 18, 682–693. doi:10.1094/MPMI-18-0682.

Raina, J.-B., Tapiolas, D., Willis, B. L., and Bourne, D. G. (2009). Coral-associated bacteria and their role in the biogeochemical cycling of sulfur. *Appl. Environ. Microbiol.* 75, 3492–3501. doi:10.1128/AEM.02567-08.

Rasmussen, T. B., Manefield, M., Andersen, J. B., Eberl, L., Anthoni, U., Christophersen, C., et al. (2000). How *Delisea pulchra* furanones affect quorum sensing and swarming motility in *Serratia liquefaciens* MG1. *Microbiology* 146, 3237–3244. doi:10.1099/00221287-146-12-3237.

Richardson, A. E., Barea, J.-M., McNeill, A. M., and Prigent-Combaret, C. (2009). Acquisition of phosphorus and nitrogen in the rhizosphere and plant growth promotion by microorganisms. *Plant Soil* 321, 305–339. doi:10.1007/s11104-009-9895-2.

Riedel, K., Steidle, A., Wu, H., Eberl, L., Geisenberger, O., Hentzer, M., et al. (2001). N-Acylhomoserine-lactone-mediated communication between *Pseudomonas aeruginosa* and *Burkholderia cepacia* in mixed biofilms. *Microbiology* 147, 3249–3262. doi:10.1099/00221287-147-12-3249.

Riemann, L., Steward, G. F., and Azam, F. (2000). Dynamics of bacterial community composition and activity during a mesocosm diatom bloom. *Appl. Environ. Microbiol.* 66, 578–587. doi:10.1128/AEM.66.2.578-587.2000.

Rodeheaver, G., Bellamy, W., Kody, M., Spatafora, G., Fitton, L., Leyden, K., et al. (1982). Bactericidal activity and toxicity of iodine-containing solutions in wounds. *Arch. Surg.* 117, 181–186. doi:10.1001/archsurg.1982.01380260051009.

Rodríguez-Echeverría, S. (2010). Rhizobial hitchhikers from Down Under: invasional meltdown in a plant-bacteria mutualism? *J. Biogeogr.* doi:10.1111/j.1365-2699.2010.02284.x.

Rohwer, F., Prangishvili, D., and Lindell, D. (2009). Roles of viruses in the environment. *Environ. Microbiol.* 11, 2771–2774. doi:10.1111/j.1462-2920.2009.02101.x.

Romero, M., Martin-Cuadrado, A.-B., Roca-Rivada, A., Cabello, A. M., and Otero, A. (2011). Quorum quenching in cultivable bacteria from dense marine coastal microbial communities. *FEMS Microbiol. Ecol.* 75, 205–217. doi:10.1111/j.1574-6941.2010.01011.x.

Roossinck, M. J. (2010). Lifestyles of plant viruses. *Philos. Trans. R. Soc. B Biol. Sci.* 365, 1899–1905. doi:10.1098/rstb.2010.0057.

Roossinck, M. J. (2015). Metagenomics of plant and fungal viruses reveals an abundance of persistent lifestyles. *Front. Microbiol.* 5. doi:10.3389/fmicb.2014.00767.

Rosenberg, E., and Zilber-Rosenberg, I. (2012). “The Hologenome Concept,” in *Beneficial Microorganisms in Multicellular Life Forms*, eds. E. Rosenberg and U. Gophna (Berlin, Heidelberg: Springer Berlin Heidelberg), 323–340. doi:10.1007/978-3-642-21680-0_24.

Rosenberg, E., and Zilber-Rosenberg, I. (2018). The hologenome concept of evolution after 10 years. *Microbiome* 6. doi:10.1186/s40168-018-0457-9.

Roth-Schulze, A. J., Pintado, J., Zozaya-Valdés, E., Cremades, J., Ruiz, P., Kjelleberg, S., et al. (2018). Functional biogeography and host specificity of bacterial communities associated with the Marine Green Alga *Ulva* spp. *Mol. Ecol.* 27, 1952–1965. doi:10.1111/mec.14529.

Roussel, S., Caralp, C., Leblanc, C., Le Grand, F., Stiger-Pouvreau, V., Coulombet, C., et al. (2019). Impact of nine macroalgal diets on growth and initial reproductive investment in juvenile abalone *Haliotis tuberculata*. *Aquaculture* 513, 734385. doi:10.1016/j.aquaculture.2019.734385.

Rousvoal, S., Bouyer, B., López-Cristoffanini, C., Boyen, C., and Collén, J. (2016). Mutant swarms of a totivirus-like entities are present in the red macroalga *Chondrus crispus* and have been partially transferred to the nuclear genome. *J. Phycol.* 52, 493–504. doi:10.1111/jpy.12427.

Ruperez, P. (2002). Mineral content of edible marine seaweeds. *Food Chem.* 79, 23–26. doi:10.1016/S0308-8146(02)00171-1.

Rutherford, S. T., and Bassler, B. L. (2012). Bacterial quorum sensing: its role in virulence and possibilities for its control. *Cold Spring Harb. Perspect. Med.* 2, a012427–a012427. doi:10.1101/cshperspect.a012427.

Safari, M., Amache, R., Esmaeilishirazifard, E., and Keshavarz, T. (2014). Microbial metabolism of quorum-sensing molecules acyl-homoserine lactones, γ-heptalactone and other lactones. *Appl. Microbiol. Biotechnol.* 98, 3401–3412. doi:10.1007/s00253-014-5518-9.

Saha, M., and Weinberger, F. (2019). Microbial “gardening” by a seaweed holobiont: Surface metabolites attract protective and deter pathogenic epibacterial settlement. *J. Ecol.*, 1365-2745.13193. doi:10.1111/1365-2745.13193.

Sampayo, E. M., Ridgway, T., Bongaerts, P., and Hoegh-Guldberg, O. (2008). Bleaching susceptibility and mortality of corals are determined by fine-scale differences in symbiont type. *Proc. Natl. Acad. Sci.* 105, 10444–10449. doi:10.1073/pnas.0708049105.

Sawabe, T., Makino, H., Tatsumi, M., Nakano, K., Tajima, K., Iqbal, M. M., et al. (1998a). *Pseudoalteromonas bacteriolytica* sp. nov., a marine bacterium that is the causative agent of red spot disease of *Laminaria japonica*. *Int. J. Syst. Bacteriol.* 48, 769–774. doi:10.1099/00207713-48-3-769.

Sawabe, T., Sawada, C., Suzuki, E., and Ezura, Y. (1998b). Intracellular alginate-oligosaccharide degrading enzyme activity that is incapable of degrading intact sodium alginate from a marine bacterium *Alteromonas* sp. *Fish. Sci.* 64, 320–324. doi:10.2331/fishsci.64.320.

Schaefer, A. L., Lappala, C. R., Morlen, R. P., Pelletier, D. A., Lu, T.-Y. S., Lankford, P. K., et al. (2013). LuxR- and LuxI-type quorum-sensing circuits are prevalent in members of the *Populus deltoides* microbiome. *Appl. Environ. Microbiol.* 79, 5745–5752. doi:10.1128/AEM.01417-13.

Schauder, S., Shokat, K., Surette, M. G., and Bassler, B. L. (2001). The LuxS family of bacterial autoinducers: biosynthesis of a novel quorum-sensing signal molecule: AI-2 biosynthesis. *Mol. Microbiol.* 41, 463–476. doi:10.1046/j.1365-2958.2001.02532.x.

Schiel, D., and Lilley, S. (2007). Gradients of disturbance to an algal canopy and the modification of an intertidal community. *Mar. Ecol. Prog. Ser.* 339, 1–11. doi:10.3354/meps339001.

Schiel, D. R., and Foster, M. S. (2006). The population biology of large brown seaweeds: ecological consequences of multiphase life histories in dynamic coastal environments.

Annu. Rev. Ecol. Evol. Syst. 37, 343–372. doi:10.1146/annurev.ecolsys.37.091305.110251.

Schiener, P., Black, K. D., Stanley, M. S., and Green, D. H. (2015). The seasonal variation in the chemical composition of the kelp species *Laminaria digitata, Laminaria hyperborea, Saccharina latissima* and *Alaria esculenta*. *J. Appl. Phycol.* 27, 363–373. doi:10.1007/s10811-014-0327-1.

Schmid, S., Ranz, D., He, M. L., Lukowicz, M. V., Reiter, R., Arnold, R., et al. (2003). Marine algae as natural source of iodine in the feeding of freshwater fish: A new possibility to improve iodine supply of man. *Rev. Médecine Vét. Fr.*

Schneider, R. P., and Marshall, K. C. (1994). Retention of the Gram negative marine bacterium SW8 on surfaces — effects of microbial physiology, substratum nature and conditioning films. *Colloids Surf. B Biointerfaces* 2, 387–396. doi:10.1016/0927-7765(94)80002-2.

Schroeder, D. C., and Mckeown, D. A. (2021). "Viruses of Seaweeds," in *Studies in Viral Ecology*, ed. C. J. Hurst (Wiley), 121–138. doi:10.1002/9781119608370.ch4.

Segev, E., Wyche, T. P., Kim, K. H., Petersen, J., Ellebrandt, C., Vlamakis, H., et al. (2016). Dynamic metabolic exchange governs a marine algal-bacterial interaction. *eLife* 5, e17473. doi:10.7554/eLife.17473.

Selosse, M.-A., Richard, F., He, X., and Simard, S. W. (2006). Mycorrhizal networks: des liaisons dangereuses? *Trends Ecol. Evol.* 21, 621–628. doi:10.1016/j.tree.2006.07.003.

Seyedsayamdost, M. R., Case, R. J., Kolter, R., and Clardy, J. (2011). The Jekyll-and-Hyde chemistry of *Phaeobacter gallaeciensis*. *Nat. Chem.* 3, 331–335. doi:10.1038/nchem.1002.

Sifri, C. D. (2008). Quorum Sensing: Bacteria Talk Sense. *Clin. Infect. Dis.* 47, 1070–1076. doi:10.1086/592072.

Simon, J.-C., Marchesi, J. R., Mougel, C., and Selosse, M.-A. (2019). Host-microbiota interactions: from holobiont theory to analysis. *Microbiome* 7, 5. doi:10.1186/s40168-019-0619-4.

Singh, R. P., Baghel, R. S., Reddy, C. R. K., and Jha, B. (2015). Effect of quorum sensing signals produced by seaweed-associated bacteria on carpospore liberation from *Gracilaria dura*. *Front. Plant Sci.* 6. doi:10.3389/fpls.2015.00117.

Sjøtun, K. (1993). Seasonal lamina growth in two age groups of *Laminaria saccharina* (L.) Lamour. in western Norway. *Bot. Mar.* 36. doi:10.1515/botm.1993.36.5.433.

Skopina, M. Yu., Vasileva, A. A., Pershina, E. V., and Pinevich, A. V. (2016). Diversity at low abundance: The phenomenon of the rare bacterial biosphere. *Microbiology* 85, 272–282. doi:10.1134/S0026261716030139.

Slattery, M., Rajbhandari, I., and Wesson, K. (2001). Competition-mediated antibiotic induction in the marine bacterium *Streptomyces tenjimariensis*. *Microb. Ecol.* 41, 90–96. doi:10.1007/s002480000084.

Smale, D. A. (2020). Impacts of ocean warming on kelp forest ecosystems. *New Phytol.* 225, 1447–1454. doi:10.1111/nph.16107.

Smit, A. J. (2004). Medicinal and pharmaceutical uses of seaweed natural products: A review. *J. Appl. Phycol.* 16, 245–262. doi:10.1023/B:JAPH.0000047783.36600.ef.

Song, S. J., Amir, A., Metcalf, J. L., Amato, K. R., Xu, Z. Z., Humphrey, G., et al. (2016). Preservation methods differ in fecal microbiome stability, affecting suitability for field studies. *mSystems* 1, e00021-16. doi:10.1128/mSystems.00021-16.

Sperandio, V., Torres, A. G., Jarvis, B., Nataro, J. P., and Kaper, J. B. (2003). Bacteria-host communication: the language of hormones. *Proc. Natl. Acad. Sci.* 100, 8951–8956. doi:10.1073/pnas.1537100100.

Spoerner, M., Wichard, T., Bachhuber, T., Stratmann, J., and Oertel, W. (2012). Growth and thallus morphogenesis of *Ulva mutabilis* (Chlorophyta) depends on a combination of two bacterial species excreting regulatory factors. *J. Phycol.* 48, 1433–1447. doi:10.1111/j.1529-8817.2012.01231.x.

Stal, L. J., and Cretoiu, M. S. eds. (2016). *The Marine Microbiome*. Cham: Springer International Publishing doi:10.1007/978-3-319-33000-6.

Staufenberger, T., Thiel, V., Wiese, J., and Imhoff, J. F. (2008). Phylogenetic analysis of bacteria associated with *Laminaria saccharina*. *FEMS Microbiol. Ecol.* 64, 65–77. doi:10.1111/j.1574-6941.2008.00445.x.

Stein, J. R., and Borden, C. A. (1984). Causative and beneficial algae in human disease conditions: a review. *Phycologia* 23, 485–501. doi:10.2216/i0031-8884-23-4-485.1.

Steinberg, P. D., and De Nys, R. (2002). Chemical mediation of colonization of seaweed surfaces. *J. Phycol.* 38, 621–629. doi:10.1046/j.1529-8817.2002.02042.x.

Steindler, L., and Venturi, V. (2007). Detection of quorum-sensing *N* -acyl homoserine lactone signal molecules by bacterial biosensors. *FEMS Microbiol. Lett.* 266, 1–9. doi:10.1111/j.1574-6968.2006.00501.x.

Steneck, R. S., Graham, M. H., Bourque, B. J., Corbett, D., Erlandson, J. M., Estes, J. A., et al. (2002). Kelp forest ecosystems: biodiversity, stability, resilience and future. *Environ. Conserv.* 29, 436–459. doi:10.1017/S0376892902000322.

Stout, M. J., Zhou, Y., Wylie, K. M., Tarr, P. I., Macones, G. A., and Tuuli, M. G. (2017). Early pregnancy vaginal microbiome trends and preterm birth. *Am. J. Obstet. Gynecol.* 217, 356.e1-356.e18. doi:10.1016/j.ajog.2017.05.030.

Stratil, S. B., Neulinger, S. C., Knecht, H., Friedrichs, A. K., and Wahl, M. (2014). Salinity affects compositional traits of epibacterial communities on the brown macroalga *Fucus vesiculosus*. *FEMS Microbiol. Ecol.* 88, 272–279. doi:10.1111/1574-6941.12292.

Stubbendieck, R. M., and Straight, P. D. (2016). Multifaceted Interfaces of bacterial competition. *J. Bacteriol.* 198, 2145–2155. doi:10.1128/JB.00275-16.

Sunagawa, S., Coelho, L. P., Chaffron, S., Kultima, J. R., Labadie, K., Salazar, G., et al. (2015). Structure and function of the global ocean microbiome. *Science* 348, 1261359. doi:10.1126/science.1261359.

Suntharalingam, P., and Cvitkovitch, D. G. (2005). Quorum sensing in streptococcal biofilm formation. *Trends Microbiol.* 13, 3–6. doi:10.1016/j.tim.2004.11.009.

Surette, M. G., Miller, M. B., and Bassler, B. L. (1999). Quorum sensing in *Escherichia coli*, *Salmonella typhimurium*, and *Vibrio harveyi*: A new family of genes responsible for autoinducer production. *Proc. Natl. Acad. Sci.* 96, 1639–1644. doi:10.1073/pnas.96.4.1639.

Suttle, C. A. (2005). Viruses in the sea. *Nature* 437, 356–361. doi:10.1038/nature04160.

Suttle, C. A. (2007). Marine viruses — major players in the global ecosystem. *Nat. Rev. Microbiol.* 5, 801–812. doi:10.1038/nrmicro1750.

Suzuki, M. T., and Giovannoni, S. J. (1996). Bias caused by template annealing in the amplification of mixtures of 16S rRNA genes by PCR. *Appl. Environ. Microbiol.* 62, 625–630. doi:10.1128/aem.62.2.625-630.1996.

Suzuki, S., Furuya, K., Kawai, T., and Takeuchi, I. (2007). Growth and annual production of the brown alga *Laminaria religiosa* introduced into the Uwa Sea in southern Japan. *Phycol. Res.* 55, 272–277. doi:10.1111/j.1440-1835.2007.00471.x.

Tait, K., Joint, I., Daykin, M., Milton, D. L., Williams, P., and Camara, M. (2005). Disruption of quorum sensing in seawater abolishes attraction of zoospores of the green alga *Ulva* to bacterial biofilms. *Environ. Microbiol.* 7, 229–240. doi:10.1111/j.1462-2920.2004.00706.x.

Tapia, J. E., González, B., Goulitquer, S., Potin, P., and Correa, J. A. (2016). Microbiota influences morphology and reproduction of the brown alga *Ectocarpus sp. Front. Microbiol.* 7, 197. doi:10.3389/fmicb.2016.00197.

Taylor, B. F., and Visscher, P. T. (1996). “Metabolic Pathways Involved in DMSP Degradation,” in *Biological and Environmental Chemistry of DMSP and Related Sulfonium Compounds*, eds. R. P. Kiene, P. T. Visscher, M. D. Keller, and G. O. Kirst (Boston, MA: Springer US), 265–276. doi:10.1007/978-1-4613-0377-0_23.

The NIH HMP Working Group, Peterson, J., Garges, S., Giovanni, M., McInnes, P., Wang, L., et al. (2009). The NIH Human Microbiome Project. *Genome Res.* 19, 2317–2323. doi:10.1101/gr.096651.109.

Theis, K. R., Dheilly, N. M., Klassen, J. L., Brucker, R. M., Baines, J. F., Bosch, T. C. G., et al. (2016). Getting the hologenome concept right: an eco-evolutionary framework for hosts and their microbiomes. *mSystems* 1. doi:10.1128/mSystems.00028-16.

Theodorou, I., and Charrier, B. (2021). “Brown Algae: *Ectocarpus* and *Saccharina* as experimental models for developmental biology,” in *Handbook of Marine Model Organisms in Experimental Biology*, eds. A. Boutet and B. Schierwater (Boca Raton: CRC Press), 27–47. doi:10.1201/9781003217503-2.

Thomas, F., Dittami, S. M., Brunet, M., Le Duff, N., Tanguy, G., Leblanc, C., et al. (2019). Evaluation of a new primer combination to minimize plastid contamination in 16S rDNA metabarcoding analyses of alga-associated bacterial communities. *Environ. Microbiol. Rep.* 12, 30–37. doi:10.1111/1758-2229.12806.

Thomas, T., Moitinho-Silva, L., Lurgi, M., Björk, J. R., Easson, C., Astudillo-García, C., et al. (2016). Diversity, structure and convergent evolution of the global sponge microbiome. *Nat. Commun.* 7, 11870. doi:10.1038/ncomms11870.

Thompson, A. W., Foster, R. A., Krupke, A., Carter, B. J., Musat, N., Vaulot, D., et al. (2012). Unicellular cyanobacterium symbiotic with a single-celled eukaryotic alga. *Science* 337, 1546–1550. doi:10.1126/science.1222700.

Toishi, K. (1959). Humidity control in a closed package. *Stud. Conserv.* 4, 81–87. doi:10.1179/sic.1959.018.

Tourneroche, A., Lami, R., Burgaud, G., Domart-Coulon, I., Li, W., Gachon, C., et al. (2020). The bacterial and fungal microbiota of *Saccharina latissima* (Laminariales, Phaeophyceae). *Front. Mar. Sci.* 7, 587566. doi:10.3389/fmars.2020.587566.

Tourneroche, A., Lami, R., Hubas, C., Blanchet, E., Vallet, M., Escoubeyrou, K., et al. (2019). Bacterial–fungal interactions in the kelp endomicrobiota drive autoinducer-2 quorum sensing. *Front. Microbiol.* 10, 1693. doi:10.3389/fmicb.2019.01693.

Tseng, C. K. (1987). *Laminaria* mariculture in China. *FAO Fish. Tech. Pap. FAO*. Available at: https://www.fao.org/3/X5819E/x5819e09.htm#TopOfPage.

Twigg, M. S., Tait, K., Williams, P., Atkinson, S., and Cámara, M. (2014). Interference with the germination and growth of *Ulva* zoospores by quorum-sensing molecules from *Ulva*-associated epiphytic bacteria. *Environ. Microbiol.* 16, 445–453. doi:10.1111/1462-2920.12203.

Ul-Hassan, A., and Wellington, E. M. (2009). "*Actinobacteria*," in *Encyclopedia of Microbiology* (Elsevier), 25–44. doi:10.1016/B978-012373944-5.00044-4.

Vacheron, J. (2015). Plant-beneficial rhizobacteria selection by plant : impact on plant-beneficial property distribution in fluorescent Pseudomonas. Available at: https://tel.archives-ouvertes.fr/tel-01433752.

Vacheron, J., Moënne-Loccoz, Y., Dubost, A., Gonçalves-Martins, M., Muller, D., and Prigent-Combaret, C. (2016). Fluorescent *Pseudomonas* strains with only few plant-beneficial properties are favored in the maize rhizosphere. *Front. Plant Sci.* 7. doi:10.3389/fpls.2016.01212.

Vairappan, C. S., Suzuki, M., Motomura, T., and Ichimura, T. (2001). Pathogenic bacteria associated with lesions and thallus bleaching symptoms in the Japanese kelp *Laminaria religiosa* Miyabe (Laminariales, Phaeophyceae). *Hydrobiologia* 445, 183–191. doi:10.1023/A:1017517832302.

Vallet, M., Strittmatter, M., Murúa, P., Lacoste, S., Dupont, J., Hubas, C., et al. (2018). Chemically-mediated interactions between macroalgae, their fungal endophytes, and protistan pathogens. *Front. Microbiol.* 9, 3161. doi:10.3389/fmicb.2018.03161.

Van Alstyne, K. L., and Puglisi, M. P. (2007). DMSP in marine macroalgae and macroinvertebrates: Distribution, function, and ecological impacts. *Aquat. Sci.* 69, 394–402. doi:10.1007/s00027-007-0888-z.

Van Alstyne, K., Wolfe, G., Freidenburg, T., Neill, A., and Hicken, C. (2001). Activated defense systems in marine macroalgae: evidence for an ecological role for DMSP cleavage. *Mar. Ecol. Prog. Ser.* 213, 53–65. doi:10.3354/meps213053.

van de Water, J. A. J. M., Allemand, D., and Ferrier-Pagès, C. (2018). Host-microbe interactions in octocoral holobionts - recent advances and perspectives. *Microbiome* 6. doi:10.1186/s40168-018-0431-6.

van der Meer, J. P., and Simpson, F. J. (1984). Cryopreservation of *Gracilaria tikvahiae* (Rhodophyta) and other macrophytic marine algae. *Phycologia* 23, 195–202. doi:10.2216/i0031-8884-23-2-195.1.

Vandenkoornhuyse, P., Baldauf, S. L., Leyval, C., Straczek, J., and Young, J. P. W. (2002). Extensive fungal diversity in plant roots. *Science* 295, 2051–2051. doi:10.1126/science.295.5562.2051.

Vandenkoornhuyse, P., Quaiser, A., Duhamel, M., Le Van, A., and Dufresne, A. (2015). The importance of the microbiome of the plant holobiont. *New Phytol.* 206, 1196–1206. doi:10.1111/nph.13312.

Verbeke, F., De Craemer, S., Debunne, N., Janssens, Y., Wynendaele, E., Van de Wiele, C., et al. (2017). Peptides as quorum sensing molecules: measurement techniques and obtained levels *in vitro* and *in vivo*. *Front. Neurosci.* 11. doi:10.3389/fnins.2017.00183.

Vesty, E. F., Kessler, R. W., Wichard, T., and Coates, J. C. (2015). Regulation of gametogenesis and zoosporogenesis in *Ulva linza* (Chlorophyta): comparison with *Ulva mutabilis* and potential for laboratory culture. *Front. Plant Sci.* 6. doi:10.3389/fpls.2015.00015.

Visch, W., Rad-Menéndez, C., Nylund, G. M., Pavia, H., Ryan, M. J., and Day, J. (2019). Underpinning the development of seaweed biotechnology: Cryopreservation of Brown Algae (*Saccharina latissima*) gametophytes. *Biopreservation Biobanking*, bio.2018.0147. doi:10.1089/bio.2018.0147.

Wahl, M., Goecke, F., Labes, A., Dobretsov, S., and Weinberger, F. (2012). The Second Skin: ecological role of epibiotic biofilms on marine organisms. *Front. Microbiol.* 3, 292. doi:10.3389/fmicb.2012.00292.

Walker, V., Bertrand, C., Bellvert, F., Moënne-Loccoz, Y., Bally, R., and Comte, G. (2011). Host plant secondary metabolite profiling shows a complex, strain-dependent response of maize to plant growth-promoting rhizobacteria of the genus Azospirillum. *New Phytol.* 189, 494–506. doi:10.1111/j.1469-8137.2010.03484.x.

Walters, W. A., Xu, Z., and Knight, R. (2014). Meta-analyses of human gut microbes associated with obesity and IBD. *FEBS Lett.* 588, 4223–4233. doi:10.1016/j.febslet.2014.09.039.

Wang, Q., Garrity, G. M., Tiedje, J. M., and Cole, J. R. (2007). Naive bayesian classifier for rapid assignment of rRNA sequences into the new bacterial taxonomy. *Appl. Environ. Microbiol.* 73, 5261–5267. doi:10.1128/AEM.00062-07.

Wegner, C.-E., Richter-Heitmann, T., Klindworth, A., Klockow, C., Richter, M., Achstetter, T., et al. (2013). Expression of sulfatases in *Rhodopirellula baltica* and the diversity of sulfatases in the genus *Rhodopirellula*. *Mar. Genomics* 9, 51–61. doi:10.1016/j.margen.2012.12.001.

Weigel, B. L., and Pfister, C. A. (2019). Successional dynamics and seascape-level patterns of microbial communities on the canopy-forming kelps *Nereocystis luetkeana* and *Macrocystis pyrifera*. *Front. Microbiol.* 10, 346. doi:10.3389/fmicb.2019.00346.

Weinberger, F., Beltran, J., Correa, J. A., Lion, U., Pohnert, G., Kumar, N., et al. (2007). Spore release in *Acrochaetium* sp. (Rhodophyta) is bacterially controlled. *J. Phycol.* 43, 235–241. doi:10.1111/j.1529-8817.2007.00329.x.

Weisburg, W. G., Barns, S. M., Pelletier, D. A., and Lane, D. J. (1991). 16S ribosomal DNA amplification for phylogenetic study. *J. Bacteriol.* 173, 697–703. doi:10.1128/JB.173.2.697-703.1991.

Weiss, A., Costa, R., and Wichard, T. (2017). Morphogenesis of *Ulva mutabilis* (Chlorophyta) induced by *Maribacter* species (Bacteroidetes, Flavobacteriaceae). *Bot. Mar.* 60. doi:10.1515/bot-2016-0083.

Wichard, T. (2015). Exploring bacteria-induced growth and morphogenesis in the green macroalga order Ulvales (Chlorophyta). *Front. Plant Sci.* 6, 86. doi:10.3389/fpls.2015.00086.

Wiese, J., Thiel, V., Nagel, K., Staufenberger, T., and Imhoff, J. F. (2009). Diversity of antibiotic-active bacteria associated with the brown alga *Laminaria saccharina* from the Baltic Sea. *Mar. Biotechnol.* 11, 287–300. doi:10.1007/s10126-008-9143-4.

Williams, P., Winzer, K., Chan, W. C., and Cámara, M. (2007). Look who's talking: communication and quorum sensing in the bacterial world. *Philos. Trans. R. Soc. B Biol. Sci.* 362, 1119–1134. doi:10.1098/rstb.2007.2039.

Wilson, K. A., Able, K. W., and Heck Jr, K. L. (1990). Predation rates on juvenile blue crabs in estuarine nursery habitats: evidence for the importance of macroalgae (*Ulva lactuca*). *Mar. Ecol. Prog. Ser.* 58, 243–251. doi:10.3354/meps058243.

Zhang, Q., Zhang, J., Shen, J., Silva, A., Dennis, D. A., and Barrow, C. J. (2006). A simple 96-well microplate method for estimation of total polyphenol content in seaweeds. *J. Appl. Phycol.* 18, 445–450. doi:10.1007/s10811-006-9048-4.

Zhang, R., Chang, L., Xiao, L., Zhang, X., Han, Q., Li, N., et al. (2020). Diversity of the epiphytic bacterial communities associated with commercially cultivated healthy and diseased

Saccharina japonica during the harvest season. *J. Appl. Phycol.* 32, 2071–2080. doi:10.1007/s10811-019-02025-y.

Zhou, W., Sailani, M. R., Contrepois, K., Zhou, Y., Ahadi, S., Leopold, S. R., et al. (2019). Longitudinal multi-omics of host–microbe dynamics in prediabetes. *Nature* 569, 663–671. doi:10.1038/s41586-019-1236-x.

Zilber-Rosenberg, I., and Rosenberg, E. (2008). Role of microorganisms in the evolution of animals and plants: the hologenome theory of evolution. *FEMS Microbiol. Rev.* 32, 723–735. doi:10.1111/j.1574-6976.2008.00123.x.

Zinger, L., Amaral-Zettler, L. A., Fuhrman, J. A., Horner-Devine, M. C., Huse, S. M., Welch, D. B. M., et al. (2011). Global patterns of bacterial beta-diversity in seafloor and seawater ecosystems. *PLoS ONE* 6, e24570. doi:10.1371/journal.pone.0024570.

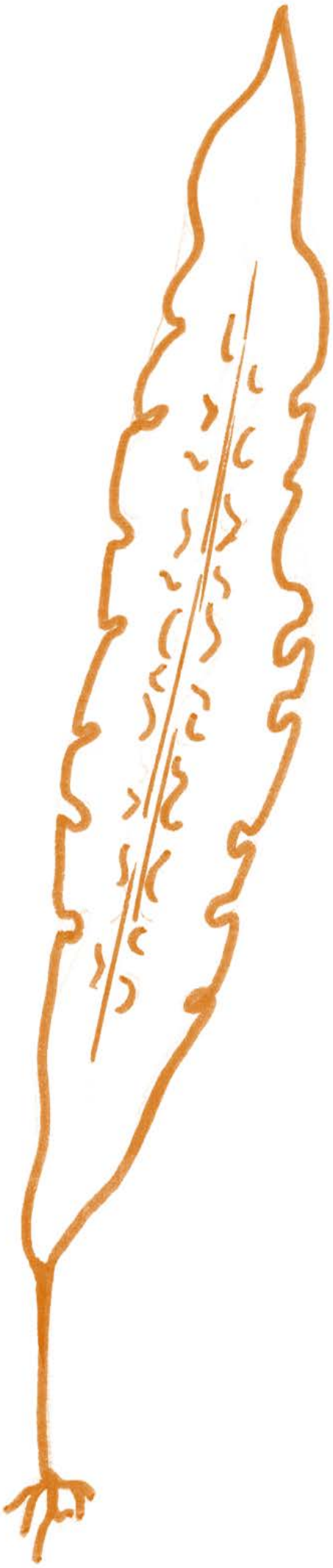

- ANNEXES -

ANNEXES

Annexe I - Présentations orales 178

Annexe II - Poster 179

Annexe III - Article M2 N°1 180

Annexe IV - Article M2 N°2 191

Annexe V - Article *Ectocarpus* Australie 203

Annexe I - Présentations orales

- Bertille Burgunter-Delamare et al. (Septembre 2021). **Exploring the microbiota of *Saccharina latissima***. Session #2 Chemical Ecology of Marine Holobiont. ISCE 2021, 36th Annual meeting of the International Society of Chemical Ecology, Stellenboch (Afrique du Sud).

- Bertille Burgunter-Delamare et al. (Mars 2021). **Exploring the microbiota of *Saccharina latissima***. Symposium #06 Algae and biotic interactions: introducing the symbiome. IPC 2021, 12th International Phycological Congress, Chili.

- Bertille Burgunter-Delamare et al. (Février 2021). **Exploring the microbiota of *Saccharina latissima***. 12èmes Journées des Jeunes Chercheurs de la Station Biologique, Roscoff (France).

- Bertille Burgunter-Delamare et al. (Février 2021). **The Holobiont: Because together, we are not alone**. 12èmes Journées des Jeunes Chercheurs de la Station Biologique, Roscoff (France).

- Bertille Burgunter-Delamare et al. (Novembre 2019). **Le microbiote des algues brunes et ses réseaux d'interactions.** FORUM 2019 ANR IDEALG**,** Roscoff (France).

- Bertille Burgunter-Delamare et al. (Novembre 2019). **In vitro testing of metabolic complementarity as a predictor of mutualistic interactions.** SYMSYM**,** Symbiosis Symposium, Roscoff (France).

- Bertille Burgunter-Delamare et al. (Octobre 2019). **In vitro testing of metabolic complementarity as a predictor of mutualistic interactions.** Journée Scientifique Biogenouest « Du phénome au métabolome »**,** Nantes (France).

- Bertille Burgunter-Delamare et al. (Août 2019). **Because together we are not alone… The holobiont concept.** EPC7, 7th European Phycological Congress, Zagreb (Croatie).

- Bertille Burgunter-Delamare, Clémence Frioux et al. (Novembre 2018). **In silico prediction and experimental validation of metabolic interactions between the brown alga *Ectocarpus* and associated bacteria.** Assemblée Générale 2018 ANR IDEALG**,** Saint-Brieuc (France).

Annexe II - Poster

7th European Phycological Congress (2019, Zagreb, Croatie), 11èmes Journées des Jeunes Chercheurs de la Station Biologique (2019, Roscoff, France)., Assemblée Générale 2019 ANR IDEALG (Roscoff, France)

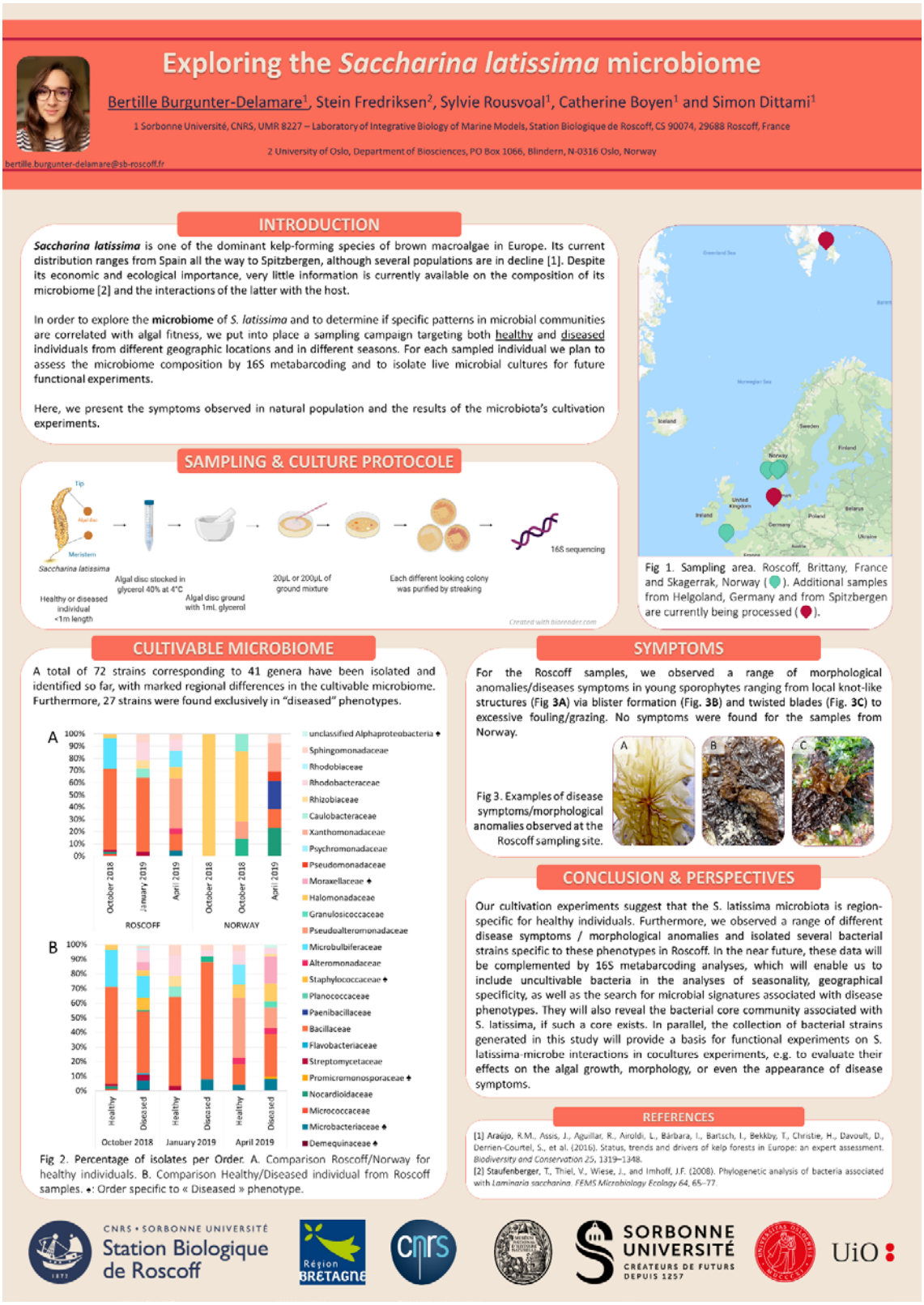

Annexe III - Article M2 N°1

Burgunter-Delamare Bertille et al. (2020) **Metabolic complementarity between a brown alga and associated cultivable bacteria provide indications of beneficial interactions**. Frontiers in Marine Science 7:85. https://doi.org/10.3389/fmars.2020.00085

frontiers in Marine Science

ORIGINAL RESEARCH
published: 21 February 2020
doi: 10.3389/fmars.2020.00085

Metabolic Complementarity Between a Brown Alga and Associated Cultivable Bacteria Provide Indications of Beneficial Interactions

*Bertille Burgunter-Delamare[1†], Hetty KleinJan[1†‡], Clémence Frioux[2], Enora Fremy[2], Margot Wagner[2], Erwan Corre[3], Alicia Le Salver[3], Cédric Leroux[3], Catherine Leblanc[1], Catherine Boyen[1], Anne Siegel[2] and Simon M. Dittami[1]**

[1] CNRS, Integrative Biology of Marine Models (LBI2M), Sorbonne Université, Roscoff, France, [2] Inria, CNRS, IRISA, Université de Rennes, Rennes, France, [3] CNRS, FR2424, Station Biologique de Roscoff, Sorbonne Université, Roscoff, France

OPEN ACCESS

Edited by:
Bernardo Antonio Perez Da Gama, Universidade Federal Fluminense, Brazil

Reviewed by:
Frithjof Kuepper, University of Aberdeen, United Kingdom
Fabiano Thompson, Federal University of Rio de Janeiro, Brazil

***Correspondence:**
Simon M. Dittami
simon.dittami@sb-roscoff.fr; simon.dittami@gmail.com

† These authors have contributed equally to this work

‡ Present address:
Hetty KleinJan, CEBEDEAU, Research and Expertise Center for Water, Liège, Belgium

Specialty section:
This article was submitted to Marine Ecosystem Ecology, a section of the journal Frontiers in Marine Science

Received: *29 October 2019*
Accepted: *03 February 2020*
Published: *21 February 2020*

Citation:
Burgunter-Delamare B, KleinJan H, Frioux C, Fremy E, Wagner M, Corre E, Le Salver A, Leroux C, Leblanc C, Boyen C, Siegel A and Dittami SM (2020) Metabolic Complementarity Between a Brown Alga and Associated Cultivable Bacteria Provide Indications of Beneficial Interactions. Front. Mar. Sci. 7:85. doi: 10.3389/fmars.2020.00085

Brown algae are key components of marine ecosystems and live in association with bacteria that are essential for their growth and development. *Ectocarpus siliculosus* is a genetic and genomic model for brown algae. Here we use this model to start disentangling the complex interactions that may occur between the algal host and its associated bacteria. We report the genome-sequencing of 10 alga-associated bacteria and the genome-based reconstruction of their metabolic networks. The predicted metabolic capacities were then used to identify metabolic complementarities between the algal host and the bacteria, highlighting a range of potentially beneficial metabolite exchanges between them. These putative exchanges allowed us to predict consortia consisting of a subset of these ten bacteria that would best complement the algal metabolism. Finally, co-culture experiments were set up with a subset of these consortia to monitor algal growth as well as the presence of key algal metabolites. Although we did not fully control but only modified bacterial communities in our experiments, our data demonstrated a significant increase in algal growth in cultures inoculated with the selected consortia. In several cases, we also detected, in algal extracts, the presence of key metabolites predicted to become producible via an exchange of metabolites between the alga and the microbiome. Thus, although further methodological developments will be necessary to better control and understand microbial interactions in *Ectocarpus*, our data suggest that metabolic complementarity is a good indicator of beneficial metabolite exchanges in the holobiont.

Keywords: *Ectocarpus siliculosus*, symbiotic/mutualistic bacteria, genome-scale metabolic networks, metabolic complementarity, holobiont

INTRODUCTION

Microbial symbionts are omnipresent and important for the development and functioning of multicellular eukaryotes. Together the eukaryote hosts and their microbiota form meta-organisms also called holobionts. Elucidating the interactions within microbial communities and how they affect host physiology is a complex task and requires an understanding of the dynamics within

the microbiome and the host, as well as of possible inter-species interactions and/or metabolic exchanges that could occur between the partners. One way to dissect those interactions is via targeted co-culture experiments using culturable bacteria, and monitoring potential interaction, *e.g.*, via transcriptomics (de Oliveira et al., 2017). This approach works particularly well for 1:1 or 1:2 interactions, but as the number of potentially interacting organisms increases, selecting the "right" bacterial consortia becomes a major bottleneck (Lindemann et al., 2016).

Metabolic complementarity has previously been proposed as an indicator for potentially beneficial host–symbiont interactions and can be assessed *in silico* using the metabolic networks of the host and the microbiota (Dittami et al., 2014b; Levy et al., 2015). Common examples of metabolic complementarity are associations of autotrophic and heterotrophic organisms such as corals and their photosynthetic symbionts (Rohwer et al., 2002), or algae, and their heterotrophic bacterial biofilm (Wahl et al., 2012). In this case, the autotrophic partner has a metabolic capacity (photosynthesis) that allows for the production of metabolic intermediates (organic carbon), which can be further metabolized by the heterotrophic partners. However, especially in systems with long-lasting interactions more complex metabolic interdependencies are likely to evolve (e.g., Amin et al., 2015).

As a tool to further explore such interactions, Frioux et al. (2018) have proposed the pipeline MiSCoTo. Given the metabolic networks of a host and several symbionts, this tool predicts potential metabolic capacities of one partner that could be unlocked by a contribution of a metabolite from another (e.g., the provision of carbohydrates by a photosynthetic organism unlocking the biochemical processes related to primary metabolism in heterotrophs). Furthermore, this computational approach uses these complementarities to define minimal consortia (i.e., with the lowest possible number of exchanges/contributors) allowing the host to reach its maximum metabolic potential. However, the actual predictive value of these models, both in terms of the effect on host growth and fitness, and in terms of the metabolic scope (i.e., the metabolites producible by the holobiont system), remains to be assessed.

Here we have applied the MiSCoTo tool to the filamentous brown alga *Ectocarpus siliculosus*, a model filamentous brown alga with an available metabolic network (Prigent et al., 2014), as well as a selection of 10 *Ectocarpus*-derived bacteria (KleinJan et al., 2017). We then selected specific minimal microbial consortia for *in vivo* testing of the proposed hypotheses (growth rate, production of specific metabolites). Our results demonstrate a clear positive effect of inoculation with the predicted bacterial consortia on algal growth as well as an effect on the production of algal metabolites predicted to depend on bacterial contributions. *In vivo* observations largely corresponded to *in silico* predictions despite the incomplete input data (with models limited to annotated pathways) and the fact that we had only limited control of the microbiome. The present work thus generates numerous testable hypotheses on specific beneficial interactions between *Ectocarpus* and its microbiome, but also provides a proof of concept for the overall predictive power of network-based metabolic complementarity for beneficial host–microbe interactions.

MATERIALS AND METHODS

Bacterial Cultures and Genome Sequencing

Ten bacterial strains were selected from the 46 isolated by KleinJan et al. (2017) from *Ectocarpus subulatus*. They were grown in liquid Zobell and/or diluted R2A until bacterial growth was visible with the naked eye (∼3 days at room temperature), and their identity was confirmed by sequencing of the 16S rRNA gene with the primers 8F and 1492R (KleinJan et al., 2017). Bacterial DNA was extracted using the UltraClean® Microbial DNA isolation kit (MoBio, Qiagen, Hilden, Germany) and used for standard pair-end sequencing at the GENOMER platform (FR2424, Station Biologique de Roscoff), using Illumina Miseq technology (V3 chemistry, 2 × 300 bp). After cleaning with Trimmomatic v0.38, default parameters (Bolger et al., 2014), the paired-end reads were assembled using SPADES v3.7.0 (Bankevich et al., 2012; default parameters for long reads). The RAST/SEED server (Aziz et al., 2008) was used for gene annotation, and sequences were later also incorporated into the MAGE platform (Vallenet et al., 2006).

In silico Predictions of Metabolic Interactions and Selection of Consortia

Bacterial metabolic networks were constructed using Pathway Tools version 20.5 (Karp et al., 2016) and version 2 of the *Ectocarpus siliculosus* EC32 metabolic network for the host, prior to any gap-filling step, in order to prevent the presence of possibly false positive reactions in the model. (because these false positive reactions could hide algal bacterial interactions). Both host and bacterial networks are provided as SBML file in **Supplementary File S1**. This network comprised a total of 2,118 metabolites, 1,887 metabolic reactions, and was able to produce five of the 50 metabolites known to be a part of the *Ectocarpus* biomass (Aite et al., 2018) with only the culture medium as input. For the remaining 45 compounds the lack of producibility can be explained by the presence of metabolic gaps – either because a reaction was missed during the reconstruction of the network (missing annotation etc.), or because the corresponding pathways require metabolite exchanges with other partners in the environment, e.g., bacteria. The more such gaps can be filled by exchanging compounds between two metabolic networks, the higher we consider the degree of metabolic complementarity between the corresponding organisms.

Here we used the MiSCoTo tool (Frioux et al., 2018) to compute such potential metabolic exchanges between *Ectocarpus* and any of the ten targeted bacteria. The underlying model of MiSCoTo assumes that a compound is producible by a host-symbiont community if there is a chain of metabolic reactions which transforms the culture medium into the expected compound without taking into consideration flux accumulations or competition for resources, and allowing for the exchange of compounds across cell boundaries. These simplifications imply that compounds predicted to be producible *in silico* may, in some

cases, remain unproducible *in vivo*, although the consortium has all the genes to activate the pathways.

In this study MiSCoTo was run twice, first to determine the scope of all algal compounds that become producible via exchanges with all 10 bacterial genomes together, and as second time to select minimal bacterial consortia for the production of these compounds. In both cases the Provasoli culture medium was used as a source as defined previously (Prigent et al., 2014).

Algal Cultures

Two of the six predicted bacterial consortia were tested experimentally via algal-bacterial co-culture experiments. Additionally, each member of the two consortia was tested individually, as well one other sequenced strain that was not part of any of the predicted minimal consortia, *i.e.*, *Sphingomonas* sp. 391. *Ectocarpus siliculosus* (strain 32; accession CCAP 1310/4, origin San Juan de Marcona, Peru) was cultured under standard conditions (13°C; 12 h light regime) in Provasoli-enriched natural seawater until the start of antibiotic treatment. Prior to co-culture experiments, algal filaments were treated with a mixture of the following liquid antibiotics: 45 μg/ml Penicillin G, 22.5 μg/ml streptomycin, and 4.5 μg/ml chloramphenicol dissolved in Provasoli-enriched artificial seawater 450 mM Na^+, 532 mM Cl^-, 10 mM K^+, 6 mM Ca^{2+}, 46 mM Mg^{2+}, 16 mM SO_4^{2-}. Filaments were exposed to 25 ml of this solution for 3 days and then placed in Provasoli-enriched artificial seawater for 3 days to recover. The absence of bacteria on the algal surface was verified by microscopy using phase-contrast (Olympus BX60, 1.3- PH3 immersion objective, 800x magnification) and by plating of algal filaments on Petri dishes with Zobell medium followed by 3 weeks of incubation at room temperature.

Co-culture Experiments

For co-culture experiments, cell densities of bacterial cultures were determined using a BD FACS CantoTM II flow cytometer (BD Bioscience, San Jose, CA, United States) using samples fixed in Tris-EDTA. Before the start of the experiment, antibiotic-treated algae (three replicate cultures per condition) were inoculated with $2.3*10^5$ bacterial cells per strain and ml medium. Each co-culture was then incubated for 4 weeks under standard algal growth conditions (see above). During this time, algal growth was quantified by measuring the filament length of the algae each week using the binocular microscope (3 measurements per replicate). Furthermore, bacterial abundance in the algal growth medium was estimated using flow cytometry (described above) and bacteria attached to algal cell walls were counted by microscopy (5 × 10 μm long filaments observed per biological replicate, 800x magnification in phase contrast). At the end of the experiment, general algal morphology was observed using a LEICA DMi8 microscope and in parallel, remaining algal tissues were frozen in liquid nitrogen and freeze-dried for downstream analyses. Two controls (three replicates each) were run in parallel: a non-antibiotic treated positive control (CTRL w/o. ATB), and an antibiotic-treated non-inoculated alga as a negative control (CTRL w. ATB).

Bacterial Community Composition After Co-culture Experiments

A metabarcoding approach was implemented to investigate the composition of the bacterial community after the co-culture experiments. For each culture, 20 mg ground freeze-dried tissue (TissueLyserII Qiagen, Hilden, Germany; 2 × 45 s, 30 Hz) was used for DNA extraction (DNeasy Plant Mini Kit, Qiagen; standard protocol). Nucleotide concentrations were verified with NanodropONE (Thermo Fisher Scientific). A mock community comprised of DNA from 32 bacterial strains (covering a variety of taxa) as well as a negative control were included in addition to the samples (see Thomas et al., 2020 for details). Libraries were prepared according to the standard Illumina protocol for metabarcoding MiSeq technology targeting the V3–V4 region (Illumina, 2017) and sequenced using Illumina MiSeq Technology (2 × 300 bp, pair-end reads; MiSeq Reagent v3 kit; Platform de Séquencage-Génotypage GENOMER, FR2424, Roscoff).

Resulting raw sequences (7,354,164 read pairs) were trimmed using fastq_quality_trimmer from the FASTX Toolkit (quality threshold 30; minimum read length 200) and assembled into 6,804,772 contigs using PandaSeq v2.11 (Masella et al., 2012). Data were analyzed with Mothur (V.1.40.3) according to the MiSeq Standard Operating Procedures (Kozich et al., 2013). Contigs were pre-clustered (allowing for four mismatches), and aligned to the Silva_SEED 132b database for sequence classification. Chimeric sequences were removed (Vsearch) and the remaining sequences classified taxonomically (Wang et al., 2007). Non-bacterial sequences were removed and the remaining sequences were then clustered into operational taxonomic units (OTUs) at a 97% identity level and each OTU was classified to the genus level where possible (Wang et al., 2007). All OTUs with $n \leq 10$ sequences were removed resulting in a final data matrix with 1,834,992 sequences. The OTU matrix was subsampled to have the same number of sequences per sample for downstream analyses.

Targeted Metabolomics

Seven metabolites predicted to be producible by the algae only in presence of metabolic exchanges with specific bacteria were selected for targeted metabolite profiling after manual verification of automatic predictions of corresponding pathways in the algal and bacterial networks and based on their biological importance for the alga: L-histidine, putrescine, beta-alanine, nicotinic acid, folic acid, auxin, and spermidine. Metabolites were extracted from 10 mg of ground, freeze-dried tissue using a triple extraction protocol based on the method of Bligh and Dyer (1959): two ml of methanol:chloroform:water (6:4:1) were used as first extraction solvent, then the remaining pellet was extracted with 1 ml of chloroform:methanol (1:1), and finally, a 3rd extraction was performed using 1 ml of H_2O. The supernatants of each extraction were pooled and evaporated under a stream of nitrogen. The residue was then resuspended in 100 μl methanol:water (1:1) and analyzed on an ACQUITY Ultra-performance convergence chromatography (UPC^2) system (Waters®, Milford, United States) equipped with a Viridis BEH

column (3 × 100 mm, 1.7 μm). A linear gradient of two solvents was used to separate peaks: supercritical carbon dioxide (Solvent A), and methanol spiked with 0.1% formic acid (Solvent B). The gradient ran from 5% to 25% of solvent B (35% for spermidine and nicotinic acid) during 2 min, was kept at this level for another 2 min and then gradually reduced back to 5% during 3 min. The UPC^2 system was coupled to a Xevo G2 Q-Tof mass spectrometer (Waters), operating in positive ESI ion mode (m/z 20–500). Blanks, as well as standards of all 7 compounds obtained from Sigma-Aldrich (St. Louis, MO, United States), were run in parallel to samples. The resulting chromatograms were then used to examine the presence/absence of the target compounds in the other samples based on retention time and the mass spectra. Analyses were performed at the METABOMER platform (FR2424, Station Biologique de Roscoff).

Statistical Analyses

Growth data (both algal and bacterial) were confirmed to follow a normal distribution using a Shapiro–Wilk test (Rstudio v1.0.44). Significant differences between all treatments after 4 weeks of co-culture (day 28) were calculated with an ANOVA and a Tukey honestly significant difference (HSD) *post hoc* test with a significance level α 0.05 using the PAST software version 3.20 (Hammer et al., 2001).

RESULTS

Predicted Metabolic Interactions and Selection of Beneficial Bacterial Consortia

Genome sequencing and subsequent bioinformatics analyses yielded bacterial genome assemblies with sufficient coverage and 11–72 scaffolds per genome (**Table 1**). Metabolic networks were then reconstructed for these ten genomes. On average, 1,714 reactions, 111 transport reactions, and 1,405 metabolites (**Table 2**) were predicted per bacterium. These reactions belonged, again on average, to 261 pathways, 137 of which were complete and 124 were incomplete (i.e., missing one or more reactions). Based on metabolic complementarity analysis carried out using MiSCoTo, these bacterial networks were predicted to enable the production of 160 additional compounds with the algal networks, including several polyamines (Cadaverine, Spermidine, Agmatine), amino acids (Histidine, Tyrosine, beta-alanine), vitamins B3, B9, and E, several lipids and lipid derivatives, and nucleic acids. Please refer to **Supplementary Table S1** for a complete list of compounds. Many of these compounds were also previously predicted via the metabolic interaction between the same strain of *E. siliculosus* and the associated bacterium *Candidatus* Phaeomarinobacter ectocarpi (Dittami et al., 2014a; Prigent et al., 2017). A total of six bacterial consortia comprising three bacterial strains each (**Table 3**) were predicted to be sufficient to enable the production of all of these compounds. Of these six proposed consortia, two comprised one phylogenetically distinct bacterium each (i.e., the *Bacteroidetes Imperialibacter* vs. the *Gammaproteobacterium Marinobacter*) were chosen for *in vivo* testing using algal-bacterial co-cultures.

Growth Rates in Co-culture Experiments

The inoculation with one or several bacterial strains significantly enhanced algal growth by a factor of 2 compared to controls (**Figure 1A**). This positive effect was observed both for the predicted bacterial consortia and for all the individual strains tested. At the same time, the abundance of bacteria on algal filaments after 4 weeks of cultivation was significantly lower in cultures initially inoculated with bacteria compared to both controls with and without initial antibiotic treatment (**Figure 1B**), although bacterial cell counts in the medium were similar between co-culture experiments and the non-inoculated control after 28 days (**Supplementary Figure S1**).

Bacterial Impact on Morphology

Compared to the negative control, which exhibited a ball-like morphology typical for "axenic" cultures (Tapia et al., 2016), all bacterial inocula tested resulted in filamentous thalli with clear branching patterns (**Figure 2**). We furthermore observed differences in the branching patterns depending on the bacterial inocula. For example, *Sphingomonas*-inoculated cultures produced relatively long filaments with few branching sites (**Figure 2G**), whereas *Hoeflea*-inoculated cultures produced filaments with frequent branching (**Figure 2E**). *Imperialibacter* induced aggregation of individual filaments (**Figure 2F**), while in all other co-cultures, filaments remained more or less separated. These differences were, however, difficult to quantify given complexity of their morphology.

(Algal) Metabolome in Co-culture Conditions

Seven putatively key metabolites (l-histidine, putrescine, beta-alanine, nicotinic acid, folic acid, auxin, and spermidine) predicted to be non-producible by the alga alone but producible via exchanges with some bacterial consortia, were quantified in algal tissues by UPC^2-MS after 4 weeks of co-culture. The presence/absence of these metabolites is shown in **Figure 3**, comparing both the predicted producibility by metabolic network analysis and the experimental UPC^2-MS results. In the negative control, i.e., antibiotic-treated algae that were not inoculated with bacteria, none of the compounds could be identified by UPC^2-MS confirming the computational predictions. In contrast, in all co-cultures, at least one target compound was experimentally detected. Furthermore, each compound became producible in at least one of the co-cultures. Overall, across the 56 predictions made based on the metabolic networks (7 metabolites × 8 consortia including the individual bacteria and the negative control) *in silico* and *in vivo* data agreed in 28 cases (**Figure 3**). Only in four cases did we observe the presence of a metabolite although it was not predicted by the networks. Finally, in 24 cases we did not detect the presence of a metabolite predicted to be producible in the co-cultures.

TABLE 1 | Overview of bacterial genomes used in this study and corresponding assembly statistics.

	Raw reads	# Scaffolds	Genome size (mbp)	N50 (mbp)	Coverage	Mapped reads
Bosea sp. 5A	1,863,417	26	6.34	0.98	133 X	99.91%
Erythrobacter sp. 430	1,065,278	11	3.14	0.44	157 X	99.93%
Hoeflea sp. 425	3,734,649	41	5.22	1.26	326 X	99.94%
Imperialibacter sp. R6	1,553,981	65	6.8	0.21	111 X	99.94%
Marinobacter sp. HK15	1,587,675	14	4.39	1.11	172 X	99.93%
Rhizobium sp. 404	1,332,560	27	4.2	0.45	148 X	99.93%
Roseovarius sp. 134	987,463	73	4.68	0.18	150 X	99.92%
Roseovarius sp. 420	803,175	85	4.68	0.12	79 X	99.89%
Sphingomonas sp. 361	1,111,277	25	3.28	0.29	150 X	99.87%
Sphingomonas sp. 391	1,150,343	74	4.6	0.16	113 X	99.91%

TABLE 2 | Number of predicted metabolic pathways (complete pathways in parentheses), reactions and metabolites in bacterial metabolic networks.

	Number of pathways	Number of reactions	Transport reactions	Number of metabolites
Bosea sp. 5A	298 (187)	1892	153	1557
Erythrobacter sp. 430	218 (91)	1532	63	1247
Hoeflea sp. 425	315 (170)	1920	129	1558
Imperialibacter sp. R6	239 (131)	1711	100	1425
Marinobacter sp. HK15	249 (128)	1679	128	1364
Rhizobium sp. 404	289 (142)	1814	125	1462
Roseovarius sp. 134	263 (146)	1703	125	1418
Roseovarius sp. 420	263 (143)	1701	125	1418
Sphingomonas sp. 361	224 (108)	1519	69	1239
Sphingomonas sp. 391	254 (126)	1671	92	1358

The networks are available in the SBML format as ***Supplementary File S1****.*

TABLE 3 | Minimal bacterial consortia predicted by MiSCoTo that enabled the production of 160 algal compounds.

Solution proposed by MiSCoTo	*In vivo* testing?
Marinobacter sp. HK15, *Roseovarius* sp. 420, *Hoeflea* sp. 425	Yes
Roseovarius sp. 420, *Imperialibacter* sp. R6, *Hoeflea* sp. 425	Yes
Marinobacter sp. HK15, *Bosea* sp. 5a, *Roseovarius* sp. 420	No
Marinobacter HK15, *Hoeflea* sp. 425, *Roseovarius* sp. 134	No
Imperialibacter sp. R6, *Hoeflea* sp. 425, *Roseovarius* sp. 134	No
Marinobacter sp. HK15, *Bosea* sp. 5a, *Roseovarius* sp. 134	No

See ***Supplementary Table S1*** *for a detailed list of compounds.*

Bacterial Community Composition After Co-culture Experiments

The bacterial community composition of each sample was analyzed by 16S rDNA metabarcoding at the end of the co-culture experiments. This was done to verify if the bacteria inoculated had grown in the co-cultures and to determine to what extent other bacteria were present and affected by the inoculations. The results (**Table 4**) show that, except for *Imperialibacter*, all of the bacterial strains inoculated were detected in the corresponding co-cultures 28 days after inoculation. However, except for *Marinobacter* and *Hoeflea*, read abundances of these strains were low compared to the total number of reads. In parallel, several other OTUs that had not been inoculated were detected in our co-culture experiments, suggesting that these bacteria were at least partially resistant to or protected from (*e.g.*, within the cell wall) the antibiotic treatments applied, and were able to recover under the experimental conditions: in total 30 additional OTUs with a minimal abundance of 1% of total reads were detected in our samples, accounting for 63–82% of the total reads. Furthermore, *Hoeflea* reads were dominant in all samples including the non-Hoeflea-inoculated cultures (14–30% of total reads).

DISCUSSION

Metabolic Complementarity, a Powerful Metric Despite Limitations

Metabolic complementarity intuitively seems like an excellent marker for beneficial metabolic interactions. The more organisms are complementary at the metabolic and by extension the gene level, the more they can potentially benefit from each other (Levy et al., 2015); the more they overlap in terms of metabolic pathways, the more likely they are to compete for the same resources (Kreimer et al., 2012). There are, however, two important restrictions that limit the applicability of this simple idea. First, the possibility of a beneficial exchange does not necessarily mean that it will occur, because this may require the presence and activation of

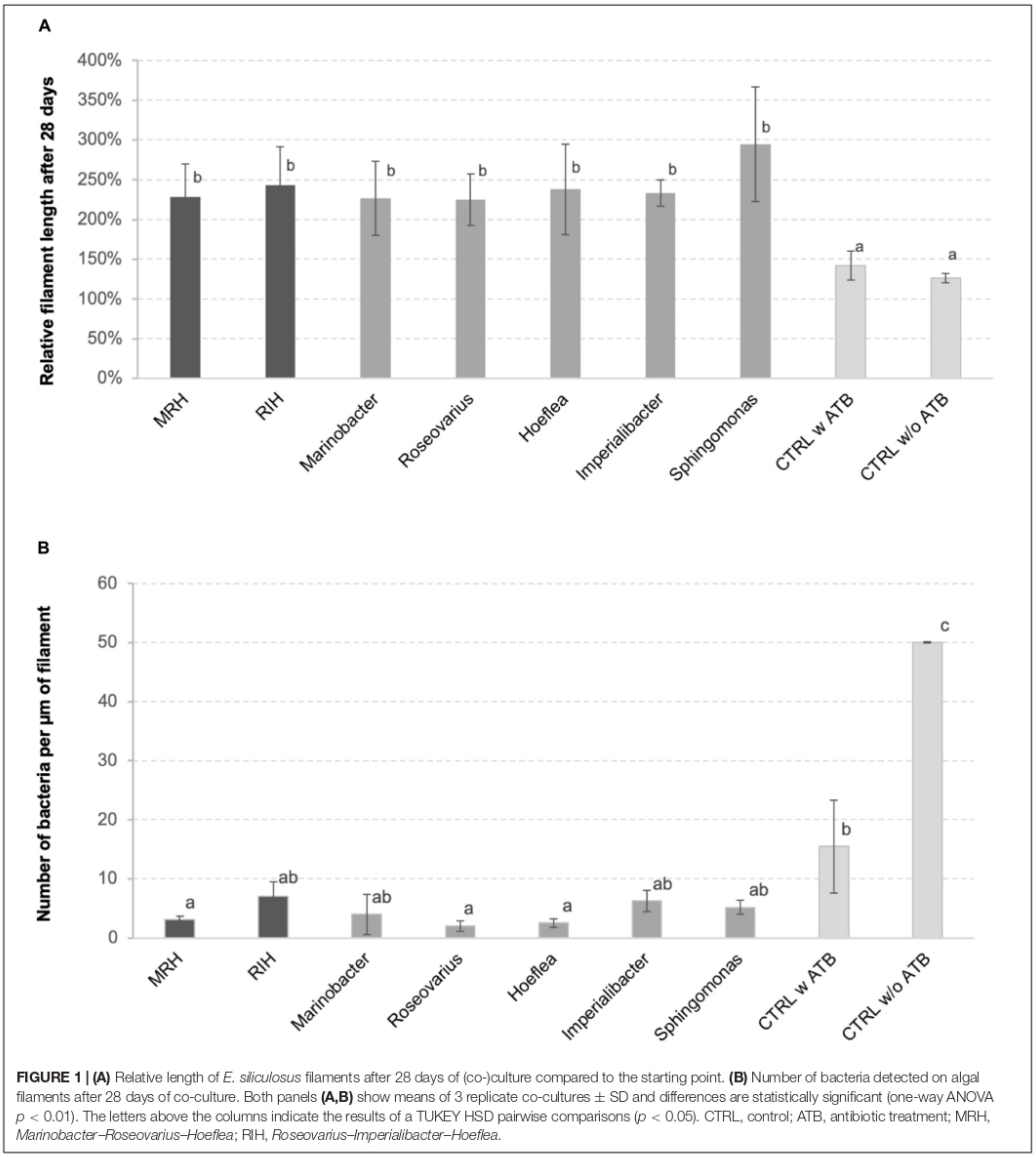

FIGURE 1 | (A) Relative length of *E. siliculosus* filaments after 28 days of (co-)culture compared to the starting point. **(B)** Number of bacteria detected on algal filaments after 28 days of co-culture. Both panels **(A,B)** show means of 3 replicate co-cultures ± SD and differences are statistically significant (one-way ANOVA $p < 0.01$). The letters above the columns indicate the results of a TUKEY HSD pairwise comparisons ($p < 0.05$). CTRL, control; ATB, antibiotic treatment; MRH, *Marinobacter–Roseovarius–Hoeflea*; RIH, *Roseovarius–Imperialibacter–Hoeflea*.

excretion/uptake mechanisms in both partners, *e.g.,* via chemical or environmental cues. Secondly, the genome-scale metabolic models used to predict metabolic complementarities may be partially erroneous and incomplete. For instance, metabolic networks frequently do not comprise interactions of chemical signals with receptor molecules, which may be key to regulate interactions (Zhou et al., 2016; Wang et al., 2018). Furthermore, in many cases, they are based on automatic predictions and annotations of protein sequences, which may, in some cases, miss genes or introduce overpredictions of functions (Schnoes et al., 2009). In this paper, we provide first *in vivo* tests of host-microbe interactions inferred from genome-based predictions

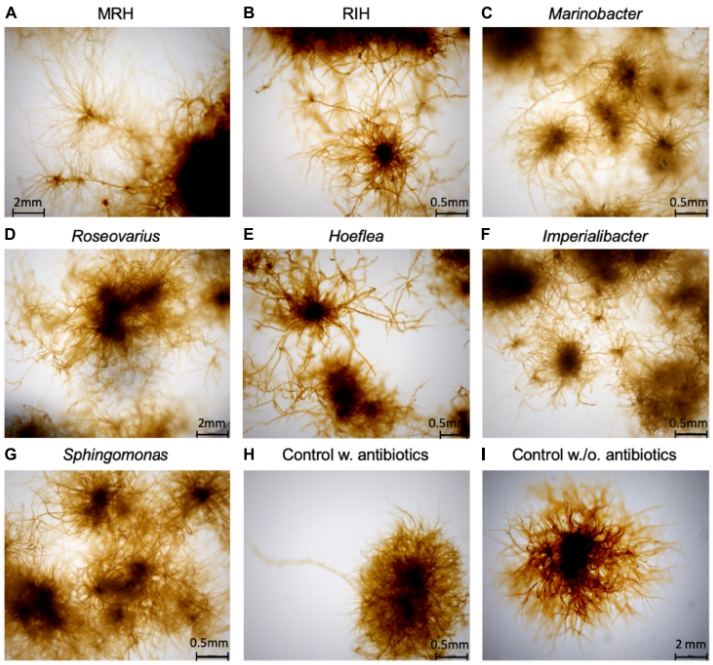

FIGURE 2 | Morphological effect co-cultures with bacteria on *E. siliculosus* after 4 weeks of co-culturing. Panels **(A–G)** correspond to different bacterial inoculations, panels **(H,I)** to controls. MRH, *Marinobacter–Roseovarius–Hoeflea*; RIH, *Roseovarius–Imperialibacter–Hoeflea*.

Target	Exchange	MRH	RIH	Marinobacter	Roseovarius	Hoeflea	Imperialibacter	Sphingomonas	CTRL w ATB
Spermidine	Dehydrospermidine	+/–	+/–	+/–	+/+	+/–	+/–	+/–	–/–
Putrescine	Agmatine	+/–	+/+	+/+	+/+	+/–	+/–	+/–	–/–
Nicotinic acid	Nicotinic acid	+/–	+/+	+/–	+/–	+/–	–/+	+/–	–/–
Folic acid	dihydrofolate	+/–	+/–	–/–	–/–	–/–	–/–	–/+	–/–
Auxine	Indole-3-acetaldehyde	+/+	+/+	–/–	–/–	–/+	+/+	–/+	–/–
L-histidine	Histidinol	+/–	+/–	+/–	+/–	+/+	+/+	+/+	–/–
Beta-Alanine	3-ureidopropanoate	+/–	+/+	+/+	+/–	+/+	+/–	–/–	–/–

FIGURE 3 | Comparison of predicted production of target metabolites in co-cultures based on metabolic networks (symbol before the slash) and results from targeted UPC^2-MS analyses of algal filaments after 28 days (symbol after the slash). The column "Exchange" indicates one possible compound provided by the microbiome leading to the production of the compound in the column "Target" in the algal metabolome; it was these target metabolites that were tested for using UPC^2-MS. All experiments were carried out in triplicate, each replicate of the same condition yielding identical results. (–): a target metabolite was not predicted/detected (+): a metabolite was predicted/detected. Green highlights conditions where predictions correspond to the *in vivo* observations, red highlights compounds that were detected although no pathway was predicted. Yellow indicates compounds potentially producible via bacterial exchanges that were not detected. MRH, *Marinobacter–Roseovarius–Hoeflea*; RIH, *Roseovarius–Imperialibacter–Hoeflea*; CTRL, control; ATB, antibiotic treatment.

of metabolic complementarity. Despite the aforementioned restrictions and simplifications, our results discussed below provide a strong indication that genome-based predictions of metabolic complementarity are a powerful tool to handle the complexity of host microbe systems and to generate hypotheses on their interactions.

TABLE 4 | Observed abundance of target OTUs after 4 weeks of co-culture.

	MRH	RIH	*Marinobacter*	*Roseovarius*	*Hoeflea*	*Imperialibacter*	*Sphingomonas*	CTRL w. ATB	CTRL w./o. ATB
Marinobct. OTU00030	**82 ± 48**	0 ± 0	**1103 ± 1068**	0 ± 0	0 ± 0	0 ± 0	38 ± 38	0 ± 0	1 ± 1
Roseovarius OTU00055	**8 ± 7**	**11 ± 3**	1 ± 1	**41 ± 10**	1 ± 1	0 ± 0	0 ± 0	0 ± 0	0 ± 0
Hoeflea OTU00001	**10265 ± 1586**	**7644 ± 889**	4483 ± 2777	15635 ± 1349	**15321 ± 3515**	13426 ± 5338	10216 ± 4345	8899 ± 2811	3618 ± 1055
Imperialib. OTU00044	0 ± 0	**0 ± 0**	0 ± 0	0 ± 0	0 ± 0	**0 ± 0**	0 ± 0	0 ± 0	0 ± 0
Sphingomn. OTU00097	0 ± 0	0 ± 0	0 ± 0	0 ± 0	0 ± 0	1 ± 1	**4 ± 4**	0 ± 0	0 ± 0
Other OTUs*	39403 ± 2138	23458 ± 1828	26223 ± 3187	36374 ± 7810	34190 ± 5508	38076 ± 4292	29066 ± 3302	42323 ± 9670	28009 ± 5897

*The table shows number of reads obtained corresponding to each OTU (mean three replicates ± SD). Bold numbers indicate OTUs expected to be present based on the inoculations. *See* ***Supplementary Figure S2*** *for details.*

Similar Complementarities Found Across Studies and *Ectocarpus* Symbionts

Compared to a previous analysis of metabolic complementarity between *Ectocarpus* and another associated bacterium, *Candidatus* Phaeomarinobacter ectocarpii, (Dittami et al., 2014a; Prigent et al., 2017), newly producible compounds predicted in this study were largely similar, notably regarding polyamines, histidine, beta-alanine, and auxin. This similarity persists even though metabolic complementarity analyses were performed using MiSCoTo, which incorporates the notion of different compartments minimizing the number metabolite exchanges (Frioux et al., 2018) and despite the fact that different bacteria were examined. The main difference compared to the previous study is that numerous additional compounds were predicted to be exchanged, which can be explained by the fact that ten rather than one bacterial network were available to complete the algal network.

Inoculation With Metabolically Complementary Bacteria Enhances Growth Rate and Impacts Morphology and Metabolism

As described above, both the bacterial consortia tested, as well as all of the bacteria inoculated individually had clear positive effects on algal growth and impacted algal morphology and metabolite profiles, even though, by the time the co-cultures were harvested, some of the inoculated bacteria were present only in very low abundance or even below the detection limit. These positive effects could be due either to interactions early in the co-culture experiments followed by a decline in bacterial abundance, or due to the capacity of bacteria to impact and interact with their algal hosts even at very low cell concentrations. The latter would support the hypothesis that part of the observed effects may not be due to the exchanges of (abundant) primary metabolites, such as the predicted histidine/histidinol, but due to lowly concentrated signaling molecules or growth hormones. One such compound could be the examined auxin, which was detected in 5 of the 7 tested co-cultures, and which has previously been shown to modify the developmental patterns and morphology of *Ectocarpus* cultures (Le Bail et al., 2010) in a similar way as bacterial inoculations. Another observation was that the abundance of bacteria on algal filaments but not in the medium was significantly lower in co-culture conditions compared to the controls. This suggests that the inoculated bacteria, either directly, or indirectly, by stimulating algal growth or defense, can also regulate biofilm formation (see Goecke et al., 2010 for a review).

Interestingly, although differences in the effects of individual bacteria and bacterial consortia were observed on metabolite profiles and morphology, all consortia had similar effects on algal growth. Indeed, all of the tested bacteria, including *Sphingomonas*, which was not part of the minimal solutions proposed by MiSCoTo, were to a great extent complementary to the alga, already covering a large part of the metabolic gaps. In future studies, it may be particularly useful to incorporate

a larger range of bacteria, possibly from other sources so that they are not expected to have evolved mutualistic interactions with brown algae. These negative controls could then be used to correlate growth rates with the presence or absence of specific metabolic capacities in the network. Once the list of candidate metabolite exchanges has been narrowed down by such comparisons, supplying these metabolites from artificial sources but also testing for their excretion into the medium by bacteria can be used to corroborate their role.

Predicted Metabolic Exchanges Likely to Occur in Part

With respect to the predictions of target metabolites, we observed that for a large number of cases, predictions from the metabolic networks corresponded to the observations made by experimental metabolic profiling: none of the target metabolites were detected in the negative control, and only in four cases (**Figure 3**) did we detect compounds in co-cultures that were not predicted to be there. This could either be attributed to undetected metabolic pathways in the examined/added bacteria (e.g., due to missing annotations) or, more likely, to the activity of other bacteria present in our co-culture experiments (see below). Furthermore, there were several cases in which a potentially co-producible metabolite was not detected in our co-cultures. Here two explanations appear particularly likely: first, the metabolites in question may be produced but quickly metabolized in certain consortia, so that they do not accumulate sufficiently to be detectable in our cultures; secondly, it is possible that the corresponding biosynthetic pathway of the metabolite was not active or that the necessary exchange of metabolites was not taking place. To resolve this point in future experiments, the addition of gene expression data may help to establish whether or not biosynthetic or degradation pathways are active. From a global perspective, however, the fact that none of the compounds in question were detected in negative controls, but all of them it at least one co-culture condition, constitutes a highly promising result.

Outlook

In our opinion, the main challenge for future *in vivo* studies of metabolic complementarity will be to better control the *Ectocarpus*-associated microbiome in co-culture experiments, and thus to avoid any impact of non-inoculated microbes. The currently applied antibiotic treatments are successful in removing bacteria from the algal surface to a level where they are no longer detectable by microscopy and spreading on culture medium, but once the treatment is stopped and algae are left to recover, so do parts of the microbiome, possibly from spores that were inactive or embedded in the algal cell wall and thus less susceptible to our treatments (Tetz and Tetz, 2017). In light of these results, we strongly recommend routine metabarcoding analysis for any type of coculture experiment, also in other model systems. One possibility in the future would be to use axenization protocols based on the movement of gametes, as has been done for *Ulva mutabilis* (Spoerner et al., 2012); at least some strains of *Ectocarpus* have previously been shown to produce phototactic gametes (Kawai et al., 1990). A second alternative is the continuous use of antibiotics throughout the experiment, and working with antibiotic-resistant bacterial strains. In this context a better understanding of the metabolic requirements of the algae will help to durably maintain axenic cultures.

Despite these challenges, the present study constitutes an important proof of concept for the use of metabolic complementarity to study simplified system of mutualistic host–symbiont interactions. We anticipate that, in the long run, this concept can be applied not only to controlled co-culture experiments, but that it will also prove useful for the interpretation of more complex datasets such as metatranscriptomic or metagenomic data.

DATA AVAILABILITY STATEMENT

The metabarcoding data generated for this study has been deposited at the European Nucleotide Archive (ENA) under project accession number PRJEB34356. The bacterial genomes have been deposited at the ENA under the sample accessions CABVLD010000000–CABVLL010000000, CABVLT010000000.

AUTHOR CONTRIBUTIONS

BB-D, HK, and SD conceived the experiments. CF and AS conceived *in silico* analyses. BB-D and HK performed the experiments. BB-D, AL, EF, CF, MW, SD, EC, and CLer performed the analyses. SD, HK, and BB-D wrote the manuscript. All authors corrected and approved of the final manuscript.

FUNDING

This work was funded partially by the CNRS Momentum call, the ANR project IDEALG (ANR-10-BTBR-04) "Investissements d'Avenir, Biotechnologies-Bioressources," the European Union's Horizon 2020 research and innovation Programme under the Marie Sklodowska-Curie grant agreement number 624575 (ALFF), and joint Ph.D. scholarship from the Brittany region (Project HOSALA) and the Sorbonne University (ED227).

ACKNOWLEDGMENTS

We thank Laurence Dartevelle for advice on algal culturing; Sylvie Rousvoal for extractions of bacterial DNA; Gwenn Tanguy and Erwan Legeay from the GENOMER platform (FR2424, Station Biologique de Roscoff) for access to the sequencing platform and support during library preparation; François Thomas, Angélique Gobet, and Maeva Brunet for helpful discussions and for sharing their mock community; Dominique Marie and Christian Jeanthon for granting us access to their flow cytometer; and the ABIMS platform and the GenOuest bioinformatics core facility (https://www.genouest.org) for providing the computing infrastructure for amplicon analyses and community predictions. The LABGeM (CEA/Genoscope

and CNRS UMR8030), the France Génomique and French Bioinformatics Institute national infrastructures (funded as part of Investissement d'Avenir program managed by Agence Nationale pour la Recherche, contracts ANR-10-INBS-09 and ANR-11-INBS-0013) are acknowledged for support within the MicroScope annotation platform. This manuscript has been released as a Pre-Print at BioRXiv (Burgunter-Delamare et al., 2019).

SUPPLEMENTARY MATERIAL

The Supplementary Material for this article can be found online at: https://www.frontiersin.org/articles/10.3389/fmars.2020.00085/full#supplementary-material

FIGURE S1 | Number of bacteria detected in the algal culture medium after 28 days of co-culture. The graph shows means of 3 replicates ± SD and differences are statistically significant (one-way ANOVA $p < 0.01$). The letters above the columns indicate the results of a TUKEY HSD pairwise comparisons ($p < 0.05$). CTRL, control; ATB, antibiotic treatment.

FIGURE S2 | Heatmap of relative OTU abundance for all 30 OTUs that made up over 1% of the total number of reads and that were not inoculated (see **Table 4** for the latter). This heatmap as generated using the ClustVis service (Metsalu and Vilo, 2015) using "correlation" as a distance measure and "average linkage" as clustering method. The color code corresponds to the mean sequence abundance for each OTU in the three replicates a percentage of total reads; uc., unclassified.

TABLE S1 | Metabolites predicted to become producible by the alga as a result of metabolite exchanges between the alga and bacteria.

FILE S1 | Metabolic networks of the algal host and the tested bacteria in the SBML format.

REFERENCES

Aite, M., Chevallier, M., Frioux, C., Camille, T., Jeanne, G., María, P. C., et al. (2018). Traceability, reproducibility and wiki-exploration for "à-la-carte" reconstructions of genome-scale metabolic models. *PLoS Comput. Biol.* 14:e1006146. doi: 10.1371/journal.pcbi.1006146

Amin, S. A., Hmelo, L. R., van Tol, H. M., Durham, B. P., Carlson, L. T., Heal, K. R., et al. (2015). Interaction and signalling between a cosmopolitan phytoplankton and associated bacteria. *Nature* 522, 98–101. doi: 10.1038/nature14488

Aziz, R. K., Bartels, D., Best, A. A., DeJongh, M., Disz, T., Edwards, R. A., et al. (2008). The RAST server: rapid annotations using subsystems technology. *BMC Genom.* 9:75. doi: 10.1186/1471-2164-9-75

Bankevich, A., Nurk, S., Antipov, D., Gurevich, A. A., Dvorkin, M., Kulikov, A. S., et al. (2012). SPAdes: a new genome assembly algorithm and its applications to single-cell sequencing. *J. Comput. Biol.* 19, 455–477. doi: 10.1089/cmb.2012.0021

Bligh, E. G., and Dyer, W. J. (1959). A rapid method of total lipid extraction and purification. *Can. J. Biochem. Physiol.* 37, 911–917.

Bolger, A. M., Lohse, M., and Usadel, B. (2014). Trimmomatic: a flexible trimmer for Illumina sequence data. *Bioinformatics* 30, 2114–2120. doi: 10.1093/bioinformatics/btu170

Burgunter-Delamare, B., KleinJan, H., Frioux, C., Enora, F., Margot, W., Erwan, C., et al. (2019). Metabolic complementarity between a brown alga and associated cultivable bacteria provide indications of beneficial interactions. *bioRxiv* [Preprint], doi: 10.1101/813683

de Oliveira, L. S., Tschoeke, D. A., Magalhães Lopes, A. C. R., Sudatti, D. B., Pedro, M. M., Cristiane, C. T., et al. (2017). Molecular mechanisms for microbe recognition and defense by the red seaweed Laurencia dendroidea. *mSphere* 2:e00094. doi: 10.1128/mSphere.00094-17

Dittami, S. M., Barbeyron, T., Boyen, C., Jeanne, C., Guillaume, C., Ludovic, D., et al. (2014a). Genome and metabolic network of "Candidatus Phaeomarinobacter ectocarpi" Ec32, a new candidate genus of Alphaproteobacteria frequently associated with brown algae. *Front. Genet.* 5:241. doi: 10.3389/fgene.2014.00241

Dittami, S. M., Eveillard, D., and Tonon, T. (2014b). A metabolic approach to study algal-bacterial interactions in changing environments. *Mol. Ecol.* 23, 1656–1660. doi: 10.1111/mec.12670

Frioux, C., Fremy, E., Trottier, C., and Siegel, A. (2018). Scalable and exhaustive screening of metabolic functions carried out by microbial consortia. *Bioinformatics* 34, i934–i943. doi: 10.1093/bioinformatics/bty588

Goecke, F., Labes, A., Wiese, J., and Imhoff, J. (2010). Chemical interactions between marine macroalgae and bacteria. *Mar. Ecol. Prog. Ser.* 409, 267–299.

Hammer, Ø, Harper, D., and Ryan, P. (2001). PAST: paleontological statistics software package for education and data analysis. *Palaeontol. Electronica* 4:9.

Illumina, (2017). *16S Metagenomic Sequencing Library Preparation*. Available at: https://support.illumina.com/documents/documentation/chemistry_documentation/16s/16s-metagenomic-library-prep-guide-15044223-b.pdf (accessed March 15, 2018).

Karp, P. D., Latendresse, M., Paley, S. M., Krummenacker, M., Ong, Q. D., Billington, R., et al. (2016). Pathway tools version 19.0 update: software for pathway/genome informatics and systems biology. *Brief. Bioinform.* 17, 877–890. doi: 10.1093/bib/bbv079

Kawai, H., Müller, D. G., Fölster, E., and Häder, D.-P. (1990). Phototactic responses in the gametes of the brown alga, *Ectocarpus siliculosus*. *Planta* 182, 292–297. doi: 10.1007/BF00197124

KleinJan, H., Jeanthon, C., Boyen, C., and Dittami, S. M. (2017). Exploring the cultivable *Ectocarpus* microbiome. *Front. Microbiol.* 8:2456. doi: 10.3389/fmicb.2017.02456

Kozich, J. J., Westcott, S. L., Baxter, N. T., Highlander, S. K., and Schloss, P. D. (2013). Development of a dual-index sequencing strategy and curation pipeline for analyzing amplicon sequence data on the miseq illumina sequencing platform. *Appl. Environ. Microbiol.* 79, 5112–5120. doi: 10.1128/AEM.01043-13

Kreimer, A., Doron-Faigenboim, A., Borenstein, E., and Freilich, S. (2012). NetCmpt: a network-based tool for calculating the metabolic competition between bacterial species. *Bioinformatics* 28, 2195–2197. doi: 10.1093/bioinformatics/bts323

Le Bail, A., Billoud, B., Kowalczyk, N., Mariusz, K., Morgane, G., Sophie, L. P., et al. (2010). Auxin metabolism and function in the multicellular brown alga *Ectocarpus siliculosus*. *Plant Physiol.* 153, 128–144. doi: 10.1104/pp.109.149708

Levy, R., Carr, R., Kreimer, A., Freilich, S., and Borenstein, E. (2015). NetCooperate: a network-based tool for inferring host-microbe and microbe-microbe cooperation. *BMC Bioinformatics* 16:164. doi: 10.1186/s12859-015-0588-y

Lindemann, S. R., Bernstein, H. C., Song, H. S., Jim, K. F., Matthew, W. F., Wenying, S., et al. (2016). Engineering microbial consortia for controllable outputs. *ISME J.* 10, 2077–2084. doi: 10.1038/ismej.2016.26

Masella, A. P., Bartram, A. K., Truszkowski, J. M., Brown, D. G., and Neufeld, J. D. (2012). PANDAseq: paired-end assembler for Illumina sequences. *BMC Bioinform.* 13:31. doi: 10.1186/1471-2105-13-31

Metsalu, T., and Vilo, J. (2015). ClustVis: a web tool for visualizing clustering of multivariate data using principal component analysis and heatmap. *Nucleic Acids Res.* 43, W566–W570. doi: 10.1093/nar/gkv468

Prigent, S., Collet, G., Dittami, S. M., Delage, L., Ethis de Corny, F., Dameron, O., et al. (2014). The genome-scale metabolic network of *Ectocarpus siliculosus* (EctoGEM): a resource to study brown algal physiology and beyond. *Plant J.* 80, 367–381. doi: 10.1111/tpj.12627

Prigent, S., Frioux, C., Dittami, S. M., Thiele, S., Larhlimi, A., Collet, G., et al. (2017). Meneco, a topology-based gap-filling tool applicable to degraded genome-wide metabolic networks. *PLoS Comput. Biol.* 13:e1005276. doi: 10.1371/journal.pcbi.1005276

Rohwer, F., Seguritan, V., Azam, F., and Knowlton, N. (2002). Diversity and distribution of coral-associated bacteria. *Mar. Ecol. Prog. Ser.* 243, 1–10.

Schnoes, A. M., Brown, S. D., Dodevski, I., and Babbitt, P. C. (2009). Annotation error in public databases: misannotation of molecular dunction in enzyme

superfamilies. *PLoS Comput. Biol.* 5:e1000605. doi: 10.1371/journal.pcbi.1000605

Spoerner, M., Wichard, T., Bachhuber, T., Stratmann, J., and Oertel, W. (2012). Growth and thallus morphogenesis of Ulva mutabilis (Chlorophyta) depends on a combination of two bacterial species excreting regulatory factors. *J. Phycol.* 48, 1433–1447. doi: 10.1111/j.1529-8817.2012.01231.x

Tapia, J. E., González, B., Goulitquer, S., Potin, P., and Correa, J. A. (2016). Microbiota influences morphology and reproduction of the brown alga *Ectocarpus* sp. *Front. Microbiol.* 7:197. doi: 10.3389/fmicb.2016.00197

Tetz, G., and Tetz, V. (2017). Introducing the sporobiota and sporobiome. *Gut Pathog.* 9:38. doi: 10.1186/s13099-017-0187-8

Thomas, F., Dittami, S. M., Brunet, M., Le Duff, N., Tanguy, G., Leblanc, C., et al. (2020). Evaluation of a new primer combination to minimize plastid contamination in 16S rDNA metabarcoding analyses of alga-associated bacterial communities. *Environ. Microbiol. Rep.* 12, 30–37.

Vallenet, D., Labarre, L., Rouy, Z., Valérie, B., Stéphanie, B., Stéphane, C., et al. (2006). MaGe: a microbial genome annotation system supported by synteny results. *Nucleic Acids Res.* 34, 53–65.

Wahl, M., Goecke, F., Labes, A., Dobretsov, S., and Weinberger, F. (2012). The second skin: ecological role of epibiotic biofilms on marine organisms. *Front. Microbiol.* 3:292. doi: 10.3389/fmicb.2012.00292

Wang, Q., Garrity, G. M., Tiedje, J. M., and Cole, J. R. (2007). Naive Bayesian classifier for rapid assignment of rRNA sequences into the new bacterial taxonomy. *Appl. Environ. Microbiol.* 73, 5261–5267.

Wang, Q., Liu, J., and Zhu, H. (2018). Genetic and molecular mechanisms underlying symbiotic specificity in legume-*Rhizobium* interactions. *Fron. Plant Sci.* 9:313. doi: 10.3389/fpls.2018.00313

Zhou, J., Lyu, Y., Richlen, M. L., Anderson, D. M., and Cai, Z. (2016). Quorum sensing is a language of chemical signals and plays an ecological role in algal-bacterial interactions. *Crit. Rev. Plant Sci.* 35, 81–105. doi: 10.1080/07352689.2016.1172461

Conflict of Interest: The authors declare that the research was conducted in the absence of any commercial or financial relationships that could be construed as a potential conflict of interest.

Copyright © 2020 Burgunter-Delamare, KleinJan, Frioux, Fremy, Wagner, Corre, Le Salver, Leroux, Leblanc, Boyen, Siegel and Dittami. This is an open-access article distributed under the terms of the Creative Commons Attribution License (CC BY). The use, distribution or reproduction in other forums is permitted, provided the original author(s) and the copyright owner(s) are credited and that the original publication in this journal is cited, in accordance with accepted academic practice. No use, distribution or reproduction is permitted which does not comply with these terms.

Annexe IV - Article M2 N°2

Burgunter-Delamare Bertille et al (2020) **Effect of essential oil- and iodine treatments on the bacterial microbiota of the brown alga *Ectocarpus siliculosus***. Journal of Applied Phycology. https://doi.org/10.1007/s10811-020-02286-y

Author's personal copy

Journal of Applied Phycology
https://doi.org/10.1007/s10811-020-02286-y

Effect of essential oil- and iodine treatments on the bacterial microbiota of the brown alga *Ectocarpus siliculosus*

Bertille Burgunter-Delamare[1] · Catherine Boyen[1] · Simon M. Dittami[1]

Received: 26 May 2020 / Revised and accepted: 28 September 2020
© Springer Nature B.V. 2020

Abstract
Macroalgae live in tight association with bacterial communities, which impact most aspects of their biology. Clean, ideally axenic, algal starting material is required to control and study these interactions. Antibiotics are routinely used to generate clean tissue; however, bacterial resistance to antibiotics is increasingly widespread and sometimes related to the emergence of potentially pathogenic, multi-resistant strains. In this study, we explore the suitability of two alternative treatments for use with algal cultures: essential oils (EOs; thyme, oregano and eucalyptus) and povidone-iodine. The impact of these treatments on bacterial communities was assessed by bacterial cell counts, inhibition diameter experiments and 16S-metabarcoding. Our data show that thyme and oregano essential oils (50% solution in DMSO, 15 h incubation) efficiently reduced the bacterial load of algae without introducing compositional biases, but they did not eliminate all bacteria. Povidone-iodine (2% and 5% solution in artificial seawater, 10 min incubation) both reduced and changed the alga-associated bacterial community, similar to the antibiotic treatment. The proposed EO- and povidone-iodine protocols are thus promising alternatives when only a reduction of bacterial abundance is necessary and where the phenomena of antibiotic resistance are likely to arise.

Keywords Antibiotics · Essential oils · Povidone-iodine · Brown algae · Microbiome · Metabarcoding

Introduction

The biology of macroalgae can only be fully understood by taking into account the interactions with their microbiomes which impact their health, performance and resistance to stress (Goecke et al. 2010). Together both components form a singular functional entity, the holobiont (Margulis 1991). Studying holobiont systems implies studying the individual components of the holobiont, their diversity, their activities and the (chemical) interactions between them (Goecke et al. 2010; Wahl et al. 2012; Hollants et al. 2013; Dittami et al. 2020). Elucidating these interactions requires controlled algal-bacterial co-cultivation experiments to test hypotheses about the functions of specific microbes. This, in turn, equally depends on the isolation of bacterial strains and the availability of aposymbiotic algal starting material, i.e. algae without the presence of any symbionts.

Antibiotics are routinely used to generate such aposymbiotic cultures, yet bacterial resistance to antibiotics is increasingly widespread and sometimes related to the emergence of potentially pathogenic, multi-resistant strains (Fair and Tor 2014). Spices and essential oils (EOs) are promising alternatives to antibiotics and have been used as antiseptics since antiquity (McCulloch 1936). However, it was only towards the end of the nineteenth century that Chamberland (1887) first systematically evaluated the antibacterial properties of several EOs. Today, numerous studies assessing the efficiency of EOs against bacteria are available (e.g. Deans and Ritchie 1987; Burt 2004; Bakkali et al. 2008) including one in marine bacteria (Mousavi et al. 2011), but none so far targeting algae-associated microbiomes.

A second alternative to antibiotics may be iodine-based treatments. Berkelman et al. (1982) have shown that diluted solutions of povidone-iodine have antibacterial effects on *Staphylococcus aureus*, *Klebsiella pneumoniae*, *Pseudomonas cepacia* and *Streptococcus mitis*. Furthermore, povidone-iodine may be active against anaerobic or sporulated organisms, moulds, protozoans and viruses (Zamora 1986). Kerrison et al. (2016) have obtained promising results using potassium iodine solutions to

Supplementary Information The online version of this article (https://doi.org/10.1007/s10811-020-02286-y) contains supplementary material, which is available to authorized users.

✉ Bertille Burgunter-Delamare
bertille.burgunter-delamare@sb-roscoff.fr

✉ Simon M. Dittami
simon.dittami@sb-roscoff.fr

[1] Sorbonne Université, CNRS, Integrative Biology of Marine Models (LBI2M) Station Biologique de Roscoff, 29680 Roscoff, France

Published online: 05 November 2020

Author's personal copy

remove parts of the microbiota of red and green algae. However, the effect of povidone-iodine on brown algae and their associated microbiota may be different as some brown algae are known to naturally accumulate high concentrations of iodide in their cell wall. The algae use this iodine for defence reactions (Küpper et al. 2008; La Barre et al. 2010) and brown algae-associated microbes may have developed higher tolerance levels for such treatments.

In this study we examined the suitability of three different EO treatments (thyme, oregano, peppermint eucalyptus) as well as one povidone-iodine treatment to reduce and control the microbiome associated with the filamentous brown alga *Ectocarpus siliculosus*. *Ectocarpus siliculosus* has been established as a genomic model for the brown algal lineage (Cock et al. 2010), but the genus *Ectocarpus* has recently also gained in importance for the study of brown algal-bacterial interactions (Dittami et al. 2016; Tapia et al. 2016; KleinJan et al. 2017; Burgunter-Delamare et al. 2020). Our data show that all tested EOs efficiently reduced the bacterial load of algae without introducing compositional biases, but they did not eliminate all bacteria. Povidone-iodine treatments, just as the antibiotics, both reduced and changed the algae-associated bacterial community.

Materials and methods

Algal cultures

Ectocarpus siliculosus strain Ec32 (CCAP accession 1310/04, isolated from San Juan de Marcona, Peru) was cultivated in 90-mm Petri dishes at 13 °C under a 12 h/12 h day-night cycle and 40 μmol photons $m^{-2}s^{-1}$ irradiance provided by daylight-type fluorescent tubes. The culture medium was composed of autoclaved natural seawater (NSW) enriched with Provasoli nutrients (PES; Provasoli and Carlucci 1974).

Essential oil treatments

We tested the effect of three EOs known for their antibacterial properties on the *E. siliculosus* bacterial microbiome: thyme (*Thymus vulgaris*), oregano (*Origanum vulgare*) and peppermint eucalyptus (*Eucalyptus dives piperitoniferum*) (Nelson 1997; Dorman and Deans 2000; Burt and Reinders 2003; De Billerbeck 2007; Kaloustian et al. 2008; Da Silva 2010; Amrouni et al. 2014). The EOs were purchased from AromaZone (Paris, France) and were rated as 100% pure.

EOs are, however, natural products and, as such, their complex chemical composition is subject to variation. For this reason, the composition of the EOs used in our experiments was determined by GC/MS analyses based on a protocol adapted from Habbadi et al. (2017). Ten μL of each EO was diluted in 990 μL of pure hexane (Supelco Analytical, USA) and 1 μL of the solution was injected in an Agilent GC7890 gas chromatograph (Agilent Technologies, USA) equipped with a DB-5MS capillary column (30 m × 0.25 mm i.d., film thickness 0.25 μm, Agilent Technologies) and coupled to a model 5975C mass selective detector (positive mode). Pure hexane was run as blank. This experiment was carried out in triplicate. The oven temperature was initially maintained at 50 °C and then increased to 300 °C at a rate of 7 °C min^{-1}. The injector temperature was 290 °C. The carrier gas was purified helium, with a flow rate of 1 mL min^{-1}, and the split ratio was 60:1. Mass spectra were obtained in EI mode at 70 eV ionization energy, and the mass range was from m/z 35 to 400. For each compound, the Kovats retention index (RI) was calculated relative to a standard mix of n-alkanes between C7 and C40 (Sigma-Aldrich, USA), which was analysed under identical conditions. Constituents were identified by comparing the RI and MS spectra to those reported in the literature (Adams 2007) and by comparison with the NIST reference database. These analyses were performed at the Corsaire-Metabomer platform at the Station Biologique de Roscoff.

Algal filaments were treated with EOs by EO diffusion on Zobell plates (tryptone 5 g L^{-1}, yeast extract 1 g L^{-1}, sterile seawater 80%, milliQ water 20%, agar 15 g L^{-1}), similar to an antibiogram in two rounds: the first round consisted of testing several dilutions of the separate EOs in DMSO (Sigma-Aldrich, USA) as well as combinations of different EOs. In the second round, we focussed on the most promising treatments, and an assessment of the microbial composition was added. Under a laminar flow hood, sterile filter paper discs (diameter 10 mm, Whatman, GE Healthcare, UK) were soaked with 15 μL of EO solution and then placed in the centre of a 90-mm Zobell plate. We included pure DMSO, NSW and olive oil as controls. *E. siliculosus* filaments were placed at 2 cm of the disc limit, and plates were incubated for 15 h at 13 °C. Next, we briefly incubated the filaments in 25 mL NSW to remove traces of the treatment and left them to recover for 2 weeks in PES medium at 13 °C. All experiments were carried out in triplicate. Treatments were considered lethal when algal filaments entirely lost their pigmentation, and no growth was observed during the recovery period.

Microbial colonization of the algal surface was determined both at the start of the experiment and after the 2-week recovery period. Bacterial cell counts were performed by phase-contrast microscopy (Olympus BX60 microscope, 1.3-PH3 immersion objective, at 1000X magnification). The total number of bacteria was determined over a distance of 100 μm, and five independent counts were averaged per biological replicate.

Povidone-iodine treatments

Povidone-iodine treatments were carried out by immersion of *E. siliculosus* filaments in povidone-iodine solutions as

Author's personal copy

described by Kerrison et al. (2016). Again, a first round of experiments was carried out to determine the most efficient concentrations and incubation times: solutions at 100 mg mL^{-1} (Bétadine dermique 10%, Meda Manufacturing, Mérignac, France) and dilutions at 75, 10, 5, 1.33 and 0.67 mg mL^{-1} were tested with incubation times of 30 s, 1 min, 2 min and 10 min (Berkelman et al. 1982; Kerrison et al. 2016). Each algal filament was placed in a sterile 1.5-mL Eppendorf tube, incubated with 1 mL of iodine solution for the given duration and washed with NSW before leaving the alga to recover for 2 weeks in PES medium. The bacterial abundance on the algal surfaces was examined by microscopy both at the start of the experiment and after recovery, as described above.

The second round of experiments was then carried out focusing on one promising experimental condition (10 min treatment, 1/20 dilution), adding notably an assessment of the microbial community composition.

Antibiotic treatments

We included a standard antibiotic treatment parallel to the EO- and iodine treatments (KleinJan et al. 2017) as a comparison to the new alternative methods. For this treatment, filaments of *E. siliculosus* were incubated in 90-mm Petri dishes with 25 mL of antibiotic solution (penicillin G 45 μg mL^{-1}, streptomycin 22.5 μg mL^{-1}, chloramphenicol 4.5 μg mL^{-1} dissolved in NSW) for 4 days. The algae were left to recover for 3 days in 25 mL of NSW and then re-treated for 4 days with 25 mL of antibiotic solution. This was followed by another recovery period of 2 weeks in PES medium. Bacterial cells on algal surfaces were counted before the experiments and after recovery, as described above.

Determination of inhibition diameters

In addition to examining the treatment effect on bacteria in algal cultures, we determined inhibition diameters as a direct measure of the treatment efficiency. *Ectocarpus siliculosus* filaments cultivated in PES were ground in a mortar with 1 mL of NSW. Fifty μL of the obtained suspension was then plated on Zobell plates. Sterile paper filter discs (10 mm, Whatman) were each soaked with 15 μL of the EO and iodine treatment solutions described above, and one disc was placed in the centre of each inoculated plate. Plates were cultivated for 1 week, which was followed by measurement of inhibition diameter. Results were separated according to two levels of activities for the discs soaked with the EO solutions and povidone-iodine solutions: resistant (ID < 12 mm) or susceptible (ID > 24 mm) (adapted from Ponce et al. 2003). Contrary to classical determinations of inhibition diameters which usually focus on one strain of bacteria, results from these experiments apply to the entire community of bacteria associated with *E. siliculosus* at the time of the experiments.

Impact of treatments on microbial community

We determined the bacterial community composition associated with algal cultures by 16S metabarcoding analyses before selected treatments (50% EO, 1/20 dilution of povidone-iodine for 10 min) as well as after the recovery period. For each sample, about 20 mg of freeze-dried algae was ground (2 × 45 s at 30 Hz) with a TissueLyser II (Qiagen, Germany). DNA was extracted using the DNeasy Plant Mini Kit (Qiagen) following the manufacturer's protocol. A mock community, comprising a mix of DNA from 26 cultivated bacterial strains (Thomas et al. 2019), as well as a negative control, were run and treated in parallel to the DNA extracts. For all of these samples, we amplified the V3 and V4 regions of the 16S rDNA gene following the standard Illumina protocol for metabarcoding (Illumina 2013) and using the Q5 High-Fidelity PCR Kit (New England BioLabs, USA), the AMPure XP for PCR Purification Kit (Beckman Coulter, USA) and the Nextera XT DNA Library Preparation Kit (Illumina, USA). Libraries were quantified with a Qubit High-Sensitivity dsDNA Assay (Life Technologies, USA), and mean fragment size was determined using a Bioanalyzer 2100 system (Agilent Technologies, USA). An equimolar pool of all samples was generated at a concentration of 4 nM, diluted to 5 pM, spiked with 20% PhiX (Illumina) and sequenced on an Illumina MiSeq sequencer on the Genomer platform (Station Biologique de Roscoff) using a MiSeq v3 kit (2x300bp, paired-end).

The obtained reads were cleaned using Trimmomatic version 0.38 (Bolger et al. 2014), assembled using Pandaseq v2.9 (Masella et al. 2012) and then analysed with Mothur 1.40.3 according to the MiSeq standard operating procedures developed by Kozich et al. (2013). Briefly, we aligned the sequences with the Silva_SEED database version 132 and removed non-aligning sequences, chimeric sequences (identified by vsearch), organellar sequences (identified by RDP classifier) and sequences that were represented only once in the dataset (singletons). The remaining sequences were then clustered into operational taxonomic units (OTUs) at a 97% identity level. OTUs that were more abundant in the blank samples compared with all other samples as well as rare OTUs (<5 reads in all samples taken together) were removed from the dataset. Finally, the OTU matrix was sub-sampled to avoid biases in the subsequent analyses.

Statistical tests

We compared bacterial counts and inhibition diameters across conditions using an ANOVA test followed by a Tukey HSD test using the Multcomp package of the R software (version

Author's personal copy

1.0.44) and a p value cutoff of 0.05. The normality of the input data was verified with a Shapiro-Wilk test, but slight deviations from a normal distribution were tolerated (Underwood 1981).

Principal component analyses (PCAs) were carried out on the bacterial sequence abundance data using the DESeq2 package (Love et al. 2014). This package was also used to determine OTUs that differed significantly in relative abundance between treatments allowing for a false discovery rate of 5%. Binomial tests followed by a Benjamini and Hochberg correction (Benjamini and Hochberg 1995) were carried out to determine the overrepresented families among the impacted OTUs.

Results

Essential oil composition

GC-MS analyses of the thyme, oregano and eucalyptus EOs led to the identification of 34 different chemical compounds (Table 1), mainly phenols, monoterpenols and monoterpenes. The EO of *Thymus vulgaris* was mainly composed of thymol (57.44%), γ-terpinene (20.88%), p-cymene (5.41%) and carvacrol (4.64%). The major constituents of *Eucalyptus dives piperitoniferum* EO were piperitone (63.74%), α-phellandrene (12.9%) and terpinen-4-ol (4.45%). The EO of *Origanum vulgare* was mainly composed of carvacrol (78.01%), p-cymene (7.82%), γ-terpinene (4.31%) and thymol (4%). These chemical compositions are consistent with the literature (Gilles et al. 2010; Amrouni et al. 2014; Habbadi et al. 2017).

Antimicrobial effects of EOs and povidone-iodine in cultures

The number of bacteria on the algal surface at the start of the experiments compared with the number of bacteria on the algal surface after the treatments and the 2-week recovery are shown in Table 2. For the EO treatments, the olive oil and DMSO control showed no antibacterial effect. All combinations of different EOs were lethal for the algae at the concentrations tested. The remaining individual EOs exhibited various levels of antimicrobial activity with the 50% solutions being the most efficient. Concordant results were also obtained in the second round of experiments (Table 3), although the effect of eucalyptus was no longer statistically significant. The inhibition experiments with ground cultures revealed that only the thyme and oregano EOs resulted in inhibition diameters (IDs) > 25 mm (Table 4). For the eucalyptus treatments, IDs were below the defined threshold for at least one of the bacteria present in the alga-associated microbiota.

The stock solution of povidone-iodine was lethal for the algae, but the 1/20 and 1/50 diluted solutions, combined with a treatment time of 10 min, proved to be efficient in both experiments (Table 2, Table 3). In the inhibition diameter experiments, only the 75 mg mL^{-1} solution of povidone-iodine resulted in an inhibition diameter > 25 mm (Table 4). For the other treatments, including the antibiotic treatment, inhibition diameters were below the defined threshold for at least one of the bacteria present in the alga-associated microbiota.

In algal cultures, unlike in the inhibition diameter experiments, the efficiency of all EO and povidone-iodine treatments was low compared with that of the treatment with antibiotic-solution, which generally resulted in two- to tenfold lower bacterial loads after recovery (Table 2, Table 3).

Effect of treatments on bacterial community composition

16S metabarcoding analyses were carried out for all control samples as well as for those treated with the 20-fold dilution of povidone-iodine, the 50% EO solutions or the antibiotics. The sequences obtained corresponded predominantly to *Alphaproteobacteria* (59% of reads), followed by *Bacteroidetes* (28.3% of reads), *Gammaproteobacteria* (4.6% of reads) and *Actinobacteria* (2.2% of the reads across all experiments; Fig. 1). A total of 9818 OTUs were identified in the dataset.

For the EO treatments, DESeq2 analyses revealed no significant effect on the microbial community composition as confirmed by the PCA plots (Fig. 2a). For the povidone-iodine treatments, the PCA showed a clear separation of controls kept in NSW and treated samples for the iodine treatment (Fig. 2b). A total of 252 OTUs were found to differ significantly (adjusted $p < 0.05$) in relative abundance between the treated and non-treated samples (69 OTUs decreased and 183 increased in treated samples; Supplementary data Table S1). The taxonomic affiliation of those OTUs is shown in Table 5. Among the OTUs that were negatively impacted by the povidone-iodine treatment and that were significantly overrepresented (adjusted $p < 0.05$) are an unclassified family of *Acidiicrobiia,* an unclassified family of *Microtrichales,* an unclassified family of *Actinobacteria,* as well as the *Saprospiraceae* and *Rhodobacteraceae* families. Among the OTUs that increased in relative abundance in response to the povidone-iodine treatments and that were significantly overrepresented (adjusted $p < 0.05$) are the *Cyclobacteriaceae*, *Hyphomonadaceae*, *Sphingomonadaceae*, *Alteromonadaceaea*, *Halieaceae* and *Pseudohongiellaceae* families.

For the antibiotic treatments, due to their high efficiency, no visible bands were obtained during PCR amplification for metabarcoding. Library preparation was nevertheless carried out, but only 10 reads remained after cleaning. These reads

Author's personal copy

Table 1 Chemical composition of *Origanum vulgaris, Thymus vulgaris,* and *Eucalyptus dives piperitoniferum* essential oils. Compounds that represent more than 1% of the total peak area are indicated in italic. RI = retention index

RI	Compounds	% peak area		
		Origanum vulgare	*Thymus vulgaris*	*Eucalyptus dives piperitoniferum*
927	*α-thujene*	0.22	_	1.28
935	α-pinene	0.59	0.16	_
952	Camphene	0.11	0.26	_
980	β-pinene	0.18	_	_
989	β-myrcene	0.50	0.16	0.55
1008	*α-phellandrene*	_	_	12.90
1019	α-terpinene	0.51	0.24	0.84
1026	*p-cymene*	7.82	5.41	4.05
1033	*β-phellandrene*	_	_	1.76
1035	Eucalyptol	0.06	0.80	_
1046	3-carene	_	_	0.25
1060	*γ-terpinene*	4.31	20.88	0.60
1087	*Terpinolene*	_	_	1.73
1100	*Linalool*	1.29	1.53	0.58
1127	Menth-2-en-l-ol < cis-p->	_	_	0.22
1139	Trans-verbenol	0.23	_	_
1151	*Camphor*	_	1.43	_
1176	*Borneol*	_	1.41	_
1184	*Terpinen-4-ol*	_	0.67	4.45
1186	Thujone	_	_	0.28
1197	*α-terpineol*	_	0.24	1.12
1239	Thymol methyl ether	_	0.39	_
1257	*Piperitone*	_	_	63.74
1291	*Thymol*	4.00	57.44	_
1300	*Carvacrol*	78.01	4.64	_
1372	4,6-di-tert-butylresorcinol	_	0.18	_
1427	*β-caryophyllene*	1.61	2.11	0.77
1467	Naphthalene	_	0.36	0.46
1497	Viridiflorene	_	_	0.74
1502	*Elixene*	_	_	2.87
1591	*Caryophyllene oxide*	0.50	1.45	_

were associated with the class of *Alphaproteobacteria*, notably the *Rhizobiaceae* and *Rhodobacteraceae* families and the *Marinobacter* genus.

Discussion

Antibiotic treatments are commonly used to obtain clean algal cultures, yet bacterial resistance to antibiotics is increasingly widespread. Sometimes it is related to the emergence of pathogenic, multi-resistant bacterial strains. Thus, especially after long treatments, resistant strains may proliferate without control from the remaining microbiome, sometimes by far exceeding bacterial concentrations found in a healthy microbiome (personal data). Ethanol has been proposed as one alternative treatment to clean kelp species, e.g. in *Ecklonia radiata*, where a short bath in a 70% ethanol solution followed by sterile deionized water showed promising results (Lawlor et al. 1991). In much the same way, the surfaces of the wrack *Fucus serratus* and the red alga *Palmaria palmata* surfaces can be cleaned efficiently with a mixture of ethanol (40–50%) and sodium hypochlorite (1%) (Kientz et al. 2011). Unfortunately, such surface sterilization methods are not suitable for small filamentous algae such as *Ectocarpus*. When *Ectocarpus* filaments come in to contact with 70% ethanol or bleach, even for less than a second, this results in immediate loss of pigmentation

Author's personal copy

Table 2 Ratio after treatment/before treatment of the number of bacteria on the algal surface. (± standard deviation, $n = 3$). NSW: natural sea water, ATB: antibiotics, _: not tested, +++: bacterial proliferation. *: Significant results in comparison with the control ($p\ value < 0.05$)

		Stock solution	Dilution 3/4	Dilution 1/2	Dilution 1/10	Dilution 1/20	Dilution 1/50	Dilution 1/100	NSW
Essential oil	DMSO	1.12 ± 0.28	_	_	_	_	_	_	_
	Olive oil	+++	_	+++	+++	_	_	_	_
	Eucalyptus	0.38 ± 0.15 *	_	0.30 ± 0.12 *	_	_	3.41	_	_
	Oregano	0.49 ± 0.10 *	_	0.35 ± 0.10 *	_	_	0.79 ± 0.24	_	_
	Thyme	1.10 ± 0.17	_	0.35 ± 0.12 *	_	_	0.44 ± 0.29 *	_	_
	Thyme + oregano	algal death	_	algal death	algal death	_	_	_	_
	Thyme + eucalyptus	algal death	_	algal death	algal death	_	_	_	_
	Eucalyptus + oregano	algal death	_	algal death	algal death	_	_	_	_
	Eucalyptus + oregano + thyme	algal death	_	algal death	algal death	_	_	_	_
Antibiotics	NSW	_	_	_	_	_	_	_	0.60 ± 0.22
	ATB	0.06 ± 0.05 *	_	_	_	_	_	_	_
Iodine	NSW	_	_	_	_	_	_	_	0.60 ± 0.22
	30 s	dead	0.55 ± 0.06	_	_	_	0.33 ± 0.01 *	0.62 ± 0.15	0.54 ± 0.14
	1 min	dead	0.46 ± 0.02 *	_	_	_	0.43 ± 0.11 *	0.87 ± 0.02	1.35 ± 0.21
	2 min	dead	0.89 ± 0.09	_	_	_	0.29 ± 0.16 *	1.01 ± 0.03	17.27 ± 0.12
	10 min	_	_	_	0.51 ± 0.11	0.34 ± 0.15 *	0.17 ± 0.08 *	_	0.86 ± 0.08

and cell death. Therefore, we sought to test two other alternative treatments, EOs and povidone-iodine, to reduce the microbiota associated with the brown alga *E. siliculosus* and compared the results with the standard antibiotic treatment routinely used in our laboratory. Moreover, unlike in previous studies that focused exclusively on the direct impact of treatments on the number of bacteria on algal surfaces, our study also examined the taxonomic composition of the microbiome after recovery.

Table 3 Average number of bacteria after the treatments and 2 weeks of recovery. (± standard deviation, $n = 3$). *: Significant results compared to controls (DMSO/NSW). NSW: natural sea water

Treatment	Average number of bacteria	
Essential Oils	Before treatment	83.7 ± 9.2
	Thyme 50%	29.2 ± 10.1 *
	Eucalyptus 50%	46.1 ± 17.8
	Oregano 50%	39.5 ± 5 *
	NSW	66.7 ± 30.7
	DMSO	284.9 ± 15.4
Iodine	Before treatment	70.6 ± 11.1
	3/4 dilution	dead
	1/10 dilution	35.7 ± 7.5
	1/20 dilution	23.9 ± 10.5 *
	1/50 dilution	11.7 ± 5.8 *
	NSW	60.6 ± 6
Antibiotics	Before treatment	61.3 ± 30.3
	After treatment	3.8 ± 3.2 *
	NSW	36.5 ± 3.2

Table 4 Inhibition zone diameter of the different treatments. (± standard deviation, $n = 3$). *: Sensitive diameters. NSW: natural sea water

Treatment		Inhibition Diameter (mm)
Control	NSW	No inhibition
	DMSO	No inhibition
Essential Oils	Thyme 50%	41.3 ± 4.6 *
	Eucalyptus 50%	18 ± 6.1
	Oregano 50%	44.7 ± 9.2 *
Iodine	3/4 dilution	22.5 ± 4.7 *
	1/10 dilution	14.8 ± 3.1
	1/20 dilution	12.3 ± 3.1
	1/50 dilution	No inhibition
Antibiotics		No inhibition

Author's personal copy

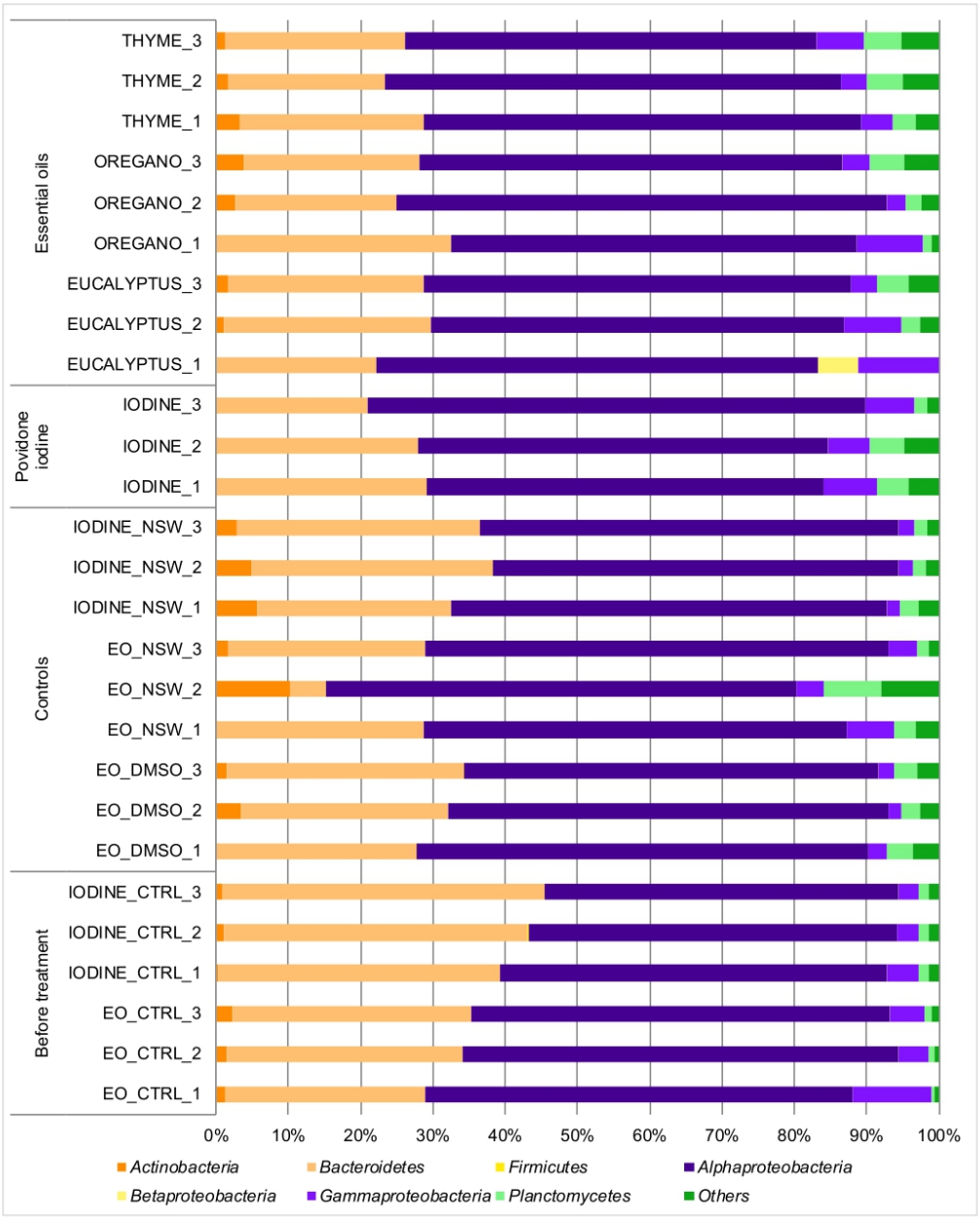

Fig. 1 Distribution of bacterial OTUs per phylum in the different samples and experiments

Author's personal copy

Table 5 Taxonomic affiliations of the OTUs impacted by the iodine treatment, compared with their occurrence in the entire iodine dataset

Taxa	OTUs decreased by iodine treatment			OTUs increased by iodine treatment			Entire dataset	
	Number of impacted OTUs	ratio	*p value*	Number of impacted OTUs	ratio	*p value*	Number of OTUs	ratio
Acidimicrobiia_unclassified	3	0.04348	0.00003 ***	0	0.00000	0.36363	13	0.00247
Microtrichales_unclassified	2	0.02899	0.00001 ***	0	0.00000	0.09896	3	0.00057
Actinobacteria_unclassified	5	0.07246	0.00001 ***	0	0.00000	0.69409	34	0.00645
Bacteria_unclassified	3	0.04348	0.98989	17	0.09290	0.95748	728	0.13814
Bacteroidetes_unclassified	0	0.00000	0.18926	1	0.00546	0.10729	16	0.00304
Bacteroidia_unclassified	11	0.15942	0.00813 *	27	0.14754	0.00070 ***	421	0.07989
Saprospiraceae	6	0.08696	< 0.00001 ***	0	0.00000	0.81904	49	0.00930
Cyclobacteriaceae	0	0.00000	0.50868	20	0.10929	< 0.00001 ***	54	0.01025
Cytophagales_unclassified	0	0.00000	0.18926	2	0.01093	0.01876	16	0.00304
Flavobacteriaceae	5	0.07246	*0.13318*	4	0.02186	0.95541	265	0.05028
Flavobacteriales_unclassified	0	0.00000	0.62309	1	0.00546	0.72888	74	0.01404
Oxyphotobacteria_unclassified	1	0.01449	0.09288	3	0.01639	0.04805	39	0.00740
Pirellulaceae	0	0.00000	0.73690	1	0.00546	0.86741	101	0.01917
Alphaproteobacteria_unclassified	10	0.14493	0.97775	30	0.16393	0.99743	1334	0.25313
Hyphomonadaceae	0	0.00000	0.58088	14	0.07650	< 0.00001 ***	66	0.01252
Rhizobiaceae	3	0.04348	*0.71437*	11	0.06011	0.62325	366	0.06945
Rhodobacteraceae	13	0.18841	0.00039 ***	4	0.02186	0.99767	383	0.07268
Sphingomonadaceae	7	0.08696	0.08099	24	0.13661	0.00041 ***	345	0.06546
Alteromonadaceae	0	0.00000	0.35172	9	0.04918	< 0.00001 ***	33	0.00626
Marinobacteraceae	0	0.00000	0.36020	1	0.00546	0.33058	34	0.00645
Halieaceae	0	0.00000	0.68711	11	0.06011	0.00007 ***	88	0.01670
Pseudohongiellaceae	0	0.00000	0.01301 *	1	0.00546	0.00059 ***	2	0.00038
Proteobacteria_unclassified	0	0.00000	0.86364	2	0.01093	0.89527	150	0.02846
TOTAL	**69**			**183**			**5270**	

* indicates significant *p* values after Benjamini-Hochberg correction (* $p < 0.05$, ** $p < 0.01$, *** $p < 0.001$)

Essential oils inhibit the growth of the complete spectrum of *Ectocarpus*-associated bacteria

Our data show that the tested EO treatments significantly reduce the number of bacteria associated with *E. siliculosus* even after 2 weeks of recovery. This is in line with data published by Mousavi et al. (2011), who observed a strong impact of a combination of four EOs on several bacterial isolates, both marine and terrestrial. A key point that has not been previously demonstrated is that this reduction occurred

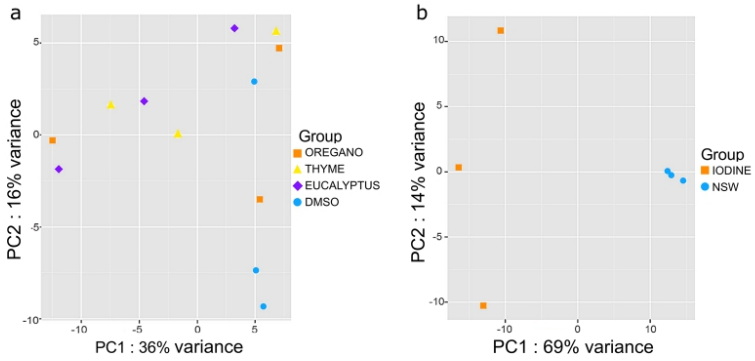

Fig. 2 PCA plot of microbiome composition 2 weeks after the different treatments (a) Essential oils treatment. **(b)** Povidone-iodine treatment. NSW: natural sea water

Author's personal copy

without significant change in the relative bacterial community composition. Indeed, EOs contain several molecules such as p-cymene, β-phellandrene, terpinolene, terpinen-4-ol, piperitone, carvacrol and thymol, which have been shown to have an antibacterial effect on a wide range of bacteria (Lambert et al. 2001; Carson et al. 2002, 2006; Eftekhar et al. 2005; Bakkali et al. 2008; Mora et al. 2011; Marchese et al. 2016, 2017). The fact that thyme and oregano were more efficient than eucalyptus in our experiments could be due to their higher concentration of linalool. This compound has been shown to have a synergic effect when combined with thymol and carvacrol molecules (the principal components of thyme and oregano EOs) (Bassolé et al. 2010; Herman et al. 2016). Both thymol and carvacrol target the bacterial cell membrane. Carvacrol changes membrane permeability for essential cations like H^+ and K^+, leading to leakage and cell death (Ultee et al. 1999), and thymol inserts itself in the lipid membrane, changing its morphology and disrupting the surface elasticity (Ferreira et al. 2016).

Furthermore, EOs contain several other potentially antimicrobial molecules. Due to this complex composition, the overall antibacterial activity of EOs is likely caused by a broad spectrum of mechanisms of action (Burt 2004; Bakkali et al. 2008), contrary to antibiotics. For this reason, it is expected that bacteria might rarely develop resistance mechanism for EOs. On the downside, host tolerance of high concentrations of EOs may also be limited, as illustrated by the lethal effect on algal hosts observed for the EO mixtures described herein.

Povidone-iodine treatments induce microbial community shifts

Povidone-iodine at low concentrations was also an efficient inhibitor of overall bacterial growth. The active compound in povidone-iodine is 'free' iodine (McDonnell and Russell 1999). Povidone-iodine is an iodophor, a complex of iodine and a solubilizing carrier (poly-vinyl-pyrrolidone, PVP), which acts as a reservoir of free iodine. The free iodine levels are dependent on the concentration of the povidone-iodine solution. The content of non-complexed free iodine increases as the dilution increases, reaching a maximum value at about 0.1% final concentration (i.e. a 1/100 dilution), but then decreases again with further dilution (Rackur 1985). The PVP component increases the antimicrobial efficiency of iodine by delivering the iodine directly to the bacterial cell surface as a result of its affinity to cell membranes (Zamora 1986).

Bacterial resistance to povidone-iodine is rare in a medical context (Houang et al. 1976), probably because its principle of action, the rapid oxidation of amino acids and nucleic acids in biological structures (Kanagalingam et al. 2015) are hard to counteract. However, iodine is also known to accumulate naturally in brown algae, which emit volatile short-lived organoiodines and molecular iodine as part of their molecular defence repertoire (Leblanc et al. 2006; Küpper et al. 2008). It is therefore likely that microbes in long-lasting associations with brown algae have at least a basic level of resistance against iodine-based defences. In fact, some marine bacteria associated with algae even have their own iodine metabolism or iodine uptake mechanisms (Amachi et al. 2007; Fournier et al. 2014; Barbeyron et al. 2016). For instance, *Zobellia galactanivorans* (*Flavobacteria*) efficiently degrades brown algal cell walls and has been suggested to cope with reactive oxygen species and the massive amounts of liberated iodine via the activity of a vanadium-dependent iodoperoxidase (Fournier et al. 2014; Barbeyron et al. 2016). The presence of such iodine-specialized marine bacteria may explain why, unlike EOs, iodine treatments resulted in a specific shift in microbial community composition after application.

Among the 69 OTUs significantly reduced by the povidone-iodine treatment, several belonged to the *Actinobacteria*, which are known to be affected by this molecule (Lachapelle et al. 2013). Furthermore, *Actinobacteria*, *Chitininophagales* and *Rhodobacteraceae* were found only among the negatively impacted OTUs. On the other hand, *Cytophagales*, *Hyphomonadaceae*, *Alteromonadaceae*, *Halieaceae* and *Oceanospirillales* comprised many OTUs that increased in relative abundance in response to the povidone-iodine treatments. An increase in relative abundance does not necessarily indicate an increase in absolute abundance as global bacterial cell counts decreased in response to the treatments; however, these taxa are likely to have more widespread resistance mechanisms to iodine and may benefit from the creation of a new niche as other bacteria in the community decline. A key question for the future is to understand how these bacteria tolerate iodine and if this tolerance correlates in any way with the iodine metabolism of the algal host.

Conclusion and outlook

While antibiotic treatments are currently the most efficient way of eliminating algal-associated microbiota and cannot be replaced by any of the tested alternative treatments in the near future both EOs and povidone-iodine offer promising alternatives when only a reduction of bacterial abundance is sought and where the phenomena of antibiotic resistance are likely to become an issue. Notably, this is the case in aquaculture, and the use of antibiotics may disrupt the equilibrium between bacteria and lead to the proliferation of resistant bacterial strains, including opportunistic pathogens (Watts et al. 2017). In seaweed aquaculture, the notion of controlling or manipulating the microbiome is not yet widespread, but it is known that microbiota impact algal fitness (Goecke et al. 2010; Wahl et al. 2012) and even the chemical properties of the algae (Burgunter-Delamare et al. 2020). In the hatchery

Author's personal copy

(closed) stages of seaweed aquaculture, both EOs and iodine treatments could potentially be used as one way of modifying the microbiome, possibly in combination with probiotics (Suvega and Arunkumar 2019). The protocols proposed here may prove useful in this context as they are more likely to be tolerated—even by small and filamentous algae. Moreover, knowledge on the compositional biases introduced by the treatments may help orient potential users towards either one of the proposed treatments depending on their aims.

Acknowledgements We thank the ABIMS platform (Station Biologique de Roscoff) and in particular Erwan Corre for support for the metabarcoding analysis; Gwenn Tanguy and Erwan Legeay from the GENOMER platform (FR2424, Station Biologique de Roscoff) for access to sequencing equipment and help during the Library preparation; Cédric Leroux and Jean Girard from the CORSAIRE-METABOMER platform (Station Biologique de Roscoff) for access to the GC/MS equipment and support; and Catherine Leblanc and Elisabeth Ficko-Blean for critical reading of the manuscript and proofreading.

Authors' contributions Designed study: BBD, SD; performed experiments: BBD; analysed data: BBD, SD; Wrote the manuscript: BBD, SD; Provided valuable input and corrected the manuscript: CB.

Funding This work was funded partially by ANR project IDEALG (ANR-10-BTBR-04) "Investissements d'Avenir, Biotechnologies-Bioressources" and CNRS momentum call (2017). BBD was funded by a joint Ph.D. scholarship from the Brittany region (Project HOSALA) and the Sorbonne University (ED227).

Data availability Raw sequence data were deposited at the European Nucleotide Archive under project accession number ENA: PRJEB37511.

Compliance with ethical standards

Competing interests The authors declare that they have no competing interests.

References

Adams RP (2007) Identification of essential oil components by gas chromatography/mass spectrometry, 4th edn. Allured Business Media, Carol Stream

Amachi S, Kimura K, Muramatsu Y, Shinoyama H, Fujii T (2007) Hydrogen peroxide-dependent uptake of iodine by marine *Flavobacteriaceae* bacterium strain C-21. Appl Environ Microbiol 73:7536–7541

Amrouni S, Touati M, Hadef Y, Djahoudi A (2014) Effet de l'huile essentielle d'*Origanum vulgare* et de *Thymus ciliatus* sur *Pseudomonas aeruginosa* VIM-2 carbapénèmase. Phytothérapie 12:309–313

Bakkali F, Averbeck S, Averbeck D, Idaomar M (2008) Biological effects of essential oils – a review. Food Chem Toxicol 46:446–475

Barbeyron T, Thomas F, Barbe V, Teeling H, Schenowitz C, Dossat C, Goesmann A, Leblanc C, Oliver Glöckner F, Czjzek M, Amann R, Michel G (2016) Habitat and taxon as driving forces of carbohydrate catabolism in marine heterotrophic bacteria: example of the model algae-associated bacterium *Zobellia galactanivorans* Dsij ^{T}. Environ Microbiol 18:4610–4627

Bassolé IH, Lamien-Meda A, Bayala B, Tirogo S, Franz C, Novak J, Nebié RC, Dicko MH (2010) Composition and antimicrobial activities of *Lippia multiflora* Moldenke, *Mentha* x *piperita* L and *Ocimum basilicum* L essential oils and their major monoterpene alcohols alone and in combination. Molecules 15:7825–7839

Benjamini Y, Hochberg Y (1995) Controlling the false discovery rate: a practical and powerful approach to multiple testing. J R Stat Soc Ser B 57:289–300

Berkelman RL, Holland BW, Anderson RL (1982) Increased bactericidal activity of dilute preparations of povidone-iodine solutions. J Clin Microbiol 15:635–639

Bolger AM, Lohse M, Usadel B (2014) Trimmomatic: a flexible trimmer for Illumina sequence data. Bioinformatics 30:2114–2120

Burgunter-Delamare B, KleinJan H, Frioux C, Fremy E, Wagner M, Corre E, Le Salver A, Leroux C, Leblanc C, Boyen C, Siegel A, Dittami SM (2020) Metabolic complementarity between a brown alga and associated cultivable bacteria provide indications of beneficial interactions. Front Mar Sci 7:85

Burt S (2004) Essential oils: their antibacterial properties and potential applications in foods—a review. Int J Food Microbiol 94:223–253

Burt SA, Reinders RD (2003) Antibacterial activity of selected plant essential oils against *Escherichia coli* O157: H7. Lett Appl Microbiol 36:162–167

Carson CF, Mee BJ, Riley TV (2002) Mechanism of action of *Melaleuca alternifolia* (tea tree) oil on *Staphylococcus aureus* determined by time-kill, lysis, leakage, and salt tolerance assays and electron microscopy. Antimicrob Agents Chemother 46:1914–1920

Carson CF, Hammer KA, Riley TV (2006) *Melaleuca alternifolia* (tea tree) oil: a review of antimicrobial and other medicinal properties. Clin Microbiol Rev 19:50–62

Chamberland M (1887) Les essences au point de vue de leurs propriétés antiseptiques. Ann Inst Pasteur 1:153–164

Cock JM, Sterck L, Rouzé P, Scornet D, Allen AE, Amoutzias G, Anthouard V, Artiguenave F, Aury JM, Badger JH, Beszteri B, Billiau K, Bonnet E, Bothwell JH, Bowler C, Boyen C, Brownlee C, Carrano CJ, Charrier B, Cho GY, Coelho SM, Collén J, Corre E, da Silva C, Delage L, Delaroque N, Dittami SM, Doulbeau S, Elias M, Farnham G, Gachon CMM, Gschloessl B, Heesch S, Jabbari K, Jubin C, Kawai H, Kimura K, Kloareg B, Küpper FC, Lang D, le Bail A, Leblanc C, Lerouge P, Lohr M, Lopez PJ, Martens C, Maumus F, Michel G, Miranda-Saavedra D, Morales J, Moreau H, Motomura T, Nagasato C, Napoli CA, Nelson DR, Nyvall-Collén P, Peters AF, Pommier C, Potin P, Poulain J, Quesneville H, Read B, Rensing SA, Ritter A, Rousvoal S, Samanta M, Samson G, Schroeder DC, Ségurens B, Strittmatter M, Tonon T, Tregear JW, Valentin K, von Dassow P, Yamagishi T, van de Peer Y, Wincker P (2010) The *Ectocarpus* genome and the independent evolution of multicellularity in brown algae. Nature 465:617–621

Da Silva F (2010) Utilisation des huiles essentielles en infectiologie ORL. Thèse pour le Diplôme d'État de Docteur en Pharmacie. Universite Henri Poincaré-Nancy 1, France. 150p

De Billerbeck V-G (2007) Huiles essentielles et bactéries résistantes aux antibiotiques. Phytothérapie 5:249–253

Deans SG, Ritchie G (1987) Antibacterial properties of plant essential oils. Int J Food Microbiol 5:165–180

Dittami SM, Duboscq-Bidot L, Perennou M, Gobet A, Corre E, Boyen C, Tonon T (2016) Host-microbe interactions as a driver of acclimation to salinity gradients in brown algal cultures. ISME J 10:51–63

Dittami SM, Arboleda E, Auguet J-C et al (2020) A community perspective on the concept of marine holobionts: current status, challenges, and future directions. https://doi.org/10.5281/ZENODO.3696771

Dorman HJD, Deans SG (2000) Antimicrobial agents from plants: antibacterial activity of plant volatile oils. J Appl Microbiol 88:308–316

Eftekhar F, Yousefzadi M, Azizian D, Sonboli A, Salehi P (2005) Essential oil composition and antimicrobial activity of *Diplotaenia damavandica*. Z Naturforsch C 60:821–825

Author's personal copy

Fair RJ, Tor Y (2014) Antibiotics and bacterial resistance in the 21st century. Perspect Med Chem 6:25–64

Ferreira JVN, Capello TM, Siqueira LJA, Lago JHG, Caseli L (2016) Mechanism of action of thymol on cell membranes investigated through lipid Langmuir monolayers at the air water interface and molecular simulation. Langmuir 32:3234–3241

Fournier J-B, Rebuffet E, Delage L, Grijol R, Meslet-Cladière L, Rzonca J, Potin P, Michel G, Czjzek M, Leblanc C (2014) The vanadium iodoperoxidase from the marine *Flavobacteriaceae* species *Zobellia galactanivorans* reveals novel molecular and evolutionary features of halide specificity in the vanadium haloperoxidase enzyme family. Appl Environ Microbiol 80:7561–7573

Gilles M, Zhao J, An M, Agboola S (2010) Chemical composition and antimicrobial properties of essential oils of three Australian *Eucalyptus* species. Food Chem 119:731–737

Goecke F, Labes A, Wiese J, Imhoff J (2010) Chemical interactions between marine macroalgae and bacteria. Mar Ecol Prog Ser 409: 267–299

Habbadi K, Meyer T, Vial L, Gaillard V, Benkirane R, Benbouazza A, Kerzaon I, Achbani EH, Lavire C (2017) Essential oils of *Origanum compactum* and *Thymus vulgaris* exert a protective effect against the phytopathogen *Allorhizobium vitis*. Environ Sci Pollut Res 25: 29943–29952

Herman A, Tambor K, Herman A (2016) Linalool affects the antimicrobial efficacy of essential oils. Curr Microbiol 72:165–172

Hollants J, Leliaert F, De Clerck O, Willems A (2013) What we can learn from sushi: a review on seaweed–bacterial associations. FEMS Microbiol Ecol 83:1–16

Houang ET, Gilmore OJ, Reid C, Shaw EJ (1976) Absence of bacterial resistance to povidone iodine. J Clin Pathol 29:752–755

Illumina (2013) 16S Metagenomic sequencing library preparation. Prep 16S Ribosomal RNA Gene Amplicons Illumina MiSeq Syst 1–28

Kaloustian J, Chevalier J, Mikail C, Martino M, Abou L, Vergnes M-F (2008) Étude de six huiles essentielles : composition chimique et activité antibactérienne. Phytothérapie 6:160–164

Kanagalingam J, Feliciano R, Hah JH, Labib H, Le TA, Lin J-C (2015) Practical use of povidone-iodine antiseptic in the maintenance of oral health and in the prevention and treatment of common oropharyngeal infections. Int J Clin Pract 69:1247–1256

Kerrison PD, Le HN, Twigg GC, Smallman DR, MacPhee R, Houston FAB, Hughes AD (2016) Decontamination treatments to eliminate problem biota from macroalgal tank cultures of *Osmundea pinnatifida, Palmaria palmata* and *Ulva lactuca*. J Appl Phycol 28:3423–3434

Kientz B, Thabard M, Cragg SM, Pope J, Hellio C (2011) A new method for removing microflora from macroalgal surfaces: an important step for natural product discovery. Bot Mar 54:457–469

KleinJan H, Jeanthon C, Boyen C, Dittami SM (2017) Exploring the cultivable *Ectocarpus* microbiome. Front Microbiol 8:2456

Kozich JJ, Westcott SL, Baxter NT, Highlander SK, Schloss PD (2013) Development of a dual-index sequencing strategy and curation pipeline for analyzing amplicon sequence data on the MiSeq Illumina sequencing platform. Appl Environ Microbiol 79:5112–5120

Küpper FC, Carpenter LJ, McFiggans GB, Palmer CJ, Waite TJ, Boneberg E-M, Woitsch S, Weiller M, Abela R, Grolimund D, Potin P, Butler A, Luther GW, Kroneck PMH, Meyer-Klaucke W, Feiters MCI (2008) Iodide accumulation provides kelp with an inorganic antioxidant impacting atmospheric chemistry. Proc Natl Acad Sci 105:6954–6958

La Barre S, Potin P, Leblanc C, Delage L (2010) The halogenated metabolism of brown algae (Phaeophyta), its biological importance and its environmental significance. Mar Drugs 8:988–1010

Lachapelle J-M, Castel O, Casado AF, Leroy B, Micali G, Tennstedt D, lambert J (2013) Antiseptics in the era of bacterial resistance: a focus on povidone iodine. Clin Pract 10:579–592.

Lambert RJW, Skandamis PN, Coote PJ, Nychas G-J (2001) A study of the minimum inhibitory concentration and mode of action of oregano essential oil, thymol and carvacrol. J Appl Microbiol 91:453–462

Lawlor HJ, Borowitzka MA, McComb JA (1991) A rapid and inexpensive method for surface sterilisation of *Ecklonia radiata* (Phaeophyta) for tissue culture. Bot Mar 34:261–264

Leblanc C, Colin C, Cosse A, Delage L, La Barre S, Morin P, Fiévet B, Voiseux C, Ambroise Y, Verhaeghe E, Amouroux D, Donard O, Tessier E, Potin P (2006) Iodine transfers in the coastal marine environment: the key role of brown algae and of their vanadium-dependent haloperoxidases. Biochimie 88:1773–1785

Love MI, Huber W, Anders S (2014) Moderated estimation of fold change and dispersion for RNA-seq data with DESeq2. Genome Biol 15:550

Marchese A, Orhan IE, Daglia M, Barbieri R, Di Lorenzo A, Nabavi SF, Gortzi O, Izadi M, Nabavi SM (2016) Antibacterial and antifungal activities of thymol: a brief review of the literature. Food Chem 210: 402–414

Marchese A, Arciola CR, Barbieri R, Silva AS, Nabavi SF, Tsetegho Sokeng AJ, Izadi M, Jafari NJ, Suntar I, Daglia M, Nabavi SM (2017) Update on monoterpenes as antimicrobial agents: a particular focus on p-cymene. Materials 10:947

Margulis L (1991) Symbiogenesis and symbionticism. In: Fester R (ed) Symbiosis as a source of evolutionary innovation. MIT Press, Cambridge, Mass, pp 1–14

Masella AP, Bartram AK, Truszkowski JM, Brown DG, neufeld JD (2012) PANDAseq: paired-end assembler for illumina sequences. BMC Bioinformatics 13:31.

McCulloch EC (1936) Sterilization and disinfection. Lea&Febiger, Philadelphia

McDonnell G, Russell AD (1999) Antiseptics and disinfectants: activity, action, and resistance. Clin Microbiol Rev 12:147–179

Mora FD, Ríos N, Rojas LB, Diaz T, Velasco J, Juan CA, Silva B (2011) Chemical composition and *in vitro* antibacterial activity of the essential oil of *Phthirusa adunca* from Venezuelan Andes. Nat Prod Commun 6:1051–1053

Mousavi SM, Wilson G, Raftos D, Mirzargar SS, Omidbaigi R (2011) Antibacterial activities of a new combination of essential oils against marine bacteria. Aquac Int 19:205–214

Nelson R (1997) In-vitro activities of five plant essential oils against methicillin-resistant *Staphylococcus aureus* and vancomycin-resistant *Enterococcus faecium*. J Antimicrob Chemother 40:305–306

Ponce AG, Fritz R, del Valle C, Roura SI (2003) Antimicrobial activity of essential oils on the native microflora of organic Swiss chard. LWT Food Sci Technol 36:679–684

Provasoli L, Carlucci AF (1974) Vitamins and growth regulators. In: Stewart WDP (ed) Algal physiology and biochemistry. Blackwell, Oxford, pp 741–787

Rackur H (1985) New aspects of mechanism of action of povidone-iodine. J Hosp Infect 6:13–23

Suvega T, Arunkumar K (2019) Probiotic bacteria promote the growth of associating host (red seaweed, *Gracilaria edulis*) also synthesize antibacterial protein. Biocatal Agric Biotechnol 19:101136

Tapia JE, González B, Goulitquer S, Potin P, Correa JA (2016) Microbiota influences morphology and reproduction of the brown alga *Ectocarpus* sp. Front Microbiol 7:197

Thomas F, Dittami SM, Brunet M, Le Duff N, Tanguy G, Leblnc C, Gobet A (2019) Evaluation of a new primer combination to minimize plastid contamination in 16S rDNA metabarcoding analyses of alga-associated bacterial communities. Environ Microbiol Rep 1758-2229:12806–12837

Ultee A, Kets EPW, Smid EJ (1999) Mechanisms of action of carvacrol on the food-borne pathogen *Bacillus cereus*. Appl Environ Microbiol 65:4606–4610

Author's personal copy

Underwood AJ (1981) Techniques of analysis of variance in experimental marine biology and ecology. Annu Rev Oceanogr Mar Biol 19: 513–605

Wahl M, Goecke F, Labes A, Dobretsov S, Weinberger F (2012) The second skin: ecological role of epibiotic biofilms on marine organisms. Front Microbiol 3:292

Watts JEM, Schreier HJ, Lanska L, Hale MS (2017) The rising tide of antimicrobial resistance in aquaculture: sources, sinks and solutions. Mar Drugs 15:158

Zamora JL (1986) Chemical and microbiologic characteristics and toxicity of povidone-iodine solutions. Am J Surg 151:400–406

Publisher's note Springer Nature remains neutral with regard to jurisdictional claims in published maps and institutional affiliations.

Annexe V - Article *Ectocarpus* Australie

Dittami, S. M., Peters, A. F., West, J. A., Cariou, T., KleinJan, H., Burgunter-Delamare, B., et al. (2020). Revisiting Australian Ectocarpus subulatus (Phaeophyceae) **From the Hopkins River: Distribution, Abiotic Environment, and Associated Microbiota**. J. Phycol. 56, 821579. doi:10.1111/jpy.12970.

J. Phycol. **56,** 719–729 (2020)
© 2020 Phycological Society of America
DOI: 10.1111/jpy.12970

REVISITING AUSTRALIAN *ECTOCARPUS SUBULATUS* (PHAEOPHYCEAE) FROM THE HOPKINS RIVER: DISTRIBUTION, ABIOTIC ENVIRONMENT, AND ASSOCIATED MICROBIOTA[1]

Simon M. Dittami[4]

CNRS, Integrative Biology of Marine Models (LBI2M), Station Biologique de Roscoff, Sorbonne Université, 29680 Roscoff, France

Akira F. Peters

Bezhin Rosko, 40 Rue des Pêcheurs, 29250 Santec, France

John A. West

Biosciences 2, University of Melbourne, Parkville, VIC 3010, Australia

Thierry Cariou

CNRS, FR2424, Station Biologique de Roscoff, Sorbonne Université, 29680 Roscoff, France

Hetty KleinJan[2]*, Bertille Burgunter-Delamare, Aurélie Prechoux*[3]

CNRS, Integrative Biology of Marine Models (LBI2M), Station Biologique de Roscoff, Sorbonne Université, 29680 Roscoff, France

Suhelen Egan

Centre for Marine Science and Innovation, School of Biological, Earth and Environmental Sciences, University of New South Wales, Sydney, NSW, Australia

and Catherine Boyen

CNRS, Integrative Biology of Marine Models (LBI2M), Station Biologique de Roscoff, Sorbonne Université, 29680 Roscoff, France

In 1995 a strain of *Ectocarpus* was isolated from Hopkins River Falls, Victoria, Australia, constituting one of few available freshwater or nearly freshwater brown algae, and the only one belonging to the genus *Ectocarpus*. It has since been used as a model to study acclimation and adaptation to low salinities and the role of its microbiota in these processes. To provide more background information on this model, we assessed if *Ectocarpus* was still present in the Hopkins river 22 years after the original finding, estimated its present distribution, described its abiotic environment, and determined its in situ microbial composition. We sampled for *Ectocarpus* at 15 sites along the Hopkins River as well as 10 neighboring sites and found individuals with ITS and *cox*1 sequences identical to the original isolate at three sites upstream of Hopkins River Falls. The salinity of the water at these sites ranged from 3.1 to 6.9, and it was rich in sulfate (1–5 mM). The diversity of bacteria associated with the algae in situ (1312 operational taxonomic units) was one order of magnitude higher than in previous studies of the original laboratory culture, and 95 alga-associated bacterial strains were isolated from algal filaments on site. In particular, species of *Planctomycetes* were abundant in situ but rare in laboratory cultures. Our results confirmed that *Ectocarpus* was still present in the Hopkins River, and the newly isolated algal and bacterial strains offer new possibilities to study the adaptation of *Ectocarpus* to low salinity and its interactions with its microbiome.

Key index words: **distribution; *Ectocarpus subulatus*; freshwater colonization; low salinity adaptation; microbiota**

***Abbreviations*: ANOSIM, analysis of similarity; BLAST, Basic Local Alignment Search Tool; ENA, European Nucleotide Archive; HPAEC, high-performance anion exchange chromatography; NCBI, National Center for Biotechnology Information; NMDS, non-metric multidimensional scaling; OTU, operational taxonomic unit; R2A agar, Reasoner's 2A agar**

Brown algae (Phaeophyceae) are widespread in the tidal and subtidal zone of rocky shores in temperate marine environments, but they are rarely

[1]Received 30 October 2019. Accepted 7 January 2020. First Published Online 21 January 2020. Published Online 28 February 2020, Wiley Online Library (wileyonlinelibrary.com).
[2]CEBEDEAU, Research and Expertise Center for Water, Allée de la découverte, 11 (B53), Quartier Polytech 1, B-4000, Liège Belgium.
[3]Present address: ALGAIA, Research & Development Center, 91 rue Edouard Branly, 50000, Saint-Lô France.
[4]Author for correspondence: e-mail simon.dittami@sb-roscoff.fr.
Editorial Responsibility: M. Roleda (Associate Editor)

found in fresh water (Dittami et al. 2017). While there are ca. 2,000 known species of marine brown algae, covering a large range of morphologies from small filamentous algae to large and morphologically complex kelp species, there is only a handful of known freshwater brown algae, all of them small and with simple morphology (crust forming or filamentous). Among these freshwater brown algae the genus *Ectocarpus* has a unique position because it corresponds to a predominantly marine genus, which, on two occasions, has been recorded also in rivers: one occurrence of *Ectocarpus crouaniorum* in a highly salt-contaminated section of the Werra river in Germany (Geissler 1983); and one occurrence of *Ectocarpus subulatus* in a nearly freshwater habitat (salinity 1) in the Hopkins River, Victoria, Australia (West and Kraft 1996, Peters et al. 2015).

The isolate from the latter site (Culture Collection of Algae and Protozoa accession 1310/196) constitutes a potential model system to study marine–freshwater transitions in brown algae. The species *Ectocarpus subulatus* (Peters et al. 2015) is related to the genomic model species *Ectocarpus siliculosus* (Cock et al. 2010) and has previously been found in highly variable environments, including environments with high levels of abiotic stressors. Its occurrence was reported, for instance, at Port Aransas, Texas, USA, where monthly average water temperatures reach 30°C in July (Bolton 1983). More recently, the nuclear genome of *E. subulatus* has been sequenced, revealing that *E. subulatus*, in comparison to *Ectocarpus siliculosus,* has lost members of gene families down-regulated in low salinities, and conserved those that were up-regulated (Dittami et al. 2020). The *E. subulatus* strain from Hopkins River Falls has further been used for physiological experiments: it can grow in both seawater and fresh water and its transcriptomic and metabolic acclimation to these conditions has been examined (Dittami et al. 2012) along with the composition of its cell wall with regard to sulfated polysaccharides (Torode et al. 2015). Moreover, the capacity of the freshwater strain to grow in low salinities has been shown to depend on its associated microbial community, although the nature of this dependence is still unknown (Dittami et al. 2016). Extensive efforts have been made to develop a collection of cultivable bacteria to study this phenomenon (KleinJan et al. 2017).

Despite this increasing quantity of data on the physiology of the Hopkins River Falls strain of *Ectocarpus subulatus*, we currently know little about its abiotic environment in situ. The original paper describing its isolation (West and Kraft 1996) states that it was isolated on March 24th, 1995 from cracks between the basalt rock of the Hopkins River, just above the Hopkins River Falls. Water temperature was 16°C, salinity was ~1, and conductivity ~3 mS · s^{-1}. However, it remains unknown if *E. subulatus* is still present at Hopkins River Falls, and if so what its current distribution is. Furthermore, the culture has undergone >20 years of cultivation in different laboratories, potentially having a strong impact on its associated microbiota.

In this study, we address both of these knowledge gaps by returning to the Hopkins River and searching for this alga for the first time since its discovery 20 years ago. We found *Ectocarpus subulatus* individuals at three locations along the Hopkins River, examined its associated microbiome in situ, and isolated several novel alga-associated bacterial strains from these samples. These data provide important background information for the use of *E. subulatus* as a model to study low salinity acclimation/adaptation and the role of microbes in these processes.

MATERIALS AND METHODS

Biological samples. The sampling campaign was carried out from March 21st to March 27th, 2017 and covered several locations along the Hopkins River between Warrnambool and Ararat (sites 1–15; selected due to their accessibility and to cover the entire length of the river), as well as 10 sites selected arbitrarily along the Southern Australian Coastline between Port Fairy and Avalon (Fig. 1, Table 1). At each sampling site, we manually searched for filamentous algae resembling a member of the Ectocarpales within a range of ca. 50 m and for at least 30 min. If filaments were found, small amounts of live samples were taken and rinsed three times in sterile 50 mL Falcon tubes with 0.2-µm-filtered local water (three replicates). A small piece of each sample was stored at max. 20°C in sterile 2 mL Eppendorf tubes filled with the surrounding water for live algal cultures. The second part of the samples was ground on-site according to Tapia et al. (2016), with 50 µL of 0.2-µm-filtered local water in a sterile mortar and the proximity of a Bunsen burner. One, 7, and 35 µL of the ground alga were diluted with 0.2-µm-filtered local water to a final volume of 50 µL and spread immediately onto preprepared Reasoner's 2A (R2A) agar plates (Sigma-Aldrich, St. Louis, MO, USA) for isolation of culturable bacteria. These plates were kept at ambient temperature (max. 25°C) and were monitored for 2 weeks. Newly emerging colonies were purified once more on fresh R2A plates and then put into culture in liquid Zobell medium (Zobell 1941) with 8-fold reduced salt concentration, identified by 16S rRNA gene sequencing (see below), and put into stock at −80°C in 40% glycerol. The remaining sample was dried using silica gel for downstream analysis of the microbial community composition, and frozen at −20°C after the sampling campaign.

For all sites, we also collected samples for germling emergence experiments to detect the presence of *Ectocarpus* spores: three to seven sediment samples including small pieces of solid substrate (shells, pebbles, and branches) if present. Approximately 0.1 mL of sediment was kept as live samples in sterile 2 mL Eppendorf tubes. After 2 weeks these samples were transferred to fresh Provasoli-enriched (Starr and Zeikus 1993) medium based on 5, 25, or 100% seawater, depending on the salinity of the water at the sampling site. Seawater for culture media was collected in Roscoff (48°46′40″ N, 3°56′15″ W), 0.45 µm filtered, and autoclaved at 120°C for 20 min prior to use. The sediment samples were then kept at 13°C in a 14:10 h light:dark cycle at an irradiance level of 25 µmol PAR · m^{-2} · s^{-1}, and the emergence of *Ectocarpus*-like germlings was monitored over 4 months.

Both live algae collected in situ and those recovered from germling emergence experiments were cleaned by rigorous

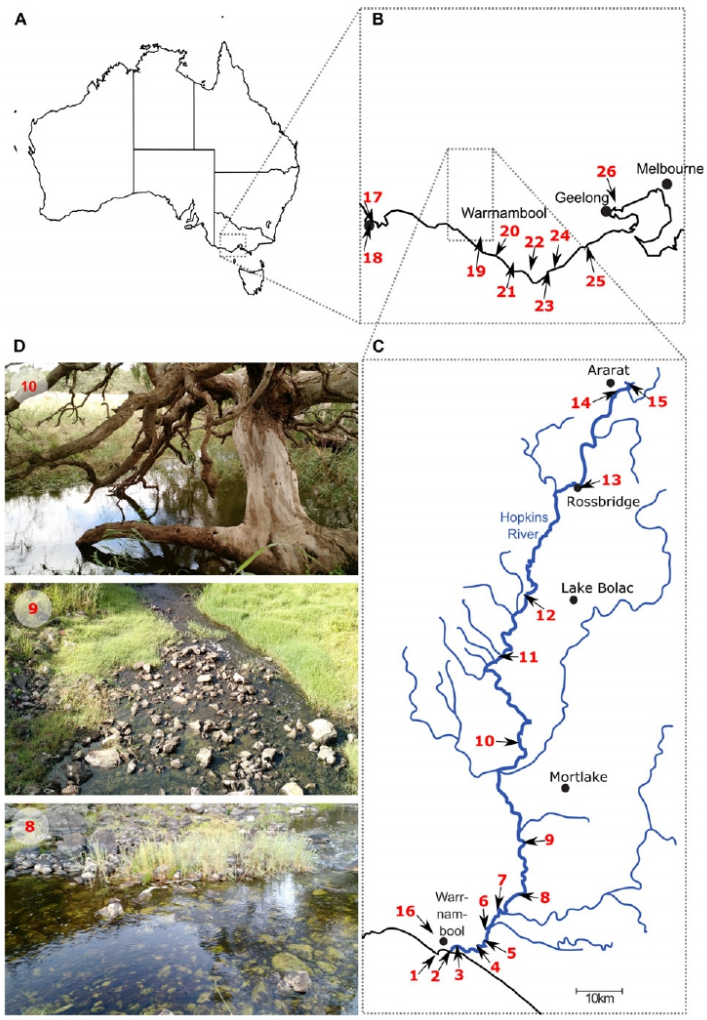

FIG. 1. Sites sampled. Panels A-C: Map of sampling sites at an increasing scale. Each sampling site is numbered (1–26, see Table 1). *Ectocarpus* individuals were found at sites 8, 9, and 10, and Panel D contains photos taken at these sites. Hopkins River Falls, the original site of isolation, corresponds to site 7. [Color figure can be viewed at wileyonlinelibrary.com]

pipetting with a Pasteur pipette and several transfers to fresh, sterile, medium. Any diatoms that remained attached to the algal filaments were removed via treatment with 3 mg · L per GeO_2 for 3 weeks.

Water samples. Approximately 100 mL of water was taken from each site, immediately filtered with 0.45 µM syringe filters to remove particulate matter, and then pasteurized for 1 h at 95–100°C to remove any remaining bacterial activity. Filtered samples were stored at ambient temperature until the end of the sampling campaign (max. 2 weeks) and then frozen at −20°C until analysis. The conductivity of water samples was determined using a Type CD78 conductivity meter (Tacussel Electronique, Villeurbanne, France) and converted to salinity according to Fofonoff and Millard (1983). Phosphate, nitrite, and nitrate concentrations were determined using an AA3 auto-analyzer (SEAL Analytical, Southampton, UK) following the method of Aminot and Kérouel (2007) with an accuracy of 0.02 µmol · L^{-1}, 0.01 µmol · L^{-1}, and 0.01 µmol · L^{-1} for NO_3^-, NO_2^-, and PO_4^{3-}, respectively. Sulfate concentrations were determined by high-performance anion-exchange chromatography (HPAEC), according to a protocol adapted from Préchoux et al. (2016). After suitable dilution, water samples were injected onto an IonPac™ AS11-HC column (4 × 250 mm) equipped with an AG11-HC guard column (4 × 50 mm), using an ICS-5000 Dionex system (SP-5 & Analytical CD Detector; Thermo Fisher Scientific, Waltham, MA, USA). Elution was performed with isocratic 12 mM NaOH at a flow rate of 1 mL · min^{-1}, and sulfate ions were detected in conductimetry mode (ASRS 500, 4 mm) and quantified using a standard calibration curve. To

TABLE 1. Overview of samples taken and species identified. The numbers in the location column correspond to site numbers in Figure 1.

Date	Location	Material sampled	*Ectocarpus* tissue found	GPS coordinates	Germling emergence	Sequence accession(s)
2017-03-22	1. Merri Island	Pebbles/mussels in tide pool	No	−38.402116, 142.471548	–	–
2017-03-22	2. Point Ritchie	Sand/sandstone	No	−38.401275, 142.509318	*Ectocarpus siliculosus*	LR735221 (*cox*1) LR735414 (ITS)
2017-03-22	3. Mahoney Road	Sand, wood/ plastic	No	−38.392103, 142.531644	–	–
2017-03-22	4. Smith Lane	Mud, wood	No	−38.397984, 142.578286	–	–
2017-03-22	5. Allan's Ford	Rock (granite)	No	−38.385325, 142.587398	–	–
2017-03-22	6. Donovans Lodge	Granit, clay	No	−38.355110, 142.599250	–	–
2017-03-22	7. Hopkins River Falls	Volcanic rock	No	−38.333509, 142.621352	–	–
2017-03-23	8. Framlingham Forest Reserve	Rock, pebbles	*E. subulatus* Au8 (abundant)	−38.297064, 142.668291	–	LR735222 (*cox*1) LR735415 (ITS)
2017-03-23	9. Kent's Ford	Rock, pebbles	*E. subulatus* Au9 (abundant)	−38.191574, 142.698058	–	LR735223 (*cox*1) LR735416 (ITS)
2017-03-23	10. Hexham	Mud, wood	*E. subulatus* Au10 (rare)	−37.995732, 142.689141	–	LR735224 (*cox*1) LR735417 (ITS)
2017-03-23	11. Chatsworth	Mud, sand, detrirus	No	−37.856357, 142.650644	–	–
2017-03-23	12. Wickliffe	Sand, detritus	No	−37.694348, 142.726074	–	–
2017-03-24	13. Rossbridge	Rock, pebbles	No	−37.480217, 142.849465	–	–
2017-03-23	14. Ararat	Sand	No	−37.300211, 142.973979	–	–
2017-03-24	15. Green Hill Lake	Pebbles	No	−37.295320, 142.979170	–	–
2017-03-24	16. Merri River, Warnambool	Concrete	No	−38.362077, 142.484414	–	–
2017-03-24	17. Killarney beach	Sand, lava pebbles, shells	No	−38.357966, 142.306880	*Kuckuckia* sp.	LR735225 (*cox*1) LR735418 (ITS)
2017-03-25	18. Belfast Lough airport	Sand, wood pollar	No	−38.361889, 142.262045	–	–
2017-03-25	19. Curdies River	Rock	No	−38.519965, 142.833558	–	–
2017-03-25	20. Port Campbell	Tide pool. sand	No	−38.620681, 142.992981	*Feldmannia* sp.	LR735226 (*cox*1)
2017-03-25	21. Gellibrand River	Mud, detritus	No	−38.727482, 143.250932	–	–
2017-03-25	22. Aire River	Mud, pebbles	No	−38.763797, 143.474727	–	–
2017-03-25	23. Wild Dog Creek	Sand	No	−38.735911, 143.683545	–	–
2017-03-25	24. Smythe's Creek	Pebbles, biofilm	No	−38.704648, 143.762856	–	–
2017-03-26	25. Lorne	Tide pool, sand shells	No	−38.531281, 143.980994	*Acinetospora* sp.	LR735227 (*cox*1)
2017-03-26	26. Hovell's Creek	Clay	No	−38.018825, 144.402156	–	–

test if variations in sulfate concentration merely mirrored variations in the overall salinity, a Pearson correlation coefficient was calculated between both variables.

Barcoding of algal and bacterial isolates. Algal isolates were identified to a species level using the mitochondrial *cox*1 and the nuclear ITS1 + 2 markers. Algal DNA was extracted from the cleaned cultures using the Macherey Nagel (Düren, Germany) NucleoSpin Plant II kit according to the manufacturer's instructions (PL1 protocol with two 25 µL elutions), and 1 µL of DNA (10–30 ng) was used in subsequent PCRs. For the ITS region, we used the AFP4LF (3′-CAATTATT GATCTTGAACGAGG-5′) and LSU38R (5′-CGCTTATTGA TATGCTTA-3′) primers (Lundholm et al. 2003, Peters et al. 2004), and for the 5′*cox*1gene the GAZF2 (3′-CCAACCAYAAA GATATWGGTAC-5′) and GAZR2 (3′-GGATGACCAAARAA CCAAAA-5′) primers (Lane et al. 2007), each at a final concentration of 0.5 µM. PCRs were carried out using a GoTaq polymerase and the following program: 2 min. 95°C followed by 30 cycles (1 min 95°C; 30 s, 50°C for ITS or 55°C for *cox*1; 3 min 72°C) and a final extension of 5 min 72°C.

Bacterial cultures were identified by partial sequencing of their 16S rRNA gene. Fifty µL of dense bacterial culture was heated to 95°C for 15 min, spun down for 1 min, and 1 µL of supernatant was used as a template in a PCR reaction with the 8F (5′-AGAGTTTGATCCTGGCTCAG-3′) and 1492R 5′-GGTTACCTTGTTACGACTT-3′; Weisburg et al. 1991) at a final concentration of 0.5 µM. Except for the annealing temperature (53°C here), the same PCR protocol as above was employed.

All PCR products were purified using ExoStar (Thermo Fisher Scientific) and the purified 16S rRNA gene amplicons were sequenced with Sanger technology at the GENOMER platform (FR2424; Roscoff Biological Station), using the BigDye Xterminator v3.1 cycle sequencing kit (Applied Biosystems, Waltham, MA, USA). For bacterial strains, sequencing was carried out only in one direction using the 8F primer, and for algal sequences both the forward and the reverse strand were sequenced and manually assembled. Sequence identification was carried out using RDP classifier (Wang et al. 2007) for bacterial 16S rRNA gene sequences, and Basic

Local Alignment Search Tool (BLAST) searches against the National Center for Biotechnology Information (NCBI) nt database (July 2017) for algal sequences. They were further aligned together with reference sequences from the NCBI nt database using the MAFFT server (Katoh et al. 2002) and the G-INS-i algorithm. All positions with less than 95% site coverage were eliminated. Phylogenetic analyses were carried out with MEGA 7 (Kumar et al. 2016) using the Maximum Likelihood method based on the GTR+G+I model and 1,000 bootstrap replicates.

Amplicon sequencing of in situ bacterial communities. Amplicon sequencing of bacterial communities was carried out to assess the in situ composition of the *Ectocarpus subulatus* microbiome. Sufficient material for these analyses was obtained at two of the three sites with *Ectocarpus* individuals: sites 8 and 9 (Fig. 1). Approximately 20 mg dry weight for each of the three replicate samples for each site were ground twice for 45 s at 30 Hz in a TissueLyser II (Qiagen, Hilden, Germany). DNA was then extracted using the Qiagen DNeasy Plant mini kit according to the manufacturer's instructions. Approximately 50 ng of DNA (as estimated using a NanodropONE; Thermo Fisher Scientific) was then used to amplify the V3-V4 region of the 16S rRNA gene. Furthermore, a mock community comprising a mix of DNA from 26 bacterial genera was cultivated in our laboratory (see Thomas et al. 2020 for details), as well as a negative control was added alongside the samples. PCR amplification, indexing, and library construction were carried out following the standard "16S Metagenomic Sequencing Library Preparation" protocol (Part # 15044223 Rev. B). Final library concentrations were measured using a BioAnalyzer (Agilent, Santa Clara, CA, USA) before pooling. Libraries for each sample were then pooled in an equimolar way, diluted to 5 nM final concentration and supplemented with 20%PhiX to add sufficient diversity for sequencing on an Illumina MiSeq using a 2 × 300 bp cartridge. Raw data were deposited at the European Nucleotide Archive (ENA) under project accession number PRJEB34906 (https://www.ebi.ac.uk/ena/data/search?query=PRJEB34906).

Raw reads were first trimmed and filtered using the fastx_quality_trimmer script (http://hannonlab.cshl.edu/fastx_toolkit/), assembled using Pandaseq 2.11 (Masella et al. 2012), and further processed with mothur according to the Miseq SOP (version April 4th, 2018; Kozich et al. 2013). Sequences were aligned to the non-redundant SSU ref database version 132, chimeric sequences removed using Vsearch (Rognes et al. 2016), and operational taxonomic units (OTUs) defined based on a 97% identity threshold (Stackebrandt and Goebel 1994). Rare sequences (<5 reads across all samples) were removed from the final analyses. Taxonomic assignments were generated for both the raw reads and the final OTUs using the RDP classifier method (Wang et al. 2007). Non-metric multidimensional scaling (NMDS) of the OTU matrix was carried out in R 3.5.1 using the isoMDS function of the Vegan package and Bray-Curtis dissimilarity as a distance measure. An Analysis of Similarity (ANOSIM) was used to test for differences in the overall community composition between the two sites (3 replicates each, 719 permutations). Statistical differences between the two sites at the level of individual OTUs were assessed by multiple two-sided *t*-tests (one test per OTU) on log-transformed abundance data with subsequent correction for multiple testing according to Benjamini and Hochberg (1995). Alpha diversity was estimated using the Shannon index with e as a base and the diversity() function of the VEGAN package. A two-sided *t*-test was used to compare these indexes obtained for the replicate samples of both sites. Differences between sites were considered significant if the Type I error rate was below 0.05.

RESULTS

Distribution of Ectocarpus subulatus *along the Hopkins River.* We found live *Ectocarpus subulatus* at 3 of the 15 sampled sites along the Hopkins River, and germlings of other Ectocarpales emerged from four additional marine sites along the Victorian coastline, including at the mouth of Hopkins River (Table 1). Despite extensive searches, no traces of *Ectocarpus* were found at the original isolation site of *E. subulatus* at Hopkins River Falls (site 7; Fig. 1). *Ectocarpus* was, however, abundant at two sites (Framlingham Forest reserve and Kent's Ford, sites 8 and 9; Fig. 1), which were ~12 km and 37 km upstream of Hopkins River Falls. The third finding of *Ectocarpus* was registered 83 km upstream (site 10), although only a few filaments were found at this site. The *cox*1 and ITS sequences obtained from *Ectocarpus* cultures from all three sites were identical to those of the strain isolated from Hopkins River Falls in 1995 (Fig. 2). We found no *E. subulatus* individuals in other sampled rivers, along the coastline, or in germling emergence experiments.

Water chemistry. The salinity of the Hopkins River was highest close to the source (8.4; ~¼ that of seawater), and then gradually decreased toward the mouth of the river, where it dropped to ca. 1, before re-spiking due to the influence of seawater (Fig. 3). This decrease corresponded to an increase in the flow of water masses toward the mouth river. Sulfate concentrations followed the same pattern as salinity (Pearson correlation $r = 0.995$, $df = 12$, $P < 0.001$) and decreased from nearly 7 mM to ~0.4 mM close to the river mouth. Finally, phosphate and nitrite/nitrate concentrations were variable along the river. They were highest at the Chatsworth site (site 11), reaching 3.3 and 22.8 μM, respectively, and then strongly decreased at sites where *Ectocarpus* was found (PO_4^{3-} 0.5–0.8 μM, NO_2^-/NO_3^- 0.8–1.7 μM; Fig. 3).

Bacterial communities associated with algae. In situ bacterial community composition was determined by 16S rRNA gene amplicon sequencing for field samples taken at Framlingham Forest reserve (site 8) and Kent's Ford (site 9; Fig. 4A). We detected 1312 OTUs across the three sampled individuals from both sites (Table S1 in the Supporting Information). The bacterial communities of both sites were dominated by *Alphaproteobacteria* (25% of reads), *Bacteriodetes* (20%), *Gammaproteobacteria* (8%), *Planctomycetes* (8%), and *Actinobacteria* (8%) (Figure 4A), and there was a significant difference in the community structure between the two sites (ANOSIM, $R_{1,4} = 1$, $P = 0.001$; Fig. 4B). Examining the OTUs individually, we identified 86 OTUs that were specific to Framlingham Forest reserve (including 31 *Proteobacteria* and 22 *Planctomycetes*), and 60 more had a higher relative abundance there. At Kent's Ford, 27 OTUs were site specific (including

13 *Proteobacteria* and 6 *Bacteroidetes*), and 13 more exhibited higher relative abundance. In three cases, site-specific OTUs from both sites were found to belong to the same genera: *Rickettsiales* of the SM2D12 group, *Flavobacterium*, and *Luteolibacter*. A detailed list of these OTUs is provided in Table S1. Alpha-diversity (Shannon index) was also slightly higher at the Framlingham Forest reserve (*t*-test, $t_4 = 3.1802$, $P = 0.03$; Fig. 4C). Amplicon sequencing analyses of bacterial communities were complemented by in situ isolation of bacterial strains from the algae after thorough rinsing with sterile river water (Fig. 5). They comprise *Gammaproteobacteria* (48 isolates, including 28 *Pseudomonas*), *Firmicutes* (27 isolates), *Actinobacteria* (8 isolates), *Alphaproteobacteria* (7 isolates), and *Bacteriodetes* (5 isolates). No members of the *Planctomycetes* were isolated.

DISCUSSION

The data presented in this study confirm that the original finding of *Ectocarpus subulatus* by West and Kraft was not the result of a transient "contamination", but that algae with identical ITS sequences are present in the river at three sites upstream of the original location. At the time of sampling, the water at these sites was saline and contained high levels of sulfate for a river, but low levels of nitrite/nitrate and phosphate compared to other upstream and downstream sites. Furthermore, the bacterial community associated with the algae in situ comprised over 1300 OTUs, which is highly diverse compared to laboratory cultures. It also included a high diversity of *Planctomycetes*. Each of these findings, discussed in more detail below, provides valuable background information when using *E. subulatus* cultures as a model system to study acclimation, adaptation, or interactions with their associated microbiome.

Based on these observations, it seems likely that *Ectocarpus subulatus* has persisted in the Hopkins River for over 20 years, maintaining a population despite the water currents. *Ectocarpus* spores and gametes are motile, but swimming speeds reported are only in the range of 150–270 $\mu m \cdot s^{-1}$ (Müller 1978). This implies that *E. subulatus* in Hopkins River either (1) does not rely on gamete releases for reproduction, (2) that its gametes are able to remain close to the substratum as has been suggested for male gametes (Müller 1978) and direct their movement upstream, or (3) that gametes rely on zoochory, as has been proposed in the case of red algae (Žuljević et al. 2016). Our findings thus open interesting perspectives for population genetics studies as well as more detailed studies of the reproductive biology of *Ectocarpus* in this area. Furthermore, the fact that no traces of *E. subulatus* were found in nearby rivers or along the coastline suggests that it may be restricted to the Hopkins River, although the range of colonization within the river may have been subject to variation, notably because individuals of *E. subulatus* were no longer found at the original isolation site.

Although limited to a single point in time, our sampling campaign also provides novel information on the chemical parameters in the Hopkins River at the time of sampling. Notably, the observed salinity at sites with *Ectocarpus subulatus* between 3.1 and 6.9 leads us to classify the water in the Hopkins River at the sites with *E. subulatus* at the time of sampling as low salinity brackish water rather than fresh water (usually defined by a salinity <0.5, International Symposium for the Classification of Brackish Waters 1958). This may be one of the factors enabling *E. subulatus* to be competitive in this environment, a hypothesis which is supported by the fact that no individuals were found in the lower portions of the river with lower salinity. High salinity in our samples also positively correlated with high sulfate concentrations between 1 and 5 mM – average sulfate concentrations in fresh water are 0.12 mM (vs. 28 on average in the ocean; Wetzel 2001). Sulfated polysaccharides are typical components of the cell walls of marine plants and algae (Popper et al. 2011) and require sulfate for their synthesis, but their importance for *Ectocarpus* remains to be explored. In the same vein the question remains open to what extent the low nitrate concentrations at sites with *E. subulatus* compared to upstream and downstream sites are related to the presence of the algae, either as a cause or as an effect. It should be noted, though, that a direct metabolomic comparison of *E. subulatus* and the marine *E. siliculosus* revealed markers for high nitrogen status (total amino acids, ratio of glutamine to glutamate) in *E. subulatus* (Dittami et al. 2012). Regardless of the physiological implications of the composition of the Hopkins River water, we argue that it may be more appropriate to refer to the *E. subulatus* strains isolated from the Hopkins River as "fluviatile" (i.e., "river" strains rather than freshwater strains) despite their capacity to grow in fresh water in laboratory conditions (Dittami et al. 2012).

In addition to these facts about the distribution and environment of *E. subulatus*, this study provides insights into its associated microbiome – a component likely connected to the capacity of this species to grow in low salinity (Dittami et al. 2016). The number of OTUs associated with *E. subulatus* in our in vivo study was one order of magnitude higher than in a previous study of the laboratory strain after 20 years of cultivation (1312 OTUs for six samples from two sites vs. 84 OTUs for six samples in two conditions; Dittami et al. 2016). Moreover, a direct taxonomic comparison of these two studies at the genus level revealed only five genera (*Acinetobacter*, *Phycisphaera*, *Maribacter*, *Marinoscillum*, and *Gaiella*) that were found in both studies. All of them were rare, that is, supported by <0.01% of reads in our study; Table S1). Both studies were based on sequencing runs with similar depth and employed

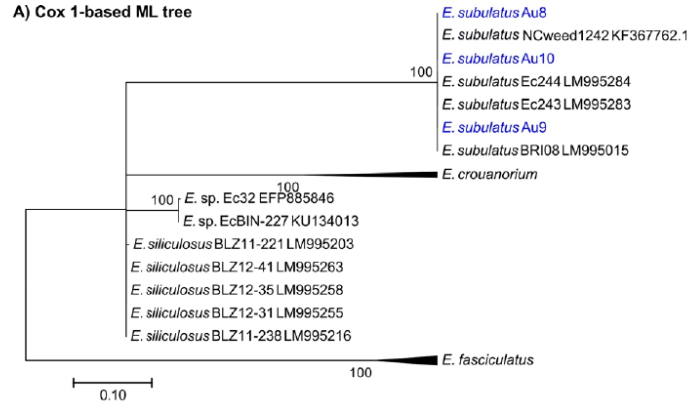

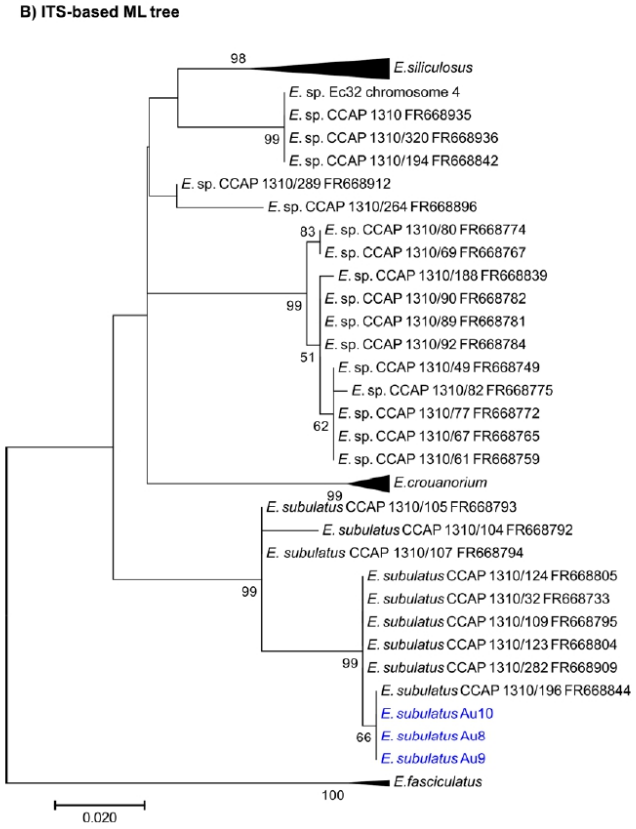

FIG. 2. Maximum-likelihood tree of *Ectocarpus* isolates from Hopkins River and related strains. Panel A displays a tree based on the *COX1* gene (alignment of 677 bp after curation), and Panel B on the ITS region (860 bp after curation). Bold names indicates isolates from this study. Support values correspond to the percentage of support using 1,000 bootstrap replicates. [Color figure can be viewed at wile yonlinelibrary.com]

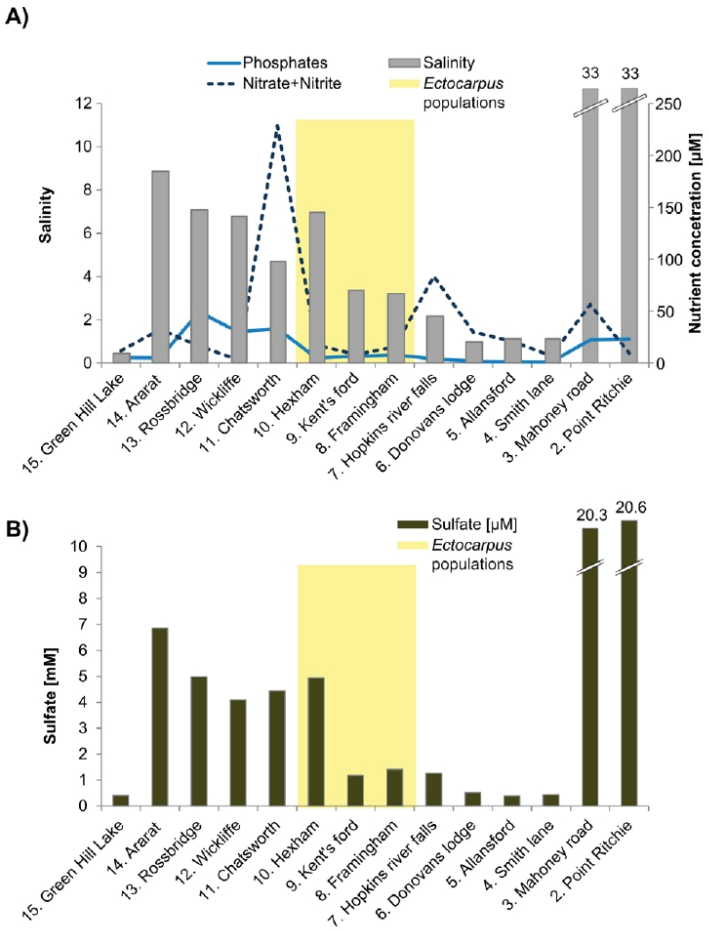

FIG. 3. Water chemistry at the different sampling sites along the Hopkins River (see Fig. 1). Panel A displays salinity (gray bars) and nutrient concentrations (solid and dashed lines), and Panel B shows sulfate concentrations. Each measurement corresponds to a single sample collected between 2017-03-22 and 2017-03-24. [Color figure can be viewed at wileyonlinelibrary.com]

similar analysis pipelines, yet many technical factors could contribute to such differences: the sampling protocol, the primers used, library preparation, the sequencing platform, and chemistry (Illumina Miseq V2 vs. V3), etc. Nevertheless, the profoundness of the observed differences suggests that either the microbiome of *E. subulatus* in the Hopkins River has evolved and diversified over time or that the cultivation of algae in the laboratory has impacted its microbiome, leading to a reduction in diversity and a change in composition. In a context of the development of new laboratory models for the study of marine holobionts (Dittami et al. 2019), a targeted examination of these potential changes (e.g., by following the evolution of alga-associated microbiomes in the field as well as over several cultivation cycles) may yield important insights on possible limitations of laboratory model systems. If confirmed, such biases would underline the necessity of devising targeted experiments to test the validity of laboratory findings in the field.

The availability of parallel amplicon sequencing data of bacterial communities and untargeted cultivation efforts further allows us to identify undersampled lineages in cultivation experiments. In this study, particularly *Planctomycetes* stand out, as

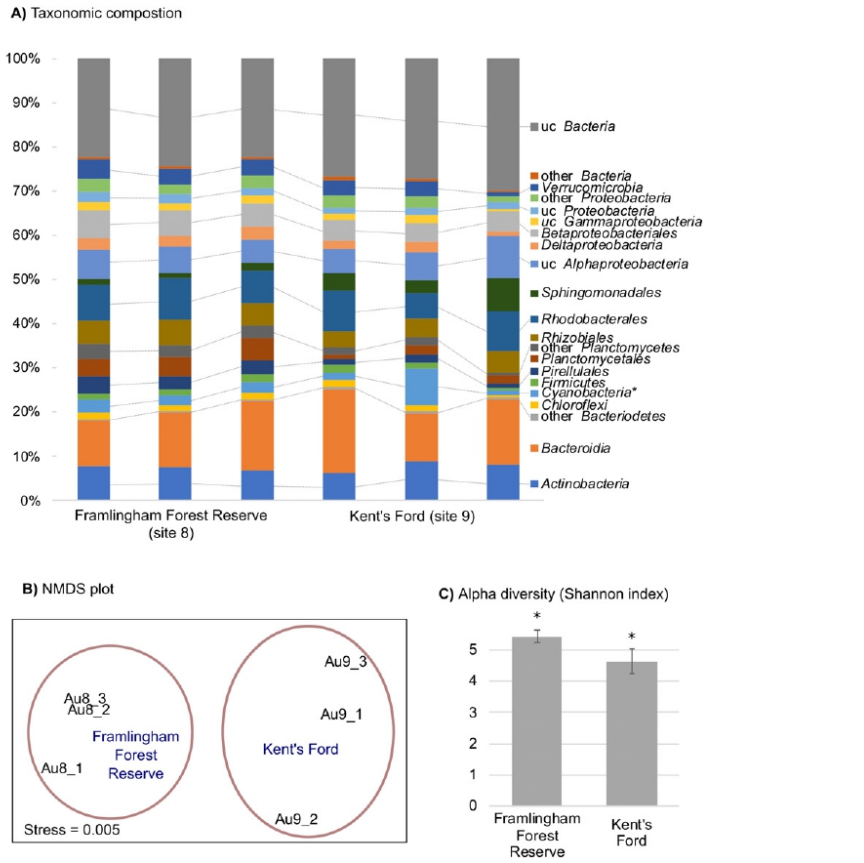

FIG. 4. Bacterial community at isolation sites determined by 16S rDNA amplicon sequencing of bacterial communities. Panel A shows the taxonomic distribution of the bacterial communities associated with each replicate at the two sampling sites with sufficient material, uc = unclassified. Panel B shows the distances between the communities (NMDS plot based on Bray-Curtis dissimilarity matrix); communities at both sites differed significantly (ANOSIM, $R_{1,4} = 1$, $P = 0.001$). Panel C shows the alpha-diversity of bacterial communities in the two sites (mean of three replicates ± SD; * indicates a significant difference, two-sided *t*-test, $t_4 = 3.1802$, $P = 0.03$). [Color figure can be viewed at wileyonlinelibrary.com]

they constituted 176 OTUs and 8% relative abundance of all algae-associated reads but did not have a single associated culture. *Planctomycetes* are notoriously difficult to cultivate, partially due to their long doubling time of up to 1 month. They require low organic content in media, physical separation from fast-growing competitors (e.g., via dilution to extinction experiments, and they may benefit from the use of fungicides; Lage and Bondoso 2012). In contrast to the present study, previous barcoding data (Dittami et al. 2016) on cultivated *Ectocarpus subulatus* revealed the presence of very few *Planctomycetes* (0.1% of reads), implying that these culturing techniques would need to be put into place using freshly collected material. In contrast, the high abundance of *Firmicutes* in the isolation experiments although they account for only 1% of the reads in the amplicon sequencing data may be because these bacteria were particularly amenable to the culture condition.

This study enhances our knowledge on *Ectocarpus subulatus* from the Hopkins River and its associated microbiome. It furthermore provides a new set of microbes for coculture experiments and thus strengthens the use of *E. subulatus* both as a model for the study of acclimation and adaptation to low salinity and of algal–bacterial interactions.

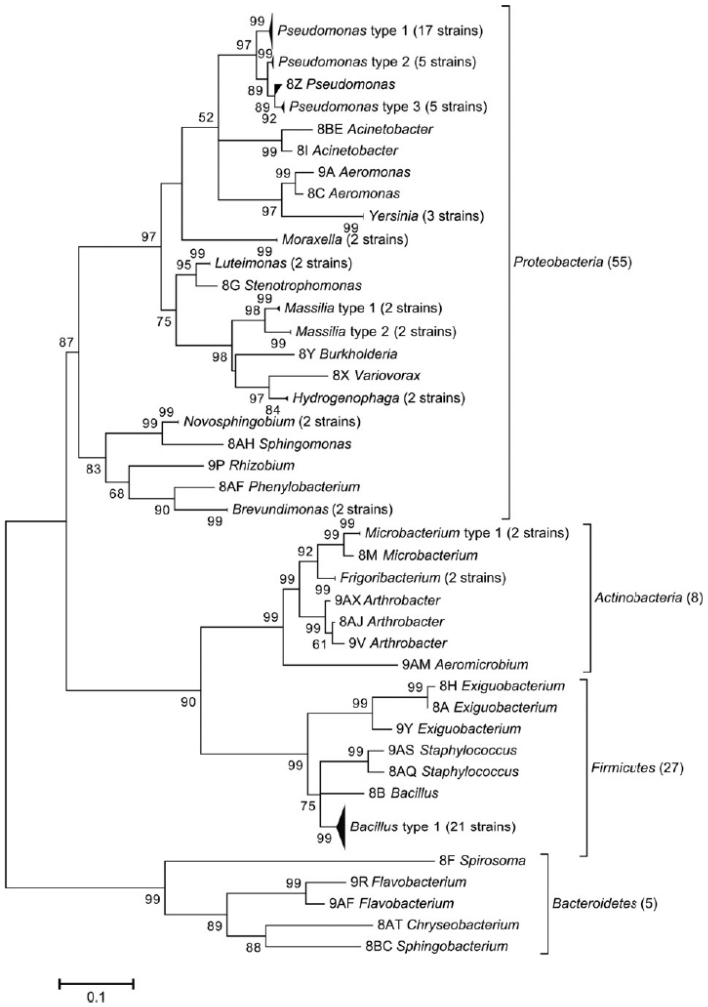

FIG. 5. Maximum-likelihood tree of bacterial isolates obtained from *Ectocarpus subulatus* in situ. The tree is based on an alignment of 16 rRNA gene sequences of all isolated strains and comprised 598 bases after cleaning. Support values correspond to the percentage of support using 1,000 bootstrap replicates. Sequence accession numbers are ENA: LR735444-LR735537.

This work was funded partially by ANR project IDEALG (ANR-10-BTBR-04) "Investissements d'Avenir, Biotechnologies-Bioressources", the European Union's Horizon 2020 research and innovation Programme under the Marie Sklodowska-Curie grant agreement number 624575 (ALFF), and an internal call for proposals from the UMR8227 (CNRS, Sorbonne University). We thank Cécile Hervé, Amandine Simeon, and Agnieszka P. Lipinska for helpful discussions; Gwenn Tanguy and Erwan Legeay from the GENOMER platform; Roscoff for support during the library construction and sequencing; and the ABIMS platform for providing the computational facilities for the amplicon sequencing analyses.

CONFLICT OF INTEREST STATEMENT

The authors declare no conflict of interest.

AUTHOR'S CONTRIBUTIONS

SD, AFP, HK, SE, JW, and CB planned the study; TC performed nutrient analyses; AP measured sulfate concentrations; BBD performed amplicon sequencing analyses of bacterial communities; SD performed sampling, culturing, in silico analyses,

and wrote the manuscript; All authors corrected the manuscript and approved the final draft.

Aminot, A. & Kérouel, R. 2007. *Dosage automatique des nutriments dans les eaux marines: méthodes en flux continu*, 1st edn. Ifremer, Versailles, 188 pp.

Benjamini, Y. & Hochberg, Y. 1995. Controlling the false discovery rate – a practical and powerful approach to multiple testing. *J. R. Stat. Soc. Series B* 57:289–300.

Bolton, J. J. 1983. Ecoclinal variation in *Ectocarpus siliculosus* (Phaeophyceae) with respect to temperature growth optima and survival limits. *Mar. Biol.* 73:131–8.

Cock, J. M., Sterck, L., Rouzé, P., Scornet, D., Allen, A. E., Amoutzias, G., Anthouard, V. et al. 2010. The *Ectocarpus* genome and the independent evolution of multicellularity in brown algae. *Nature* 465:617–21.

Dittami, S. M., Arboleda, E., Auguet, J. C., Bigalke, A., Briand, E., Cárdenas, P., Cardini, U. et al. 2019. A community perspective on the concept of marine holobionts: current status, challenges, and future directions. *PeerJ Prepr.* 7:e27519v3.

Dittami, S. M., Corre, E., Brillet-Gueguen, L., Lipinska, A. P., Pontoizeau, N., Aite, M., Avia, K. et al. 2020. The genome of *Ectocarpus subulatus* – a highly stress-tolerant brown alga. *Mar. Genomics*. https://doi.org/10.1016/j.margen.2020.100740.

Dittami, S. M., Duboscq-Bidot, L. L., Perennou, M., Gobet, A., Corre, E., Boyen, C. & Tonon, T. 2016. Host–microbe interactions as a driver of acclimation to salinity gradients in brown algal cultures. *ISME J.* 10:51–63.

Dittami, S. M., Gravot, A., Goulitquer, S., Rousvoal, S., Peters, A. F., Bouchereau, A., Boyen, C. & Tonon, T. 2012. Towards deciphering dynamic changes and evolutionary mechanisms involved in the adaptation to low salinities in *Ectocarpus* (brown algae). *Plant J.* 71:366–77.

Dittami, S. M., Heesch, S., Olsen, J. L. & Collén, J. 2017. Transitions between marine and freshwater environments provide new clues about the origins of multicellular plants and algae. *J. Phycol.* 53:731–45.

Fofonoff, N. P. & Millard, R. C. J. 1983. Algorithms for computation of fundamental properties of seawater. *UNESCO Technical Papers in Marine Science*, pp. 44–53.

Geissler, U. 1983. Die salzbelastete Flusstrecke der Werra - ein Binnenlandstandort für *Ectocarpus confervoides* (Roth) Kjellmann. *Nova Hedwigia* 37:193–217.

International Symposium for the Classification of Brackish Waters 1958. The Venice system for the classification of marine waters according to salinity. *Limnol. Oceanogr.* 3:346–7.

Katoh, K., Misawa, K., Kuma, K. & Miyata, T. 2002. MAFFT: a novel method for rapid multiple sequence alignment based on fast Fourier transform. *Nucleic Acids Res.* 30:3059–66.

KleinJan, H., Jeanthon, C., Boyen, C. & Dittami, S. M. 2017. Exploring the cultivable *Ectocarpus* microbiome. *Front. Microbiol.* 8:2456.

Kozich, J. J., Westcott, S. L., Baxter, N. T., Highlander, S. K. & Schloss, P. D. 2013. Development of a dual-index sequencing strategy and curation pipeline for analyzing amplicon sequence data on the miseq illumina sequencing platform. *Appl. Environ. Microbiol.* 79:5112–20.

Kumar, S., Stecher, G. & Tamura, K. 2016. MEGA7: molecular evolutionary genetics analysis version 7.0 for bigger datasets. *Mol. Biol. Evol.* 33:1870–4.

Lage, O. M. & Bondoso, J. 2012. Bringing *Planctomycetes* into pure culture. *Front. Microbiol.* 3:405.

Lane, C. E., Lindstrom, S. C. & Saunders, G. W. 2007. A molecular assessment of northeast Pacific *Alaria* species (Laminariales, Phaeophyceae) with reference to the utility of DNA barcoding. *Mol. Phylogenetics Evol.* 44:634–48.

Lundholm, N., Moestrup, Ø., Hasle, G. R. & Hoef-Emden, K. 2003. A study of the *Pseudo-nitzschia pseudodelicatissima/cuspidata* complex (Bacillariophyceae): what is *P. pseudodelicatissima*? *J. Phycol.* 39:797–813.

Masella, A. P., Bartram, A. K., Truszkowski, J. M., Brown, D. G. & Neufeld, J. D. 2012. PANDAseq: paired-end assembler for illumina sequences. *BMC Bioinformatics* 13:31.

Müller, D. G. 1978. Locomotive responses of male gametes to the species specific sex attractant in *Ectocarpus siliculosus* (Phaeophyta). *Arch. Protistenk.* 120:371–7.

Peters, A. F., Coucerio, L., Tsiamis, K., Küpper, F. C. & Valero, M. 2015. Barcoding of cryptic stages of marine brown algae isolated from incubated substratum reveals high diversity. *Cryptogamie, Algologie* 36:3–29.

Peters, A. F., Scornet, D., Müller, D. G., Kloareg, B. & Cock, J. M. 2004. Inheritance of organelles in artificial hybrids of the isogamous multicellular chromist alga *Ectocarpus siliculosus* (Phaeophyceae). *Eur. J. Phycol.* 39:235–42.

Popper, Z. A., Michel, G., Hervé, C., Domozych, D. S., Willats, W. G. T., Tuohy, M. G., Kloareg, B. & Stengel, D. B. 2011. Evolution and diversity of plant cell walls: from algae to flowering plants. *Annu. Rev. Plant Biol.* 62:567–90.

Préchoux, A., Genicot, S., Rogniaux, H. & Helbert, W. 2016. Enzyme-assisted preparation of furcellaran-like κ-/β-carrageenan. *Mar. Biotech.* 18:133–43.

Rognes, T., Flouri, T., Nichols, B., Quince, C. & Mahé, F. 2016. VSEARCH: a versatile open source tool for metagenomics. *PeerJ* 4:e2584.

Stackebrandt, E. & Goebel, B. M. 1994. Taxonomic note: a place for DNA-DNA reassociation and 16S rRNA sequence analysis in the present species definition in bacteriology. *Int. J. Syst. Evol. Microbiol.* 44:846–9.

Starr, R. C. & Zeikus, J. A. 1993. Utex – the culture collection of algae at the University of Texas at Austin: 1993 list of cultures. *J. Phycol.* 29:1–106.

Tapia, J. E., González, B., Goulitquer, S., Potin, P. & Correa, J. A. 2016. Microbiota influences morphology and reproduction of the brown alga *Ectocarpus* sp. *Front. Microbiol.* 7:197.

Thomas, F., Dittami, S. M., Brunet, M., Le Duff, N., Tanguy, G., Leblanc, C. & Gobet, A. 2020. Evaluation of a new primer combination to minimize plastid contamination in 16S rDNA metabarcoding analyses of alga-associated bacterial communities. *Environ. Microbiol. Rep.* 12:30–37. https://doi.org/10.1111/1758-2229.12806.

Torode, T. A., Marcus, S. E., Jam, M., Tonon, T., Blackburn, R. S., Hervé, C. & Knox, J. P. 2015. Monoclonal antibodies directed to fucoidan preparations from brown algae. *PLoS ONE* 10:e0118366.

Wang, Q., Garrity, G. M., Tiedje, J. M. & Cole, J. R. 2007. Naive Bayesian classifier for rapid assignment of rRNA sequences into the new bacterial taxonomy. *Appl. Environ. Microbiol.* 73:5261–7.

Weisburg, W. G., Barns, S. M., Pelletier, D. A. & Lane, D. J. 1991. 16S ribosomal DNA amplification for phylogenetic study. *J. Bacteriol.* 173:697–703.

West, J. & Kraft, G. 1996. *Ectocarpus siliculosus* (Dillwyn) Lyngb. from Hopkins River Falls, Victoria – the first record of a freshwater brown alga in Australia. *Muelleria* 9:29–33.

Wetzel, R. G. 2001. *Limnology: Lake and River Ecosystems*, 3rd edn. Academic Press, San Diego, California, 1006 pp.

Zobell, C. E. 1941. Studies on marine bacteria. I. Cultural requirements of marine heterotrophic aerobes. *J. Mar. Res.* 4:42–75.

Žuljević, A., Kaleb, S., Peña, V., Despalatović, M., Cvitković, I., De Clerck, O., Le Gall, L., Falace, A., Vita, F., Braga, J. C. & Antolić, B. 2016. First freshwater coralline alga and the role of local features in a major biome transition. *Sci. Rep.* 6:19642.

Supporting Information

Additional Supporting Information may be found in the online version of this article at the publisher's web site:

Table S1. Amplicon sequencing results of bacterial communities.

ABSTRACT

Saccharina latissima is a kelp-forming species of brown algae and, as such, is considered a so-called ecosystem engineer. Several populations of this alga are exploited around the world. *S. latissima* is also currently undergoing increasing development in aquaculture. Despite its economic and ecological interest, only a few data are available on the composition of microbiota associated with *S. latissima* and its role in algal physiology.

My PhD thesis aims to characterise the bacterial microbiota and study host-microbiota interactions within the *S. latissima* holobiont to understand how the microbiota composition influences algal growth.

16S metabarcoding analyses were used to study the microbiota of *S. latissima* natural populations from Roscoff (France), Helgoland (Germany), Southern Norway (Skagerrak) and Svalbard. Since the study of these populations requires a simple sampling protocol, we have tested and validated the use of silica gel as an alternative to liquid nitrogen. We have shown a difference in bacterial composition depending on the algal blade part (apex/meristem), the geographical area and the algal physiologic state. The microbiota is predominantly composed of the phyla *Alphaproteobacteria*, *Gammaproteobacteria,* and *Bacteroidota*. In parallel, bacterial isolations were performed to obtain the cultivable part of this microbiota, and we have obtained 69 taxonomically unique bacterial strains (377 isolates), belonging mainly to the *Firmicutes*, the *Alphaproteobacteria*, and the *Gammaproteobacteria*. Combining these results with the 16S metabarcoding data allowed us to select bacterial strains associated specifically with healthy algae (*Granulosicoccus* sp.), associated specifically with algae with symptoms (*Sulfitobacter* sp., *Maribacter* sp., *Pseudoalteromonas* sp., *Psychromonas* sp.) or associated with both groups (*Bacillus* sp.).

These strains were co-cultivated with *S. latissima* plantlets for two weeks, and we observed their impact on the algal growth. In several co-culture experiments, we observed decreased algal growth coupled with a “recovery” phenomenon when adding a second strain, but these results were only partially reproducible, leading us to consider others parameters. Different experimental outcomes from one set of experiments to the next could, for instance, be due to the plantlet’s general state at the beginning or to its initial microbiota composition. Adding the tested strains could also have triggered a Quorum Sensing phenomenon (QS), a bacterial mode of communication/perception, leading to an imbalance in the microbiota (dysbiosis). Analysis of all combined data (algal growth, QS production, bacterial composition of co-cultures) shows a correlation between an increase of QS molecules and a decrease in algal growth.

Together, these results on *S. latissima* microbiota’s composition help to decipher its impact on the algal host and, more generally, contribute to a better understanding of the algal holobiont. They support the idea of interdependence between the host and its microbiota.

RESUME DE THESE

Saccharina latissima est une des espèces de macroalgues brunes dites ingénieures qui participent à la formation des forêts de laminaires. Plusieurs populations naturelles sont exploitées autour du monde et *S. latissima* fait également l'objet de développements croissants en aquaculture. Malgré l'importance économique et écologique de *S. latissima*, il existe actuellement peu de données sur la composition de son microbiote associé et sur le rôle de celui-ci dans la physiologie de l'algue.

Le but de ma thèse est de caractériser le microbiote bactérien et d'étudier les interactions hôte-microbiote au sein de l'holobionte *S. latissima*, pour comprendre dans quelles mesures la composition du microbiote influence la croissance de l'algue.

Des approches de metabarcoding 16S nous ont permis d'étudier le microbiote de *S. latissima* issues de populations naturelles de Roscoff (France), Helgoland (Allemagne), Norvège sud (Skagerrak) et Svalbard. L'étude de ces populations nécessitant la mise en place d'un protocole d'échantillonnage simple d'utilisation, nous avons testé et validé l'utilisation du silica-gel comme alternative à l'azote liquide. Nous avons montré une différence de composition en fonction de la zone de la lame (apex/méristème), en fonction de la zone géographique et de l'état physiologique de l'algue. Le microbiote est majoritairement composé des phylums *Alphaproteobacteria, Gammaproteobacteria* et *Bacteroidota*. En parallèle, des isolements bactériens ont été fait pour avoir accès à la part cultivable de ce microbiote, et nous avons obtenu 69 souches taxonomiquement uniques (377 isolats), appartenant principalement aux *Firmicutes*, *Alphaproteobacteria* et *Gammaproteobacteria*. La combinaison de ces résultats avec les données de métabarcoding 16S a permis de sélectionner des souches associées à des algues saines *(Granulosicoccus* sp.), à des souches associées à des algues porteuses de symptômes (*Sulfitobacter* sp., *Maribacter* sp., *Pseudoalteromonas* sp., *Psychromonas* sp.) ou associées aux deux groupes d'algues (*Bacillus* sp.).

Ces souches ont été mises en cocultures avec des plantules de *S. latissima* pendant 2 semaines et nous avons observé leur impact sur la croissance algale. L'observation d'une diminution de la croissance, couplée à des phénomènes de « récupération » lors de l'ajout d'une deuxième souche, résultats inattendus mais partiellement reproductibles, nous a mené à prendre en compte d'autres paramètres. Ces résultats pourraient être dus à l'état général de la plantule de départ ou à la composition de son microbiote initial. L'ajout de ces souches a pu déclencher un phénomène de quorum sensing (QS), mode bactérien de communication/perception, entrainant alors un déséquilibre dans le microbiote (dysbiose). L'analyse de l'ensemble des résultats obtenus (croissance algale, production de QS, composition bactérienne des cocultures) montre une corrélation entre l'augmentation du QS et une baisse de la croissance.

Ensemble, ces résultats apportent de nouvelles données sur la composition du microbiote de *S. latissima*, de son impact sur l'hôte, et de manière générale participent à la meilleure compréhension de l'holobionte algue. Ils viennent à l'appui de l'idée d'interdépendance entre l'hôte et son microbiote.